

Copyright Warning & Restrictions

The copyright law of the United States (Title 17, United States Code) governs the making of photocopies or other reproductions of copyrighted material.

Under certain conditions specified in the law, libraries and archives are authorized to furnish a photocopy or other reproduction. One of these specified conditions is that the photocopy or reproduction is not to be “used for any purpose other than private study, scholarship, or research.” If a user makes a request for, or later uses, a photocopy or reproduction for purposes in excess of “fair use” that user may be liable for copyright infringement,

This institution reserves the right to refuse to accept a copying order if, in its judgment, fulfillment of the order would involve violation of copyright law.

Please Note: The author retains the copyright while the New Jersey Institute of Technology reserves the right to distribute this thesis or dissertation

Printing note: If you do not wish to print this page, then select “Pages from: first page # to: last page #” on the print dialog screen

The Van Houten library has removed some of the personal information and all signatures from the approval page and biographical sketches of theses and dissertations in order to protect the identity of NJIT graduates and faculty.

ABSTRACT

OBSERVERS FOR DISCRETE-TIME NONLINEAR SYSTEMS

by
Walter D. Grossman

Observer synthesis for discrete-time nonlinear systems with special applications to parameter estimation is analyzed. Two new types of observers are developed. The first new observer is an adaptation of the Friedland continuous-time parameter estimator to discrete-time systems. The second observer is an adaptation of the continuous-time Gauthier observer to discrete-time systems. By adapting these observers to discrete-time continuous-time parameter estimation problems which were formerly intractable become tractable.

In addition to the two newly developed observers, two observers already described in the literature are analyzed and deficiencies with respect to noise rejection are demonstrated. Improved versions of these observers are proposed and their performance demonstrated.

The issues of discrete-time observability, discrete-time system inversion, and optimal probing are also addressed.

OBSERVERS FOR DISCRETE-TIME NONLINEAR SYSTEMS

by
Walter D. Grossman

**A Dissertation
Submitted to the Faculty of
New Jersey Institute of Technology
in Partial Fulfillment of the Requirements for the Degree of
Doctor of Philosophy**

Department of Electrical and Computer Engineering

May 1999

Copyright © 1999 by Walter D. Grossman

ALL RIGHTS RESERVED

APPROVAL PAGE

OBSERVERS FOR DISCRETE-TIME NONLINEAR SYSTEMS

Walter D. Grossman

Dr. Bernard Friedland, Dissertation Advisor Distinguished Professor, Department of Electrical and Computer Engineering, NJIT	Date
--	------

Dr. Andrew U. Meyer, Committee Member Professor of Electrical Engineering, Department of Electrical and Computer Engineering, NJIT	Date
--	------

Dr. Timothy N. Chang, Committee Member Associate Professor of Electrical and Computer Engineering Department of Electrical and Computer Engineering, NJIT	Date
---	------

Dr. Denis Blackmore, Committee Member Professor of Mathematics Department of Mathematics, NJIT	Date
--	------

Dr. Zoran Gajic, Committee Member Associate Professor of Electrical Engineering, Department of Electrical Engineering, Rutgers University	Date
---	------

BIOGRAPHICAL SKETCH

Author: Walter D. Grossman

Degree: Doctor of Philosophy

Date: May 1999

Date of Birth: March 7, 1957

Place of Birth: New York City

Undergraduate and Graduate Education:

- Doctor of Philosophy in Electrical Engineering, New Jersey Institute of Technology, Newark, NJ, 1999
- Degree of Engineer in Electrical Engineering, Polytechnic University, Brooklyn, NY, 1991
- Master of Science in Electrical Engineering, Polytechnic University, Brooklyn, NY, 1988
- Bachelor of Science in Electrical Engineering, Massachusetts Institute of Technology, Cambridge, MA, 1979

Major: Electrical Engineering

Presentations and Publications:

- A. Grodzinsky, W. Grossman, and R. Lee, "The significance of electromechanical and osmotic forces in the swelling behavior of articular cartilage in tension," *Trans. ASMEJ. Biochemical Engineering*, Nov. 1981.
- D. G. Edwards and W. D. Grossman, "A high voltage zener diode with an array structure," *IEEE Device Letters*, Nov. 1982.
- W. Grossman, F. Khorrami, and B. Friedland, "An observer-based design for robust control of robot manipulators," *Proc. American Control Conference*, pp. 731-736, May 1990.
- F. Khorrami, S. Jain, A. Tzes, W. Grossman, and W. Blesser, "Nonlinear control with input preshaping for flexible link manipulators," *Proc. Fifth Int. Conf. on Advanced Robotics*, June 1991.
- W. Grossman, "Algebraic Approach to the bearings-only estimation equations," *AIAA Journal of Guidance, Control, and Dynamics*, vol. 14, pp. 1086-1088, Sep. 1991.

- W. Grossman, "Bearings-only tracking: A hybrid coordinate system approach," *AIAA J. of Guidance, Control, and Dynamics*, vol. 17, May-June 1994.
- M. Carrol and W. Grossman, "Passive emitter location for tactical applications," *Exponent-The Loral Technical Journal*, pp. 24-28, 1991.
- W. Grossman, "Bias and divergence in bearings-only extended kalman filters," in *Proceedings of the 1st Regional Control Conference*, (Brooklyn, NY), pp. 137-140, 1992.
- B. Friedland and W. Grossman, "On continuous-time processes with data on occurrence of discrete events," in *Proceedings of the 2d Regional Control Conference*, (Newark, NJ), 1993.
- W. Grossman, "Extension of the friedland parameter estimator to discrete-time systems," *AIAA J. of Guidance, Control, and Dynamics*, vol. 20, no. 5, pp. 1047-1049, 1997.

To my beloved wife Vered

ACKNOWLEDGMENT

Needless to say it was very difficult for me to study for my doctorate while working and raising my family. I received much help from many kind people affiliated with various offices at NJIT and I owe them all a debt of gratitude. I would like to thank Jean Ebenholtz, formerly with the ECE Graduate Studies office, for assisting me in making sure I was always registered properly and for taking care of matters which were difficult for me to take care of from Virginia. I would like to thank Annette Damiano, Assistant Director of Graduate Studies, for helping me by supporting my various petitions and for her critical review of the dissertation format.

I wish to thank the members of my dissertation committee, Professor Andrew Meyer, Professor Timothy Chang, Professor Denis Blackmore, and Professor Zoran Gajic for their efforts on my behalf, for reviewing my work, and for their critical comments which served to clarify and sharpen my work.

I wish to thank my friend and colleague Dave Haessig for our long and intellectually stimulating telephone conversations. He and I worked somewhat parallel paths and it was my pleasure to talk with him and, during the difficult times, to commiserate with.

To “thank” Professor Friedland for his help in completing my doctorate does him a great injustice. On the professional level, Professor Friedland gave me the critical guidance to move my work forward. He suggested directions to pursue, directions to avoid, and he kept my feet on the ground. He asked the theoretical questions which had to be asked and which made me think more deeply about my work. He guided the organization of my dissertation to give it the necessary clarity which it lacked in early drafts. On the personal level, Professor Friedland understood the “human side” of my effort to complete my doctorate. My work did not always advance at an even pace due to various family or work commitments. He understood these difficulties and showed great patience. On a deeper level I

cannot thank Professor Friedland enough for giving me a career. I met Professor Friedland thirteen years ago at a time where my career focus was unclear. It was from his lectures and those of our mutual colleague Jack Richman that my focus was sharpened. His lectures were delivered with contagious enthusiasm. I quickly became fascinated by the magic of state estimation whereby entire states are estimated from single measurements. I immediately put this knowledge to work and I became a specialist. To date I have designed the control systems of many satellites and I have a critical role in the control system design of the International Space Station. These accomplishments are all thanks to Professor Friedland.

It is from my late mother, Frances Gaezer Grossman *z"l*, and from my father, Jacob Grossman, I received the encouragement and the drive for scholarship. This drive is in the spirit of the great *Jewish* tradition of scholarship and I am a fortunate beneficiary of this great tradition. In an age where material pursuits are paramount, my parents preferred I concentrate on learning. Both of my parents were scholars in their own right and it is fair to say that this drive for scholarship with which I was imbued caused me to seek a doctorate and kept my efforts on track. I only wish my mother could see and enjoy the fruits of her efforts.

To my beloved wife Vered I owe everything and I have dedicated this dissertation to her. I owe her for the encouragement when I wanted to quite, for the countless cups of coffee when I wanted to sleep, for shuttling the children out of my office when they (and I) wanted to play, for organizing my office when I could no longer see the floor, for taking the children to the mall so they would not dance on my keyboard, and for holding her list of home improvements in abeyance until I finished this dissertation. The list is endless. Her love, selflessness, and devotion to me made this work possible and I am the luckiest guy on earth to have her for my wife.

Lastly, with all my love I thank my three wonderful children, Yarden, Edan, and Tal, for without their help I would have finished in about half the time. Yet, without their smiles, it wouldn't have been worth continuing.

Walter D. Grossman

Fairfax Station, Virginia

May 1999

TABLE OF CONTENTS

Chapter	Page
1 INTRODUCTION	1
1.1 Nonlinear Systems	2
1.2 Discrete-Time Systems	4
1.3 Advantages of Direct Design of Discrete-Time Control Systems	5
2 BACKGROUND	8
2.1 Observers for Time-Varying Linear Systems	8
2.2 Continuous-Time Nonlinear Observers	8
2.2.1 The Extended Kalman Filter	8
2.2.2 Differential Geometry-based Nonlinear Observers	9
2.2.3 The Gauthier Observer	10
2.2.4 The Ciccarella Observer	10
2.2.5 Hybrid Coordinate Kalman Filter	10
2.2.6 Reduced-Order Observers for Nonlinear Systems	11
2.3 Discrete-time Nonlinear Systems Analysis	11
2.4 Parameter Estimation for Nonlinear Systems	13
2.4.1 Parameter-Adaptive Control System Design	13
2.4.2 Optimal Probing Signal Design	15
2.4.3 Methods of Parameter Estimation	18
2.5 Contribution of Present Work	19
2.5.1 Summary of Present State-of-the-Art	19
2.5.2 New Contributions	20
3 OBSERVABILITY	23
3.1 Introduction and Background	23
3.2 Properties of Observability	25

Chapter	Page
3.3 Algebra for Discrete-time Nonlinear Systems	25
3.4 Observability of Nonlinear Discrete-time Systems	27
3.5 Rank test for “Strong” Observability	29
3.6 Degree of Strong Observability	31
4 MODIFICATIONS FOR IMPROVEMENT OF OBSERVERS	32
4.1 The Moraal/Grizzle Observer	32
4.1.1 Original Form	32
4.1.2 Noise “Bandwidth” Properties of the Moraal/Grizzle Observer	35
4.1.3 Modified Form	37
4.2 The Ciccarella Observer	39
4.2.1 Original Form	39
4.2.2 Noise “Bandwidth” Properties of the Ciccarella Observer	43
4.2.3 Modified Form	45
4.3 Coordinate Transformation, Noise, and Observability	47
4.4 Extension of the Friedland Observer	48
4.4.1 Observer Derivation	49
4.4.2 The Newton and Least-Square Observer Subclass	51
5 A NEW OBSERVER – THE “GROSSMAN” OBSERVER	55
5.1 Introduction	55
5.1.1 Continuous-Time Origins of the “Grossman Observer”	55
5.1.2 Tractability of Discrete-Time Formulation	57
5.2 A New Observer for the General Discrete-time Nonlinear Systems . . .	60
5.2.1 The Unforced System	60
5.2.2 Observer for Forced Discrete-time Nonlinear Systems	63
5.2.3 Structure of Grossman Observer	64
5.2.4 Example	66
6 APPLICATIONS	68

Chapter	Page
6.1 Discrete-time Friedland Observer for Identification of an AR Filter . .	68
6.2 Simultaneous State and Parameter Estimation	73
6.2.1 Grossman Observer	73
6.2.2 Modified Moraal/Grizzle Observer	77
6.2.3 Modified Ciccarella Observer	83
6.3 Canine Blood Pressure Response to Nitropruside	89
6.3.1 Grossman Observer	91
6.3.2 Original Moraal/Grizzle Observer	91
6.3.3 Modified Moraal/Grizzle Observer	92
6.3.4 Original Ciccarella Observer	94
6.3.5 Modified Ciccarella Observer	114
7 NUMERICAL AND IMPLEMENTATION CONSIDERATIONS	128
7.1 Newton's Methods of Solving Nonlinear Systems of Equations	128
7.2 Propagation of Solver Seed	129
8 MISCELLANEOUS RESULTS	130
8.1 The Ciccarella Observer and the Hybrid Kalman Filter	130
8.2 Generalized Continuous-time Friedland Parameter Estimator	133
8.3 Unified Theory of Friedland Parameter and State Estimators	135
8.3.1 The Generalized Friedland Nonlinear Reduced-order Observer .	135
8.3.2 Application to Parameter Estimation In Affine Systems	137
8.4 Quasi-Optimal Discrete-Time Friedland Observer	137
9 CONCLUSIONS AND RECOMMENDATIONS	140
9.1 Conclusion	140
9.2 Further Research	143
9.2.1 Optimal Pole Locations	144
9.2.2 Unification of Discrete-Time and Continuous-Time Theory . . .	145
9.2.3 Unification of Discrete-time Friedland Observer and the SDREF	145

Chapter	Page
9.2.4 The Dynamic Observer and Static Root finding	146
APPENDIX A SIMULATION PLOTS	149
APPENDIX B MATLAB CODE	192
REFERENCES	215

LIST OF TABLES

Table	Page
4.1 Effect of “slowing-factor” on Moraal/Grizzle Observer.	39
6.1 Grossman observer initial conditions	74
6.2 Modified Moraal/Grizzle observer for ARMA parameter estimation.	78
6.3 Modified Ciccarella observer for ARMA parameter estimation.	85
6.4 Initial conditions for Canine blood pressure simulation.	91
6.5 Steady-state statistics of Grossman Observer, with noise.	92
6.6 Steady-state statistics of Moraal/Grizzle Observer, with noise.	93
9.1 Observer application summary chart.	141

LIST OF FIGURES

Figure	Page
4.1 Newton root finder – Input/Output form.	34
4.2 d -stage Newton solver.	34
4.3 Moraal/Grizzle d -stage Newton observer.	35
4.4 Transient response of Moraal/Grizzle observer for scalar example.	37
4.5 Steady-state noise of Moraal/Grizzle observer for scalar example.	38
4.6 Block diagram of second “robust” form of the Ciccarella observer.	44
5.1 Grossman observer block diagram.	65
5.2 Grossman observer state estimate.	67
6.1 Estimates of ARMA characteristic polynomial coefficients.	72
6.2 Estimates of ARMA characteristic polynomial coefficients, w/ noise.	72
6.3 Observer convergence of state x_1	75
6.4 Observer convergence of state x_2	75
6.5 Observer convergence of parameter p_1	76
6.6 Observer convergence of parameter p_2	76
6.7 Modified Moraal/Grizzle estimation of ARMA coefficient p_1 , w/o noise.	79
6.8 Modified Moraal/Grizzle estimation of ARMA coefficient p_2 , w/o noise.	79
6.9 Modified Moraal/Grizzle error of ARMA state x_1 , w/o noise.	80
6.10 Modified Moraal/Grizzle error of ARMA state x_2 , w/o noise.	80
6.11 Modified Moraal/Grizzle estimation of ARMA coefficient p_1 , w/noise.	81
6.12 Modified Moraal/Grizzle estimation of ARMA coefficient p_2 , w/noise.	81
6.13 Modified Moraal/Grizzle estimation error of ARMA state x_1 , w/noise.	82
6.14 Modified Moraal/Grizzle estimation error of ARMA state x_2 , w/noise.	82
6.15 Modified Ciccarella observer error for ARMA process, w/o noise.	85
6.16 Observability condition number for modified Ciccarella observer.	86

Figure	Page
6.17 Modified Ciccarella estimation of ARMA coefficient p_1 , w/noise.	86
6.18 Modified Ciccarella estimation of ARMA coefficient p_2 , w/noise.	87
6.19 Modified Ciccarella estimation of ARMA state x_1 , w/noise.	87
6.20 Modified Ciccarella estimation of ARMA state x_2 , w/noise.	88
6.21 Grossman observer state estimate w/o noise. $\alpha = 0.5, d = 1$	95
6.22 Grossman observer estimation error w/o noise. $\alpha = 0.5, d = 1$	96
6.23 Grossman observer residual process w/o noise.	97
6.24 Noisy measurement driving observer.	98
6.25 Grossman observer state estimate w/noise. $\alpha = 0.5, d = 1$	99
6.26 Grossman observer estimation error w/noise. $\alpha = 0.5, d = 1$	100
6.27 Grossman observer residual process for example 6.3 w/noise.	101
6.28 Moraal/Grizzle observer state estimate w/o noise. $\alpha = 1.0, d = 1$	102
6.29 Moraal/Grizzle observer estimation error w/o noise. $\alpha = 1.0, d = 1$	103
6.30 Moraal/Grizzle observer state estimate w/noise. $\alpha = 1.0, d = 1$	104
6.31 Moraal/Grizzle observer estimation error w/noise. $\alpha = 1.0, d = 1$	105
6.32 Moraal/Grizzle observer state estimate w/o noise. $\alpha = 0.1, d = 1$	106
6.33 Moraal/Grizzle observer estimation error w/o noise. $\alpha = 0.1, d = 1$	107
6.34 Moraal/Grizzle observer state estimate w/noise. $\alpha = 0.1, d = 1$	108
6.35 Moraal/Grizzle observer estimation error w/noise. $\alpha = 0.1, d = 1$	109
6.36 Ciccarella observer state estimate w/o noise, arbitrary gains.	110
6.37 Ciccarella observer estimation error w/o noise, arbitrary gains.	111
6.38 Ciccarella observer state estimate w/noise, arbitrary gains.	112
6.39 Ciccarella observer estimation error w/noise, arbitrary gains.	113
6.40 Ciccarella observer estimate w/o noise, arbitrary gains, w/o feedforward.	116
6.41 Ciccarella observer error w/o noise, arbitrary gains, w/o feedforward.	117
6.42 Ciccarella observer estimate w/noise, arbitrary gains, w/ feedforward.	118
6.43 Ciccarella observer error w/noise, reduced gains, w/feedforward.	119

Figure	Page
6.44 Modified Ciccarella observer estimate w/noise, w/o feedforward.	120
6.45 Modified Ciccarella observer error w/noise, w/o feedforward.	121
6.46 Modified Ciccarella observer gain history.	122
6.47 Modified Ciccarella observer estimate, increased process noise.	123
6.48 Modified Ciccarella observer error, increased process noise.	124
6.49 Modified Ciccarella observer gain history, increased process noise.	125
6.50 Modified Ciccarella observer estimate w/noise, w/feedforward.	126
6.51 Modified Ciccarella observer error w/noise, w/feedforward.	127

CHAPTER 1

INTRODUCTION

State observers combine measurements of system output, knowledge of the system input, knowledge of the system and measurement noise, and knowledge of the system dynamics to estimate the dynamic state. Often some of the states are not available for direct measurement and the observer provides a “window” into the internal dynamics of a process. Often a system state is available for direct measurement and the observer is implemented to mitigate the effects of measurement noise.

Estimates of state observers are used in closed-loop control and as data products themselves. Examples of the former include any type of process control. Examples of the latter include navigation, spacecraft attitude determination, and system fault detection and isolation.

The general theory of *linear* observers has been developed over the past thirty-five years. Linear observers vary in complexity. For most applications the fixed-gain filter, the gains of which are calculated from the steady-state Riccati equation, provides satisfactory performance. In high-performance applications, a variable gain filter is required, the gains of which are calculated from propagation of the Riccati equation in either real-time or off-line.

Many, if not most systems of practical interest are nonlinear. Linear observers have been applied to *nonlinear* systems by local linearization of the dynamics and measurement equations about the current estimated state. Even though the observer is “suboptimal,” and convergence often cannot be proved, this approach has been applied very successfully in many applications.

Local linearization almost always requires the real-time propagation of the Riccati equation to calculate the gains. Therefore, most linearized filters are variable gain. To stabilize linearized filters they need to be “tuned.” Tuning requires

adjustment of the process noise and measurement noise covariance matrices to “mask” the nonlinearity of the system. Tuning is best achieved by running Monte Carlo analysis and adjusting the noise matrices such that the statistical errors (the statistical state covariance matrix) matches closely with that propagated by the Riccati equation.

“Masking” the nonlinearity with process noise or measurement noise impairs filter performance by failing to exploit all the knowledge one has of the system process and measurement equations. The system and measurement equations, though nonlinear, may be known very well, as in the case of satellite dynamics. Yet, to fit the linear observer paradigm, this knowledge cannot be exploited to its fullest.

In other situations where the nonlinearity is “hard,” such as a zero-velocity stiction, the linearized observer may fail to converge.

Discrete-time observers for nonlinear systems are of interest because observers, linear, nonlinear, continuous-time, or discrete-time are implemented with discrete-time digital computers. Continuous-time observers are approximated by combining high sample rates and low-order approximations to system dynamics. For low sample-rate systems the techniques for implementing continuous-time observers are less clear.

1.1 Nonlinear Systems

The dynamics of many completely known systems are described by nonlinear equations. The simple pendulum is described

$$\dot{x}_1 = x_2 \tag{1.1}$$

$$\dot{x}_2 = -\frac{g}{l} \sin x_1 \tag{1.2}$$

where $x_1 = \theta$, the pendulum angle. In fact, the broad class of Lagrangian systems is nonlinear and can be written [48]

$$J(q)\ddot{q} + H(q, \dot{q})\dot{q} + G(q) = u, \tag{1.3}$$

or in state-space form

$$\dot{x}_1 = x_2 \quad (1.4)$$

$$\dot{x}_2 = J(x_1)^{-1} [u - H(x_1, x_2)x_2 - G(x_1)]. \quad (1.5)$$

Nonlinear systems also occur as a result of describing a parametrically-uncertain *linear* system in terms of an unknown system parameter by augmenting the system state vector with the unknown parameter. The simplest example is the single-pole filter with an unknown pole p . If p is known, the dynamics are linear

$$\dot{x}_1 = -px_1 + u. \quad (1.6)$$

If p is unknown it can be adjoined to the state vector. Letting $x_2 = p$, the previous system is described by the nonlinear equations

$$\dot{x}_1 = -x_2x_1 + u \quad (1.7)$$

$$\dot{x}_2 = 0. \quad (1.8)$$

Sometimes nonlinear systems are both parametrically uncertain *and* intrinsically nonlinear. The coulomb model for friction is an example

$$\dot{x}_1 = x_2 \quad (1.9)$$

$$\dot{x}_2 = u - \theta \operatorname{sign} x_2 \quad (1.10)$$

$$\dot{\theta} = 0 \quad (1.11)$$

where θ is the unknown coefficient of coulomb friction.

It is important to note is that by augmenting the state vector with the system parameters *the parameter estimation problem can be considered as a subclass of the general nonlinear estimation problem.*

1.2 Discrete-Time Systems

Many economic processes, chemical processes, and pharmacokinetic processes are described better in discrete-time than in continuous time [30]. This class of discrete-time systems usually involves discrete-time measurement and discrete-time control. Sometimes the dynamic process is a combination of subprocesses which are completed in discrete batches.

Most commonly, however, discrete-time nonlinear systems are derived from discrete-time measurement and control of continuous-time systems. In many situations a controller or an observer can be designed in continuous-time and adapted to discrete-time by sampling “fast enough.” The required sampling speed is defined as that which works. The rule-of-thumb for the usual starting point is to sample 10-20 times the faster than the fastest time constant of the system.

In other situations it is better to design the controller or observer using a “direct digital” design. Such methods accounts for the effects of sampling and is particularly appropriate for slow sampling systems.

Direct digital design is also appropriate when the vendor hardware functions in discrete-time. A rate-integrating gyroscope outputs a discrete-time rotation pseudo-vector

$$\delta\theta = \begin{bmatrix} \delta\theta_x & \delta\theta_y & \delta\theta_z \end{bmatrix}' \quad (1.12)$$

and the rigid-body kinematics are described in closed-form

$$T(k+1) = [\exp -\delta\theta_k^\times] T(k), \quad (1.13)$$

where T is the attitude matrix and

$$\delta\theta^\times = \begin{bmatrix} 0 & -\delta\theta_z & \delta\theta_y \\ \delta\theta_z & 0 & -\delta\theta_x \\ -\delta\theta_y & \delta\theta_x & 0 \end{bmatrix} \quad (1.14)$$

is the skew-symmetric matrix generated from the measured output of the rate-integrating three-axis gyro.

1.3 Advantages of Direct Design of Discrete-Time Control Systems

In many practical circumstances the direct design of a discrete-time control system is advantageous in comparison to the digital redesign by (rapid) sampling of the continuous-time system. Slow sampling and accommodating vendor hardware are two practical reasons for direct digital design. It is often difficult to calculate the gains in the digital re-design of nonlinear systems leaving more of the design to the “cut-and-try” method.

Certain problems have better *theoretical* formulation in discrete-time than in continuous-time. Almost all work on system identification is developed for discrete-time systems [2, 35]. Delayed or retarded systems are better formulated in discrete-time where the theory is fairly complete [34, 14].

The impetus to the present work is one sentence from Friedland’s “Advanced Control System Design,” [14], page 326. Describing parameter estimation in ARMA models Friedland writes

Methods for estimating the parameters of a linear, discrete-time system are available that have no obvious counterparts in continuous-time systems.

This statement is true because discrete-time inputs and outputs are known at every sampling interval. By comparison, the derivatives of the input and outputs of continuous-time systems are rarely, if ever, completely available.

In 1993 Ciccarella *et al* [5] proposed a globally convergent continuous-time observer. The observer is of general applicability except that its use is restricted to systems of relative degree¹ $r = n$, where n is the dimension of state. This restriction

¹The relative degree of a system is equal to the minimum derivative of the output plus one which is directly affected by the system input.

precludes its application to the parameter estimation problem since, as seen in the following example, the parameter estimation problem usually has relative degree $r < n$.

1.3.1 Example

The dynamics of a two-pole filter are nonlinear if the proper state vector is augmented with the unknown filter coefficients, i.e.,

$$x = \begin{bmatrix} x_1 & x_2 & p_1 & p_2 \end{bmatrix}' \quad (1.15)$$

$$\dot{x}_1 = x_2 \quad (1.16)$$

$$\dot{x}_2 = -p_1x_1 - p_2x_2 + u \quad (1.17)$$

$$\dot{p}_1 = 0 \quad (1.18)$$

$$\dot{p}_2 = 0 \quad (1.19)$$

$$y = x_1. \quad (1.20)$$

The transformed variable z is the four element vector given by y and its first three derivatives

$$z \equiv \begin{bmatrix} y \\ \dot{y} \\ \ddot{y} \\ \dddot{y} \end{bmatrix} = \begin{bmatrix} x_1 \\ x_2 \\ -p_1x_1 - p_2x_2 + u \\ p_1p_2x_1 + (p_2^2 - p_1)x_2 - p_2u + \dot{u} \end{bmatrix}. \quad (1.21)$$

The control input appears in the third element of the derivative vector making this system one of relative degree $r = 3$. The state vector is four element, $n = 4$. Since $r < n$ this system does not satisfy the conditions for the Ciccarella observer. *For any system in which $n > 1$ and the dynamics are affine in the parameters, the Ciccarella observer is inappropriate for estimating the parameters.* Furthermore, since most parameter estimation problems require persistent excitation to enhance observability, the unforced version of the Ciccarella observer is of no utility.

In spite of extensive research it was not possible to extend the Ciccarella continuous-time results to systems of relative degree $r < n$. The difficulty arises when $r < n$ because the linearizing transformation upon which the Ciccarella results are based is very complicated. The resulting observer requires explicitly the derivatives of the input and the output of the system.

Moraal and Grizzle [42] and Ciccarella [6, 7] developed nonlinear discrete-time observers which do not have a relative degree requirement. They did not, however, address the practical implementation of their observers in real systems with noise. Performance of their observers in practical applications is limited by measurement noise and process uncertainty. Neither observer provides the right design “handle” for implementation in a noisy environment.

In light of Friedland’s above comment it appeared to this author that it may be possible to cast the continuous-time Ciccarella observer into a discrete-time form to overcome its relative degree limitations. In this present work this author develops two new discrete-time observers which demonstrate excellent performance in systems with noise. This author further demonstrates that the discrete-time observers of Moraal/Grizzle and of Ciccarella, while not satisfactory for practical application in their present form, can be modified to significantly enhance their noise robustness. With this improved noise robustness the Moraal/Grizzle the Ciccarella observers can be implemented in real systems.

CHAPTER 2

BACKGROUND

2.1 Observers for Time-Varying Linear Systems

Theory of observers for *idealized* time-varying linear systems with known dynamics and measurement equations is fairly complete. Kalman's original work [29] was written in terms of known, time-varying systems in which the statistics of the process and measurement noise were zero-mean Gaussian with a known, possibly time-varying covariance. Luenberger [37] coined the term "observer" and developed the general, sub-optimal form.¹

Current research in linear time-varying systems explores issues when the systems of interest depart from this idealized model. Such issues include:

- Observer robustness with system or parametric uncertainty.
- Observer performance with non-Gaussian or incompletely known noise statistics.
- Observer performance of linearized approximations of nonlinear systems.
- Observer performance for linearized systems in which time-variation linear system is "exchanged" for the time-invariant nonlinear system.
- Performance of reduced-order observers.

Since most practical systems represent a departure from the idealized model presented by Kalman further important research continues in these areas.

2.2 Continuous-Time Nonlinear Observers

2.2.1 The Extended Kalman Filter

The earliest work on nonlinear observers, both discrete-time and continuous-time, used some form of the *extended* Kalman filter (EKF). The extended Kalman filter

¹It is interesting that Kalman developed the optimal form of the Luenberger observer *prior* to Luenberger's development of the general, suboptimal form.

was, in fact, invented by Swerling [49] to estimate satellite orbits before Kalman developed the general theory. The term “extended” means that the filter dynamics, the observation, or both are nonlinear and that the filter gains are calculated by linearizing the equations about the current state estimate. Such filters have been applied to intrinsically nonlinear systems and to systems made nonlinear by state vector augmentation of unknown parameters. This method has been used successfully by many practitioners and yet lacks a firm theoretical basis. Jazwinski [27] provides an in-depth presentation of the EKF and its many variants with application to the nonlinear problems of orbit determination and parameter estimation. His presentation emphasizes continuous-time (possibly nonlinear) dynamics and discrete-time, nonlinear observation updates—which are the most common application in practice.

Ljung [35] further studied the theoretical asymptotic properties of the EKF in parameter estimation. He demonstrated that in spite of its wide application, the EKF can produce biased estimates or may even diverge.

2.2.2 Differential Geometry-based Nonlinear Observers

Isidori [26] presents a solution of the nonlinear observer problem using a nonlinear transformation of coordinates to map the nonlinear system into the linear Brunowski chain-integrator form. Linear observer theory is then used to assign eigenvalues of the estimation error dynamics and guarantee convergence (but not necessary optimality.)

The example given by Isidori in [26] is an unforced system. The relative degree of an unforced system is not defined or irrelevant since the input is zero by construction. Isidori does not address the n -dimension forced system with relative degree $r < n$, which is common for most parameter estimation problems. Parameter estimation problems usually require some probing or persistent excitation to make the system observable. A *complete* linearizing transformation for forced systems with

relative degree $r < n$ does not exist. (It may still be possible to linearize a portion of the system.)

2.2.3 The Gauthier Observer

Gauthier *et al* [16] developed a fixed-gain nonlinear observer for continuous-time systems and proved convergence. The observer requires nonlinear transformation into Brunowski form (chain of integrators). A Sylvester equation, similar to the steady-state Riccati equation is solved in the transformed coordinates to calculate the fixed gain. An inverse transformation of coordinates is required to recover the original states. In the general case, this inverse transformation requires the solution of a set of partial differential equations.

2.2.4 The Ciccarella Observer

Ciccarella *et al* [5] extended Gauthier's work and improved upon it by eliminating the nonlinear transformation. Ciccarella used nonlinear transformations to develop his observer and to prove convergence. The final form of the observer, however, does not require a nonlinear transformation.

2.2.5 Hybrid Coordinate Kalman Filter

The approaches of Gauthier and Ciccarella are forms of the hybrid approach used by Grossman [23] for the bearings-only estimation problem. In [23] two coordinate systems are used – one for the propagation of the dynamics and one for the measurement update. The coordinate system for the dynamics propagation was chosen to simplify mechanization of the integration of the state and covariance equations. The coordinate system for the update is chosen for its good performance under conditions of noisy measurements and poor observability. The covariance matrix is propagated in the “dynamics” coordinate system and converted to the “measurement” coordinate system using the Jacobian matrix relating the two

systems. The Gauthier and Ciccarella observers use a similar approach where the two systems are the native one and the one transformed to Brunowski normal form of n derivatives of the output. (See section 8.1 for further discussion of this similarity.)

2.2.6 Reduced-Order Observers for Nonlinear Systems

In comparison with the large volume of work on full-order observers, very little has been written about reduced-order observers, linear or nonlinear, despite their great potential for simplifying controller design and improving controller robustness. Friedland [12] derived the reduced order observer for linear systems. Properties of the reduced-order Kalman Filter are summarized by Friedland in [13].

For nonlinear systems Friedland [14] developed the general form of the reduced-order observer and described a new approach to parameter estimation for nonlinear systems when the complete state is measurable and the system is affine in the unknown parameter.²

2.3 Discrete-time Nonlinear Systems Analysis

In contrast to the large volume of work on continuous-time nonlinear systems, very little work has been done on the analogous problem of discrete-time nonlinear observers.

A discrete-time system is one in which values for the state, the controlling input, and the measured output are defined at discrete times. The general (possibly nonlinear) discrete-time system of interest can be described

$$x_{k+1} = f(x_k, u_k) \quad (2.1)$$

$$y_k = h(x_k, u_k). \quad (2.2)$$

²This author has extended Friedland's technique to apply to the more general problem of nonlinear reduced-order state estimation when the system is affine in the unmeasured state. See section 8.2.

The *linear* discrete-time system is a subset of the systems described above

$$x_{k+1} = A_k x_k + B_k u_k \quad (2.3)$$

$$y_k = C_k x_k + D_k u_k. \quad (2.4)$$

Functions f and h in (2.1), (2.2) could be functions of the index k resulting in a time-varying nonlinear discrete-time system.

The development of the differential geometric analysis of nonlinear systems in the 1980's provided a new set of tools to analyze and develop nonlinear continuous-time observers. Development of discrete-time nonlinear observers has not followed their continuous time counterparts because little work has been done on the analogous problem of discrete-time nonlinear system inversion. The reason is that smoothness, continuity, existence of high-order derivatives is required for the application of differential geometric analysis techniques. Discrete-time systems are characterized by *discrete jumps* and thus cannot satisfy the typical smoothness requirements.

Most of the limited amount of the literature in the field of nonlinear discrete-time systems relates to system inversion applied to the controller design problem with the presumption of full-state measurability. Scant attention has been given to nonlinear discrete-time observer design and the fundamental issue of observability of such systems.

The earliest work addressing the controller design problem is that of Grizzle *et al* [20], [21] where they demonstrate that the willy-nilly application of the discrete-time sample-and-hold on the input can destroy the linearization. Grizzle then proposes a multirate scheme to mitigate the deleterious effects of the sample-and-hold. Grizzle does not develop general theory, analogous to the differential geometry, to be applied to discrete-time systems.

More recently Kotta [30], [31] has developed a theoretical framework for feedback linearization i.e., right inversion of discrete-time state-space systems. His work applies to the feedback control problem under the assumption that full-state feedback is available. Kotta does not address the issue of nonlinear observers or the inversion problem using partial state feedback.

Fleigner, Kotta, Nijmeijer have addressed the problem of feedback linearization of discrete-time implicit systems [11].

The issue of observability of nonlinear discrete-time systems is addressed by Sontag [47] and Nijmeijer [43]. Their results are summarized in chapter 3.

2.4 Parameter Estimation for Nonlinear Systems³

Parameter estimation for closed-loop feedback control systems provided the original impetus for this work on nonlinear discrete-time observers. In particular, this dissertation was motivated by a series of failed attempts to apply the continuous-time Ciccarella observer [5] to estimate parameters in systems for which measurements for all the states were unavailable. The cause of these failures, as stated in section 1.3 and section 5.1.2, was the conflicting requirements that the relative degree of the augmented system be equal to the dimension the augmented state and that the system be persistently excited. Formulating the problem in discrete-time and applying a discrete-time observer, as shown in section 5.1.2, provides a means to work around this conflict.

2.4.1 Parameter-Adaptive Control System Design

The notion of parameter-adaptive or “indirect-adaptive” control originated *simultaneously* with the birth of modern control theory. In 1958 Kalman wrote “Design of a Self-Optimizing Control System” [28] in which he describes a system which

³See Åström and Wittenmark [2], chapter 2, for further discussion of parameter estimation as related to adaptive control and robust control.

first identifies the pulse transfer function.⁴ The article includes photographs of the apparatus. In 1961 Kalman and Bucy wrote [29]

The generality of our results should be of considerable usefulness in the theory of adaptive systems, which is as yet in a primitive stage of development.

An *adaptive system* is one which changes its parameters in accordance with measured changes in its environment. In the estimation problem, the changing environment is reflected in the time-dependence of F , G , H , Q , R . Our theory shows that such changes affect only the values of the parameters but not the structure of the optimal filter. This is what one would expect intuitively and we now have a rigorous proof. Under ideal circumstances, the changes in the environment could be detected instantaneously and exactly. The adaptive filter would then behave as required by the fundamental equations (I-IV) [the Kalman filter and variance equations]. In other words, our theory establishes a basis of comparison between actual and ideal adaptive behavior. It is clear therefore that *a fundamental problem in the theory of adaptive systems is the further study of the properties of the variance equation (IV)*. [Emphasis in original text].

Kalman does not address the methods by which “measured changes” in environment (i.e., measurements) are to be processed to establish the time-dependent values for system matrices F , G , H , Q , R from which his optimal filter is constructed. This processing of “measured changes” into refined system and noise models has been the subject of parameter-adaptive control system for the past thirty years.⁵

⁴It is interesting to note that in this paper Kalman first raises the then unanswered question of defining optimality of the controller once the system is identified. It is for design of optimal systems rather than adaptive ones in which he made his greatest contribution and for which he is best known.

⁵Kalman does imply that the parameter estimation is *not* achieved by augmentation of the state vector by the unknown parameters. For estimation of parameters in linear systems, state vector augmentation is equivalent to exchanging the original linear time-varying problem for a time-invariant nonlinear problem. Kalman developed the theoretical optimal solution for the former and not the latter.

Many control systems are designed by substituting a (more tractable) time-varying linear dynamics equation for the true nonlinear dynamics equation. State augmentation techniques for parameter estimation is the opposite approach whereby a time-invariant nonlinear system is substituted for a parameter-dependent, time-varying linear system. See note 3.2, page 110 of [12] for further discussion of time-varying versus nonlinear systems.

In 1965 Fel'dbaum hinted at a hierarchical control structure in which a supervisory level “measures” the environment and establishes system parameters for which the lower level optimal controller is designed [10], page 4. Implementation of this hierarchy leads to the dual loop slow-loop/fast-loop adaptive controller structure later developed by researchers in adaptive control:⁶

For a sufficiently slow change in the characteristics of the controlled object, a primary controller can be constructed according to optimal system theory, by providing it, however, with variable parameters. A secondary controller—an automatic optimizer—by observing the operation of the system, changes the parameters of the primary device, such that on the whole the system remains close to optimal, in spite of an unexpected variation in the characteristics of the controlled object.

2.4.2 Optimal Probing Signal Design

The issue of “optimal probing” input is an inherent part of dual control and has been explored by many investigators. Fel'dbaum identified the requirement of probing signals for parameter identification [9, 10]. Fel'dbaum [10], pages 30-31, expounded the dual nature of the control input, i.e., the control input should be used probe and characterize the system parameters as well as to drive the system to the desired trajectory:

A study of the disturbance \bar{z} [plant disturbance], i.e., by essentially varying the characteristics of the object B [the plant] in an unexpected manner, can be made...not by passive observations but by an active method, by means of rational “experiments.” The object would be “sensed” by the actions \bar{u} [plant input], having a trial perceptive character, and the results \bar{y} [plant output] of these actions analyzed by the controller A . The purpose of such actions is to further the more rapid and precise “study” of the characteristics of the object B [the plant], which will help to choose the best control law for the object.

Bar Shalom, Tse, *et al* [50], [52], [4], [51] extended Fel'dbaum's work and derived “optimal probing” signals for identifying systems. Their work and the work

⁶This dual loop structure is based upon the separation of time constants between plant parameters and proper state variables. It is ubiquitous in the adaptive control literature and is featured on the front cover of [2].

of Mehra [39], [40], [41] and Goodwin *et al* [18], [17] is based upon maximizing the norm of the Fisher information matrix (the inverse covariance matrix). Åström's work [2] in persistent excitation is based upon minimizing the condition number of the deterministic observability matrix. This approach is closely related to the maximizing the norm of the Fisher information matrix. The issue of optimal probing is not relevant to linear systems since the separation theorem proves that for a linear system the optimal observer problem is independent of control [12, 33, 19].

It has not been generally recognized that for nonlinear systems which can be feedback-linearized *the "optimal" probing signal is the linearizing feedback*. The linearizing feedback transforms the nonlinear system into Brunowski Normal form with an observability matrix equal to the identity matrix.⁷

For the continuous-time SISO system with relative degree $r = n$, where n is the order of the system

$$\dot{x} = f(x) + g(x)u \quad (2.5)$$

$$y = h(x) \quad (2.6)$$

let $z = \phi(x)$ be the function mapping the system to Brunowski normal form, i.e.,

$$z = \phi(x) = \begin{bmatrix} h(x) \\ L_f h(x) \\ \vdots \\ L_f^{n-1} h(x) \end{bmatrix}. \quad (2.7)$$

The linearizing feedback [26] is

$$u = \frac{1}{L_g L_f^{n-1} h(x)} (-L_f^n h(x) + v) \quad (2.8)$$

⁷This development follows Isidori [26]. It is interesting to note that Isidori was primarily interested in differential geometry of control and did not recognize or at least state explicitly that by driving the system to Brunowski form, the linearizing feedback also drives the system to optimal observability.

where v is the external input to this linearizing compensator.

In the z coordinates the system equations are

$$\dot{x} = Az + Bv \quad (2.9)$$

$$y = Cz \quad (2.10)$$

where

$$A = \begin{bmatrix} 0 & 1 & 0 & \dots & 0 \\ 0 & 0 & 1 & \dots & 0 \\ \vdots & \vdots & \vdots & \ddots & \vdots \\ 0 & 0 & 0 & 0 & 1 \\ 0 & 0 & 0 & 0 & 0 \end{bmatrix} \quad (2.11)$$

$$B = \begin{bmatrix} 0 \\ 0 \\ \vdots \\ 0 \\ 1 \end{bmatrix} \quad (2.12)$$

$$C = [1 \ 0 \ 0 \ \dots \ 0]. \quad (2.13)$$

The observability matrix Ω in the z coordinates is the identity matrix

$$\Omega = \begin{bmatrix} C \\ CA \\ CA^2 \\ \vdots \\ CA^{n-1} \end{bmatrix} = I, \quad (2.14)$$

thus, no other probing signal can make z *more* observable.

The sensitivity of the x coordinates to changes in the z coordinates is an important question in using feedback linearization control system design. The

Jacobian of ϕ provides insight into this sensitivity. Define the Jacobian

$$J = \frac{\partial z}{\partial x} = \frac{\partial \phi(x)}{\partial x}. \quad (2.15)$$

If $\text{cond } J \gg 1$ then transformation $z = \phi(x)$ is likely poorly conditioned in which small changes in x , depending upon the direction, may hardly be visible from the z coordinates and others greatly magnified. Also, $\text{cond } J^{-1} = \text{cond } J$ so that even if the z system is very observable, this observability may not translate well to observability in the x coordinates. It is prudent to assess the condition number of J prior to implementing inverse dynamics.

The same results apply to discrete-time systems.⁸ The linearizing control is the optimal probing input in terms of minimizing the condition number of the observability matrix. Presumably, the caveats regarding sensitivity presented for continuous-time systems also apply for discrete-time systems.

2.4.3 Methods of Parameter Estimation

Since the 1960's Åström [2] *et al* developed much theory for estimating parameters in discrete-time systems. This work is limited to systems which are affine in the unknown parameters, i.e.,

$$y_k = \phi_{1k}\theta_1 + \phi_{2k}\theta_2 + \cdots + \phi_{nk}\theta_n = \phi'_k\theta \quad (2.16)$$

where θ is the vector of unknown parameters and ϕ is the vector of *known* functions which may depend upon other known variables.

Åström places particular emphasis on the identification of transfer functions. His methods require direct measurement of the state variables in the ϕ functions. If the system is transformed to a chain of output delays his techniques are applicable using the measured system output and imposing an n stage delay. His work

⁸The theory regarding linearization of discrete-time nonlinear systems is not as mature as that for continuous-time systems. Recent work by Kotta [30] describes methods for applying feedback linearization to discrete-time nonlinear systems.

is limited to discrete-time systems due to the practical simplicity of obtaining $\{u_k, u_{k+1}, \dots, y_k, y_{k+1}, \dots\}$ in contrast to the practical difficulties of obtaining $\{u, \dot{u}, \ddot{u}, \dots, y, \dot{y}, \ddot{y}, \dots\}$ in continuous-time systems.

Ljung and Söderström [36] devote their entire book to the subject of recursive identification. Their work is much along the lines of Åström with similar applicability and limitations.

Because the parameter estimation problem is a subclass of the general nonlinear state estimation problem, the discrete-time observers developed in this dissertation can be applied to parameter estimation. These new observers are, in fact, generalized estimation methods of which the aforementioned methods of Åström, Ljung and Söderström are a subclass. As such, these new methods are free of many of the limitations of the earlier methods.

2.5 Contribution of Present Work

2.5.1 Summary of Present State-of-the-Art

Much work has been done in applying extended Kalman filters (EKF) to discrete-time problems, continuous-time problems, and mixed continuous-dynamics/discrete-update problems. A strong theoretical foundation does not exist, but the observers often work well when the nonlinearity is “soft” and initial estimates are “close.” The EKF may perform poorly or fail to perform completely when the nonlinearity is “hard” or the initial estimates are not “close enough.” [35, 22]

Gauthier and Ciccarella have developed observers for continuous-time nonlinear systems with relative degrees equal to the state dimension. They have not addressed the design of nonlinear observers for systems with relative degree less than the state dimension. Such systems occur in the parameter estimation problem.

Moraal and Grizzle and Ciccarella *et al* have developed discrete-time nonlinear observers which are applicable to systems with relative degree less than the state

dimension but they did not address the essential issue of observer performance in the presence of measurement noise or process uncertainty.

2.5.2 New Contributions

The original impetus for the present work was this author's consistent failure to make continuous-time simultaneous parameter and state estimation work. The good results obtained from the Ciccarella observer when applied to nonlinear state estimation problem were not obtained when the observer was applied to the parameter estimation problem. The parameter estimation problem when cast into a state estimation problem by augmenting the state vector with the parameters invariably yields a system with a relative degree $r < n$. The continuous-time Ciccarella observer cannot be applied to such systems unless the input excitation is zero. Typically parameters are not observable without persistent excitation and the parameter states of the augmented vector are not observable with zero input. Thus a conflict exists between the relative degree requirement of the continuous-time Ciccarella observer and the persistent excitation requirement of parameter estimation.

This problem is more tractable in the discrete-time formulation. The central contribution of the thesis is the exploration and development of discrete-time observers which solve this problem. Specifically, the primary contributions of this present work are as follows:

1. Improvement of existing discrete-time observers
 - (a) Modification of the Moraal/Grizzle Observer to enhance noise rejection thus enabling the reduction of the Moraal/Grizzle theory to practice.
 - (b) Modification of the Ciccarella Observer to enhance noise rejection by solving a Riccati equation for the gain set and thus enabling the reduction of theory to practice.

2. Development of new discrete-time observers
 - (a) Adaptation of the Friedland parameter estimator to discrete-time systems and demonstration that some previous well-known methods for parameter estimation are a subset of this more general method.⁹
 - (b) Development of the “Grossman Observer,” the discrete-time version of the Gauthier Observer (precursor to the Ciccarella observer) which allows for the relaxation of the relative degree requirement of the continuous-time Gauthier and Ciccarella observers.

Other contributions of this dissertation include:

1. Demonstration that the Ciccarella Observer is not generally appropriate for the continuous-time parameter estimation problem (section 1.3.1).
2. Demonstration that for invertible systems the inverting control is *the* observability optimizing probe signal (section 2.4.2).
3. Elucidation of the relationship between the Ciccarella observer to earlier work of Grossman regarding hybrid-coordinate system observers (section 8.1).
4. Elucidation of the relationship between the Friedland Parameter estimator described on pages 318-324 of [14] and the Friedland nonlinear reduced-order estimator described on pages 183-187 of [14] showing that with a minor modification of the latter, the former is a special case of the latter (section 8.3).

⁹Published in the *AIAA Journal of Guidance, Control, and Dynamics* [24].

5. Extension the Friedland parameter estimator to provide for “parameter dynamics” (section 8.2), i.e. to systems of the form:

$$\dot{x}_1 = f_1(x_1, u) + F_{12}(x_1, u)x_2$$

$$\dot{x}_2 = f_2(x_1, u) + F_{22}(x_1, u)x_2$$

$$y = x_1.$$

CHAPTER 3

OBSERVABILITY

3.1 Introduction and Background

Observability is well defined for discrete-time and continuous-time linear systems and for continuous-time nonlinear systems which satisfy mild “smoothness” requirements. The issue of observability for nonlinear, discrete-time systems is poorly addressed in the control literature with the notable exceptions of one paper by Sontag [47] and one paper by Nijmeijer [43].

Sontag [47] describes several forms of observability for polynomial systems.

1. Single-experiment observability.
2. Single-experiment observability with generic inputs.
3. Observability.
4. Finite observability.
5. Finite observability with generic inputs.
6. Algebraic observability.
7. Final-state determinability.
8. Final-state determinability with generic inputs.

The paper [47] is restricted to polynomial systems so that logically implicative relationships among these various types of observability can be proven. In [47] it is conjectured that the logically implicative relationships hold for non-polynomial systems.

The paper [47] predates (slightly) the explosion of work in the 1980’s in differential geometric system theory. Without this theory as extended to discrete-time

systems, it is difficult to develop a simple definition of observability. It is interesting to note that in [47] Sontag presents a rank test restricted to state-affine systems of the form

$$\begin{aligned}x_{k+1} &= F(u_k)x_k + G(u_k) \\ y_k &= Hx_k\end{aligned}$$

Without the differential geometric system theory it was not simple to eliminate this affine restriction. The rank test described in the sequel is not restricted to state-affine systems and reduces to that presented in [47] for the subclass of state-affine systems.

Nijmeijer [43] simplifies the definition of the observability using a discrete-time approach parallel to the geometric system theory developed for continuous-time systems [25], [32]. As stated in [43] this contribution is significant because this definition of observability is a natural extension of that founded on the differential geometric theory of continuous-time systems.

The definition of observability in [43] is restricted to *autonomous* discrete-time nonlinear systems. The restriction simplifies the development of the work but excludes the application of the definition to non-autonomous systems. This restriction excludes the parameter estimation problem which usually requires persistent input excitation.

The paper [43] describes an observability rank test for autonomous systems. The rank test described in the sequel reduces to that presented in [43] for the subclass of systems with zero-input excitation. Nijmeijer coined the term “strong local observability,” which he defines for autonomous systems.

3.2 Properties of Observability

Observability in the conventional sense is the canonical property of a measured system by virtue of which it is possible to determine unambiguously, the system dynamical state in a finite time from the external measurements, knowledge of the system input, and knowledge of the process dynamics. The notion of observability when extended and applied to nonlinear discrete-time systems should have this same canonical property. Furthermore, this extended notion should reduce to the conventional one when applied to linear discrete-time systems since such systems are a proper subset of the larger class of nonlinear discrete-time systems.

3.3 Algebra for Discrete-time Nonlinear Systems

A causal discrete-time nonlinear SISO system is given by¹

$$x_{k+1} = f(x_k, u_k) \quad (3.1)$$

$$y_k = h(x_k), \quad (3.2)$$

where $x \in \mathcal{R}^n$.

¹For notational simplicity the input-dependence of the output mapping functions is suppressed. Function $h(x_k)$ is understood to be possibly dependent on the present input u_k , i.e., $h(x_k) = h(x_k, u_k) = h_k(x_k)$. Output mapping functions with dependence upon past inputs are not considered. Generality is not lost since such systems can always be recast in terms of a state vector augmented with past input values.

The vector of n successive outputs is given by

$$\begin{aligned}
 \begin{bmatrix} y_k \\ y_{k+1} \\ y_{k+2} \\ \vdots \\ y_{k+n-1} \end{bmatrix} &= \begin{bmatrix} h(x_k) \\ h(x_{k+1}) \\ h(x_{k+2}) \\ \vdots \\ h(x_{k+n-1}) \end{bmatrix} = \begin{bmatrix} h(x_k) \\ h[f(x_k, u_k)] \\ h[f(x_{k+1}, u_{k+1})] \\ \vdots \\ h[f(x_{k+n-2}, u_{k+n-2})] \end{bmatrix} \\
 &= \begin{bmatrix} h(x_k) \\ h[f(x_k, u_k)] \\ h\{f[f(x_k, u_k), u_{k+1}]\} \\ \vdots \\ h[\mathcal{G}_f^{n-1}(x_k, u_k)] \end{bmatrix} \quad (3.3)
 \end{aligned}$$

where the discrete-time analog of the Lie derivative is introduced and defined recursively

$$\mathcal{G}_f^0(x_k, u_k) = x_k \quad (3.4)$$

$$\mathcal{G}_f^n(x_k, u_k) = f\{\mathcal{G}_f^{n-1}(x_k, u_k), u_{k+n-1}\}. \quad (3.5)$$

(Note that the compact notation, $\mathcal{G}_f^n(x_k, u_k)$ hides the dependence of this quantity on $u_k, u_{k+1}, \dots, u_{k+n-1}$)

Allowing for a minor abuse of notation whereby a zero on the u_k argument of the \mathcal{G}_f^n bracket implies $u_k = u_{k+1} = \dots = u_{k+n-1} = 0$ the relative degree is defined. The relative degree of the system described by (3.1), (3.2) is r if for $\{u_k \neq 0\}$

$$\mathcal{G}_f^m(x_k, u_k) = \mathcal{G}_f^m(x_k, 0), \quad m < r - 1 \quad (3.6)$$

$$\mathcal{G}_f^m(x_k, u_k) \neq \mathcal{G}_f^m(x_k, 0), \quad m \geq r. \quad (3.7)$$

3.4 Observability of Nonlinear Discrete-time Systems

Now define a coordinate transformation

$$z_k = \phi(x_k, u_k) \quad (3.8)$$

$$= \begin{bmatrix} h\{x_k\} \\ h\{f(x_k, u_k)\} \\ h\{f[f(x_k, u_k), u_{k+1}]\} \\ \vdots \\ h\{\mathcal{G}_f^{n-1}(x_k, u_k)\} \end{bmatrix}. \quad (3.9)$$

The system (3.1), (3.2) is then transformed to

$$z_{k+1} = Az_k + By_{k+n} \quad (3.10)$$

$$= Az_k + Bh\{\mathcal{G}_f^n(x_k, u_k)\} \quad (3.11)$$

where

$$A = \begin{bmatrix} 0 & 1 & 0 & 0 \\ 0 & 0 & 1 & 0 \\ \vdots & \vdots & \ddots & \vdots \\ 0 & 0 & 0 & 1 \\ 0 & 0 & 0 & 0 \end{bmatrix}, \quad B = \begin{bmatrix} 0 \\ 0 \\ \vdots \\ 0 \\ 1 \end{bmatrix}. \quad (3.12)$$

Observability is defined in terms of being able to reconstruct the system state x from the measured output $\{y_k\}$ and known input $\{u_k\}$. Referring to (3.8), define

$$g(x_k, u_k, z_k) = z_k - \phi(x_k, u_k). \quad (3.13)$$

Definition 3.4.1

The system (3.1), (3.2), is observable for input sequence $\{u_k, u_{k+1}, \dots, u_{k+n-1}\}$ iff there exists a unique x_k^* such that

$$g(x_k^*, u_k, z_k) = 0. \quad (3.14)$$

This definition is consistent with the rank test for linear systems

$$x_{k+1} = Ax_k + Bu_k \quad (3.15)$$

$$y_k = Cx_k. \quad (3.16)$$

For system described by (3.15) and (3.16), $g(x_k, u_k, z_k)$ is given by

$$g(x_k, u_k, z_k) = \begin{bmatrix} y_k \\ y_{k+1} \\ \vdots \\ y_{k+j} \\ \vdots \\ y_{k+n-1} \end{bmatrix} - \begin{bmatrix} C \\ CA \\ \vdots \\ CA^j \\ \vdots \\ CA^{k+n-1} \end{bmatrix} x_k \quad (3.17)$$

$$- \begin{bmatrix} 0 \\ CBu_k \\ \vdots \\ C \sum_{m=0}^{j-1} A^m B u_{k+j-m-1} \\ \vdots \\ C \sum_{m=0}^{k+n-2} A^m B u_{2k+n-m-2} \end{bmatrix} \quad (3.18)$$

$$= z_k - \Omega_1 x_k - \Omega_2.$$

State x_k is recovered by setting

$$g(x_k, u_k, z_k) = z_k - \Omega_1 x_k - \Omega_2 = 0. \quad (3.19)$$

Then

$$x_k = \Omega_1^{-1}(z_k - \Omega_2). \quad (3.20)$$

Solution state x_k is unique iff Ω_1 is not singular (full rank).

3.5 Rank test for “Strong” Observability of Nonlinear Discrete-time Systems

Observability as defined here implies that transformation $z_k = \phi(x_k, u_k)$ is uniquely invertible, i.e, if for

$$z_a = \phi(x_a, u) \quad (3.21)$$

$$z_b = \phi(x_b, u) \quad (3.22)$$

then

$$z_a = z_b \Leftrightarrow x_a = x_b. \quad (3.23)$$

The observability rank test provides the *sufficient* condition for the existence of inverse function $x_k = \phi^{-1}(z_k, u_k)$.

Definition 3.5.1

Let J represent the Jacobian of $g(x, u, z)$, (3.13), for input sequence $\{u_k, u_{k+1}, \dots, u_{k+n-1}\}$

i.e.,

$$J = \frac{\partial g(x, u, z)}{\partial x} \quad (3.24)$$

a nonlinear discrete-time system is strongly observable for this input sequence iff

$$\text{rank } J = n. \quad (3.25)$$

The implicit function theorem is the basis for this rank test. A rigorous proof of the theorem can be found in most books on analysis [45]. The basis of the implicit function theorem and this rank test is that for a small region about some point defined by x and z where $\zeta(x, z) = 0$, the Taylor expansion allows the nonlinear function ζ to be approximated by a tangent plane, i.e.,

$$\zeta(x, y) = 0 \quad (3.26)$$

$$\zeta(x + dx, y + dy) = 0. \quad (3.27)$$

The Taylor expansion of ζ is given,

$$\zeta(x + dx, y + dy) \approx \underbrace{\zeta(x, y)}_{=0} + \frac{\partial \zeta}{\partial x} dx + \frac{\partial \zeta}{\partial z} dz + \text{higher-order terms} \quad (3.28)$$

$$\approx \frac{\partial \zeta}{\partial x} dx + \frac{\partial \zeta}{\partial z} dz. \quad (3.29)$$

Constraining $\zeta(x + dx, y + dy) = 0$, (3.29) yields a *unique* expression for dx in terms of dz

$$dx = - \left[\frac{\partial \zeta}{\partial x} \right]^{-1} \frac{\partial \zeta}{\partial z} dz, \quad (3.30)$$

provided that $\partial \zeta / \partial x$ is invertible (full rank) and $\partial \zeta / \partial z \neq 0$.

In the observability problem under consideration $\zeta(x, z) = g(x, u, z)$, so

$$\frac{\partial g}{\partial z} = I \quad (3.31)$$

regardless of the values for u . Therefore, if the inverse of Jacobian $\partial g / \partial x$ exists for the sequence u then a local inverse exists and x is uniquely determined.

The rank test provides a *sufficient* condition for observability as defined in section 3.4 and we *define* “strong” observability in terms of the rank test. The rank test does not provide the necessary condition for observability as defined in section 3.4, i.e., a system can be observable in the sense of section 3.4 and fail the rank test for “strong” observability as the following example illustrates.

Example

For the single-state system

$$x_{k+1} = x_k \quad (3.32)$$

$$y_k = x_k^3, \quad (3.33)$$

$\phi(x, u) = x_k^3$ and $g(x_k, u_k, z_k)$ is given

$$g(x_k, u_k, z_k) = g(x_k, y_k) = y_k - x_k^3. \quad (3.34)$$

The Jacobian

$$J = \frac{\partial g}{\partial x} = -3x_k^2 \quad (3.35)$$

which is zero for $x_k = 0$. This system fails the rank test so it is *not* strongly observable as determined by the rank test. It is observable as defined in section 3.4 since the inverse function ϕ^{-1} exists

$$x_k = \phi^{-1}(y_k, u_k) = \sqrt[3]{y_k} \quad (3.36)$$

and x_k can always be reconstructed uniquely from output y_k .

3.6 Degree of Strong Observability

The condition number of the Jacobian J , from (3.24), provides a continuous measure of strong observability and the sensitivity of the reconstructed states to uncertainty (noise) in the measured system outputs.

Strong observability is a necessary condition for the synthesis and numerical stability of nonlinear discrete-time observers to be presented in chapters 4 and 5. Synthesis of observers for nonlinear discrete-time systems which are observable but not strongly observable is difficult since the state reconstruction at the singularity point of the Jacobian is *infinitely sensitive* to small changes in the measured system output.

The structure of Jacobian J , revealed by the singular value decomposition, provides much information about observability. While $\text{cond } J = \infty$ and the system is not strongly observable, some states may be very observable while others not. These issues shall be explored further in chapter 7.

CHAPTER 4

MODIFICATIONS OF OBSERVERS FOR NONLINEAR DISCRETE-TIME SYSTEMS

4.1 The Moraal/Grizzle Discrete-Time Nonlinear Observer

4.1.1 Original Form

The essence of the algorithm by Moraal and Grizzle is contained in their equations (24), (27), (28) on page 398 of [42]. Consider the discrete-time nonlinear system

$$x_{k+1} = f(x_k, u_k) \quad (4.1)$$

$$y_k = h(x_k, u_k). \quad (4.2)$$

Define input and output data “windows,” U_k and Y_k ,

$$U_k = \begin{bmatrix} u_{k-n+1} \\ \vdots \\ u_k \end{bmatrix} \quad Y_k = \begin{bmatrix} y_{k-n+1} \\ \vdots \\ y_k \end{bmatrix}. \quad (4.3)$$

A window of n estimated successive system outputs starting with the $k-n+1$ output is generated from the retarded state x_{k-n+1} using multiple compositions of the system forward dynamics (4.1) and the system output map (4.2)

$$\tilde{Y} = H(x_{k-n+1}, U_k) = \begin{bmatrix} h[x_{k-n+1}, u_{k-n+1}] \\ h[f(x_{k-n+1}, u_{k-n+1}), u_{k-n+2}] \\ \vdots \\ h[f \circ f \cdots f(f(x_{k-n+1}, u_{k-n+1}), u_{k-n+2}) \cdots u_{k-1}], u_k \end{bmatrix}. \quad (4.4)$$

The nonlinear function $g(x_{k-n+1}, U_k, Y_k)$ is synthesized

$$\bar{g}(Y_k, \tilde{Y}_k) = \bar{g}[Y_k, H(x_{k-n+1}, U_k)] \quad (4.5)$$

$$= Y_k - H(x_{k-n+1}, U_k) \quad (4.6)$$

$$= g(x_{k-n+1}, U_k, Y_k). \quad (4.7)$$

If the system is observable as defined in chapter 3 then in the noise-free situation there exists a single root x_{k-n+1}^* of g , which is the reconstructed retarded state for input/output windows U_k, Y_k . The current value of the state can be recovered by forward-propagating the retarded state $n - 1$ times using multiple compositions of (4.1).

In the Moraal/Grizzle observer the root of g is found using the multi-dimensional Newton's method. A single Newton iteration is parametrically dependent upon U_k, Y_k and is a function of "seed" estimate of the retarded state $z_k = x_{k-n+1}$. The single step Newton iteration is described by equation (24) of [42] and is rewritten below:

$$\Theta^{Y_k, U_k}(\zeta) = \zeta + \left[\frac{\partial \tilde{Y}}{\partial x} \right]^{-1} [Y_k - \tilde{Y}(\zeta, U_k)] \quad (4.8)$$

$$\hat{z}_k = \Theta^{Y_k, U_k}(\tilde{z}_k). \quad (4.9)$$

Multiple Newton iterations, written $(\Theta^{Y_k, U_k})^{(d)}(\zeta)$ are achieved by composing (4.8) with itself d times.¹ These Newton iterations yield the recursive relationship

$$\hat{z}_k = (\Theta^{Y_k, U_k})^{(d)}(\tilde{z}_k) \quad (4.10)$$

By defining z_k to be an n -delay retarded estimate of x_k , i.e., in the absence of estimation errors $z_k = x_{k-n}$, the Moraal/Grizzle observer (equations (27), (28) of [42]) is summarized

$$\tilde{z}_{k+1} = f(\hat{z}_k, u_{k-n}) \quad (4.11)$$

$$\hat{z}_{k+1} = (\Theta^{Y_k, U_k})^{(d)}(\tilde{z}_{k+1}) \quad (4.12)$$

$$\hat{x}_{k+1} = \underbrace{f \circ f \cdots f}_{n\text{-stage forward propagation}}(f(\hat{z}_{k+1}, u_{k-n+1}, u_{k-n+2}) \cdots u_k) \quad (4.13)$$

¹The term "iteration" requires clarification. A single iteration, by strict interpretation, means a composition of (4.8) with itself one time. Here and throughout the dissertation, unless otherwise indicated, the term iteration refers to number of times (stages) a recursive calculation is performed and not how many times it is composed upon itself. Thus $d = 1$ means a single execution of (4.8).

In summary, the Moraal/Grizzle observer is composed of a Newton root finder which seeks the solution x^* to the equation $Y_k = H(x_{k-n+1}, U_k)$ and an extrapolator to bring the retarded estimate forward to the current time.

The block diagram of a single stage of the Moraal/Grizzle observer is shown in figures 4.1. This block accepts the input/output windows, U_k, Y_k , which act like function parameters. In addition, the observer accepts a solution “seed”, \tilde{z}_k , and outputs a refined estimate of the retarded state, \hat{z}_k . The single Newton step represents the algebraic operation $\hat{z}_k = \Theta^{Y_k, U_k}(\tilde{z}_k)$, which occurs in zero sample time.

The Newton solver can be iterated. This iteration is achieved by concatenating single stage solvers, using the output of each prior stage as the seed for the next stage. Again, these operations occur in zero sample time. This multiple iteration is shown schematically in figure 4.2.

Figure 4.3 represents the combination of the Newton solver and state extrapolator which combine to form the Moraal/Grizzle observer.

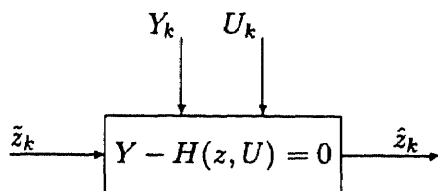


Figure 4.1 Newton root finder – Input/Output form. The n -vectors U_k, Y_k of system inputs and outputs are “parameters” of the root equation.

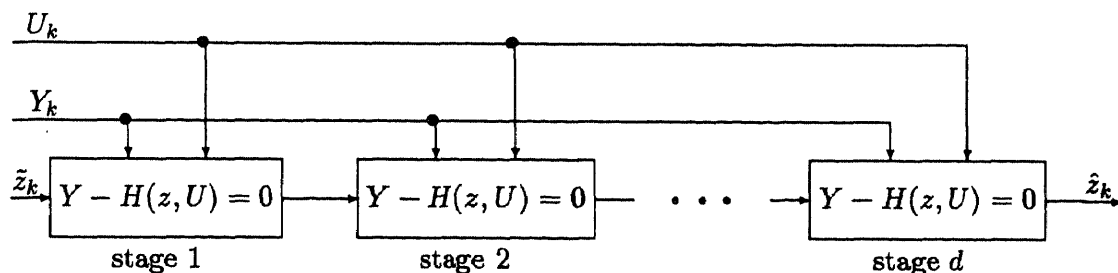


Figure 4.2 d -stage Newton solver.

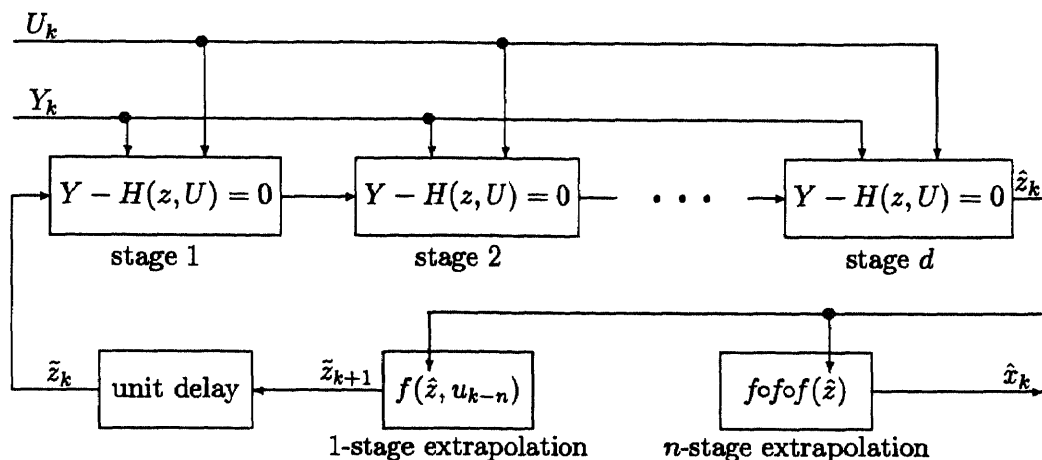


Figure 4.3 Moraal/Grizzle d -stage Newton observer.

4.1.2 Noise “Bandwidth” Properties of the Moraal/Grizzle Observer²

The filtering properties of the Newton iteration can be understood analytically from a static scalar example. Implementing a “slowing factor” α , the basic Newton iteration for solving equation $y - f(x) = 0$ is

$$\hat{x}_{k+1} = \hat{x}_k + \frac{\alpha}{f'(\hat{x}_k)} [y - f(\hat{x}_k)]. \quad (4.14)$$

If y is measurement then its true value is not known. Its measured value is its true value corrupted by noise, i.e., $\bar{y}_k = y + \eta_k$. The Newton iteration becomes

$$\hat{x}_{k+1} = \hat{x}_k + \frac{\alpha}{f'(\hat{x}_k)} [\bar{y}_k - f(\hat{x}_k)] \quad (4.15)$$

$$= \hat{x}_k + \frac{\alpha}{f'(\hat{x}_k)} [y + \eta_k - f(\hat{x}_k)] \quad (4.16)$$

$$= \hat{x}_k + \frac{\alpha}{f'(\hat{x}_k)} [y - f(\hat{x}_k)] + \frac{\alpha}{f'(\hat{x}_k)} \eta_k \quad (4.17)$$

Defining $\epsilon_k = \hat{x}_k - x_k$, the first order expansion of $f(\hat{x})$ yields

$$f(\hat{x}) \approx f(x) + f'(x)\epsilon_k \quad (4.18)$$

$$\approx y + f'(x)\epsilon_k \quad (4.19)$$

²The term “bandwidth” is enclosed in quotes to signify a rather loose definition. In this context “high bandwidth” implies the admission of a comparatively large amount of measurement noise energy into the state estimates. Likewise, “lower bandwidth” implies admission of a comparatively small amount of measurement noise energy into the state estimates.

Substituting (4.19) into (4.17) leads to a first-order approximation of the error dynamics of the noisy Newton iteration

$$\epsilon_{k+1} = x_{k+1} - x \quad (4.20)$$

$$= \epsilon_k + \frac{\alpha}{f'(\hat{x}_k)} [y - f(\hat{x}_k)] + \frac{\alpha}{f'(\hat{x}_k)} \eta_k \quad (4.21)$$

$$= \epsilon_k + \frac{\alpha}{f'(\hat{x}_k)} [y - y - f'(x)\epsilon_k] + \frac{\alpha}{f'(\hat{x}_k)} \eta_k \quad (4.22)$$

$$= (1 - \alpha)\epsilon_k + \frac{\alpha}{f'(\hat{x}_k)} \eta_k \quad (4.23)$$

The first term of (4.23) represents the free response of the first-order approximation of the error dynamics. The second term represents the noise driving term. Factor $\alpha/f'(\hat{x}_k)$ represents a state-dependent noise gain. In the Moraal/Grizzle paper $\alpha = 1$ and Newton iteration is a low-pass filter with deadbeat error dynamics that converge to zero in at most n steps. Simultaneously, the input/output gain on the measurement noise η is $1/f'(\hat{x}_k)$ which can be very large *depending upon coordinate system scaling*. If \bar{y} is noisy, this high gain can severely degrade system performance.

Example

The Newton observer is applied to the static scalar root search problem $y - x^3 = 0$. The observer searched for solution of $\bar{y}_k - x^3 = 0$ where $\bar{y}_k = y + \eta_k$ is a measured quantity y_k subject to noise η_k . Variable $y = 0$ and standard deviation $\sigma_\eta = 1.0 \times 10^{-4}$. Two thousand measurements were processed by the observer.

Figure 4.4 shows the first 200 samples of the observer and illustrates the effect of varying slowing factor α on the observer convergence rate (transient response).

Figure 4.5 shows the last 1000 samples of the observer and illustrates the effect of varying slowing factor α on the observer steady-state noise level.

Table 4.1 summarizes the effect of the slowing factor upon transient response and steady-state noise level. Decreasing the α from 1 towards 0 yields a longer transient response with improving noise rejection.

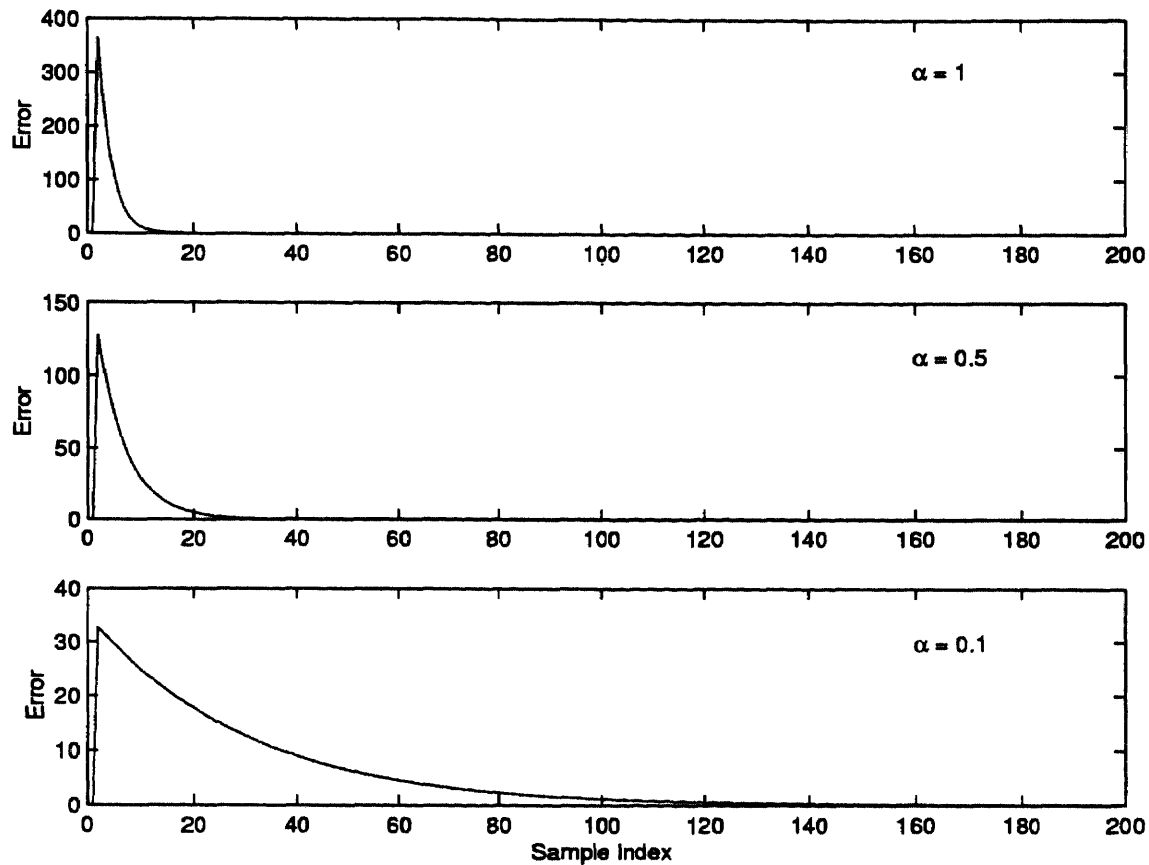


Figure 4.4 Transient response of Moraal/Grizzle Newton observer applied to scalar example illustrating the effect of different “slowing factors” α .

4.1.3 Modified Form

Modification of the number of iterations in the Newton root-finder is the only design feature of the Moraal/Grizzle observer. It can be demonstrated that increasing the number of iterations has a minimal effect upon observer performance and the effect is not always a desirable one. Experience with iterated extended Kalman filters has shown that a single Newton iteration improves the estimate of the “observation partials”, $\partial h/\partial x$, often leading to improved transient performance. Experience has also shown that *multiple iterations increase the “bandwidth” of the Newton iteration with deleterious effects to the system when noise is present.*

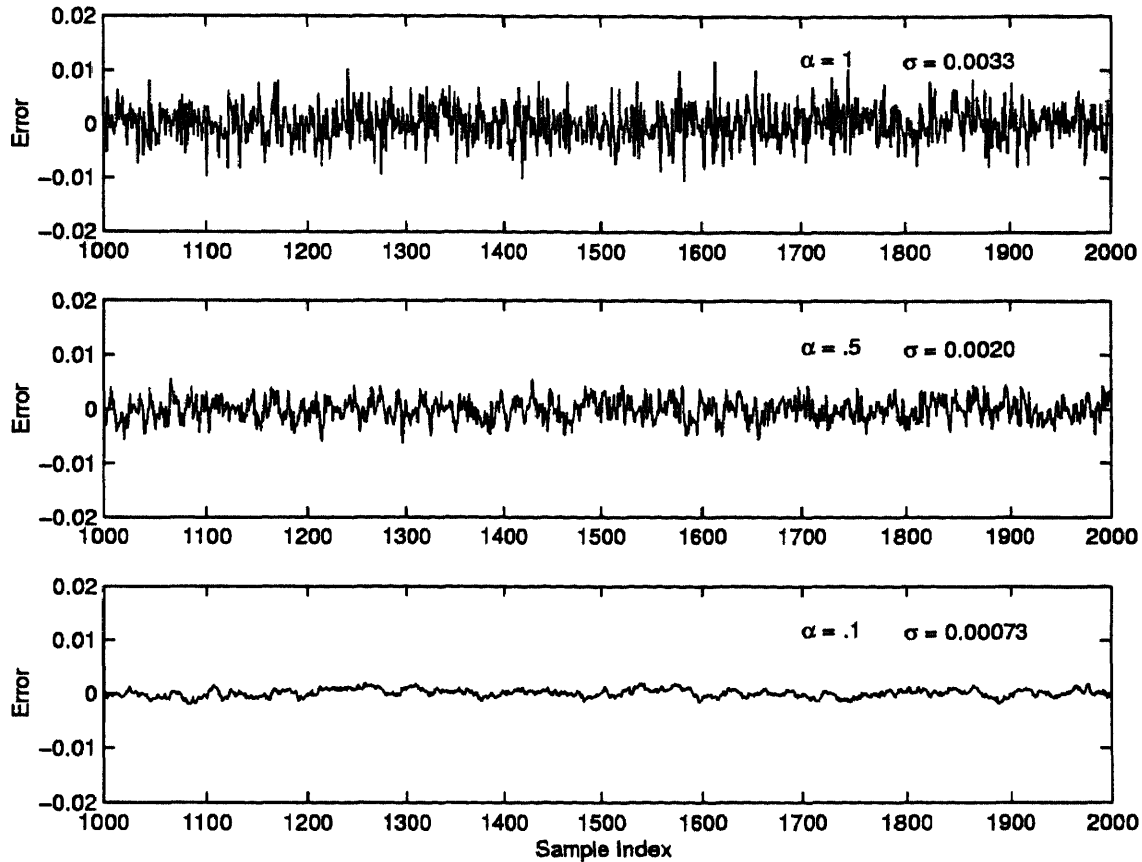


Figure 4.5 Steady state response of Moraal/Grizzle Newton observer applied to scalar example illustrating the effect of different “slowing factors” α on noise level.

The state update and error dynamics for the single Newton step, (4.14), (4.23), explain the poor noise performance of the Moraal/Grizzle observer and show the method to improve this performance. Referring to the linear error dynamics, (4.23), by setting $\alpha = 1$, the fastest possible observer is achieved (in the linear approximation) but one with poor measurement noise rejection properties. By reducing α such that $0 < \alpha < 1$ the observer is “slowed.” This slowing provides mitigation of the deleterious effects of measurement noise.

If $0 < \alpha < 1$, the error dynamics are still low-pass but lower bandwidth when compared to $\alpha = 1$. This reduced bandwidth is helpful in reducing the deleterious effects of system noise for the Moraal/Grizzle observer and for iterated extended

Table 4.1 Effect of “slowing-factor” α on Moraal/Grizzle observer transient response and noise rejection for scalar example.

α	Response Time ^a (samples)	Steady-State Noise (σ)	Noise Gain Factor
1.0	8	3.3×10^{-3}	33
0.5	15	2.0×10^{-3}	20
0.1	70	7.3×10^{-4}	7.3

^aResponse time defined as the sample number at which the estimate falls 90% from its peak value.

Kalman Filter. In addition, it reduces the input/output gain on the measurement to $\alpha/f'(\hat{x})$ which is desirable when the measurements are noisy.

It is noteworthy that Moraal and Grizzle missed this important feature since it is only major design feature of their observer. The number of iterations is the only other feature of their observer over which the designer has control.

The slowing also manifests itself as a longer time for the transient response to settle. In the presence of dynamic model mismatch the slower filter demonstrates poorer tracking performance when compared to the filter with $\alpha = 1$. Thus, as in the case of linear filters, the gain selection represents a trade-off between mitigating the effects of measurement noise and mitigating the effects of process uncertainty.

4.2 The Ciccarella Discrete-time Nonlinear Observer

4.2.1 Original Form

Ciccarella *et al* present two discrete-time forms of the nonlinear continuous-time observer presented in [5]. The first form, described in [6], is a discrete-time version of their continuous-time observer developed using a discrete-time version of the Lie derivative operators. The development follows the continuous-time development, i.e.,

1. Transform system into Brunowski normal form (chain of delays) using transformation $w = \phi(x)$. The transformed system is

$$\begin{aligned} w_{k+1} &= Aw_k + By_{k+n} \\ y_k &= Cw_k \end{aligned}$$

where

$$\begin{aligned} A &= \begin{bmatrix} 0 & 1 & 0 & 0 \\ 0 & 0 & 1 & 0 \\ \vdots & \vdots & \ddots & \vdots \\ 0 & 0 & 0 & 1 \\ 0 & 0 & 0 & 0 \end{bmatrix}, \quad B = \begin{bmatrix} 0 \\ 0 \\ \vdots \\ 0 \\ 1 \end{bmatrix} \\ C &= \begin{bmatrix} 1 & 0 & \dots & 0 \end{bmatrix} \end{aligned}$$

2. Develop a linear observer with stable gains in the transformed coordinate system.

$$\hat{w}_{k+1} = A\hat{w}_k + B(y_{k+n} - \hat{y}_{k+n}) + K(y_k - C\hat{w}_k)$$

3. Transform system back to the original coordinates. Transform the linear gains using the inverse of Jacobian $J = \partial\phi(x)/\partial x$.

The second form of the discrete-time observer [7] uses an n -dimension measurement vector synthesized from n successive measurements. This observer is essentially a full-state feedback observer where the full state measurement is “faked” by imposing a delay to collect the n -measurements and then propagating forward the estimate. Ciccarella claims global convergence for the continuous-time observer provided certain system properties were satisfied. In contrast, he claims only local convergence for the discrete-time observer. Despite the lack of global convergence, Ciccarella claims his observer to be advantageous in comparison with

the Moraal/Grizzle observer in that no nonlinear equations need be inverted. The Moraal/Grizzle observer is globally convergent if certain criteria are met but requires the solution of a set of nonlinear equations.³ Ciccarella further claims this “fake full-state feedback” form of his observer is more robust than his single measurement form. Ciccarella does not quantify robustness *per se*, but he demonstrated a parameter estimation example in which his second observer performed well in contrast to his first observer which performed poorly.

The structure of both forms of the Ciccarella observer is similar. Suppressing the control inputs for clarity, the observer equations for the first Ciccarella observer are written

$$\hat{z}_{k+1} = f(\hat{z}_k) \quad (4.24)$$

$$J = \left. \frac{\partial \phi(x)}{\partial x} \right|_{x=\hat{z}_{k+1}} \quad (4.25)$$

$$\hat{y}_{k-n-1} = h(\hat{z}_k) \quad (4.26)$$

$$\hat{y}_{k-n+2} = h(f(\hat{z}_k)) \quad (4.27)$$

$$\vdots \quad \vdots \quad (4.28)$$

$$\hat{y}_{k+1} = h(\underbrace{f(\cdots f(f(\hat{z}_k)) \cdots)}_{n\text{-stage forward propagation}}) \quad (4.29)$$

$$\hat{z}_{k+1} = \hat{z}_{k+1} + J^{-1}\{B[y_{k+1} - \hat{y}_{k+1}] + K[y_{k-n+1} - \hat{y}_{k-n+1}]\} \quad (4.30)$$

³The importance of global convergence in comparison with local convergence should not be overemphasized given the nature of most global convergence proofs. Typically some Lipschitz criteria bounding linearly the norm of the error in some function of state to the norm of the error in state is required in the proof. Satisfaction of these criteria for the given nonlinear system is difficult if not impossible to ascertain theoretically. It is possible to estimate this Lipschitz ratio constant and it is found that for convergent observers the Lipschitz condition is satisfied and for divergent observers it is not. It is also found that the divergent observers can be made to converge with closer initial estimates, and in those circumstances, the Lipschitz condition is satisfied. Thus the practitioner is left with the unconstructive result that the observer is globally convergent if the initial estimate is sufficiently *close enough* to the true state. Moraal and Grizzle [42] provide precise expression for this convergence radius and that is one of their significant contributions.

where B , $\phi(x)$ are given

$$B = \begin{bmatrix} 0 & 0 & \dots & 0 & 1 \end{bmatrix}' \quad (4.31)$$

$$\phi(x) = \begin{bmatrix} h[x_{k-n+1}] \\ h[f(x_{k-n+1})] \\ \vdots \\ h[\underbrace{f(f(\dots f(x_{k-n+1}) \dots))}_{n-1\text{-stage forward extrapolation}}] \end{bmatrix}. \quad (4.32)$$

The equations for the second form of the Ciccarella observer are the same as those of the first except the measurement is the n dimensional "fake" full-state feedback. Instead of the measurement represented y_k , the system is updated with vector Y_k , where

$$Y_k = \begin{bmatrix} y_{k-n+1} \\ \vdots \\ y_{k-1} \\ y_k \end{bmatrix}. \quad (4.33)$$

The resulting observer equations are:

$$\tilde{z}_{k+1} = f(\hat{z}_k) \quad (4.34)$$

$$J = \left. \frac{\partial \phi(x)}{\partial x} \right|_{x=\tilde{z}_{k+1}} \quad (4.35)$$

$$\hat{y}_{k-n+1} = h[\hat{z}_k] \quad (4.36)$$

$$\hat{y}_{k-n+2} = h[f(\hat{z}_k)] \quad (4.37)$$

$$\vdots \quad \vdots \quad (4.38)$$

$$\hat{y}_k = h[\underbrace{f(f(\cdots f(\hat{z}_k)\cdots))}_{n-1\text{-stage forward extrapolation}}] \quad (4.39)$$

$$\hat{Y}_k = \begin{bmatrix} \hat{y}_{k-n+1} \\ \hat{y}_{k-n+2} \\ \vdots \\ \hat{y}_k \end{bmatrix} \quad (4.40)$$

$$\hat{y}_{k+1} = h[\underbrace{f(f(\cdots f(\hat{z}_k)\cdots))}_{n\text{-stage forward extrapolation}}] \quad (4.41)$$

$$\hat{z}_{k+1} = \tilde{z}_{k+1} + J^{-1}\{B[y_{k+1} - \hat{y}_{k+1}] + K[Y_k - \hat{Y}_k]\} \quad (4.42)$$

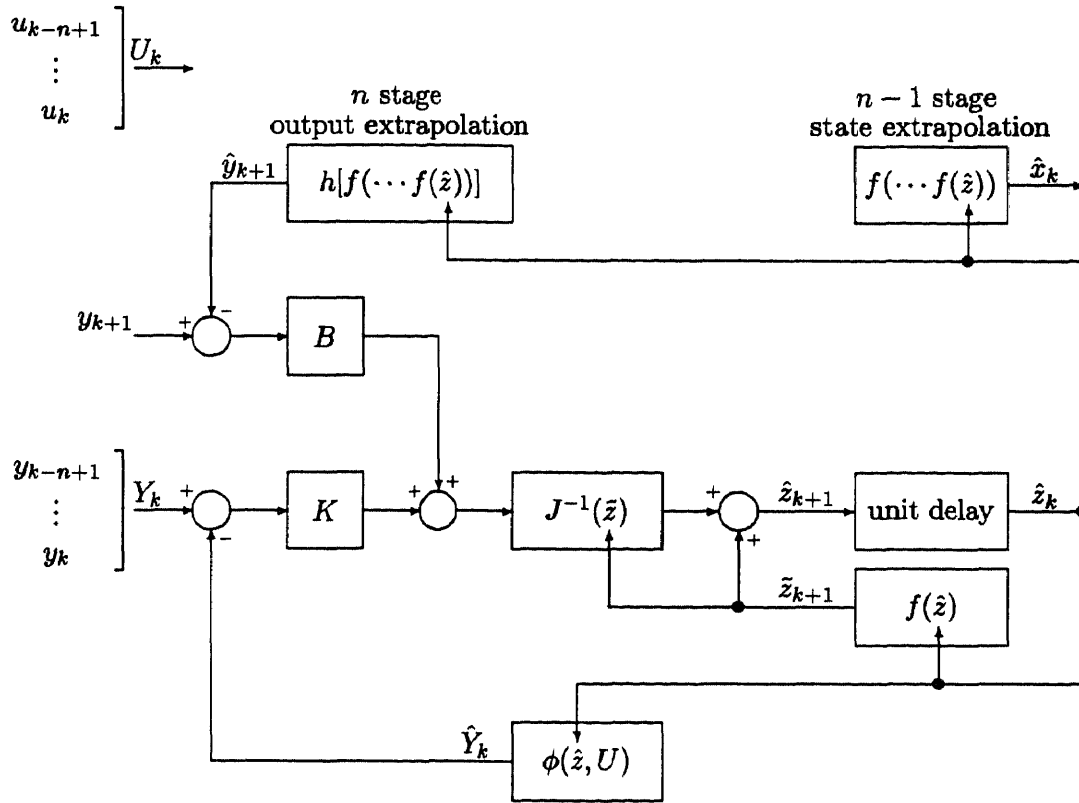
where B , $\phi(x)$ are given by (4.31) and (4.32), respectively.

The block diagram of the second form of the Ciccarella observer is shown in figure 4.6.

In both forms of his observer Ciccarella considers output mapping functions which are functions only of state and not input, i.e., $y = h(x)$ is considered but $y = h(x, u)$ is not. This simplification does not limit generality since the latter mapping function can be written in terms of the former by augmenting the state vector with $h(x, u)$.

4.2.2 Noise "Bandwidth" Properties of the Ciccarella Observer

The Ciccarella observer is driven "from both ends," i.e., from measurement y_{k-n+1} and measurement y_{k+1} . In this manner the observer thus differs from the Luenberger



$$B = \begin{bmatrix} 0 \\ \vdots \\ 0 \\ 1 \end{bmatrix}, \quad \phi(z, U) = \begin{bmatrix} h[z, U_1] \\ h[f(z, U_1), U_2] \\ \vdots \\ h[\underbrace{f(\dots f(f(z, U_1), U_2) \dots, U_{n-1}), U_n}]_{n-1\text{-stage extrapolation}} \end{bmatrix}, \quad J(z, U) = \frac{\partial \phi(z, U)}{\partial z}$$

Figure 4.6 Block diagram of second “robust” form of the Ciccarella observer.

observer structure by virtue of the y_{k+1} “feedforward” term. The Ciccarella observer measurement update is written:

$$\hat{z}_{k+1} = \tilde{z} + J^{-1}(\tilde{z}) \left\{ \underbrace{B[y_{k+1} - \hat{y}_{k+1}]}_{\text{Feedforward}} + \underbrace{K[y_{k-n+1} - \hat{y}_{k-n+1}]}_{\text{Innovation}} \right\} \quad (4.43)$$

This departure from the Luenberger structure significantly affects the observer by limiting performance when measurement noise is present. Whereas the eigenvalues of $A - KC$ can be set to much less than unity, the gain on y_{k+1} is fixed at unity. This unity gain provides a direct pass-through for the measurement noise.

In neither of the two observer forms does Ciccarella specify how gains are to be chosen other than to state that the eigenvalues of $A - KC$ must be within the unit circle. In the second form of the observer (“fake” full-state feedback) Ciccarella describes a gain structure

$$K = \begin{bmatrix} K_{11} & K_{12} & 0 & \cdots & 0 \\ 0 & K_{22} & K_{23} & \cdots & 0 \\ \vdots & \vdots & \ddots & \cdots & \vdots \\ 0 & 0 & 0 & K_{n-1,n-1} & K_{n-1,n} \\ 0 & 0 & 0 & 0 & K_{n,n} \end{bmatrix}.$$

Ciccarella uses this structure for the convenience to simply place all the closed-loop eigenvalues of $A - K$ (observation matrix C is the identity matrix on the second form of the observer). The eigenvalues of $A - K$ are the diagonal elements of K_{ii} and are unaffected by elements $K_{i,i+1}$. Elements $K_{i,i+1}$ are weights chosen to control the weighting of measurement $i + 1$ on element i of the state vector estimate. This form of gain weighting provides some control of the filter “memory” and therefore some control of the noise level and transient response of the state estimates. *This approach does not provide a quantitative method to select gains which balances the state estimate noise level and state estimate transient response for some given metric of the measurement noise and process uncertainty.*

4.2.3 Modified Form

In the absence of measurement and process noise, the second version of the Ciccarella observer works over a large variation of gain matrix K .

When noise is present, however, the Ciccarella observer performance is strongly dependent upon the chosen gain matrix. As in the linear observer the gains should represent some *engineering compromise* between the certainty of the process model and the quality of the sensor measurement.

In the presence of measurement noise and process uncertainty the performance of the Ciccarella observer can be improved by

1. Solving for the gain by propagating the Riccati equation in the transformed coordinates.
2. Eliminating the feedforward of $B(y_{k+1} - \hat{y}_{k+1})$.

The Riccati gain equation is developed as follows. The noise-free, untransformed system dynamics are given (suppressing control u for clarity)

$$x_{k+1} = f(x_k) \quad (4.44)$$

$$y_k = h(x_k). \quad (4.45)$$

The system, subject to Gaussian noise with known statistics, is written

$$x_{k+1} = f(x_k) + \nu \quad (4.46)$$

$$y_k = h(x_k) + \omega \quad (4.47)$$

with

$$E[\nu] = 0, \quad E[\nu\nu'] = V \quad (4.48)$$

$$E[\omega] = 0, \quad E[\omega\omega'] = W \quad (4.49)$$

Applying transformation $w = \phi(x)$ the transformed system is written

$$w_{k+1} = Aw_k + By_{k+n} + B\eta \quad (4.50)$$

$$y_k = Cw_k + \xi \quad (4.51)$$

In this transformed system the process noise enters the system *only through the single n th state variable*. The first order process noise covariance can be modeled as

$$Q = E[BB'\eta^2] = E[\eta^2] \begin{bmatrix} 0 & 0 & 0 \\ 0 & 0 & 0 \\ 0 & 0 & 1 \end{bmatrix} \quad (4.52)$$

$$W = E[\xi^2] \quad (4.53)$$

(For a first order approximation of the nonlinear transformation of the process noise, $B\eta = J^{-1}\nu$. This relationship implies that noise vector ν is orthogonal to every row of J^{-1} except for the last.)

Now a Kalman filter is defined by the matrices of the transformed system A, C, Q, W and some initial state covariance P . In practice the initial state covariance can be some large diagonal matrix if no state knowledge is available. If state knowledge is available P can be approximated

$$P_w(0) = J^{-1}P_x(0)J^{-T}. \quad (4.54)$$

The gains are thus calculated at every cycle and the state covariance is updated

$$C = I \quad (4.55)$$

$$\tilde{P} = A\hat{P}A' + Q \quad (4.56)$$

$$K = \tilde{P}(\tilde{P} + W)^{-1} \quad (4.57)$$

$$\hat{P} = (I - K)\tilde{P}. \quad (4.58)$$

4.3 Coordinate Transformation, Noise, and Observability

The Moraal/Grizzle observer and the Ciccarella observers belong to a class of observers synthesized by coordinate transformation. It was shown by this author [22] that proper coordinate system transformation is crucial to assuring satisfactory performance of the nonlinear observer operating with measurement noise. The consequence of the work in [22] is that a noise-free nonlinear observer may demonstrate excellent performance but if the observer uses an implicit or explicit coordinate transformation, like the Moraal/Grizzle and Ciccarella observers, the noise distribution may become pathological.⁴ In these situations even small levels of noise can degrade observer performance.

⁴It is important to note that in the absence of noise the nonlinear observer requires only n measurements and, with knowledge of the control, the state is estimated once and forever.

The issue of noise is especially important for systems with marginal observability. The Jacobian matrix J ,

$$J = \frac{\partial Y(x)}{\partial x} \quad (4.59)$$

where

$$Y(x) = \begin{bmatrix} y_{k-n+1} \\ y_{k-n+2} \\ \vdots \\ y_k \end{bmatrix} = \begin{bmatrix} h[x, u_{k-n+1}] \\ h[f(x, u_{k-n+1}), u_{k-n+2}] \\ \vdots \\ h[f \circ f \cdots f(f(x, u_{k-n+1}), u_{k-n+2}) \cdots u_{k-1}), u_k] \end{bmatrix} \quad (4.60)$$

is the observability matrix. For poorly observable systems the Jacobian matrix is poorly conditioned and the state x may not be determined by the measurements with great certainty. The inverse Jacobian, J^{-1} will amplify the noise greatly in certain directions such that the noise will limit the performance and applicability of the observer.

4.4 Extension of the Friedland Parameter Estimator to Discrete-Time Systems with Special Structure

Friedland developed a continuous-time parameter estimator for systems in which the entire state was accessible for measurement and the state dynamics were affine in the unknown parameters [14]. In section 8.2 the continuous-time results of [14] are extended to a broader class of general state estimation problems. With some modifications, the continuous-time results of section 8.2 can be adapted to the problem of discrete-time nonlinear state estimation for systems with a special structure.

4.4.1 Observer Derivation

Define a discrete-time dynamic system:

$$x_{1k+1} = f_1(x_{1k}, u_k) + F_{12}(x_{1k}, u_k)x_{2k} \quad (4.61)$$

$$x_{2k+1} = f_2(x_{1k}, u_k) + F_{22}(x_{1k}, u_k)x_{2k} \quad (4.62)$$

$$y_k = x_{1k} \quad (4.63)$$

where x_1 is the directly measured state and x_2 is not measured.

The following reduced-order observer is proposed

$$\hat{x}_{1k} = y_k \quad (4.64)$$

$$\hat{x}_{2k} = \hat{x}_{2k-1} + K(y_{k-1})y_k + z_k \quad (4.65)$$

$$z_{k+1} = \phi_1(y_k, u_k) + \Phi_2(y_k, u_k)\hat{x}_{2k} \quad (4.66)$$

where $K(y_k)$ is a nonlinear gain matrix dependent upon measurement y_k .

The error dynamics are derived

$$e_k = \hat{x}_{2k} - x_{2k} \quad (4.67)$$

$$e_{k+1} = \hat{x}_{2k+1} - x_{2k+1} \quad (4.68)$$

$$= \hat{x}_{2k} + K(y_k)y_{k+1} + z_{k+1} - [f_2 + F_{22}x_{2k}] \quad (4.69)$$

$$= [e_k + x_{2k}] + K(y_k)y_{k+1} + z_{k+1} - [f_2 - F_{22}x_{2k}] \quad (4.70)$$

$$= [e_k + x_{2k}] + K(y_k)[f_1 + F_{12}x_{2k}] + z_{k+1} - [f_2 + F_{22}x_{2k}] \quad (4.71)$$

$$= [e_k + x_{2k}] + K(y_k)[f_1 + F_{12}x_{2k}] + \phi_1 + \Phi_2\hat{x}_{2k} - [f_2 + F_{22}x_{2k}] \quad (4.72)$$

$$= [e_k + x_{2k}] + K(y_k)[f_1 + F_{12}x_{2k}] + \phi_1 + \Phi_2[e_k + x_{2k}] - [f_2 + F_{22}x_{2k}] \quad (4.73)$$

$$= [I + \Phi_2]e_k + [\phi_1 + K(y_k)f_1 - f_2] + [I + \Phi_2 + K(y_k)F_{12} - F_{22}]x_{2k} \quad (4.74)$$

where for clarity functions $f_1, F_{12}, f_2, F_{22}, \phi_1, \Phi_2$ are abbreviated

$$f_1 = f_1(x_{1k}, u_k) \quad (4.75)$$

$$F_{12} = F_{12}(x_{1k}, u_k) \quad (4.76)$$

$$f_2 = f_2(x_{1k}, u_k) \quad (4.77)$$

$$F_{22} = F_{22}(x_{1k}, u_k) \quad (4.78)$$

$$\phi_1 = \phi_1(x_{1k}, u_k) \quad (4.79)$$

$$\Phi_2 = \Phi_2(x_{1k}, u_k). \quad (4.80)$$

For the error dynamics to be independent of y, u and x_2 in (4.74)

$$\phi_1 = f_2 - K(y_k)f_1 \quad (4.81)$$

$$\Phi_2 = F_{22} - K(y_k)F_{12} - I. \quad (4.82)$$

The resulting error dynamics are given

$$e_{k+1} = [I + \Phi_2] e_k \quad (4.83)$$

$$= [F_{22} - K(y_k)F_{12}] e_k. \quad (4.84)$$

These error dynamics are stable for a symmetric matrix $F_{22} - K(y_k)F_{12}$ with eigenvalues λ in the unit circle,⁵ i.e.,

$$|\lambda \{F_{22} - K(y_k)F_{12}\}| < 1. \quad (4.85)$$

Substituting (4.81), (4.82) into (4.66), the dynamics for z can be written

$$z_{k+1} = [f_2 - K(y_k)f_1] + [F_{22}(y, u) - K(y_k)F_{12}] \hat{x}_2. \quad (4.86)$$

The observer is synthesized by choosing a function $K(y_k)$ such that matrix $F_{22}(y, u) - K(y_k)F_{12}$ is stable. Then functions ϕ_1, Φ_2 are constructed from (4.81), (4.82) to propagate dynamics of intermediate state variable z , (4.66).

⁵For a general matrix the eigenvalue condition is *necessary* but not *sufficient* for guaranteeing stability since the spectral radius of a matrix is not a norm. The symmetry requirement is by itself not *necessary* but together with the eigenvalue requirement provides both the *necessary* and *sufficient* conditions for stability.

4.4.2 The Newton Observer and Nonlinear Least-Square Observers as a Subclass of the Discrete-Time Friedland Observer

For the discrete-time version of the original system studied by Friedland in section 10.2.2 of [14] it is possible to demonstrate that the Newton observer is a subclass of the discrete-time Friedland observer with a special gain structure.

Consider the discrete-time dynamic system with unknown parameter vector p

$$x_{k+1} = f(x_k, u_k)p \quad (4.87)$$

$$y_k = x_k. \quad (4.88)$$

Following section 4.4.1 the reduced-order observer is obtained

$$\hat{p}_k = \hat{p}_{k-1} + K(y_{k-1})y_k + z_k \quad (4.89)$$

$$z_{k+1} = -K(y_k)f(x_k, u_k)\hat{p}_k. \quad (4.90)$$

Equations (4.89), (4.90) can be combined to yield the observer form

$$\hat{p}_{k+1} = \hat{p}_k + K(y_k)[y_{k+1} - f(x_k, u_k)\hat{p}_k]. \quad (4.91)$$

Defining the extrapolated measurement (which equals the state in this full-state measurement system), \tilde{y}_{k+1}

$$\tilde{y}_{k+1} = \tilde{x}_{k+1} = f(x_k, u_k)\hat{p}_k, \quad (4.92)$$

the observer in (4.91) can be placed into "residual" form

$$\tilde{y}_{k+1} = f(x_k, u_k)\hat{p}_k \quad (4.93)$$

$$\hat{p}_{k+1} = \hat{p}_k + K(y_k)[y_{k+1} - \tilde{y}_{k+1}]. \quad (4.94)$$

The observer can assume one of three forms depending upon the relative dimensions of the parameter and state vectors, viz., $\dim p = \dim x$, $\dim p < \dim x$, and $\dim p > \dim x$. These three cases are addressed below.

4.4.2.1 Parameter Vector Dimension Equal to State Vector Dimension:

For the situation when the parameter vector and state vector are equal dimension the proposed candidate expression for gain matrix $K(y_k)$ is the scaled inverse of forward dynamics matrix function $f(\cdot)$

$$K(y_k) = \alpha f^{-1}(y_k, u_k). \quad (4.95)$$

The resulting observer is given

$$\tilde{y}_{k+1} = f(x_k, u_k)\hat{p}_k \quad (4.96)$$

$$\hat{p}_{k+1} = \hat{p}_k + \alpha f^{-1}(y_k, u_k)[y_{k+1} - \tilde{y}_{k+1}]. \quad (4.97)$$

For $0 < \alpha < 1$ the stability condition in (4.85) is satisfied trivially

$$\alpha f^{-1}(x_k, u_k)f(x_k, u_k) = \alpha I. \quad (4.98)$$

The resulting scaled identity matrix is symmetric with all the eigenvalues equal to α , which are within the unit circle by construction.

The observer described by (4.96), (4.97) is a Newton observer. By writing the forward dynamics

$$x_{k+1} = F(x_k, u_k, p) \quad (4.99)$$

$$(4.100)$$

where $F(x_k, u_k, p) = f(x_k, u_k)p$, it is seen that the Jacobian of the forward dynamics F is f , i.e.,

$$J = \frac{\partial F(x_k, u_k)}{\partial p} \quad (4.101)$$

$$= f(x_k, u_k). \quad (4.102)$$

This observer is similar to the Moraal/Grizzle observer except that here the system is has an n -dimensional output vector, where n is the dimension of state. The Moraal/Grizzle observer, by contrast, uses a “faked” full-state feedback synthesized from n measurements of a single-output system.

4.4.2.2 Parameter Vector Dimension Less Than State Vector Dimension:

For the situation when the parameter vector dimension is less than the state vector dimension the proposed candidate expression for gain matrix $K(y_k)$ is the scaled left pseudoinverse of forward dynamics matrix function $f(\cdot)$ of forward dynamics f

$$K(y_k) = \alpha [f(y_k, u_k)' f(y_k, u_k)]^{-1} f(y_k, u_k)'. \quad (4.103)$$

The resulting observer is given

$$\tilde{y}_{k+1} = f(x_k, u_k) \hat{p}_k \quad (4.104)$$

$$\hat{p}_{k+1} = \hat{p}_k + \alpha [f(y_k, u_k)' f(y_k, u_k)]^{-1} f(y_k, u_k)' [y_{k+1} - \tilde{y}_{k+1}]. \quad (4.105)$$

For $0 < \alpha < 1$ the stability condition in (4.85) is satisfied trivially

$$\alpha [f(y_k, u_k)' f(y_k, u_k)]^{-1} f(y_k, u_k)' f(x_k, u_k) = \alpha I. \quad (4.106)$$

The resulting scaled identity matrix is symmetric with all the eigenvalues equal to α , which is within the unit circle by construction.

4.4.2.3 Parameter Vector Dimension Greater Than State Vector Dimension:

For the situation when the parameter vector dimension is greater than the state vector dimension the proposed candidate expression for gain matrix $K(y_k)$ is the scaled right pseudoinverse of forward dynamics matrix function $f(\cdot)$ of forward dynamics f

$$K(y_k) = \alpha f(y_k, u_k)' [f(y_k, u_k) f(y_k, u_k)']^{-1}. \quad (4.107)$$

The resulting observer is given

$$\tilde{y}_{k+1} = f(x_k, u_k) \hat{p}_k \quad (4.108)$$

$$\hat{p}_{k+1} = \hat{p}_k + \alpha f(y_k, u_k)' [f(y_k, u_k) f(y_k, u_k)']^{-1} [y_{k+1} - \tilde{y}_{k+1}]. \quad (4.109)$$

For $0 < \alpha < 1$ the stability condition in (4.85) is satisfied. The closed-loop error dynamics matrix is given by

$$\alpha f(y_k, u_k)' [f(y_k, u_k) f(y_k, u_k)']^{-1} f(x_k, u_k) = \alpha M. \quad (4.110)$$

Denoting $n_p = \dim p$, $n_x = \dim x$, matrix M in (4.110) is a symmetric $n_p \times n_p$ projection matrix with n_x unity eigenvalues and $n_p - n_x$ zero eigenvalues. Matrix αM , with $0 < \alpha < 1$, is a symmetric scaled projection matrix with n_x eigenvalues of α and $n_p - n_x$ eigenvalues of zero. Matrix αM is therefore a contractor and the observer is stable.

The observer described by (4.104), (4.105) is a nonlinear least-squares observer. It is similar to the Newton observer except, for the situation where the state dimension is greater than the parameter dimension, the inverse of the (square) Jacobian matrix is replaced with the pseudoinverse of the (rectangular) Jacobian matrix. A “quasi-optimal” observer which uses a pseudoinverse that is a function of measurement noise and process uncertainty is proposed in section 8.4.

This similarity leads to question whether the Moraal/Grizzle observer and the Ciccarella observer could have been implemented with a measurement vector of dimension *greater than* the state dimension and what would the robustness properties of this observer likely be. In the absence of measurement noise and process uncertainty, the measurements would be dependent and would not contribute new information. In the situation where measurement noise is present, process uncertainty is small and observability is poor the extra measurements may be beneficial for convergence. These issues shall require future research.

CHAPTER 5

A NEW OBSERVER – THE “GROSSMAN” OBSERVER

5.1 Introduction

5.1.1 Continuous-Time Origins of the “Grossman Observer”

Gauthier *et al* [16] and later Ciccarella *et al* [5] developed observers for continuous-time nonlinear systems using state variable coordinate transformations to transform the continuous-time nonlinear system to a linear system in Brunowski form (integrator chain form). With the Gauthier observer the estimation is performed in the linearized coordinates and the state estimate is recovered by applying the inverse transformation to the estimated transformed state. With the Ciccarella observer the estimation is performed in the original nonlinear system and only the fixed gain matrix, calculated off-line in the linearized system, is transformed from the linearized system to the original nonlinear system. This inverse transformation is a simple matrix inversion and multiplication. Both observers are globally convergent provided certain conditions are satisfied for the calculation of the gains.

The Gauthier and Ciccarella observers, when applied to forced systems, are restricted to applications where the relative degree $r = n$, n being the dimension of state. This limitation exists since for systems where $r < n$, the geometric transformation and linearization is not possible. These observers cannot be applied to the parameter estimation problem where persistent excitation is, in general, required.

5.1.1.1 Gauthier Observer: Let

$$\dot{x} = f(x, u) \tag{5.1}$$

$$y = h(x) \tag{5.2}$$

and a nonlinear transformation $z = \phi(x)$ exists such that

$$z = \begin{bmatrix} y \\ \dot{y} \\ \ddot{y} \\ \vdots \\ y^{(n-1)} \end{bmatrix}. \quad (5.3)$$

The Gauthier observer is given

$$\dot{z} = Az + B\varphi + P_\infty^{-1}C'(y - Cz) \quad (5.4)$$

where P_∞ is the steady-state solution to the Sylvester equation¹

$$0 = KP_\infty + A'P_\infty + P_\infty A - C'C \quad (5.5)$$

for large K and,

$$A = \begin{bmatrix} 0 & 1 & 0 & \cdots & 0 \\ 0 & 0 & 1 & \cdots & 0 \\ \vdots & \vdots & \vdots & \ddots & \vdots \\ 0 & 0 & 0 & \cdots & 1 \\ 0 & 0 & 0 & \cdots & 0 \end{bmatrix} \quad (5.6)$$

$$B = \begin{bmatrix} 0 \\ 0 \\ \vdots \\ 0 \\ 1 \end{bmatrix} \quad (5.7)$$

$$C = \begin{bmatrix} 1 & 0 & 0 & \cdots & 0 \end{bmatrix}, \quad (5.8)$$

¹Matrix equation $AX + XB = C$ is known as the Sylvester equation [53]. For $B = A'$, the Sylvester reduces to the standard Liapunov equation. The Sylvester equation is also known as the generalized Liapunov equation [38].

and

$$\varphi(x) = L_f^n h(x) + u L_g L_f^{n-1} h(x). \quad (5.9)$$

5.1.1.2 The Ciccarella Observer: Ciccarella *et al* [5] extends Gauthier's work and improves upon it by eliminating the nonlinear transformation. Ciccarella uses nonlinear transformations to develop his observer and prove convergence but the final observer does not require a nonlinear transformation.

Referring to (5.1)-(5.3) the Ciccarella observer is given

$$\dot{\hat{x}} = f(\hat{x}, u) + J^{-1} L(\hat{x})(y - C\hat{x}) \quad (5.10)$$

where J is the observability matrix and is also the Jacobian relating the transformed z coordinates to the original x coordinates

$$J(x) = \frac{\partial \phi(x)}{\partial x}. \quad (5.11)$$

Matrix C is as given in (5.8). Fixed gain matrix L is chosen such that

$$A - LC \quad (5.12)$$

is a stable matrix. Stability of $A - LC$ is necessary but not sufficient. Gain matrix L need be chosen so the eigenvalues are fast enough to account for the unknown dynamics introduced by the estimate of the n th derivative of the output. In theory, for the unforced system, it is determined by the Lipschitz constant γ

$$|L_f^n h[\phi^{-1}(\hat{z})] - L_f^n h[\phi^{-1}(z)]| < \gamma |\hat{z} - z| \quad (5.13)$$

and $\lambda\{A - LC\} < -\gamma$.

5.1.2 Tractability of Discrete-Time Formulation

Issues related to the system relative degree are more tractable using a discrete-time formulation in comparison with the continuous-time formulation. The relative

degree of a system for which $r < n$ can always be increased by augmenting the state vector with $n - r$ values of the input sequence. This augmentation is equivalent to imposing $n - r$ input delays to the system. The *difference* between the dimension of the augmented system and the relative degree of the augmented system remains unchanged, but now the system can be *partially* inverted. The part of the augmented system which can be partially inverted is the original system.

Example²

Referring to the example in chapter 1, the dynamics of a discrete-time two-pole filter are nonlinear if the proper state vector is augmented with the unknown filter coefficients, i.e.,

$$x = \begin{bmatrix} x_1 \\ x_2 \\ p_1 \\ p_2 \end{bmatrix} = \begin{bmatrix} x_1 \\ x_2 \\ x_3 \\ x_4 \end{bmatrix} \quad (5.14)$$

$$x_{1k+1} = x_{2k} \quad (5.15)$$

$$x_{2k+1} = -x_3 x_{1k} - x_4 x_{2k} + u_k \quad (5.16)$$

$$x_{3k+1} = x_{3k} \quad (5.17)$$

$$x_{4k+1} = x_{4k} \quad (5.18)$$

$$y_k = x_{1k}. \quad (5.19)$$

²For typographical compactness the time index and state variable index are written as a combined subscript. Unless otherwise indicated, the variable x_{3k+1} represents the variable x_3 at the $k + 1$ time index and *not* the variable x at the $3k + 1$ time index.

The transformed variable z is the four element vector given by the sequence of four outputs y

$$z \equiv \begin{bmatrix} y_k \\ y_{k+1} \\ y_{k+2} \\ y_{k+3} \end{bmatrix} = \begin{bmatrix} x_{1k} \\ x_{2k} \\ -x_{3k}x_{1k} - x_{4k}x_{2k} + u_k \\ x_{3k}x_{4k}x_{1k} + (x_{4k}^2 - x_{3k})x_{2k} - x_{4k}u_k + u_{k+1} \end{bmatrix}. \quad (5.20)$$

The control input appears in the third element of the output sequence vector making this system one of relative order $r = 3$, which is less than the state dimension, $n = 4$.

If the augmented state vector in (5.14) is further augmented by a single control sample, the relative degree is increased to $r = 4$, the dimension of the augmented system is increase to $n = 5$. The augmented state vector is defined:

$$x = \begin{bmatrix} x_1 \\ x_2 \\ p_1 \\ p_2 \\ u_k \end{bmatrix} = \begin{bmatrix} x_1 \\ x_2 \\ x_3 \\ x_4 \\ x_5 \end{bmatrix}. \quad (5.21)$$

The augmented system dynamics are given

$$x_{1k+1} = x_{2k} \quad (5.22)$$

$$x_{2k+1} = -x_{3k}x_{1k} - x_{4k}x_{2k} + x_{5k} \quad (5.23)$$

$$x_{3k+1} = x_{3k} \quad (5.24)$$

$$x_{4k+1} = x_{4k} \quad (5.25)$$

$$x_{5k+1} = \bar{u}_k \quad (5.26)$$

where $\bar{u}_k = u_{k+1}$.

The transformed variable z is the five element vector given by the sequence of five outputs y

$$z \equiv \begin{bmatrix} y_k \\ y_{k+1} \\ y_{k+2} \\ y_{k+3} \\ y_{k+4} \end{bmatrix} = \begin{bmatrix} x_{1k} \\ x_{2k} \\ -x_{3k}x_{1k} - x_{4k}x_{2k} + x_{5k} \\ -x_{3k}x_{4k}x_{1k} + (x_{4k}^2 - x_{3k})x_{2k} - x_{4k}x_{5k} \\ \dots \text{expression in } x_k, \bar{u}_k, \text{ and } \bar{u}_{k+1} \end{bmatrix}. \quad (5.27)$$

For n -dimensional observable system, as defined in chapter 3, only n output samples are necessary to reconstruct the state. By imposing $n - r$ delays on the system input it is possible to create an augmented system, the partial inversion of which provides the basis for the synthesis of an observer.

5.2 A New Observer for the General Discrete-time Nonlinear Systems

The observers presented in this section are for the nonlinear discrete-time system presented by (3.1), (3.2). The system equations under consideration are repeated here for convenience:

$$x_{k+1} = f(x_k, u_k) \quad (5.28)$$

$$y_k = h(x_k, u_k), \quad (5.29)$$

5.2.1 The Unforced System

Theorem 5.1. If the nonlinear discrete-time system described by (5.28), (5.29) is:

H1 Observable as defined in chapter 3

H2 $h[G_f^n \phi^{-1}(\zeta)]$ is uniformly Lipschitz, i.e., $\forall \zeta_1, \zeta_2 \in R^n$:

$$\|h[G_f^n \phi^{-1}(\zeta_2)] - h[G_f^n \phi^{-1}(\zeta_1)]\| \leq \gamma \|\zeta_2 - \zeta_1\|$$

with $\|\gamma\| < 1$

then there exists a finite gain matrix $L = L^*$ and matrices

$$A = \begin{bmatrix} 0 & 1 & 0 & 0 \\ 0 & 0 & 1 & 0 \\ \vdots & \vdots & \ddots & \vdots \\ 0 & 0 & 0 & 1 \\ 0 & 0 & 0 & 0 \end{bmatrix}, \quad B = \begin{bmatrix} 0 \\ 0 \\ \vdots \\ 0 \\ 1 \end{bmatrix}$$

$$C = \begin{bmatrix} 1 & 0 & \dots & 0 \end{bmatrix}$$

such that the observer

$$\hat{z}_{k+1} = A\hat{z}_k + Bh[G_f^n \phi^{-1}(\hat{z}_k)] + L(y_k - C\hat{z}_k) \quad (5.30)$$

$$\hat{x}_k = \phi^{-1}(\hat{z}_k) \quad (5.31)$$

converges asymptotically to system state x .

Proof: Define estimation error $\epsilon = \hat{z} - z$. The error dynamics of the proposed observer are derived

$$\begin{aligned} \epsilon_{k+1} &= A\hat{z}_k + Bh[G_f^n \phi^{-1}(\hat{z}_k)] + L(y_k - C\hat{z}_k) - Az_k - Bh[G_f^n \phi^{-1}(z_k)] \\ &= (A - LC)(\hat{z}_k - z_k) + B\{h[G_f^n \phi^{-1}(\hat{z}_k)] - h[G_f^n \phi^{-1}(z_k)]\} \\ &= (A - LC)\epsilon_k + B\{h[G_f^n \phi^{-1}(\hat{z}_k)] - h[G_f^n \phi^{-1}(z_k)]\} \\ &= A_{cl}\epsilon_k + Bg(z_k, \epsilon_k) \end{aligned} \quad (5.32)$$

where $A_{cl} = A - LC$ and

$$g(z_k, \epsilon_k) = h[G_f^n \phi^{-1}(\hat{z}_k)] - h[G_f^n \phi^{-1}(z_k)] \quad (5.33)$$

$$= h[G_f^n \phi^{-1}(z_k + \epsilon_k)] - h[G_f^n \phi^{-1}(z_k)]. \quad (5.34)$$

Define a discrete-time Liapunov function $V(\epsilon_k) = \epsilon_k' \epsilon_k$. $V(\epsilon_k)$ is positive definite and $V(0) = 0$. For Liapunov stability $\Delta V_{k+1} = V(\epsilon_{k+1}) - V(\epsilon_k) < 0$ except when $V(\epsilon_k) = 0$.

From (5.32)

$$\Delta V_{k+1} = [A_{cl}\epsilon_k + Bg(z_k, \epsilon_k)]' [A_{cl}\epsilon_k + Bg(z_k, \epsilon_k)] - \epsilon_k' \epsilon_k \quad (5.35)$$

$$= \epsilon_k' A_{cl}' A_{cl} \epsilon_k + 2g(z_k, \epsilon_k) B' A_{cl} \epsilon_k + g^2(z_k, \epsilon_k) - \epsilon_k' \epsilon_k \quad (5.36)$$

Denoting the eigenvalue of A_{cl} with largest magnitude as $\bar{\lambda}$ and substituting the Lipschitz condition from $H2$, an upper bound on ΔV is given

$$\Delta V_{k+1} \leq \|\bar{\lambda}\|^2 \|\epsilon_k\|^2 + 2\gamma \|\bar{\lambda}\| \|\epsilon\|^2 + (\gamma^2 - 1) \|\epsilon\|^2. \quad (5.37)$$

Liapunov stability requires $\Delta V < 0$ which following (5.37) requires

$$\|\bar{\lambda}\|^2 \|\epsilon_k\|^2 + 2\gamma \|\bar{\lambda}\| \|\epsilon\|^2 + (\gamma^2 - 1) \|\epsilon\|^2 < 0 \quad (5.38)$$

$$\|\bar{\lambda}\|^2 + 2\gamma \|\bar{\lambda}\| + (\gamma^2 - 1) < 0 \quad (5.39)$$

$$[\|\bar{\lambda}\| + (\gamma + 1)] [\|\bar{\lambda}\| + (\gamma - 1)] < 0 \quad (5.40)$$

The left factor of (5.40) is always positive. To satisfy inequality relationship (5.40) the right factor must be less than zero

$$0 > \|\bar{\lambda}\| + (\gamma - 1) \quad (5.41)$$

$$\Rightarrow 0 < \|\bar{\lambda}\| < 1 - \gamma. \quad (5.42)$$

Validity of (5.42) requires two conditions:

$$\gamma < 1, \quad (5.43)$$

$$\|\bar{\lambda}\| < 1 - \gamma. \quad (5.44)$$

Condition (5.43) is satisfied by hypothesis $H2$. Condition (5.44) is satisfied by selecting $L = L^*$ such that the $\|\bar{\lambda}\| < 1 - \gamma$. This pole placement is always possible since by construction the matrix pair $\{A, C\}$ is completely observable. \square

5.2.2 Observer for Forced Discrete-time Nonlinear Systems

Theorem 5.2. If the nonlinear discrete-time system described by (5.28), (5.29) is:

H1 Observable as defined in section 3.4

H2 $h[G_f^n \phi^{-1}(\zeta, u)]$ is uniformly Lipschitz, i.e., $\forall \zeta_1, \zeta_2, u \in R^n$:

$$\|h[G_f^n \phi^{-1}(\zeta_2, u)] - h[G_f^n \phi^{-1}(\zeta_1, u)]\| \leq \gamma \|\zeta_2 - \zeta_1\|$$

with $\|\gamma\| < 1$

then the observer

$$\hat{z}_{k+1} = A\hat{z}_k + Bh[G_f^n \phi^{-1}(\hat{z}_k, u_k)] + L(y_k - C\hat{z}_k) \quad (5.45)$$

$$\hat{x}_k = \phi^{-1}(\hat{z}_k) \quad (5.46)$$

converges asymptotically to system state x for some finite gain matrix L .

Proof: Proof of theorem 5.2 is identical to that of theorem 5.1 with forcing function g defined

$$g(z_k, \epsilon_k) = h[G_f^n \phi^{-1}(z_k + \epsilon_k, u_k)] - h[G_f^n \phi^{-1}(z_k, u_k)]. \quad (5.47)$$

Remark 1. Calculation of observer forcing function $h[G_f^n \phi^{-1}(\hat{z}_k, u_k)]$ in (5.45) requires knowledge of u_{k+n-1} . This calculation requires $n - r$ delays and the state estimate output by the observer is retarded by $n - r$ delays.

Remark 2. In contrast to the continuous-time observer developed by Gauthier [16] and Ciccarella [5] there is no relative degree requirement restricting application of the discrete-time observer. Instead, the discrete-time observer requires $n - 1$ delays to estimate the state. This delay requirement need be considered in the overall control system design but in practice is less restrictive than the relative degree requirement. The “real-time” delay is the product of the $n - 1$ delays and the sample period which can made short enough such that the delay introduced by the observer has a minimal effect.

Remark 3. By transforming system (3.1), (3.2) using transformation $z = \phi(x, u)$ a globally convergent observer is given

$$\hat{z}_{k+1} = A\hat{z}_k + By_{k+n} + L(y_k - Cz_k) \quad (5.48)$$

$$\hat{x}_k = \phi^{-1}(\hat{z}_k, u_k). \quad (5.49)$$

For this observer the closed-loop error dynamics are determined by matrix $A-LC$. The observer problem is now a (possibly difficult) numerical analysis problem of inverting the nonlinear algebraic transformation $z = \phi(x, u)$. Solving for this inverse algebraic transformation, (5.49), is the discrete-time analog of the continuous-time problem in the Gauthier observer of solving an n th order system of partial differential to find the inverse transformation. *In general, it is significantly easier solving a nonlinear algebraic equation than it is to solve a system of partial differential equation.*

Remark 4. Solving for the transformation $x^* = \phi^{-1}(z, u)$ is equivalent to finding the root x^* of equation $z - \phi(x^*, u)$. This root-searching problem generally requires calculation of Jacobian matrix $J = \partial z / \partial x$. If J is singular then the root may not exist or may be difficult to find. As seen in chapter 3, J is the observability test matrix for strong observability. If the system is not strongly observable some method other than a Newton search will be required to solve for root of equation $z - \phi(x^*, u)$. Practicability of these other methods will determine the observer can be implemented in those situations.

5.2.3 Structure of Grossman Observer

The Grossman observer has the structure shown in figure 5.1. Comparing the structure of the Grossman observer, figure 5.1 with the modified Moraal/Grizzle observer, figure 4.3, the Grossman observer is essentially a nonlinear, low-pass pre-filter concatenated with a Newton solver similar to that of Moraal and Grizzle. It accepts two driving inputs, viz., a retarded measurement y_{k-n+1} and an estimate of

the $k + 1$ measurement based upon the nonlinear function of the current estimate.

It is possible that often this latter driving term may be omitted.

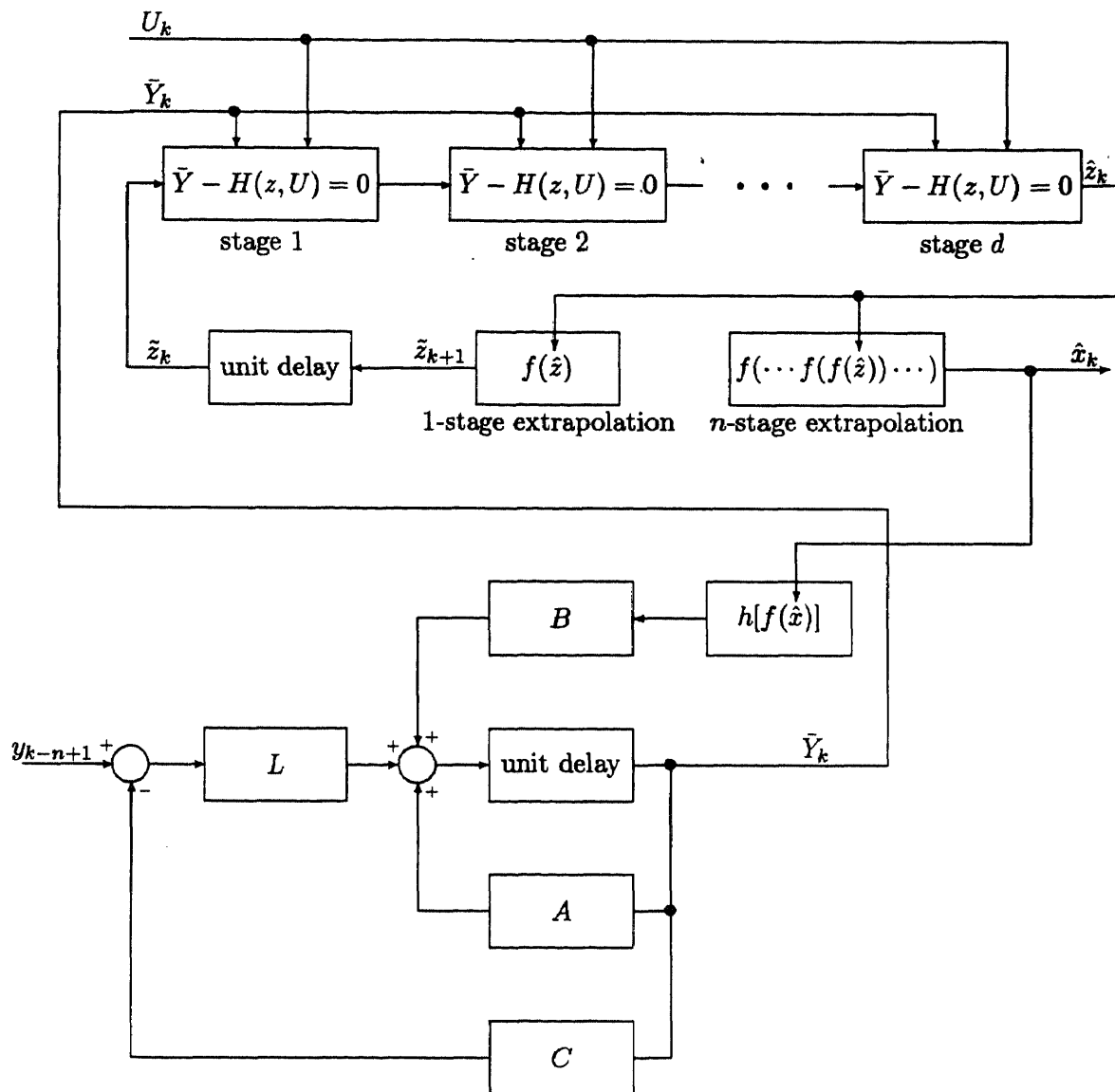


Figure 5.1 Grossman observer combines a nonlinear low-pass filter with a nonlinear equation solver. (Shown here with a Newton solver.) The low-pass filter provides for noise mitigation.

5.2.4 Example

The forced nonlinear discrete-time system is given

$$x_{k+1} = f(x_k, u_k) \quad (5.50)$$

$$y_k = h(x_k) \quad (5.51)$$

where functions $f(x_k, u_k)$, $h(x_k)$ are given by (5.52), (5.53), (5.54) below:

$$x_{1k+1} = (1 - x_{1k}^2)x_{2k} + u_{1k} \quad (5.52)$$

$$x_{2k+1} = -x_{1k}x_{2k} + u_{2k} \quad (5.53)$$

$$y_k = x_{1k}x_{2k}. \quad (5.54)$$

In this simulation the inputs are fixed to $u_1 = 0.2$, $u_2 = -0.5$. Following (5.45), (5.46) an observer is constructed. The inverse function ϕ^{-1} is calculated using a multi-dimensional nonlinear root finder to solve for \hat{x} such that

$$g(\hat{x}) = z - \phi(\hat{x}, u) = 0. \quad (5.55)$$

This root finder requires a “seed” \tilde{x} . The observer algorithm proceeds as follows:

```

L := [ -0.2500  0.0150 ]'
z0 := [ y0  y1 ]'
x_tilde_0 := 0
x_hat_0 := phi^-1(z0, x_tilde_0, u)

for k := 0 to N do
    z_hat := A z_hat + B h[G_f^2(x_hat, u_k)] + L(y_k - C z_hat)
    x_tilde := f(x_hat, u_k)           comment: propagate the seed
    x_hat := phi^-1(z_hat, x_tilde, u_k)
end

```

Simulation results are shown in figure 5.2.

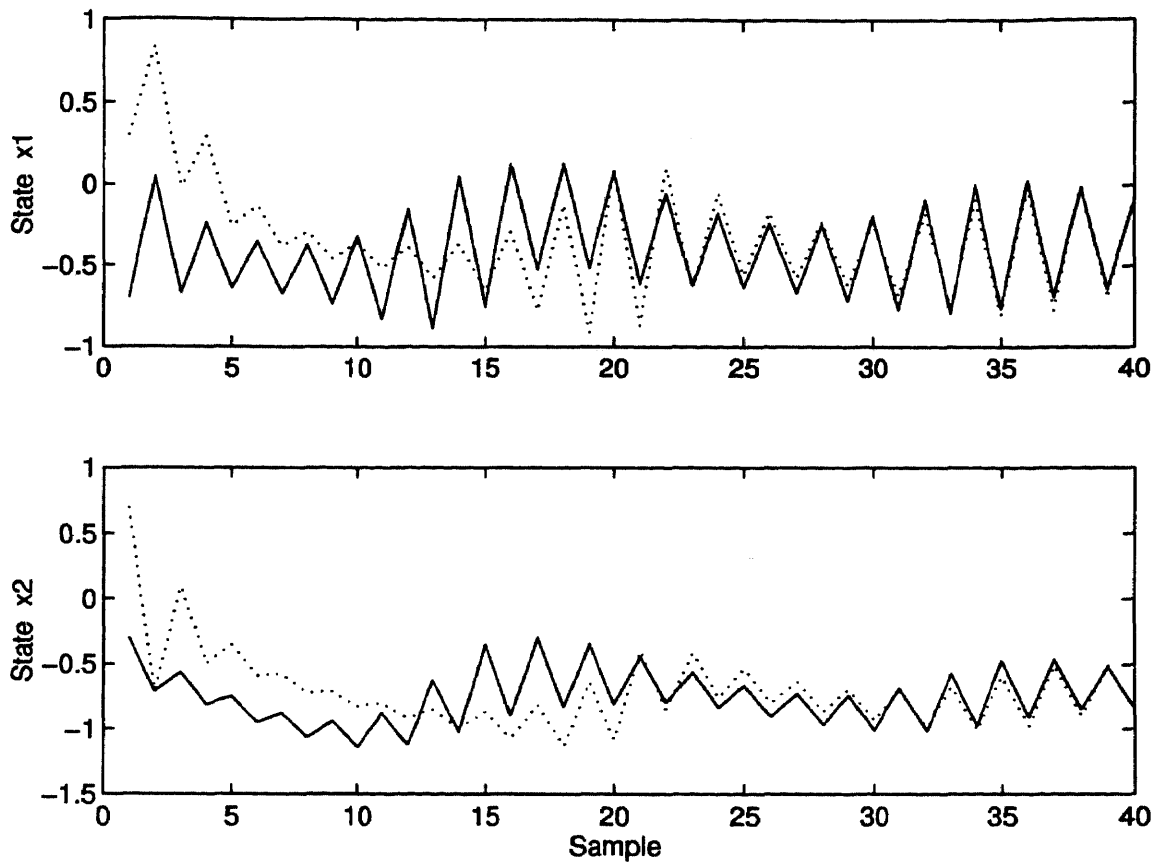


Figure 5.2 Grossman observer state estimate (solid line) and true state (dotted line) for example 5.2.4.

CHAPTER 6

APPLICATIONS

6.1 Discrete-time Friedland Observer for Identification of the Characteristic Polynomial of an Autoregressive Filter¹

With slight modification the discrete-time version of the Friedland parameter estimator developed in section 4.4 can be used to estimate parameters in systems where the n -dimensional state vector is defined as the sequence of n successive outputs. The modification requires inclusion of prior measured states and inputs into the system dynamics.²

Defining $X_k = [x_k, \dots, x_{k-n+1}]'$, $U_k = [u_k, \dots, u_{k-n+1}]'$, the autoregressive filter with nonstationary poles can be represented

$$x_{k+1} = F(X_k, U_k)p_k + g(X_k, U_k) \quad (6.1)$$

$$p_{k+1} = A(X_k)p_k, \quad (6.2)$$

and the observer is given

$$\hat{p}_k = A(X_{k-1})\hat{p}_{k-1} + M(X_{k-1})x_k + z_k \quad (6.3)$$

$$z_{k+1} = -M(X_k)[F(X_k, U_k)p_k + g(X_k, U_k)]. \quad (6.4)$$

With this modified representation the autoregressive process with nonstationary poles is given

$$x_{k+1} = F(X_k)p + u_k \quad (6.5)$$

$$p_{k+1} = A(X_k)p_k \quad (6.6)$$

¹This section is based upon the recent publication "Extension of the Friedland Parameter Estimator to Discrete-Time Systems" [24].

²This formal modification is necessary since, strictly speaking, it is not possible to have full-state measurement on a system in which the forward dynamics depends upon states other than the present state. Availability of full-state measurement is the premise underlying both the Friedland observer and the present work.

where $F(X_k) = X_k'$. The proposed observer follows (4.65), (4.65). Define state-dependent gain matrix $M(x)$ for scalar L , $0 < L < 2$, to be

$$M(X_k) = L \frac{X_k}{X_k' X_k}, \quad (6.7)$$

then the observer is given as

$$\hat{p}_k = A(X_{k-1})\hat{p}_{k-1} + L \frac{X_{k-1}}{X_{k-1}' X_{k-1}} x_k + z_k \quad (6.8)$$

$$z_{k+1} = -L \frac{X_k}{X_k' X_k} [F(X_k)\hat{p}_k + u_k]. \quad (6.9)$$

The parameter error dynamics are given as

$$\epsilon_{k+1} = \left[A(X_k) - L \frac{X_k X_k'}{X_k' X_k} \right] \epsilon_k \quad (6.10)$$

$$= G(X_k)\epsilon. \quad (6.11)$$

For $L = 1$, and $A(X_k) = I$, matrix $G(X_k)$ is a rank $n-1$ idempotent projection matrix with eigenvalues $\lambda \in \{0, 1\}$. The eigenvector corresponding to the stable eigenvalue $\lambda = 0$ is X_k . The eigenvector corresponding to the *marginally stable* eigenvalue $\lambda = 1$ is in the $n-1$ -dimension orthogonal subspace X_k^\perp . In general, $\lambda \in \{1-L, 1\}$ with eigenvector $e \in \{X_k, X_k^\perp\}$, respectively. Therefore $0 < L < 2$ guarantees marginal stability.

Remark 5. For all L , the eigenvalue corresponding to X_k^\perp remains unity and only marginal stability of the observer can be realized. The entire parameter vector p can be estimated with asymptotically zero error if $X_k \neq 0$ and the *direction* of X_k varies. This variation is achieved by nonzero input excitation.

Remark 6. The standard parameter estimation “projection algorithm” presented in [2], [36] is a special case of the new observer presented here. By combining observer (6.8), (6.9) the parameter estimation equation is

$$\rho_k = x_k - [F(X_{k-1})\hat{p}_{k-1} + u_{k-1}] \quad (6.12)$$

$$\hat{p}_k = A(X_{k-1})\hat{p}_{k-1} + L \frac{X_{k-1}}{X_{k-1}' X_{k-1}} \rho_k. \quad (6.13)$$

The parameter identification algorithm from [2] is

$$\rho_k = x_k - F(X_{k-1})\hat{p}_{k-1} \quad (6.14)$$

$$\hat{p}_k = A_{k-1}\hat{p}_{k-1} + L \frac{X_{k-1}}{X'_{k-1}X_{k-1}} \rho_k. \quad (6.15)$$

The new observer, (6.12), (6.13) provides for an explicit forcing term and a state-dependent parameter dynamics matrix.³ The observer in [2] can be viewed as a special case of the new observer for which the full n dimension-state vector in [2], which is not directly measurable, becomes directly measurable by insertion of n unit delays into the measurement epoch.

Remark 7. Matrix

$$M(X_k) = L \frac{X_k}{X'_k X_k} \quad (6.16)$$

is the scaled (by L) *right pseudoinverse* of the underdetermined equation

$$x_{k+1} = F(X_k)p_k. \quad (6.17)$$

The minimum- L_2 norm pseudoinverse $F^\#$ for underdetermined equation $x = Fp$ is $F^\# = F'(FF')^{-1}$. For this system, $F(X_k) = X'_k$ and the right pseudoinverse is given

$$F^\# = X_k(X'_k X_k)^{-1} \quad (6.18)$$

$$= \frac{X_k}{X'_k X_k} \quad (\text{since } X'_k X_k \text{ is a scalar}). \quad (6.19)$$

In this simulation the initial parameter estimates were set $\hat{p}_1 = \hat{p}_2 = 0$ and a unity amplitude square wave, $u_k = \text{sign}(\sin 2\pi 0.1k)$ was applied. Convergence of the noise-free parameter estimator is shown in figure 6.1.

When white Gaussian noise η , $\eta \in N\{0, 0.30\}$ ⁴ is added to the state measurements, observer performance is seriously degraded as shown in figure 6.2. It

³The observer in [2] can easily accommodate an input forcing function and probably can accommodate a state-dependent parameter dynamics matrix provided that the parameter variation bandwidth is much less than the bandwidth of the measured output.

⁴Expression $\eta \in N\{\bar{x}, \sigma_x\}$ means that η is from a normal (Gaussian) distribution with mean \bar{x} , standard deviation σ_x .

is difficult to generalize this noise sensitivity to the discrete-time Friedland observer because gain matrix and forward dynamics matrix are problem dependent. The application of the observer is premised upon availability of full state measurement and, at least in this application, the measurements need be relatively noise-free.

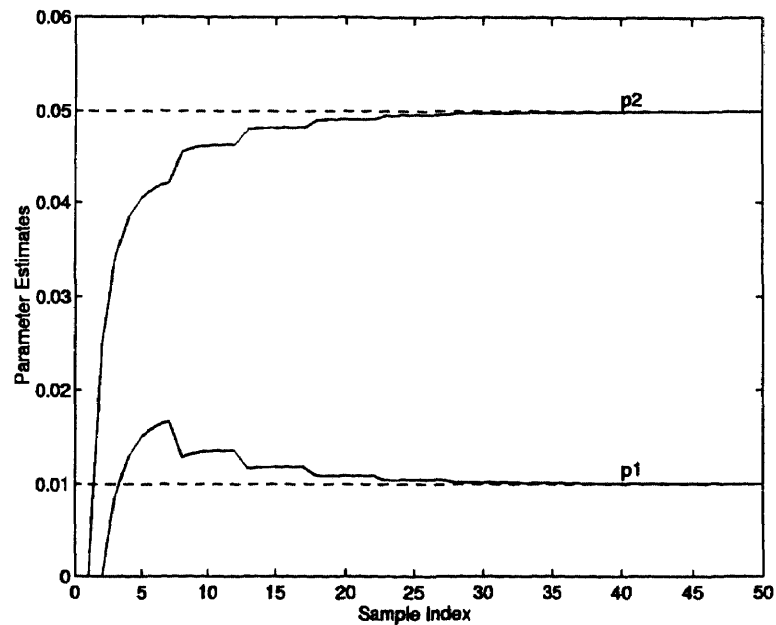


Figure 6.1 Convergence of estimates of ARMA characteristic polynomial coefficients (solid) to actual coefficient values (dashed) using discrete-time Friedland observer.

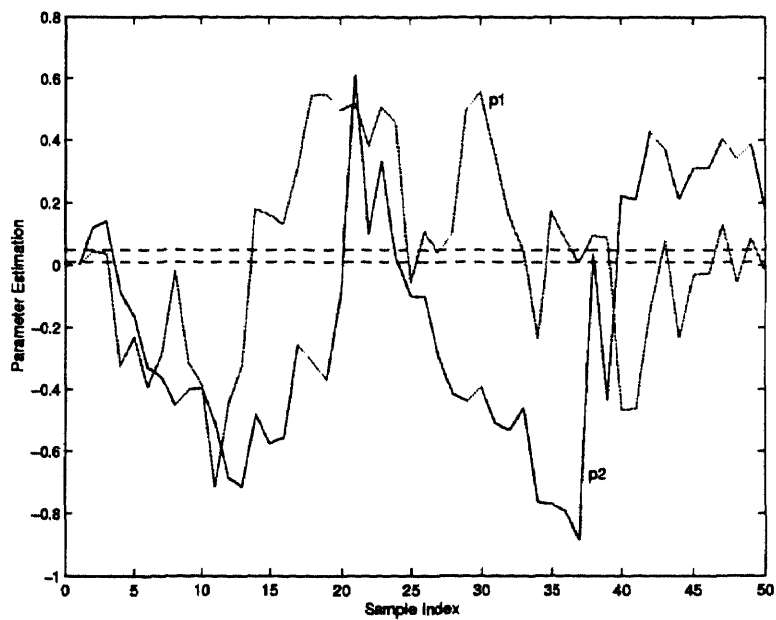


Figure 6.2 Degraded convergence of estimates of ARMA characteristic polynomial coefficients (solid) to actual coefficient values (dashed) using discrete-time Friedland observer. Noise present.

6.2 Simultaneous State and Parameter Estimation Applied to an Autoregressive Filter

This observer is derived to estimate the states and the coefficients of the characteristic polynomial of an autoregressive process. The given process is

$$x_{1k+1} = x_{2k} \quad (6.20)$$

$$x_{2k+1} = -p_1 x_{1k} - p_2 x_{2k} + u_k \quad (6.21)$$

$$y_k = x_{1k}. \quad (6.22)$$

The augmented state vector is

$$X = \begin{bmatrix} p_1 \\ p_2 \\ x_1 \\ x_2 \end{bmatrix}. \quad (6.23)$$

The (nonlinear) dynamics of the augmented system are given

$$X_{k+1} = \begin{bmatrix} p_{1k} \\ p_{2k} \\ x_{2k} \\ -p_{1k}x_{1k} - p_{2k}x_{2k} + u_k \end{bmatrix}. \quad (6.24)$$

6.2.1 Grossman Observer

The transformation of the augmented system given by (6.24), $z = \phi(x, u)$, into Brunowski form is given

$$z_k = \begin{bmatrix} x_{1k} \\ x_{2k} \\ -p_{1k}x_{1k} - p_{2k}x_{2k} + u_k \\ -p_{1k}x_{2k} - p_{2k}(-p_{1k}x_{1k} - p_{2k}x_{2k} + u_k) + u_{k+1} \end{bmatrix}. \quad (6.25)$$

Table 6.1 Grossman observer initial conditions for simultaneous ARMA parameter and state estimation.

Variable	True Value	Initial Estimate
p_1	0.5	0.1
p_2	1.0	4.0
x_1	1.0	1.2
x_2	0.5	0.0

The inverse, $x = \phi^{-1}(z, u)$ requires solving a nonlinear algebraic equation. This equation can be solved by finding the root of

$$g(x, u) = z - \phi(x, u). \quad (6.26)$$

Newton's method is used to solve (6.26). Newton's method requires calculation of the Jacobian of ϕ , (6.25). The Jacobian $J = \partial\phi/\partial x$ in closed form is given

$$J = \begin{bmatrix} 0 & 0 & 1 & 0 \\ 0 & 0 & 0 & 1 \\ -x_1 & -x_2 & -p_1 & -p_2 \\ p_2x_1 - x_2 & 2p_2x_2 + p_1x_1 - u_k & p_1p_2 & p_2^2 - p_1 \end{bmatrix}. \quad (6.27)$$

The Grossman observer⁵ was used to simultaneously estimate the states and parameters of this filter (i.e., all the states from this augmented system.) The initial conditions for the simulation are shown in table 6.1. A square wave, $u_k = 10 \text{sign}(\sin 2\pi 0.067k)$ was applied to the input and white Gaussian noise η , $\eta \in N\{0, 0.30\}$ was added to the measurement. Performance of the observer is shown in figures 6.3-6.6.

⁵See appendix B for the MATLAB code.

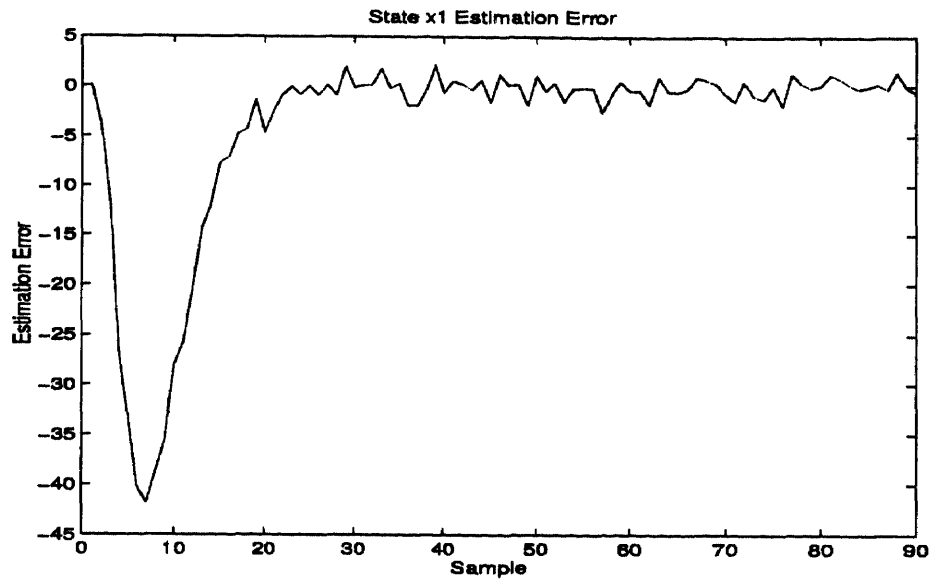


Figure 6.3 Observer convergence of state x_1 .

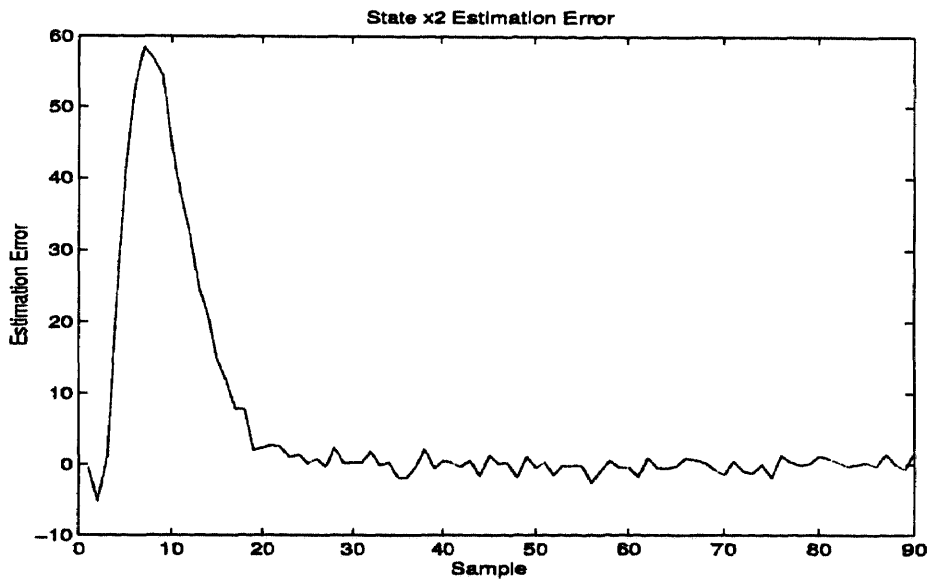


Figure 6.4 Observer convergence of state x_2 .

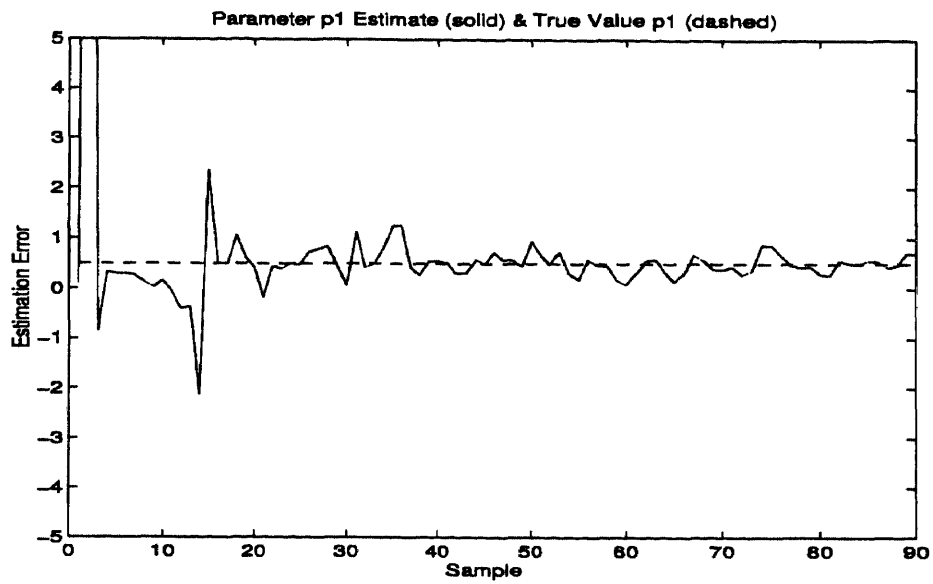


Figure 6.5 Observer convergence of parameter p_1 .

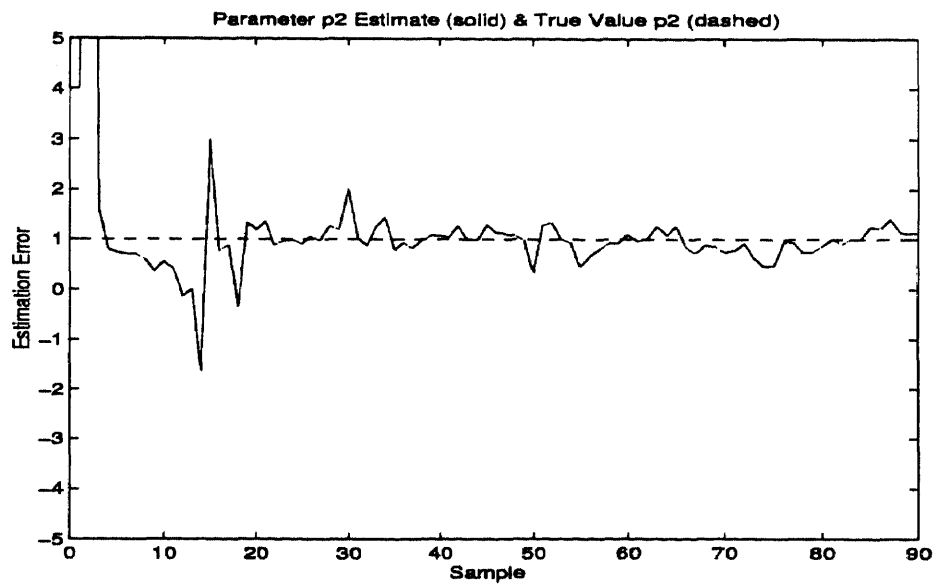


Figure 6.6 Observer convergence of parameter p_2 .

6.2.2 Modified Moraal/Grizzle Observer

Using the state vector definition of X from (6.23), the forward dynamics function for $X_{k+1} = f(X_k, u_k)$, (6.24), and output equation

$$y_k = h(X_k, u_k) \quad (6.28)$$

$$= X_{3k}, \quad (6.29)$$

the extrapolated vector of four successive measurements as a function of retarded state vector $z_k = X_{k-3}$ is given

$$\tilde{Y}_k = \begin{bmatrix} \tilde{y}_{k-3} \\ \tilde{y}_{k-2} \\ \tilde{y}_{k-1} \\ \tilde{y}_k \end{bmatrix} \quad (6.30)$$

$$= \begin{bmatrix} h(z_k) \\ h(f(z_k, u_{k-2})) \\ h(f(f(z_k, u_{k-2}), u_{k-1})) \\ h(f(f(f(z_k, u_{k-2}), u_{k-1}), u_k)) \end{bmatrix}. \quad (6.31)$$

Using the Jacobian given by (6.27), the single iteration modified Moraal/Grizzle observer is given

$$\tilde{z}_k = f(z_{k-1}, u(k-4)) \quad (6.32)$$

$$Y_k = \begin{bmatrix} y_{k-3} & y_{k-2} & y_{k-1} & y_k \end{bmatrix}' \quad (6.33)$$

$$U_k = \begin{bmatrix} u_{k-3} & u_{k-2} & u_{k-1} & u_k \end{bmatrix}' \quad (6.34)$$

$$z_k = \tilde{z}_k + \alpha J(\tilde{z}_k, U_k)^{-1} (Y_k - \tilde{Y}_k) \quad (6.35)$$

$$\hat{X}_k = f(f(f(z_k, u_{k-3}), u_{k-2}), u_{k-1}). \quad (6.36)$$

The initial conditions and the input for this simulation were the same as those used in section 6.2.1 (see table 6.1). A square wave, $u_k = 10 \text{ sign}(\sin 2\pi 0.067k)$ was

Table 6.2 Modified Moraal/Grizzle observer for ARMA parameter estimation.

α	Transient Response ^a			Steady-state Noise ^b		
	0.1	0.5	1.0	0.1	0.5	1.0
p_1	45	12	8	0.021	0.066	0.074
p_2	35	10	8	0.022	0.086	0.078
x_1	45	12	8	0.332	0.835	0.281
x_2	45	13	7	0.360	1.668	1.085

^aSample index at which error is reduced 90% from its peak value.

^bStandard deviation of simulation points 50:100.

applied to the input. Two simulations runs were made, one without noise and one with noise. The noise process, η , was white Gaussian, $\eta \in N\{0, 0.30\}$ and it was added to the measurement.

Figures 6.7–6.10 show the noise-free transient response of the estimates of the observer as a function of slowing factor α . Figures 6.11–6.14 shows the same response when the measurement is corrupted with the white Gaussian noise. Displayed in these figures is the statistical estimate of the steady-state standard deviation based upon the last fifty points of the simulation run (points 50:100).

Figures 6.7–6.10 demonstrate, as expected that the transient response is fastest for $\alpha = 1$ and slowest for $\alpha = 0.1$. Figures 6.11, 6.12, and 6.14 demonstrate clearly the beneficial effect the non-unity slowing factor has upon steady state noise mitigation. Figure 6.13 represents an interesting anomaly where in the steady state the noise mitigation for $\alpha = 1$ was *superior* to values $\alpha < 1$ for state estimate x_1 . It is also interesting to note that for this estimate the steady-state noise responses for $\alpha = 0.5$ were generally *worse* than those for $\alpha = 1$. These results are summarized in table 6.2.

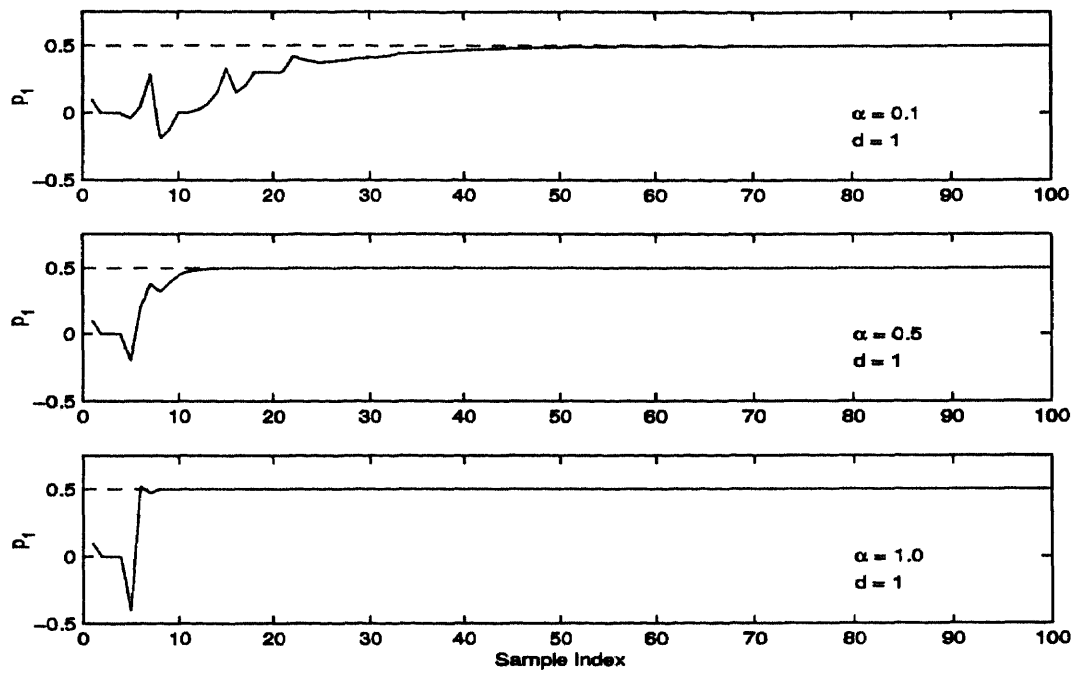


Figure 6.7 Modified Moraal/Grizzle observer estimation of p_1 (solid) and true value (dashed) for different values of α . No measurement noise.

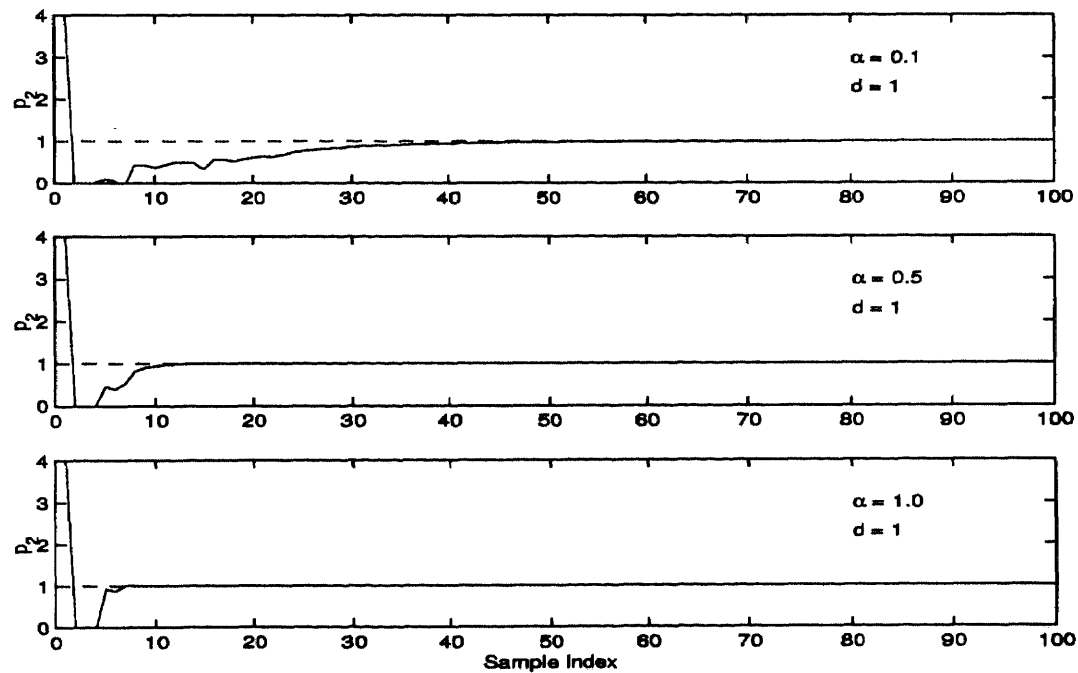


Figure 6.8 Modified Moraal/Grizzle observer estimation of p_2 (solid) and true value (dashed) for different values of α . No measurement noise.

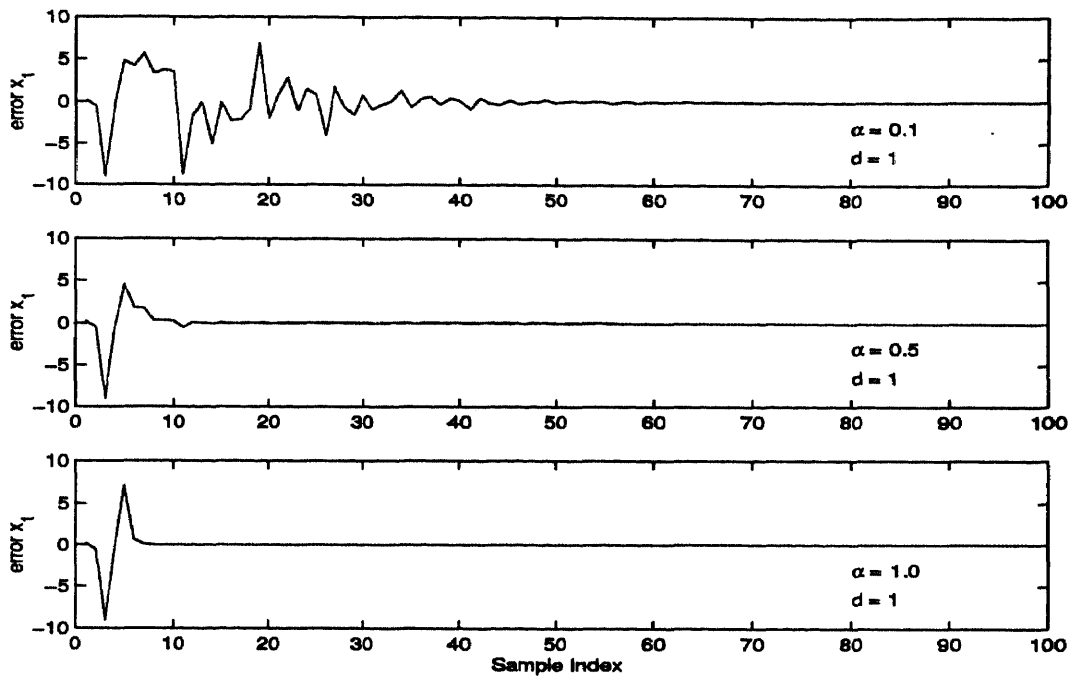


Figure 6.9 Modified Moraal/Grizzle observer estimation error of state x_1 for different values of α . No measurement noise.

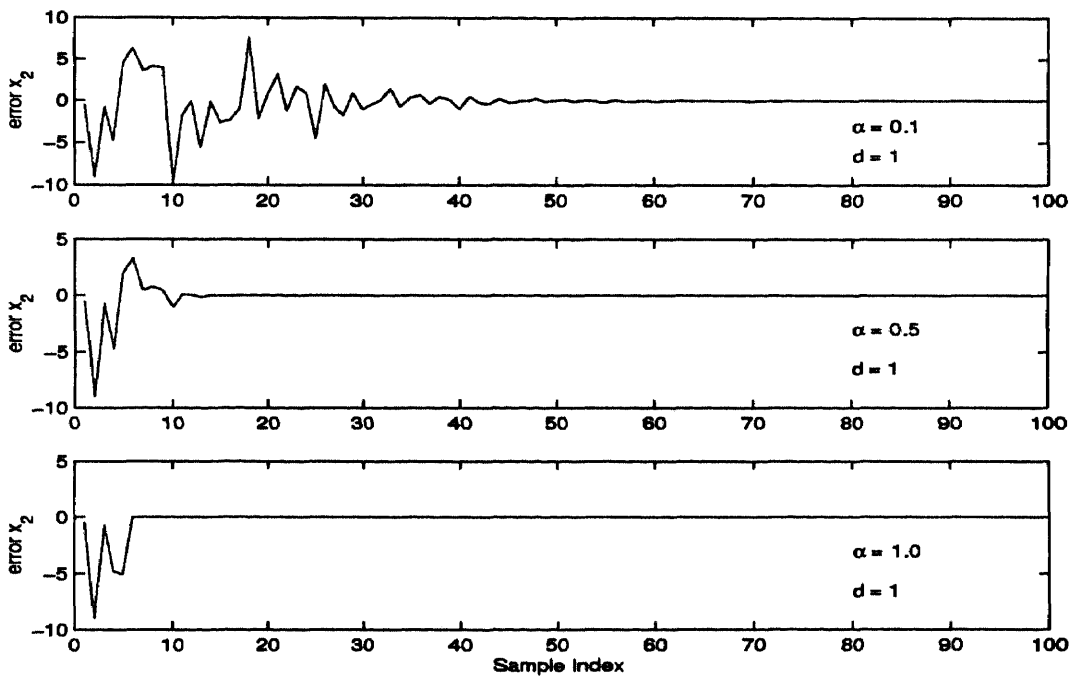


Figure 6.10 Modified Moraal/Grizzle observer estimation error of state x_2 for different values of α . No measurement noise.

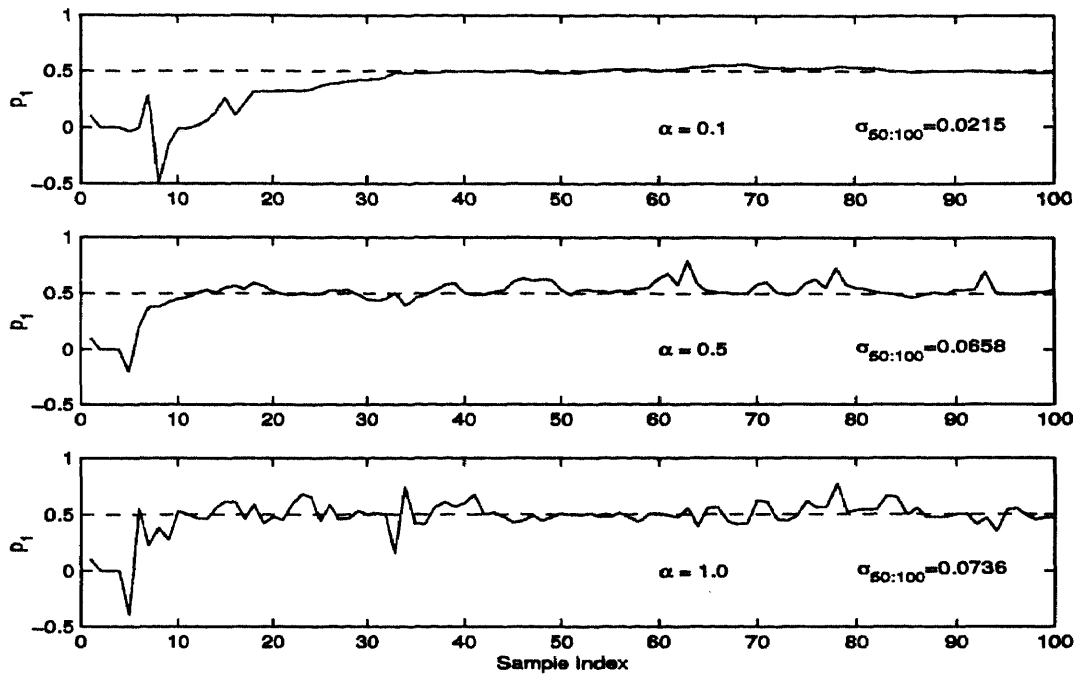


Figure 6.11 Modified Moraal/Grizzle observer estimation of p_1 (solid) and true value (dashed) for different values of α . Measurement noise present.

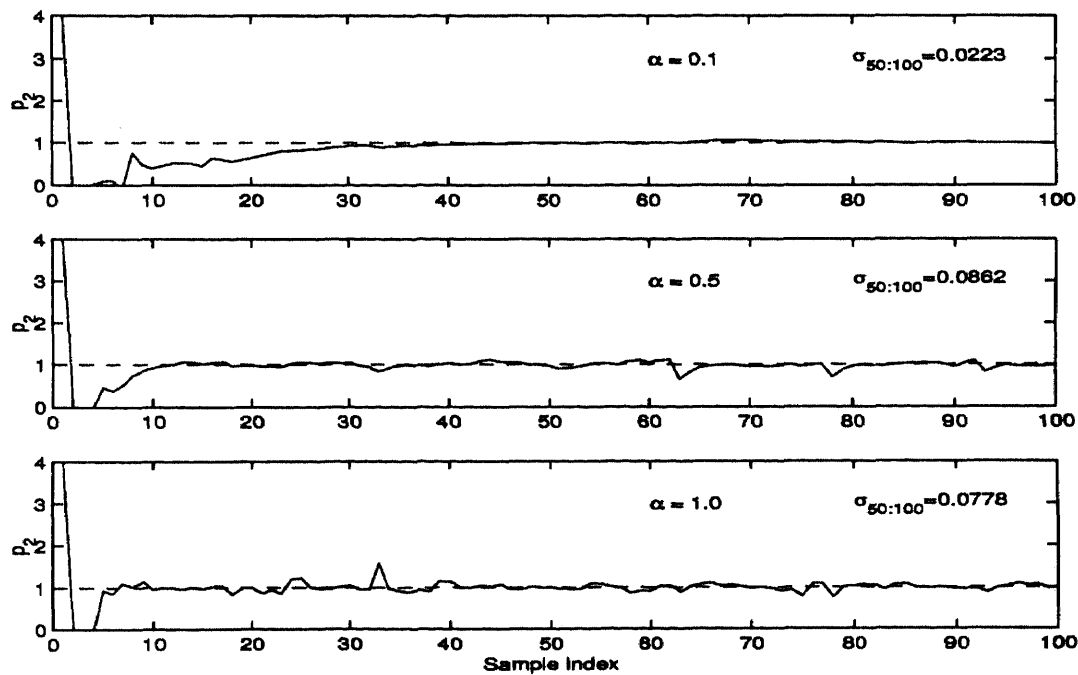


Figure 6.12 Modified Moraal/Grizzle observer estimation of p_2 (solid) and true value (dashed) for different values of α . Measurement noise present.

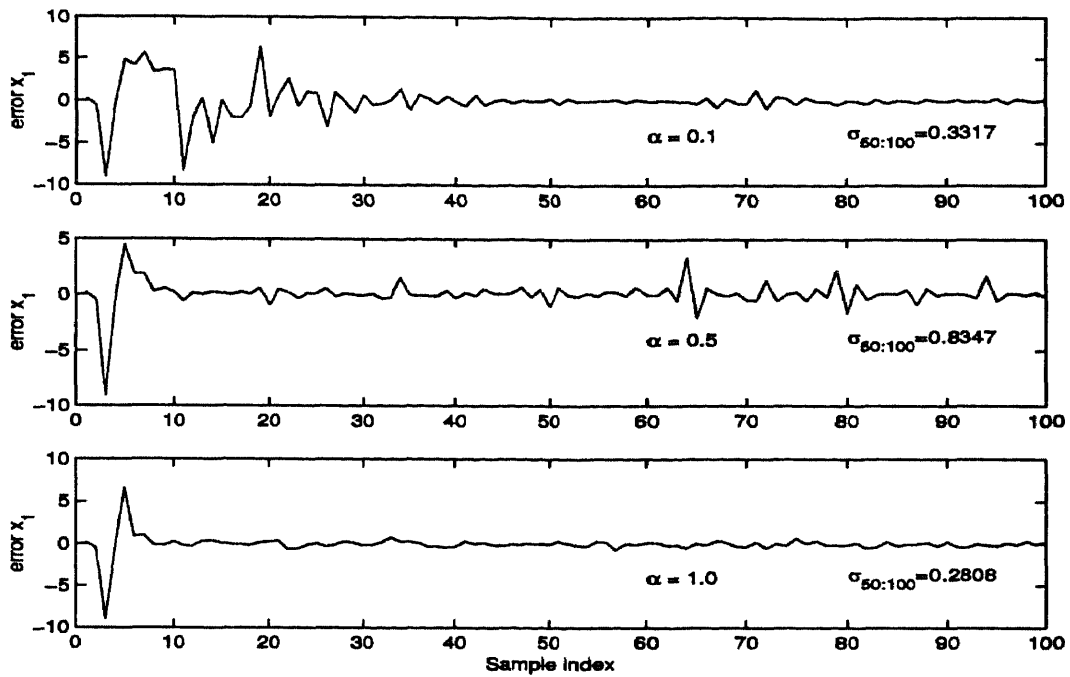


Figure 6.13 Modified Moraal/Grizzle observer estimation error of state x_1 for different values of α . Measurement noise present.

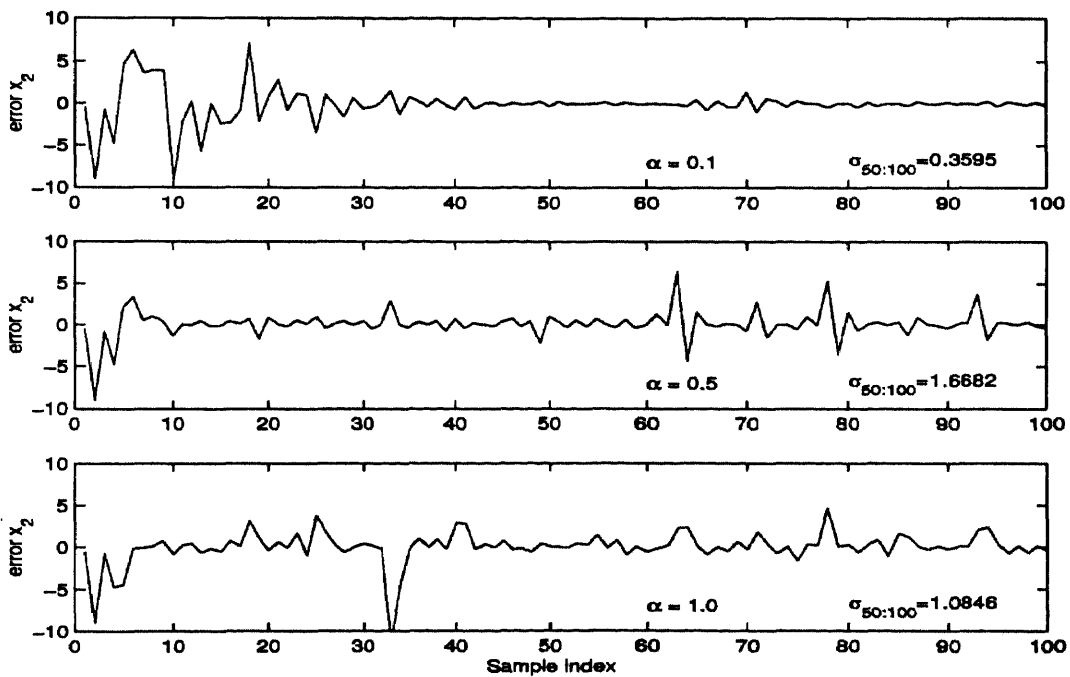


Figure 6.14 Modified Moraal/Grizzle observer estimation error of state x_2 for different values of α . Measurement noise present.

6.2.3 Modified Ciccarella Observer

Using the state vector definition of X from (6.23), the forward dynamics function for $X_{k+1} = f(X_k, u_k)$, (6.24), and output equation (6.29), the modified Ciccarella Observer was applied to this ARMA parameter estimation problem

$$\tilde{z}_{k+1} = f(z_k, u(k-3)) \quad (6.37)$$

$$P = APA' + Q \quad (6.38)$$

$$Y_k = \begin{bmatrix} y_{k-3} & y_{k-2} & y_{k-1} & y_k \end{bmatrix}' \quad (6.39)$$

$$U_k = \begin{bmatrix} u_{k-3} & u_{k-2} & u_{k-1} & u_k \end{bmatrix}' \quad (6.40)$$

$$\tilde{y}_{k+1} = h(f(f(f(\tilde{z}_k, u_{k-2}), u_{k-1}), u_k)) \quad (6.41)$$

$$K = P(P + W)^{-1} \quad (6.42)$$

$$\rho = Y_k - \tilde{Y}_k \quad (6.43)$$

$$z_{k+1} = \tilde{z}_k + J(\tilde{z}_k, U_k)^{-1}[B(y_{k+1} - \tilde{y}_{k+1}) + K\rho] \quad (6.44)$$

$$P = (I - K)P \quad (6.45)$$

$$\dot{X}_{k+1} = f(f(f(z_{k+1}, u_{k-3}), u_{k-2}), u_{k-1}), \quad (6.46)$$

where

$$A = \begin{bmatrix} 0 & 1 & 0 \\ 0 & 0 & 1 \\ 0 & 0 & 0 \end{bmatrix} \quad B = \begin{bmatrix} 0 \\ 0 \\ 1 \end{bmatrix}. \quad (6.47)$$

The initial conditions and the input for this simulation were the same as those used in section 6.2.1 (see table 6.1). A square wave, $u_k = 10 \text{ sign}(\sin 2\pi 0.067k)$ was applied to the input. Two simulations runs were made, one without noise and one with noise. The noise process, η , was white Gaussian, $\eta \in N\{0, 0.30\}$ and it was added to the measurement.

For the modified Ciccarella observer described in section 4.2.3 the feedforward term is eliminated ($B = 0$). By eliminating this term the noise properties are

improved but the stability of the observer can no longer be guaranteed. After numerous attempts using different values for Q , W , and P_0 (initial covariance), a stabilizing set was not found. The feedforward term was subsequently implemented and then a stabilizing set was found. *The necessity of this term and its implied unity gain factor on the measurement noise leads to a steady-state noise floor on the state estimates.* This noise floor does not exist for the modified Moraal/Grizzle observer.

The need for this feedforward term in this application is understood from figures 6.15 and 6.16. Figure 6.15 shows very large transient responses of the state estimates. In particular, the transient of estimate x_4 exceeds four orders of magnitude. (No transient response of this magnitude has been seen for the modified Moraal/Grizzle observer.) Figure 6.16 shows the condition number of the Jacobian used for this observer and it too has a transient exceeding four orders of magnitude.⁶ The Jacobian of this estimator is the observability matrix so this transient in condition number implies that the observer passes through a period of marginal observability. Furthermore, this poor conditioning implies a very large sensitivity of the *gains* of estimator to errors in residual since the effective gains on the residual are $J^{-1}K$.

Figures 6.17–6.20 demonstrate the performance of the observer in this application. The results are summarized in table 6.3. For parameter estimates p_1 , p_2 , the modified Moraal/Grizzle observer demonstrated better steady-state noise performance. For state estimates x_1 , x_2 , the modified Ciccarella observer and the modified Moraal/Grizzle observer demonstrated nearly equivalent performance. The transient settling time of the modified Ciccarella observer was about equivalent to that of the modified Moraal/Grizzle observer for $\alpha = 1$. The magnitude of the transient peaks of the modified Ciccarella observer were worse than that of the modified Moraal/Grizzle observer.

⁶It is also interesting to note from this figure the effect of the control upon observability. The observability is enhanced, in particular by the negative swings in the control input. The observability deteriorates over the periods of constant input.

Table 6.3 Transient peaks, transient response, and steady-state noise level for modified Ciccarella observer applied to ARMA parameter estimation.

	Transient Peak	Transient Response ^a	Steady-state Noise ^b
p_1	35	11	0.066
p_2	48	11	0.081
x_1	225	9	0.291
x_2	11000	13	0.991

^aSample index at which error is reduced 90% from its peak value.

^bSteady-state noise is given in terms of standard deviation of simulation points 50:100.

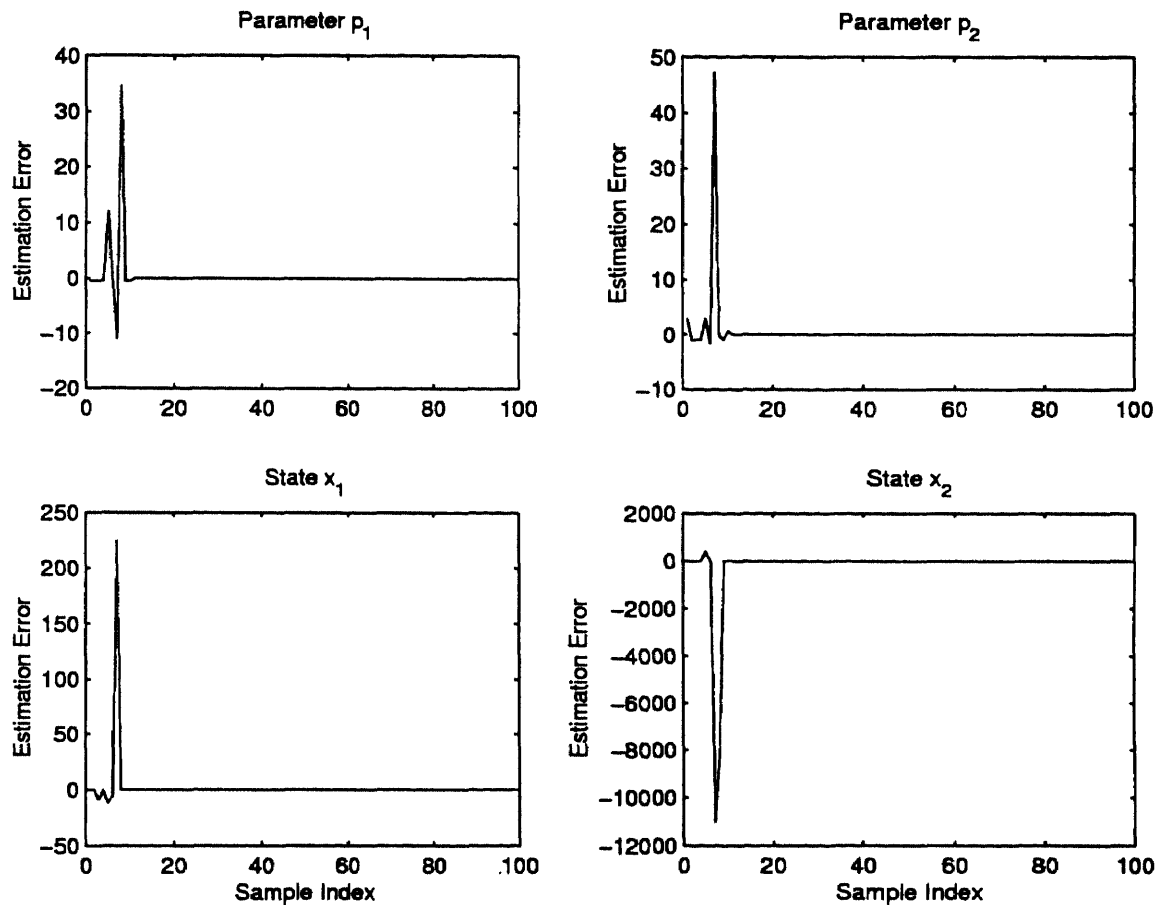


Figure 6.15 Modified Ciccarella observer error transient response for the ARMA parameters and state estimation. No noise. Feedforward present.

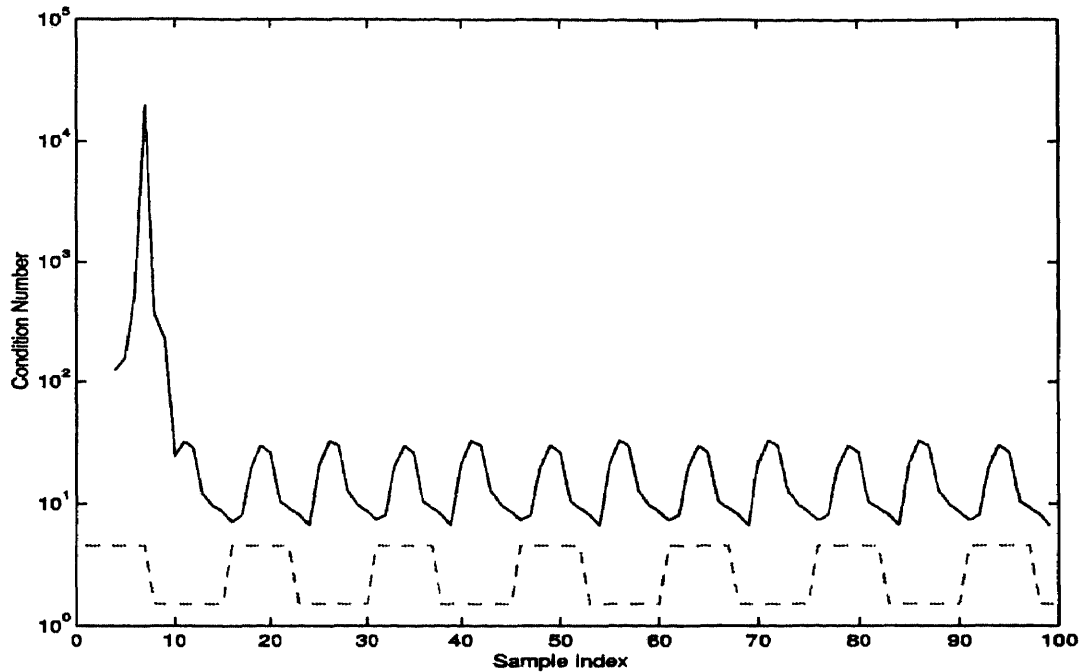


Figure 6.16 Condition number of observability matrix for the modified Ciccarella observer. Excitation input (dashed), not to scale, is also shown.

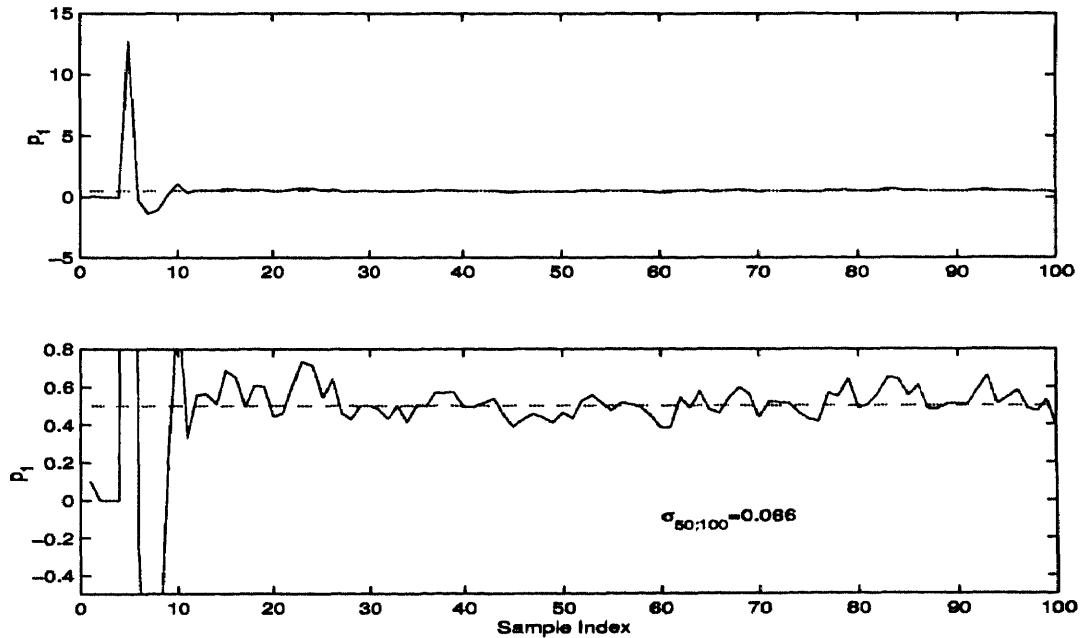


Figure 6.17 Modified Ciccarella estimation of ARMA coefficient p_1 (solid) and true value (dashed), measurement noise present, feedforward present. Magnification in bottom figure.

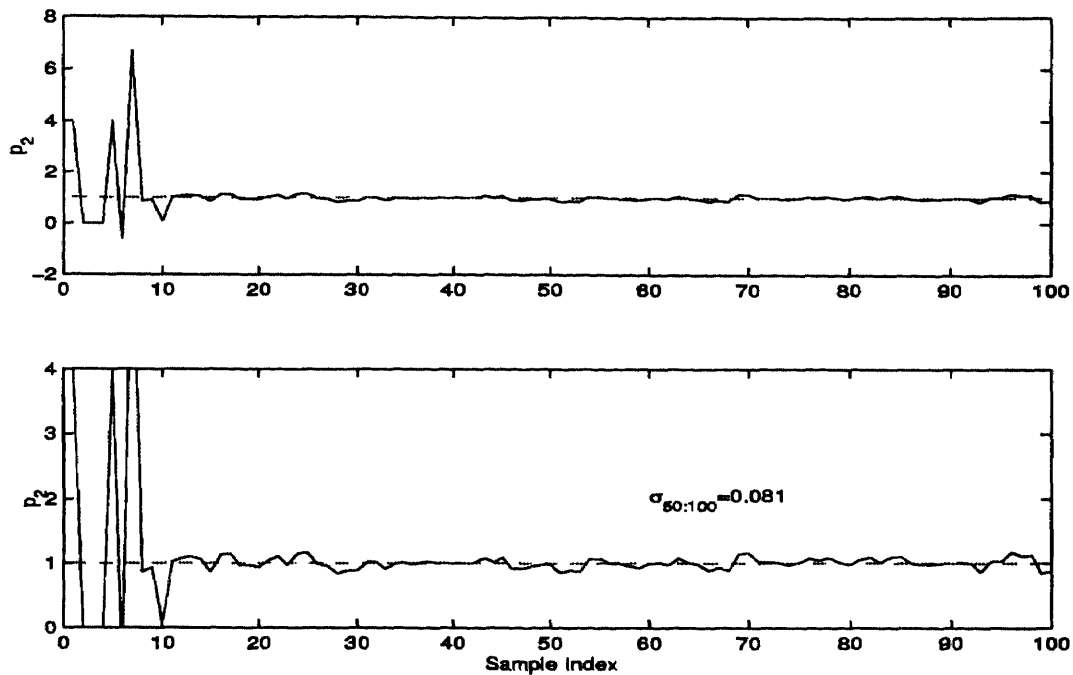


Figure 6.18 Modified Ciccarella estimation of ARMA coefficient p_2 , measurement noise present, feedforward present. Magnification in bottom figure.

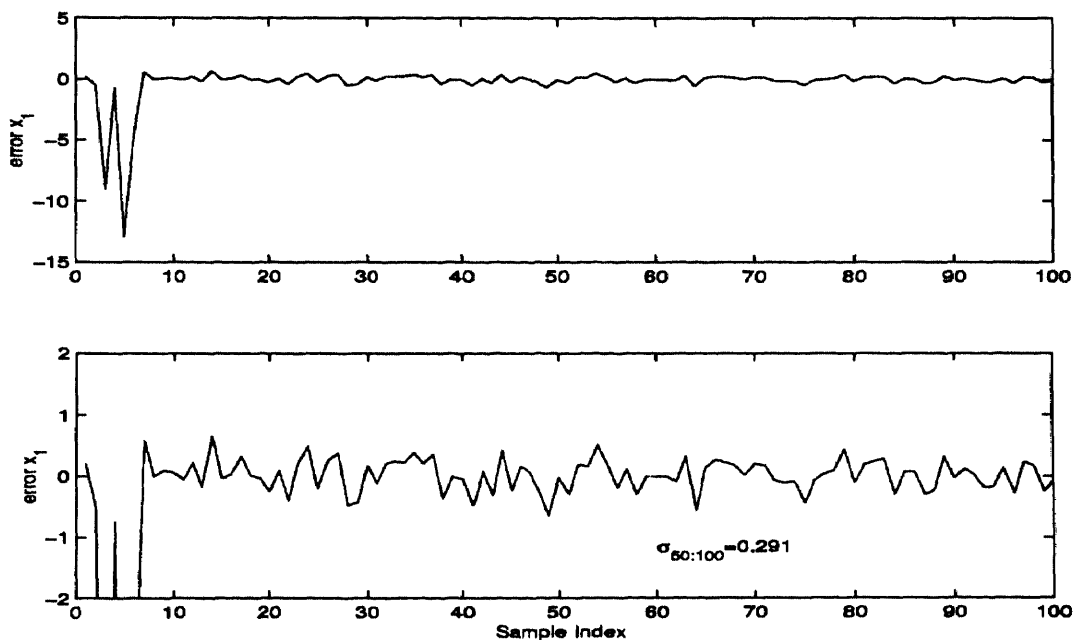


Figure 6.19 Modified Ciccarella estimation of ARMA state x_1 , measurement noise present, feedforward present. Magnification in bottom figure.

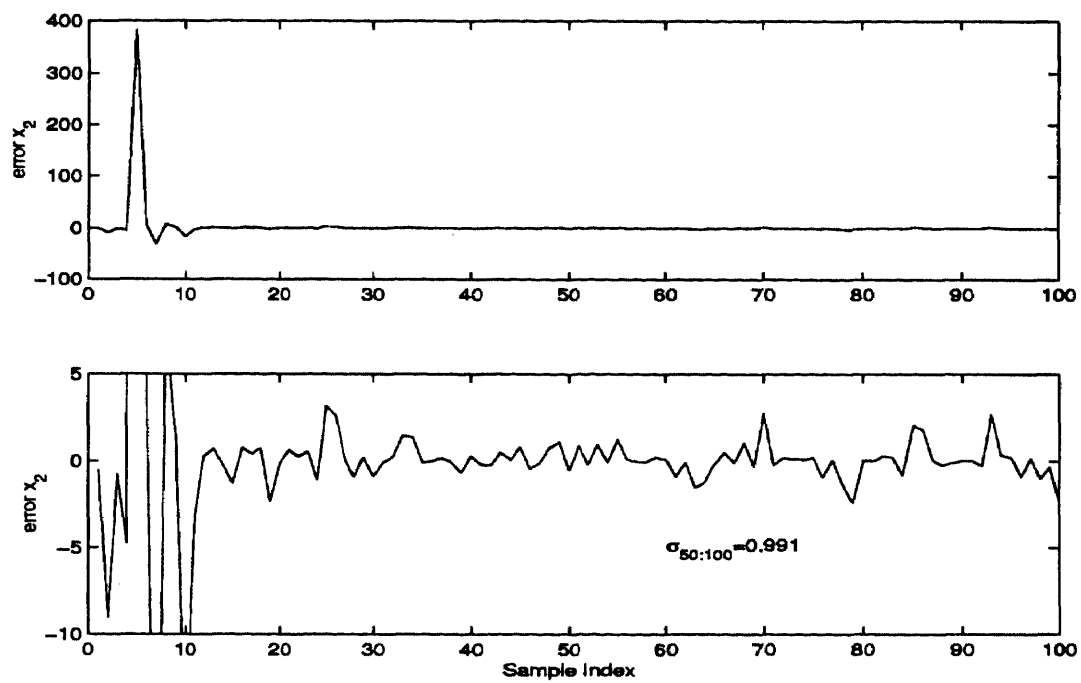


Figure 6.20 Modified Ciccarella estimation of ARMA state x_2 , measurement noise present, feedforward present. Magnification in bottom figure.

6.3 Canine Blood Pressure Response to Nitropruside

In many problems in physiology, economics, and chemical processing the basic principles underlying the plant dynamics are often not well understood. In such instances system identification techniques using polynomial models are used to describe the system. The following example, courtesy of Ü. Kotta, represents a polynomial model of canine blood pressure response to the drug nitropruside. The model was identified using the technique described in [8].

A dog was infused with the drug Nitropruside to control his blood pressure. The control input is the infusion rate measured in units milliliters/hour. The measured output is the main arterial blood pressure measured in units millimeters of mercury. The following three-state polynomial system was identified which describes the dog's response to the drug:

$$x_{k+1} = [F_0 + u_k F_1 + u_k^2 F_2] x_k + u_k G_1 + u_k^2 G_2 \quad (6.48)$$

$$y_k = [H_0 + u_k H_1] x_k \quad (6.49)$$

where

$$F_0 = \begin{bmatrix} 0.8088 & 1.0 & 0.3614 \\ 0.0857 & 0.0 & -0.296 \\ -0.1692 & 0 & 0.0898 \end{bmatrix}$$

$$F_1 = \begin{bmatrix} 0.0247 & -0.0241 & 0.0049 \\ 0.0105 & 0.0053 & 0.004 \\ -0.0055 & -0.0025 & -0.0012 \end{bmatrix}$$

$$\begin{aligned}
F_2 &= \begin{bmatrix} 0.0002 & -0.00010 & \\ -0.0002 & 0.0002 & 0 \\ -0.0002 & 0.0001 & 0 \end{bmatrix} \\
G_1 &= \begin{bmatrix} 0 & 1 & 0 \end{bmatrix}' \\
G_2 &= \begin{bmatrix} 0.0151 & -0.0289 & 0.0085 \end{bmatrix}' \\
H_0 &= \begin{bmatrix} -0.1024 & 0.019 & -0.0539 \end{bmatrix} \\
H_1 &= \begin{bmatrix} -0.0031 & -0.002 & -0.0004 \end{bmatrix}
\end{aligned}$$

Two sets simulations were performed for the Grossman observer, the Moraal/Grizzle observer, and Ciccarella observer, with these latter two observers implemented in their original and in their modified forms. In the first simulation, noise-free measurements were used. In the second simulation, measurements were corrupted with white Gaussian noise resulting in a 3 dB power signal-to-noise (S/N) ratio⁷. The observers were coded in Matlab (see appendix B). The code reveals the necessity for the delays that the theory calls for and illustrates the propagation of the seed in the nonlinear solver.

The control input consisted of a symmetric, 50% duty-cycle square wave of unity amplitude, with a ten-sample period, i.e.,

$$u_k = \begin{cases} 1 & \text{for } k \bmod 10 < 5, \\ -1 & \text{for } k \bmod 10 \geq 5. \end{cases} \quad (6.50)$$

Simulation runs with a $u_k = \pm 10$ amplitude square wave were also performed with results qualitatively similar to $u_k = \pm 1$. (See section A.4.)

The initial conditions for the three simulations were the same and are given in table 6.4.

⁷Noise standard deviation, $\sigma_{\text{noise}} = 0.707\sigma_y$, where y is measured output.

Table 6.4 Initial conditions for Canine blood pressure observer simulation.

Variable	True Value	Initial Estimate
x_1	0.5	-3.0
x_2	-.70	-3.0
x_3	2.0	-3.0

6.3.1 Grossman Observer

Figure 6.21 shows the convergence of the three state estimates to their true values for the noise-free simulation. Figure 6.22 shows the state estimation error $\epsilon = \hat{x} - x$ for this same simulation. Figure 6.23 shows the residual process of the filter.

Figure 6.24 shows the noisy measurement driving the observer (the noise-free measurement is shown for reference.) Figure 6.25 shows the convergence of the state estimates to their true values even with the 3 dB S/N of the measurement. Figure 6.26 shows the state estimation error. Figure 6.27 shows the residual process of the filter with the noisy measurement.

Table 6.5 shows a summary of mean and standard deviation ($\bar{\epsilon}_x$, σ_{ϵ_x} respectively) for the three state estimates given by the Grossman observer for different values α and d in the Newton solver. From table 6.5 it is seen that for a given $\alpha < 1$, increasing d is detrimental to noise rejection. It is also seen that increasing d compromises the *achievable* noise rejection improvement. Increasing iterations drives the observer to the instantaneous solution for the noisy data and essentially “weighs” the most recent measurements more than the past measurements.

6.3.2 Original Moraal/Grizzle Observer

Figure 6.28 shows the convergence of the three state estimates to their true values for the noise-free simulation. Figure 6.29 shows the state estimation error $\epsilon = \hat{x} - x$ for this same simulation. Figure 6.30 shows the convergence of the state estimates

Table 6.5 Estimation statistics for three-state model of dog blood pressure response to medication using Grossman Observer. Measurement noise present.

α	d	$\bar{\epsilon}_{x1}^a$	$\bar{\epsilon}_{x2}^a$	$\bar{\epsilon}_{x3}^a$	$\sigma_{\epsilon_{x1}}^b$	$\sigma_{\epsilon_{x2}}^b$	$\sigma_{\epsilon_{x3}}^b$
1.0	1	0.43049	-0.12760	-0.15481	0.72631	0.54168	0.27683
0.5	1	0.14274	-0.03927	-0.05379	0.35393	0.26761	0.13957
0.1	1	0.02189	-0.00571	-0.00858	0.06946	0.05315	0.02802
1.0	5	0.43049	-0.12760	-0.15481	0.72631	0.54168	0.27683
0.5	5	0.40535	-0.11953	-0.14617	0.70245	0.52429	0.26834
0.1	5	0.10962	-0.02979	-0.04167	0.28858	0.18790	0.11443

^aMean error.

^bStandard deviation.

to their true values with the 3 dB S/N of the measurement. Figure 6.31 shows the state estimation error.

6.3.3 Modified Moraal/Grizzle Observer

The Moraal/Grizzle observer was modified and implemented with the “slowing factor” $\alpha = 0.1$ instead of $\alpha = 1$ as in its original form. Figure 6.32 shows the convergence of the three state estimates to their true values for the noise-free run. Figure 6.33 shows the state estimation error $\epsilon = \hat{x} - x$ for the same run. The comparison between the estimation errors of the original observer, figure 6.29, with the that of the modified observer, 6.33 shows that the original observer demonstrates deadbeat response with the error converging to zero in three steps. The modified observer shows a slower transient response.

Figure 6.34 shows the convergence of the three state estimates to their true values for the run with measurement noise. Figure 6.35 shows the state estimation error for the same run. The comparison between the estimation errors of the original observer, figure 6.33, with the that of the modified observer, 6.35 shows that the modified observer demonstrates superior noise rejection performance.

Table 6.6 Estimation statistics for three-state model of dog blood pressure response to medication using Moraal/Grizzle Observer. Measurement noise present.

α	d	$\bar{\epsilon}_{x1}^a$	$\bar{\epsilon}_{x2}^a$	$\bar{\epsilon}_{x3}^a$	$\sigma_{\epsilon_{x1}}^b$	$\sigma_{\epsilon_{x2}}^b$	$\sigma_{\epsilon_{x3}}^b$
1.0	1	-0.19253	-0.03057	0.04003	1.44031	0.18483	0.27551
0.5	1	-0.18179	-0.02929	0.03799	0.81953	0.12269	0.16624
0.1	1	-0.10801	-0.01767	0.02635	0.26188	0.04273	0.05473
1.0	5	-0.19253	-0.03057	0.04003	1.44031	0.18483	0.27551
0.5	5	-0.19223	-0.03054	0.03998	1.39529	0.18062	0.26777
0.1	5	-0.17605	-0.02846	0.03682	0.71639	0.10995	0.14667

^aMean error.

^bStandard deviation.

Thus, as expected, this example demonstrates that the non-unity “slowing factor” α provides the capability to make the tradeoff between transient response and noise rejection. For the parameter estimation problem, noise rejection in the parameter estimates is critical but transient response is not. Thus in such situations it would be recommended to implement a slowing factor $\alpha \ll 1$.

Table 6.6 shows a summary of mean and standard deviation ($\bar{\epsilon}_x$, σ_{ϵ_x} respectively) for the three state estimates given by the Moraal/Grizzle observer for different values α and d . From table 6.6 it is seen that for a given $\alpha < 1$, increasing d is detrimental to noise rejection. It is also seen that increasing d compromises the *achievable* noise rejection improvement. Increasing iterations drives the observer to the instantaneous solution for the noisy data and essentially “weighs” the most recent measurements more than the past measurements.

6.3.4 Original Ciccarella Observer

The robust form of the Ciccarella observer was implemented with a stable arbitrary gain set. The gain set is given

$$K = \begin{bmatrix} -0.3 & 1 & 0 \\ 0 & -0.4 & 1 \\ 0 & 0 & -0.5 \end{bmatrix} \quad (6.51)$$

was used to place the closed-loop eigenvalues of $A - K$ at $\{0.3, 0.4, 0.5\}$.

Figures 6.36, 6.37 demonstrate the perform of the Ciccarella observer in the absence of noise. The estimator converges more slowly than the n samples required by the Moraal/Grizzle observer. The speed is a function of the gain set which, as mentioned, was chosen rather arbitrarily.

Figures 6.38, 6.39 demonstrate the performance of the same observer in the presence of 0 db S/N measurement noise. The observer estimates the general trend of the state with nearly zero mean error. The state estimates are noisy.

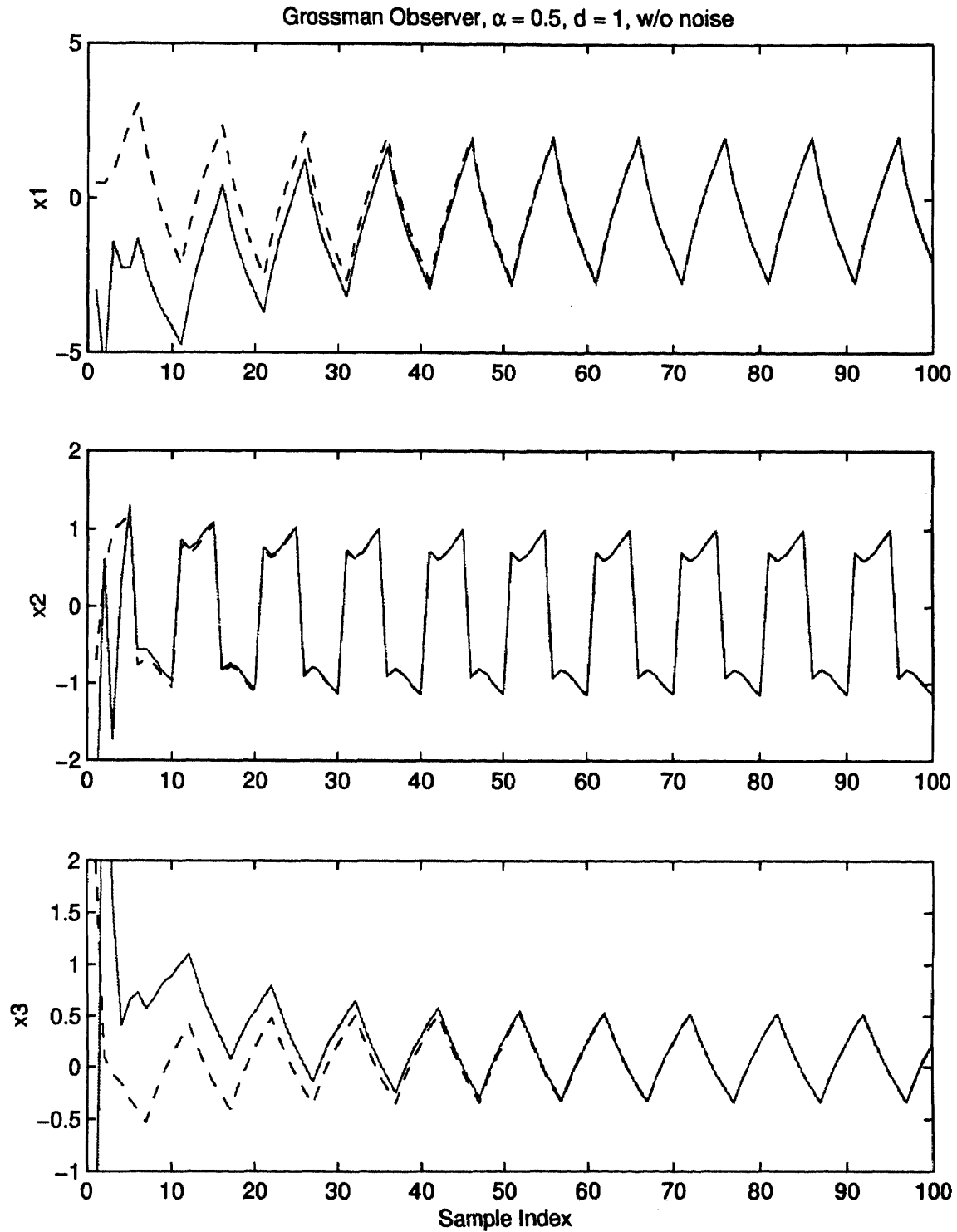


Figure 6.21 Grossman observer state estimate (solid) and true state (dotted) for three-state model of dog blood pressure response to medication. $\alpha = 0.5$, $d = 1$, no measurement noise present.

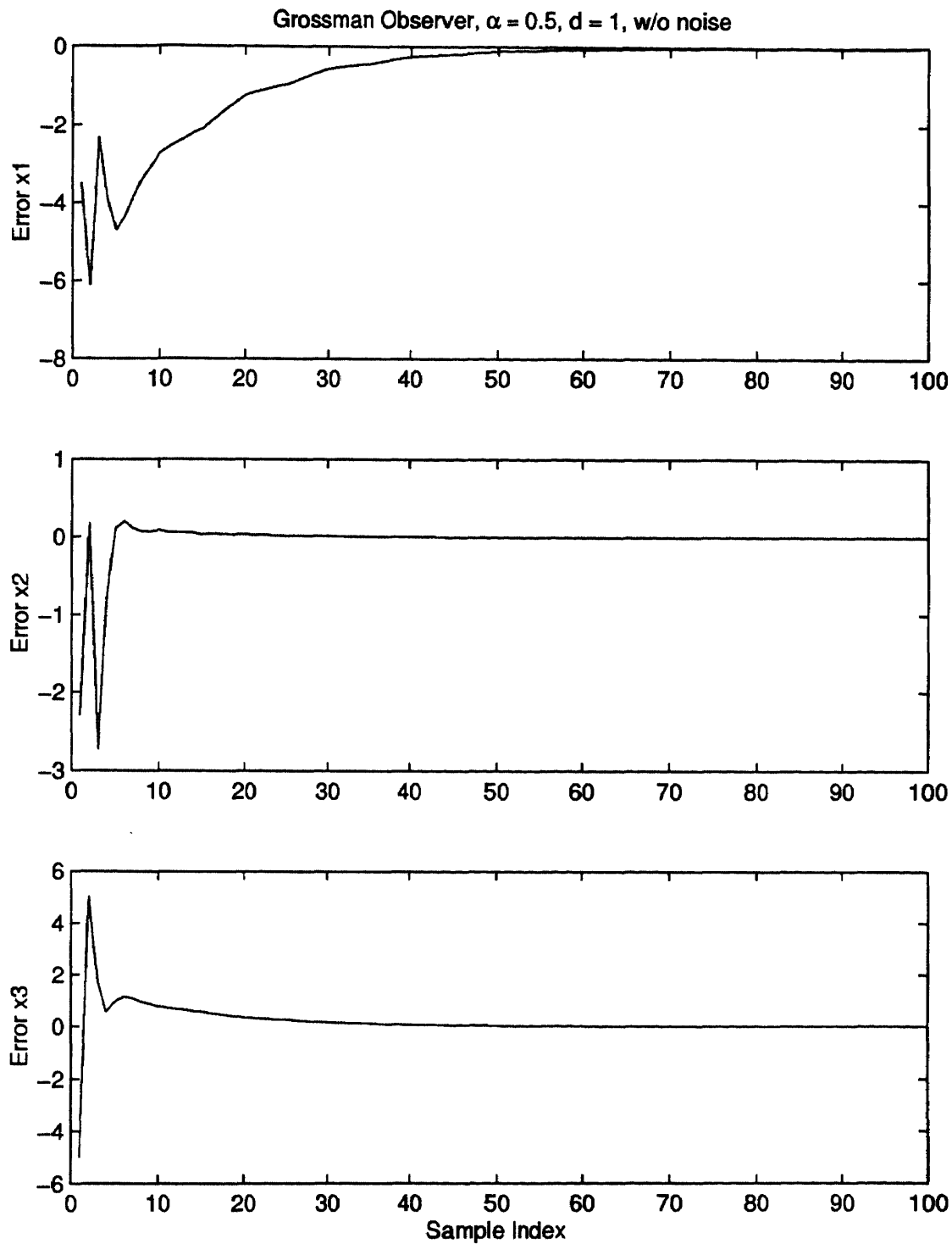


Figure 6.22 Grossman observer estimation error for three-state model of dog blood pressure response to medication. $\alpha = 0.5$, $d = 1$, no measurement noise present.

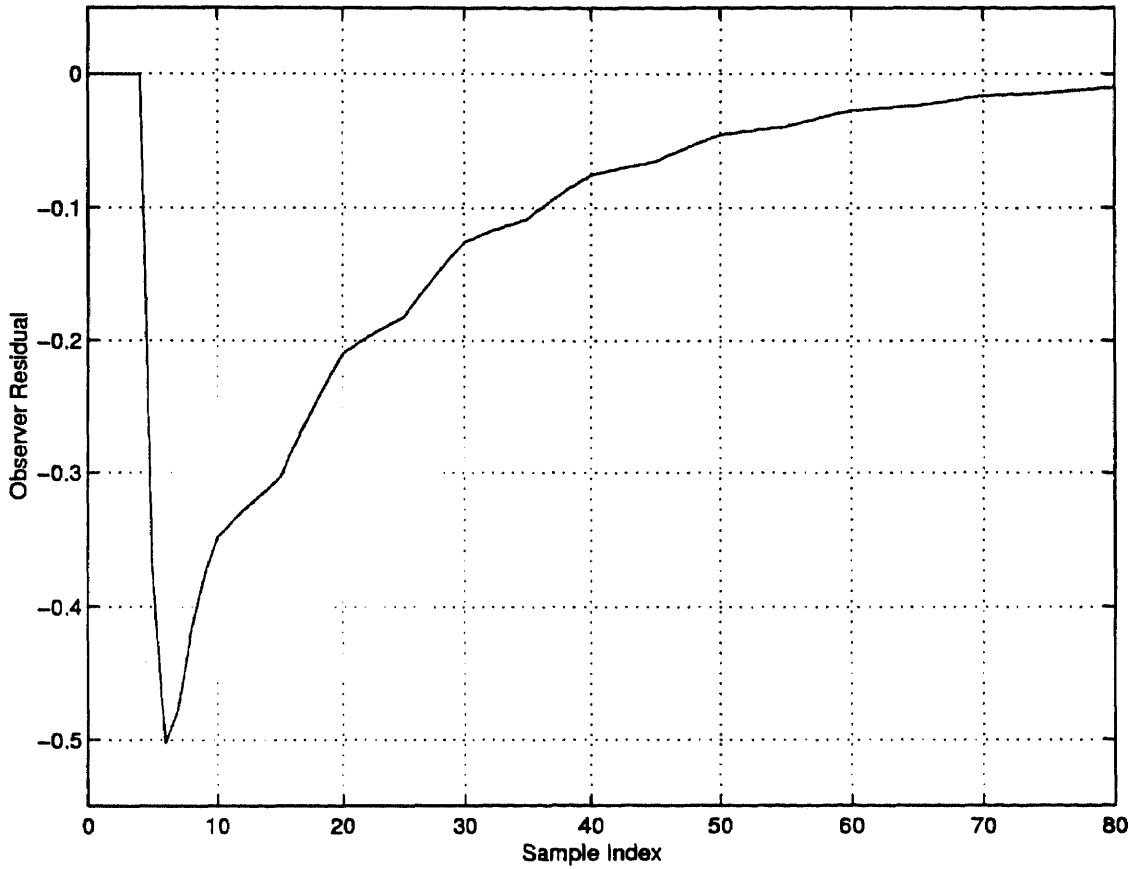


Figure 6.23 Grossman observer residual process for three-state model of dog blood pressure response to medication. No measurement noise.

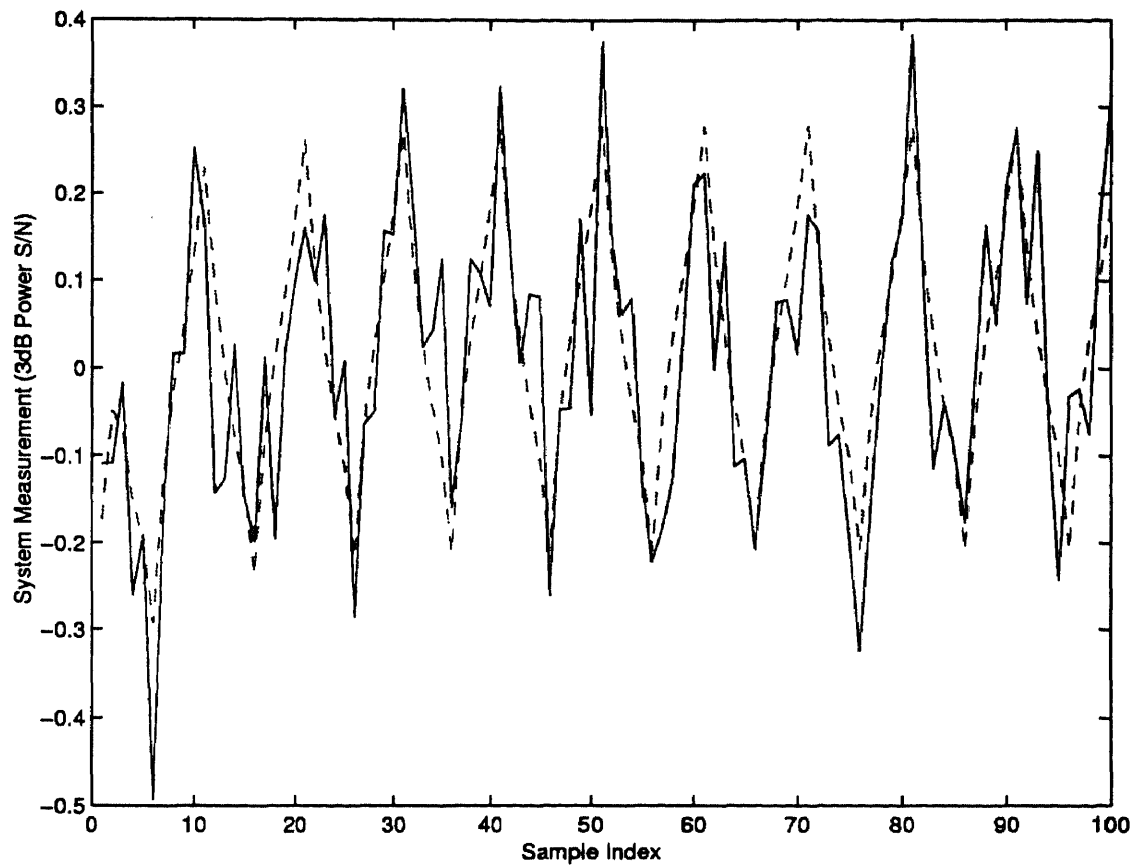


Figure 6.24 Measurement with 3 dB noise driving observer (solid). Noise-free measurement shown for reference (dashed).

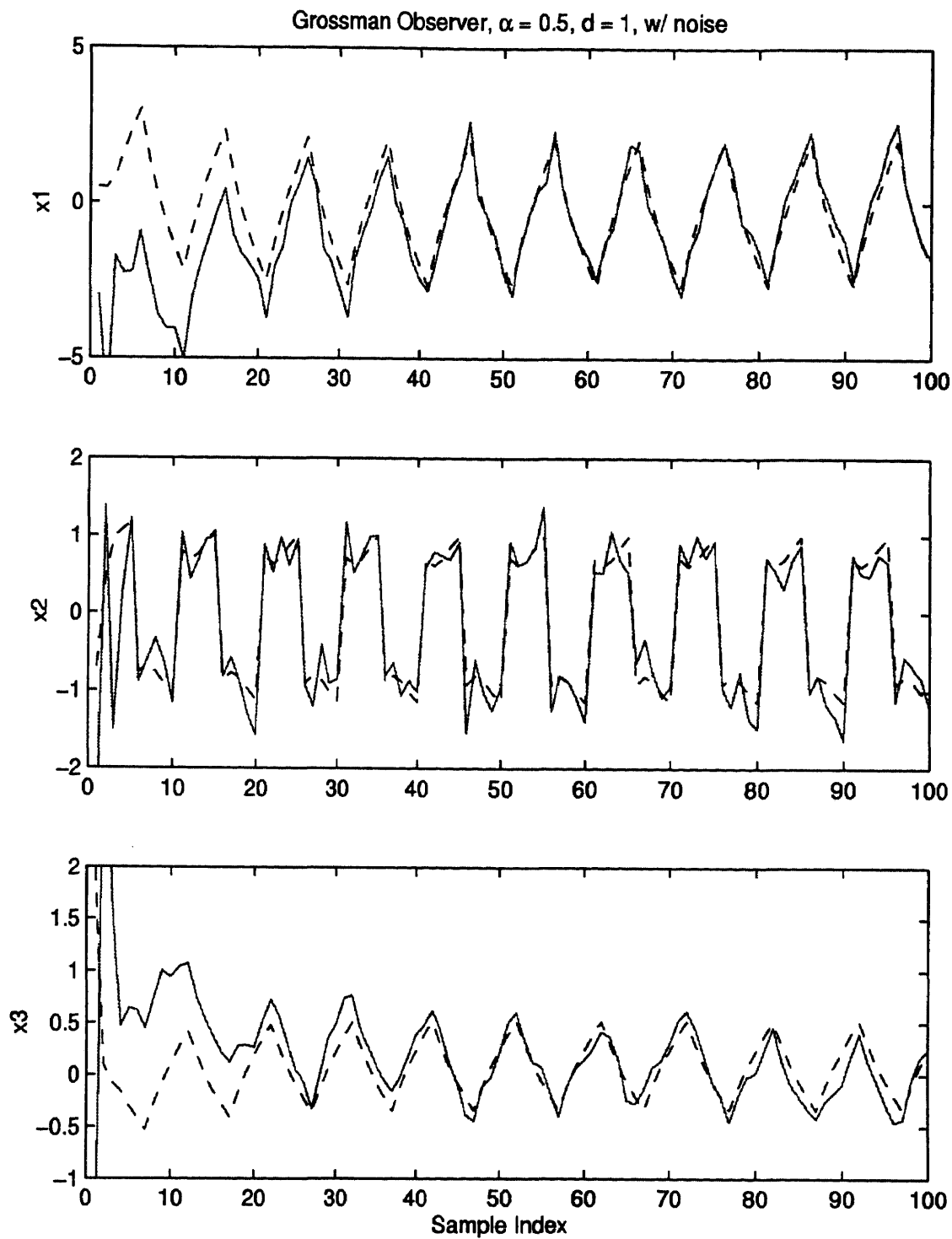


Figure 6.25 Grossman observer state estimate (solid) and true state (dotted) for three-state model of dog blood pressure response to medication. $\alpha = 0.5$, $d = 1$, measurement noise present.

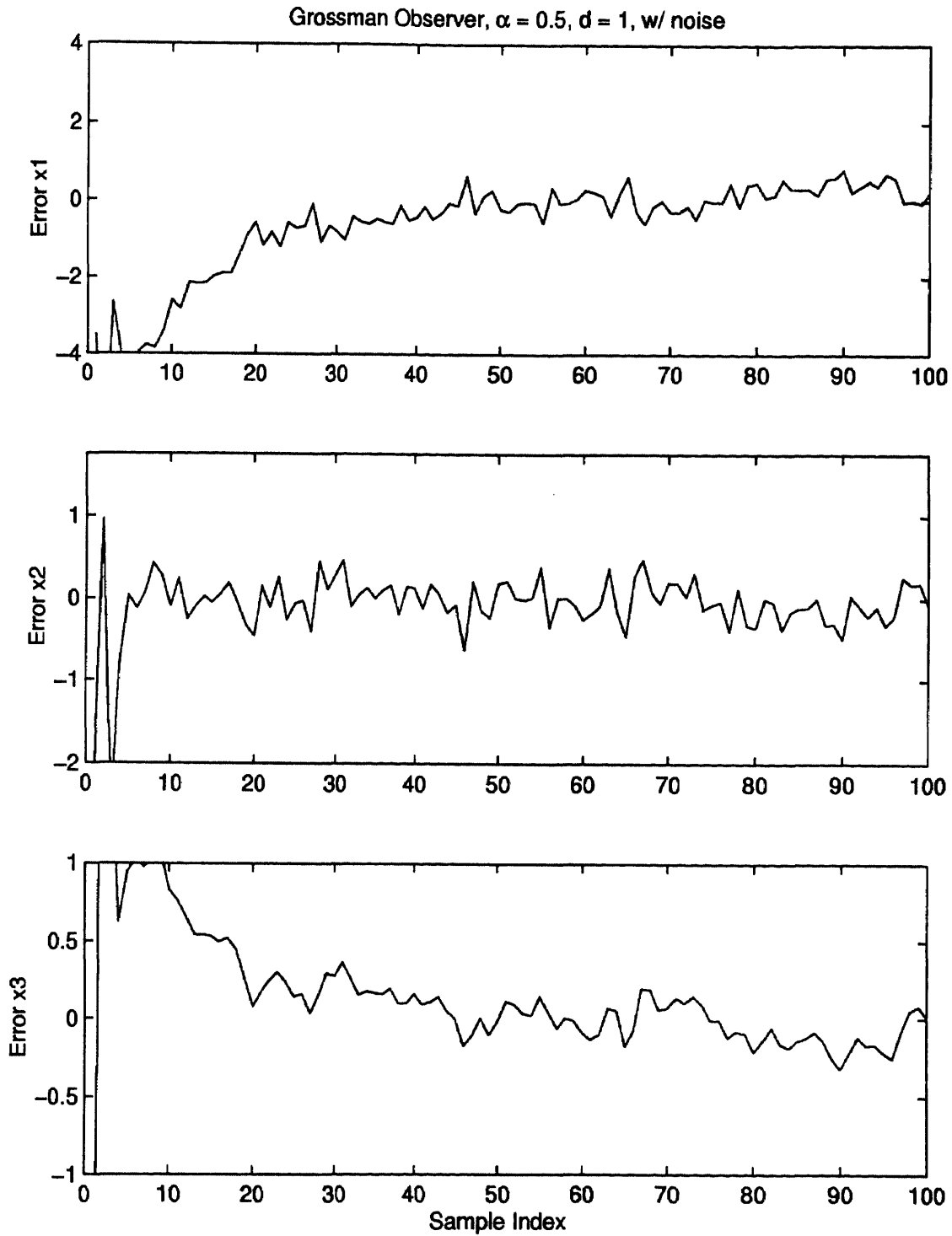


Figure 6.26 Grossman observer estimation error for three-state model of dog blood pressure response to medication. $\alpha = 0.5$, $d = 1$, measurement noise present.

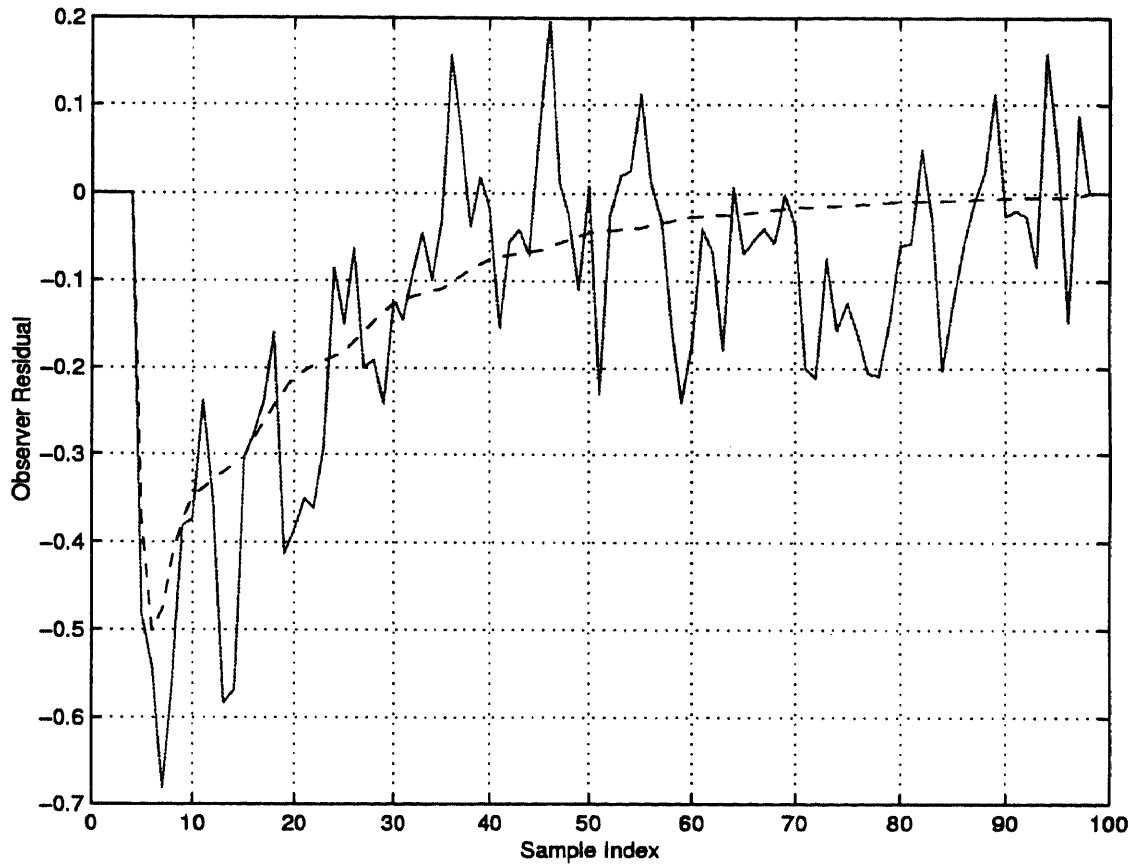


Figure 6.27 Grossman observer residual process for measurement with 3 dB S/N ratio (solid) and with no noise (dotted).

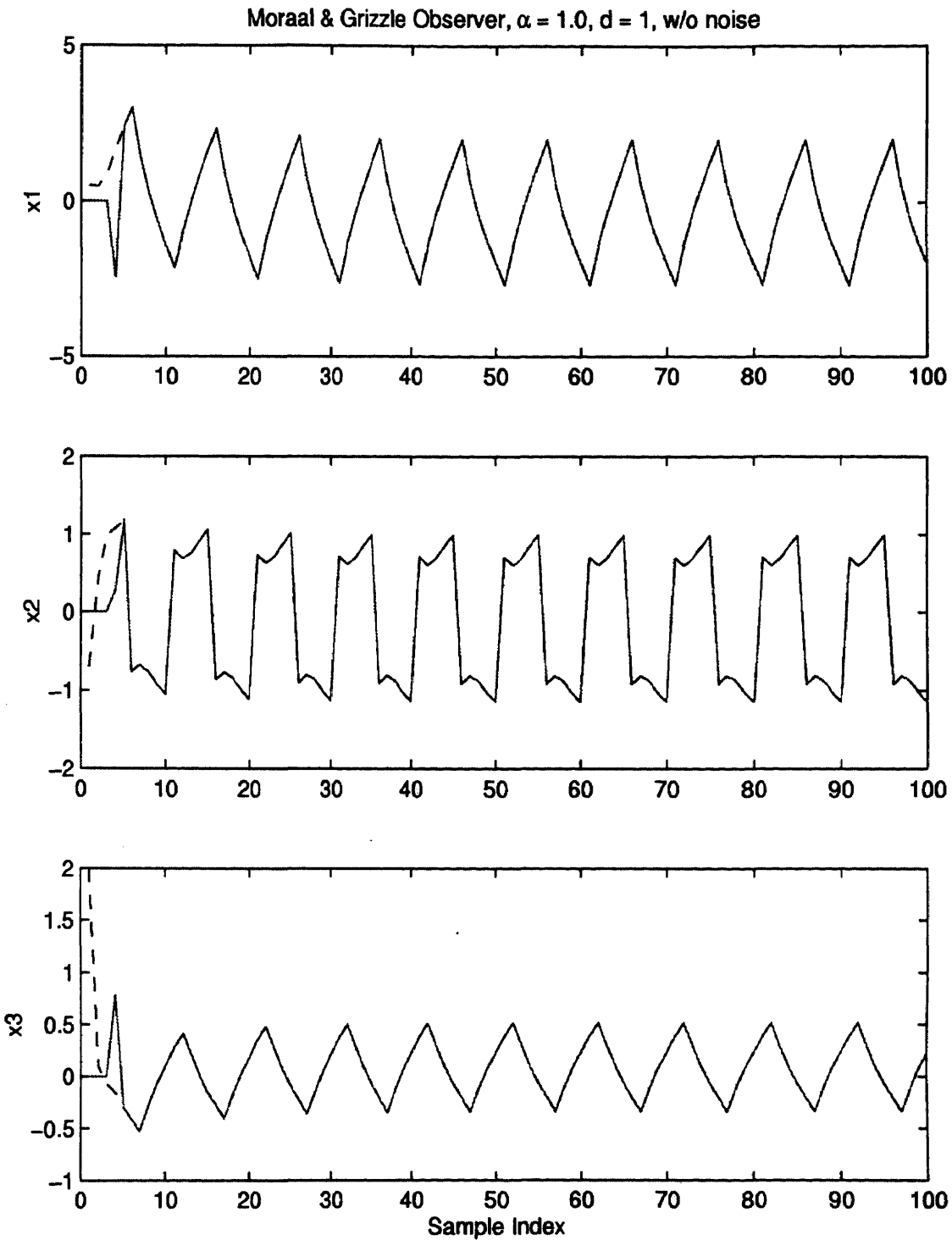


Figure 6.28 Moraal/Grizzle observer state estimate (solid) and true state (dotted) for three-state model of dog blood pressure response to medication. $\alpha = 1.0$, $d = 1$, no measurement noise present.

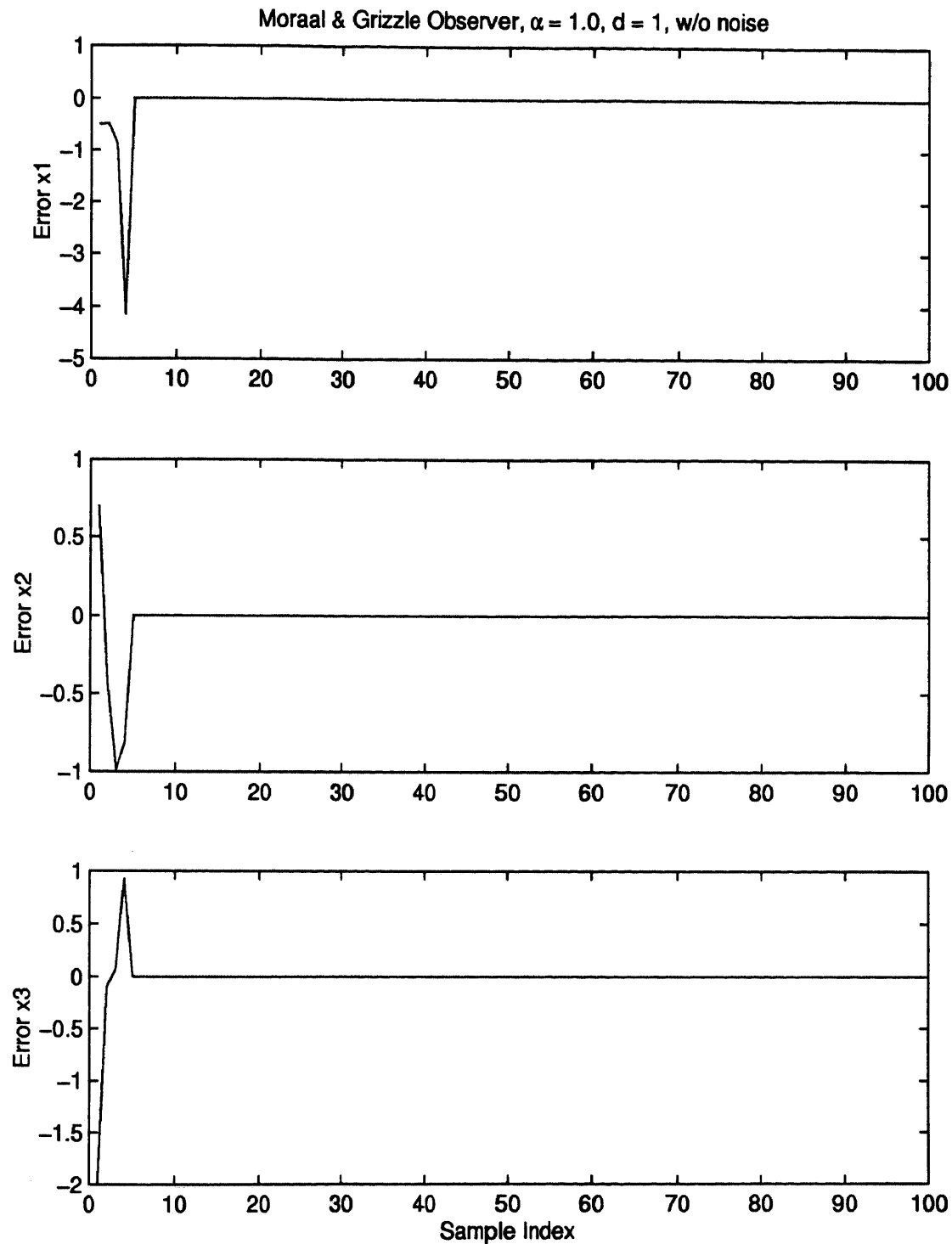


Figure 6.29 Moraal/Grizzle observer estimation error for three-state model of dog blood pressure response to medication. $\alpha = 1.0, d = 1$, no measurement noise present.

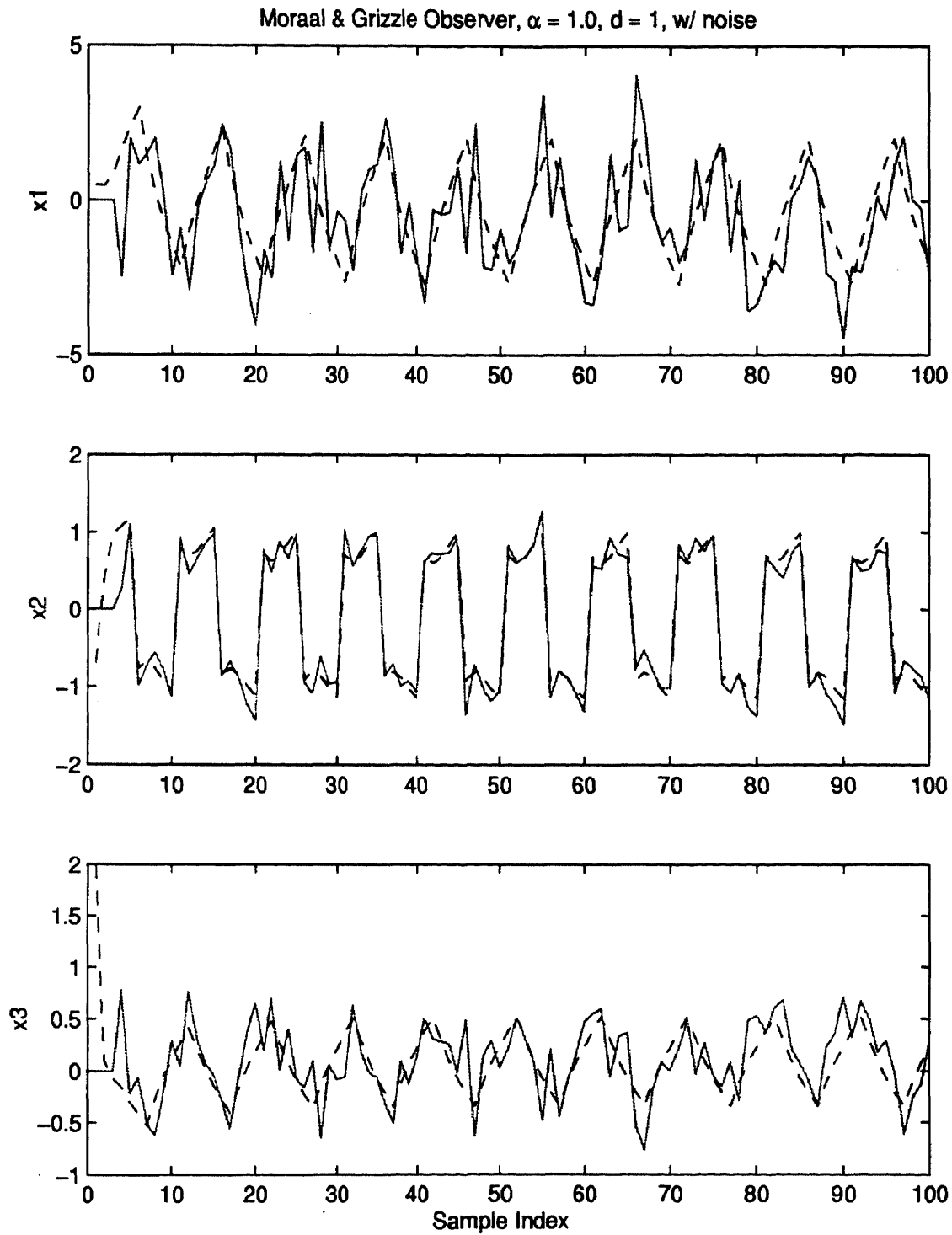


Figure 6.30 Moraal/Grizzle observer state estimate (solid) and true state (dotted) for three-state model of dog blood pressure response to medication. $\alpha = 1.0$, $d = 1$, measurement noise present.

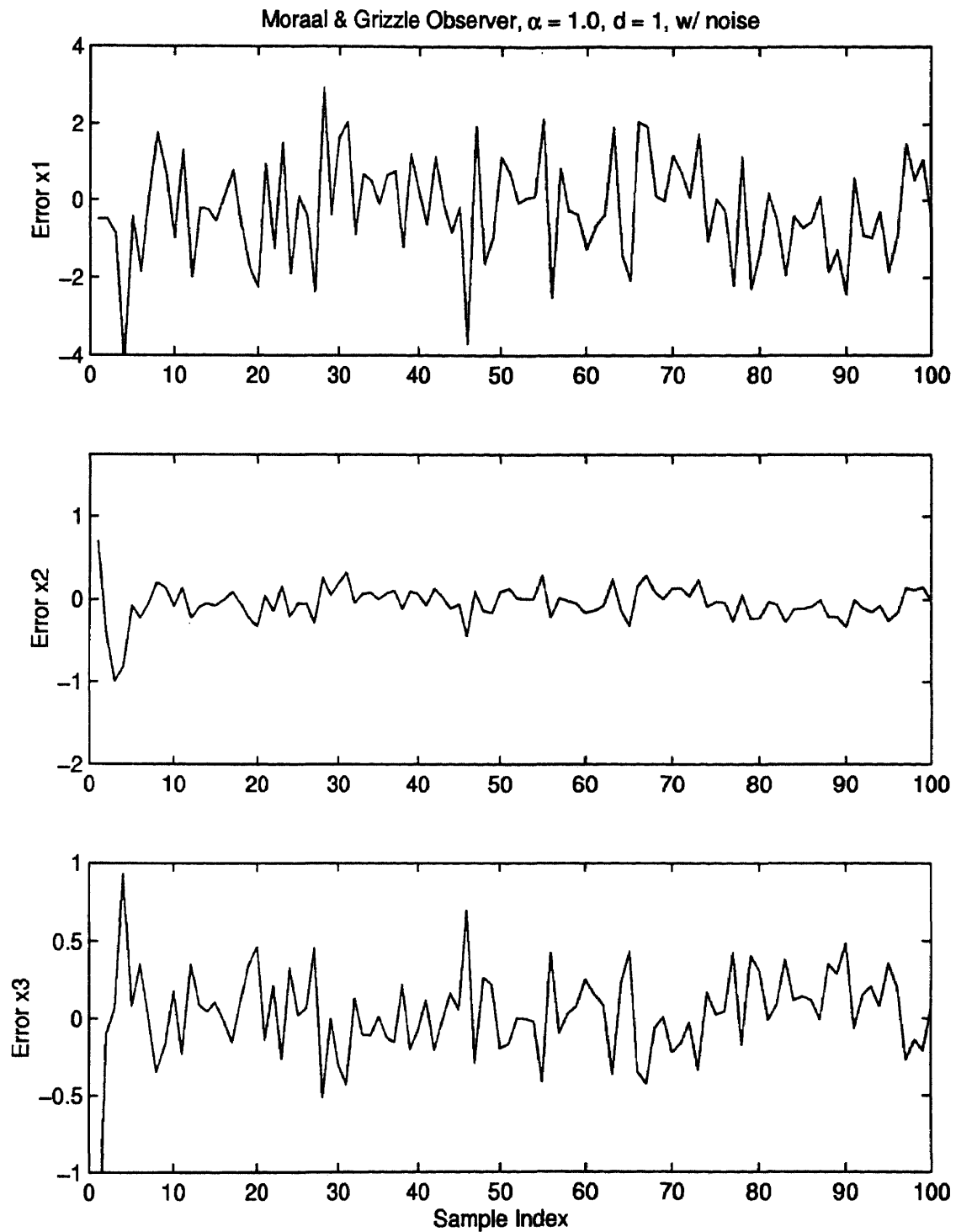


Figure 6.31 Moraal/Grizzle observer estimation error for three-state model of dog blood pressure response to medication. $\alpha = 1.0$, $d = 1$, measurement noise present.

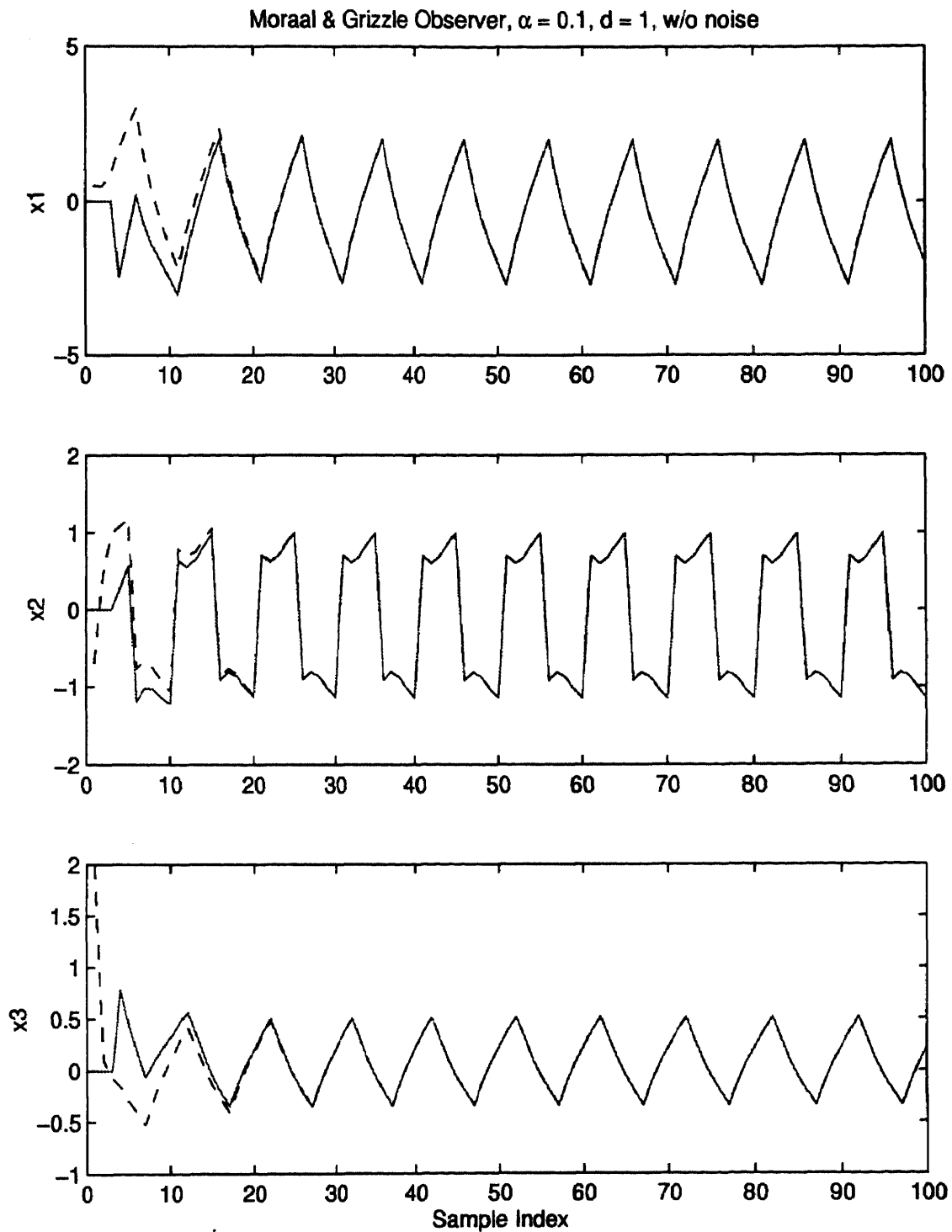


Figure 6.32 Moraal/Grizzle observer state estimate (solid) and true state (dotted) for three-state model of dog blood pressure response to medication. $\alpha = 0.1$, $d = 1$, no measurement noise present.

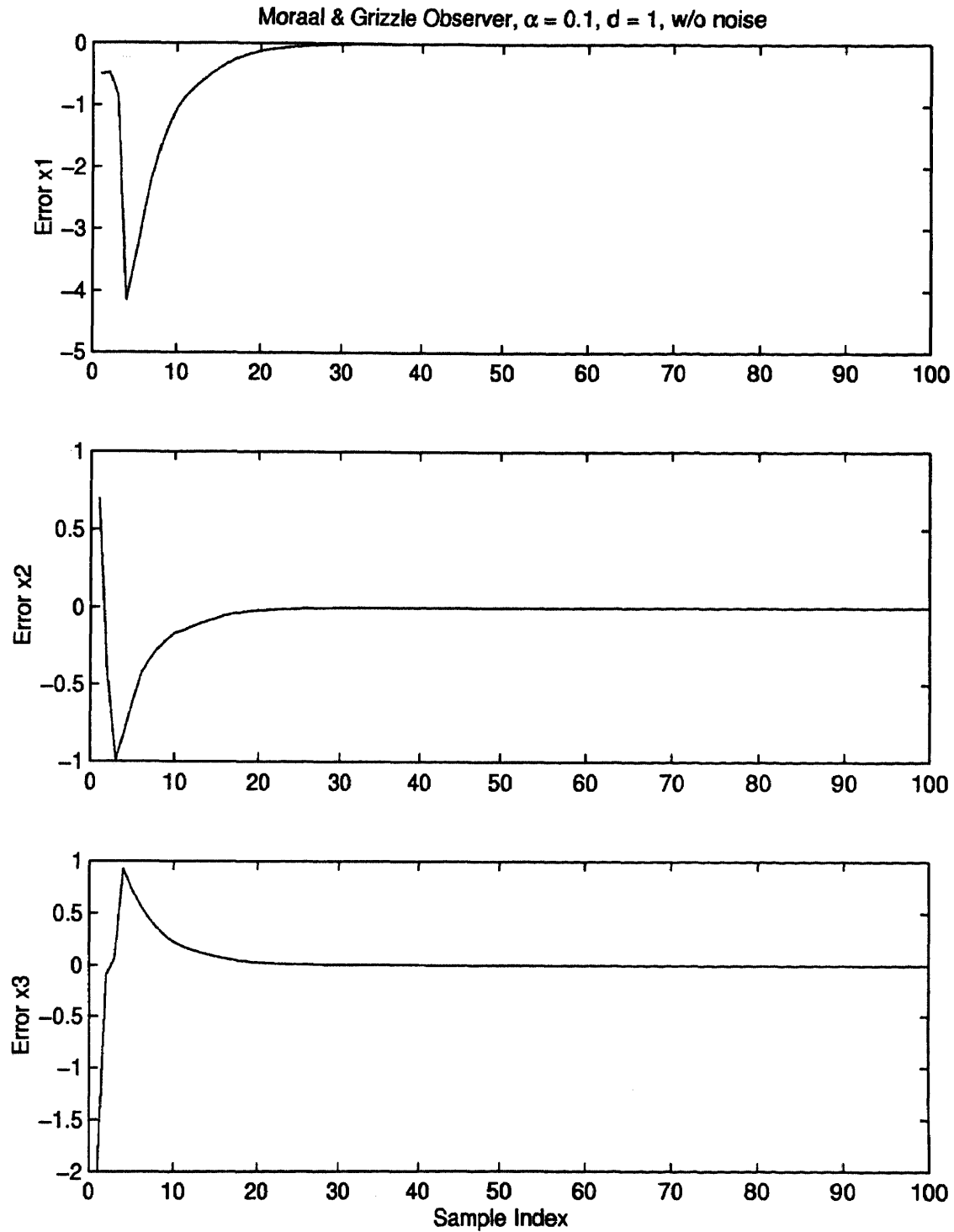


Figure 6.33 Moraal/Grizzle observer estimation error for three-state model of dog blood pressure response to medication. $\alpha = 0.1$, $d = 1$, no measurement noise present.

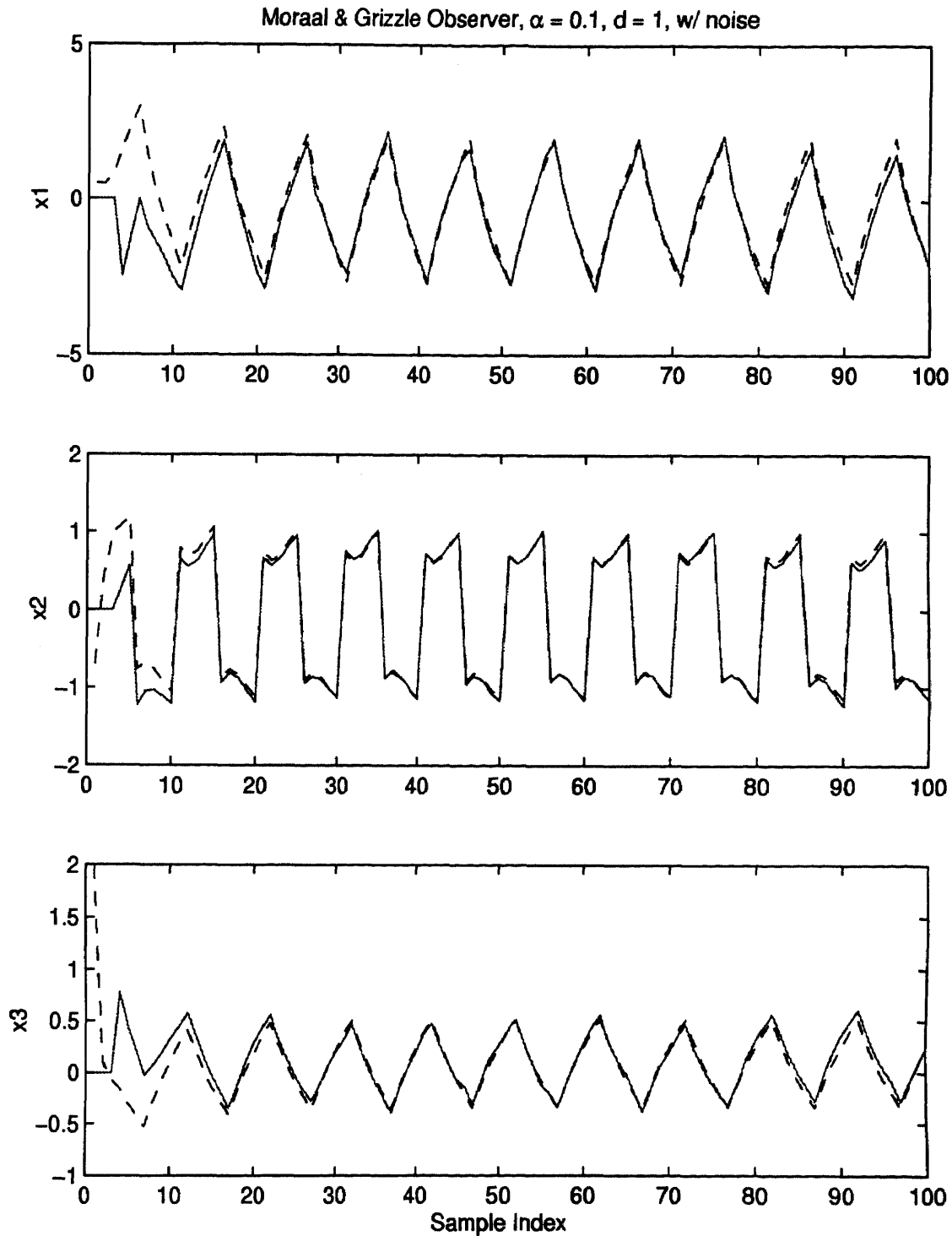


Figure 6.34 Moraal/Grizzle observer state estimate (solid) and true state (dotted) for three-state model of dog blood pressure response to medication. $\alpha = 0.1$, $d = 1$, measurement noise present.

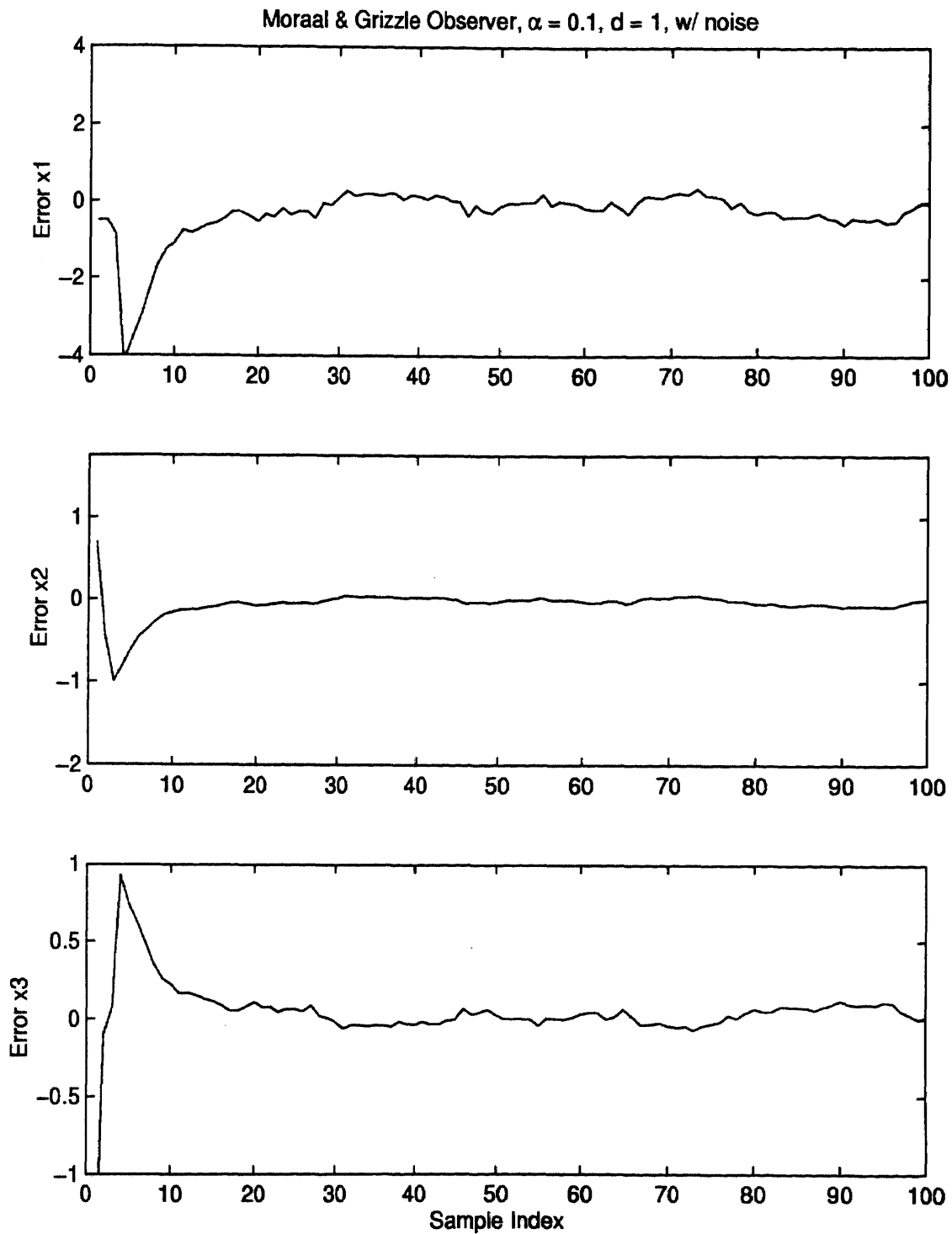


Figure 6.35 Moraal/Grizzle observer estimation error for three-state model of dog blood pressure response to medication. $\alpha = 0.1$, $d = 1$, measurement noise present.

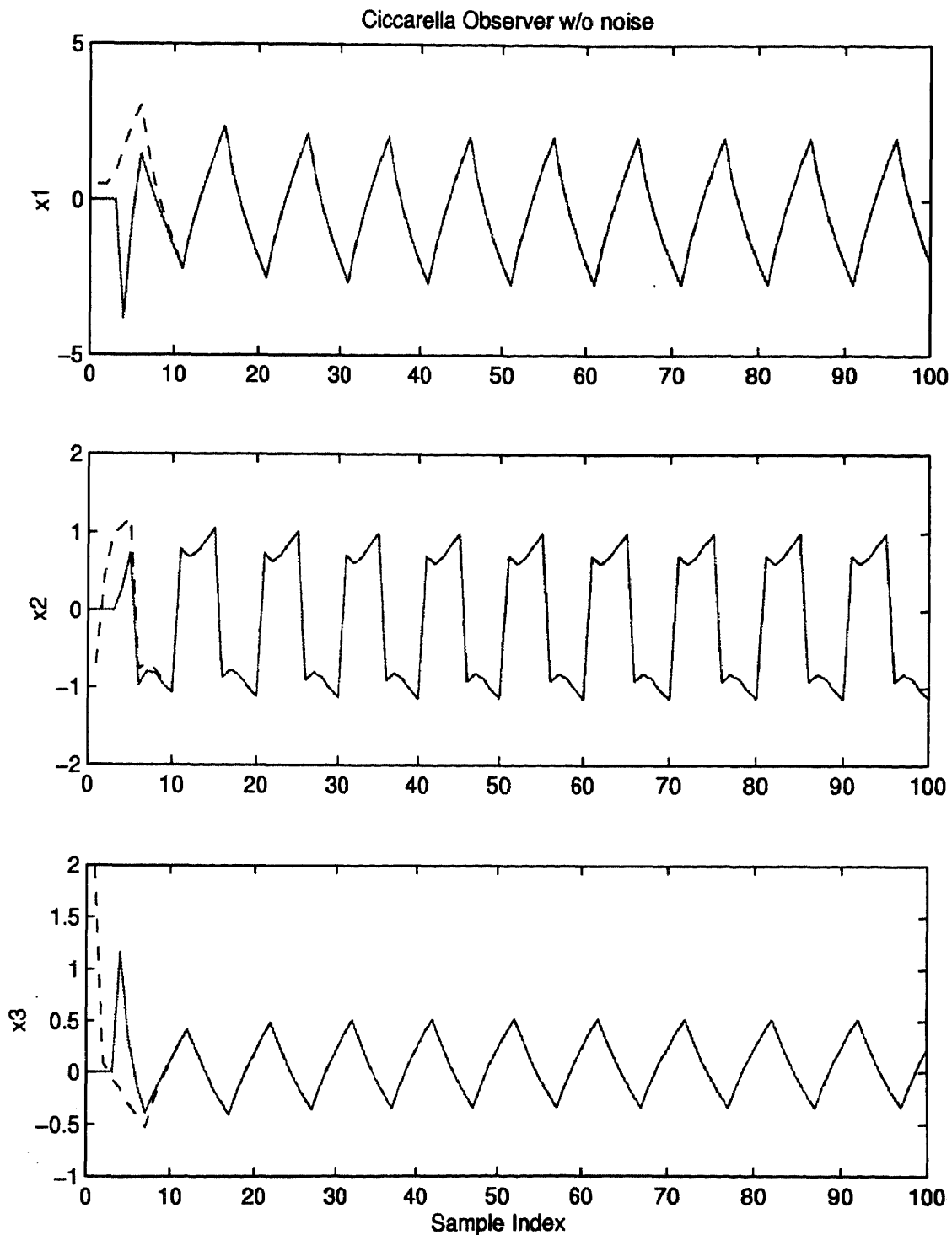


Figure 6.36 Ciccarella observer state estimate (solid) and true state (dotted), for three-state model of dog blood pressure response to medication. Arbitrary gain set ($\lambda(A - K) \in \{0.3, 0.4, 0.5\}$), no measurement noise present.

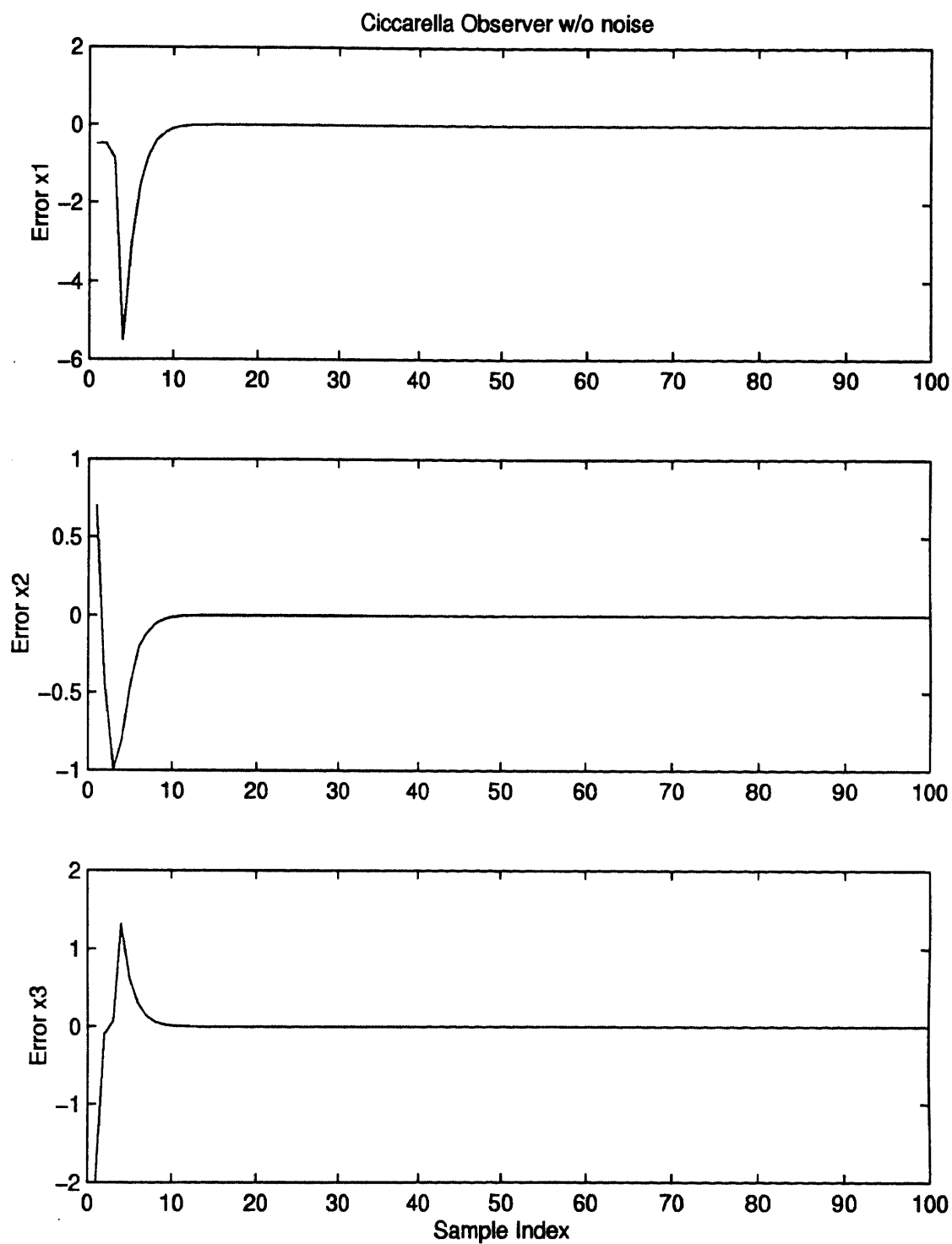


Figure 6.37 Ciccarella observer estimation error for three-state model of dog blood pressure response to medication. Arbitrary gain set ($\lambda(A - K) \in \{0.3, 0.4, 0.5\}$), no measurement noise present.

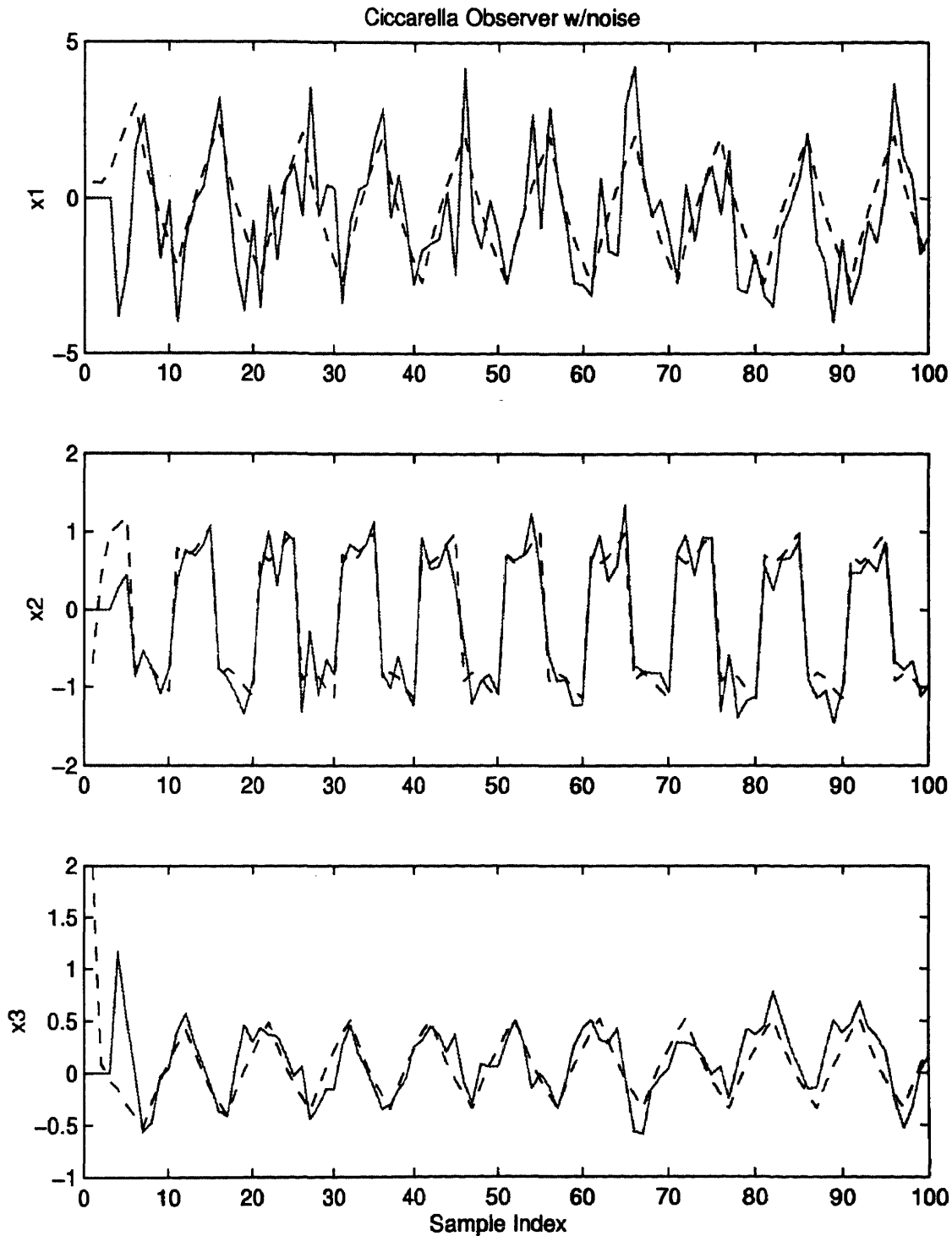


Figure 6.38 Ciccarella observer state estimate (solid) and true state (dotted), for three-state model of dog blood pressure response to medication. Arbitrary gain set ($\lambda(A - K) \in \{0.3, 0.4, 0.5\}$), measurement noise present.

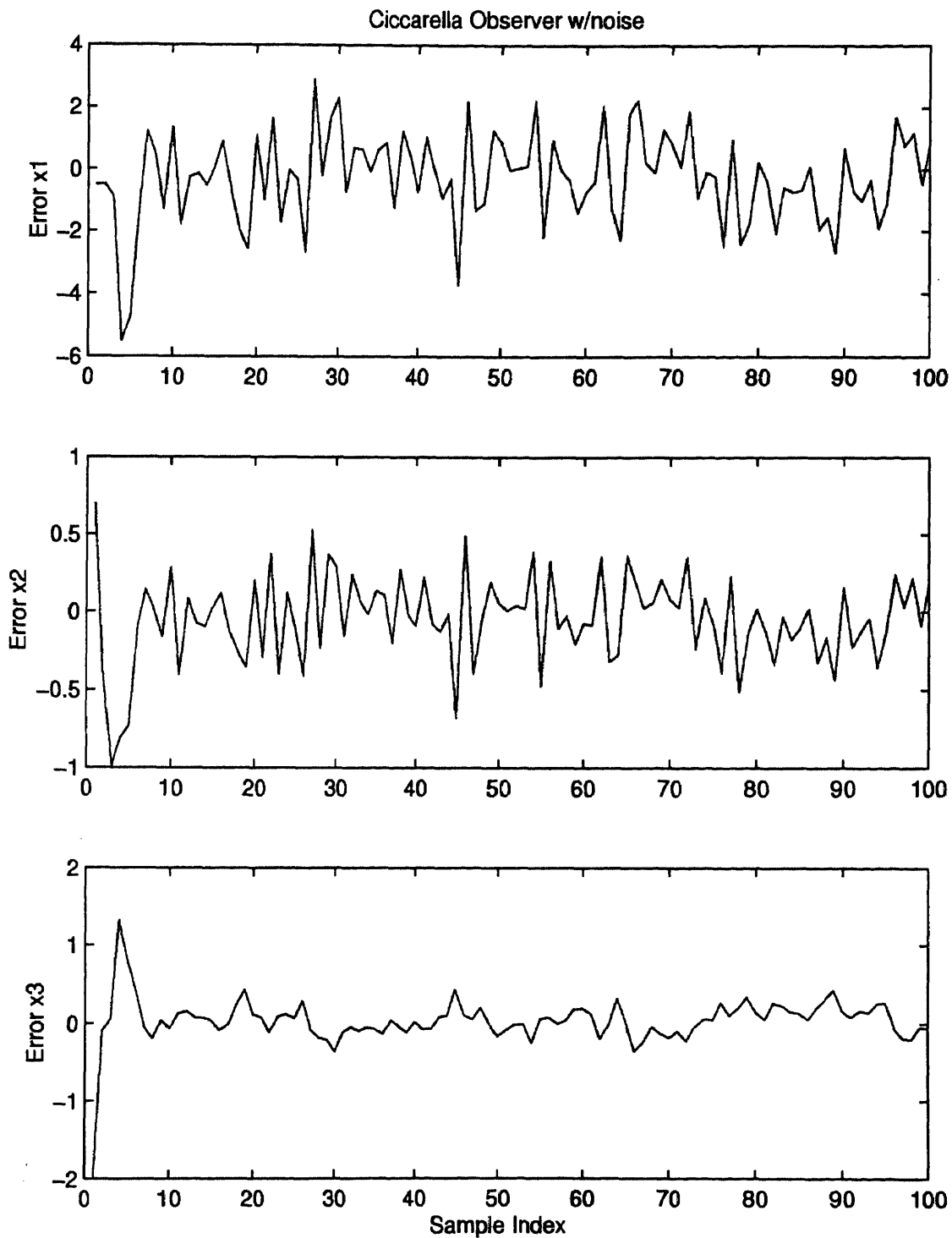


Figure 6.39 Ciccarella observer estimation error for three-state model of dog blood pressure response to medication. Arbitrary gain set ($\lambda(A - K) \in \{0.3, 0.4, 0.5\}$), measurement noise present.

6.3.5 Modified Ciccarella Observer

In the first attempt to mitigate the estimation noise of the original observer the feedforward term was eliminated by setting $B = 0$. This modification represents a departure from the theoretical basis of the Ciccarella observer and, in fact, figures 6.40, 6.41 demonstrate *filter divergence*. This observer was stabilized when the feedback gain matrix was reduced in magnitude and set to

$$K = \begin{bmatrix} -0.03 & 1 & 0 \\ 0 & -0.04 & 1 \\ 0 & 0 & -0.05 \end{bmatrix} \quad (6.52)$$

placing the closed-loop eigenvalues of $A - K$ at $\{0.03, 0.04, 0.05\}$. Figures 6.42, 6.43 demonstrate performance of this observer.

The modified Ciccarella observer using the Kalman gains and no feedforward term ($B = 0$) was implemented for comparison. The Kalman filter noise matrices used for this observer were

$$Q = 0.00018 \begin{bmatrix} 0 & 0 & 0 \\ 0 & 0 & 0 \\ 0 & 0 & 1 \end{bmatrix} \quad (6.53)$$

$$W = 0.0183I. \quad (6.54)$$

Figures 6.44, 6.45 demonstrate observer performance superior to the original Ciccarella observer. State estimation noise is essentially eliminated. Figure 6.46 shows the gain history of the modified Ciccarella observer gain matrix K (The off-diagonal elements were zero.) *Elements K_{11}, K_{22} vary over two orders of magnitude.* The gains reach steady state after three filter iterations.

Figures 6.47, 6.48 demonstrate the performance of the same observer when the assumed process noise covariance matrix used in calculation of the gain is increased by two orders of magnitude. The Kalman filter noise matrices used for this observer

were

$$Q = 0.018 \begin{bmatrix} 0 & 0 & 0 \\ 0 & 0 & 0 \\ 0 & 0 & 1 \end{bmatrix} \quad (6.55)$$

$$W = 0.0183I. \quad (6.56)$$

Filter tracking is worse than in the previous example which is expected since by supposition the knowledge of the process is inferior. Figure 6.49 shows the gain history for this filter. The steady-state gains for this filter are an order of magnitude larger than for the previous observer.

Figures 6.50, 6.51 demonstrate performance of the modified Ciccarella observer when the feedforward term is include ($B = [0 \ 0 \ 1]'$) and using noise matrices

$$Q = 0.00018 \begin{bmatrix} 0 & 0 & 0 \\ 0 & 0 & 0 \\ 0 & 0 & 1 \end{bmatrix} \quad (6.57)$$

$$W = 0.0183I. \quad (6.58)$$

In comparison to figures 6.44, 6.45, *inclusion of the feedforward term appears detrimental to the observers noise rejection behavior.* Inclusion of the feedforward term does appear to improve the system transient response somewhat.

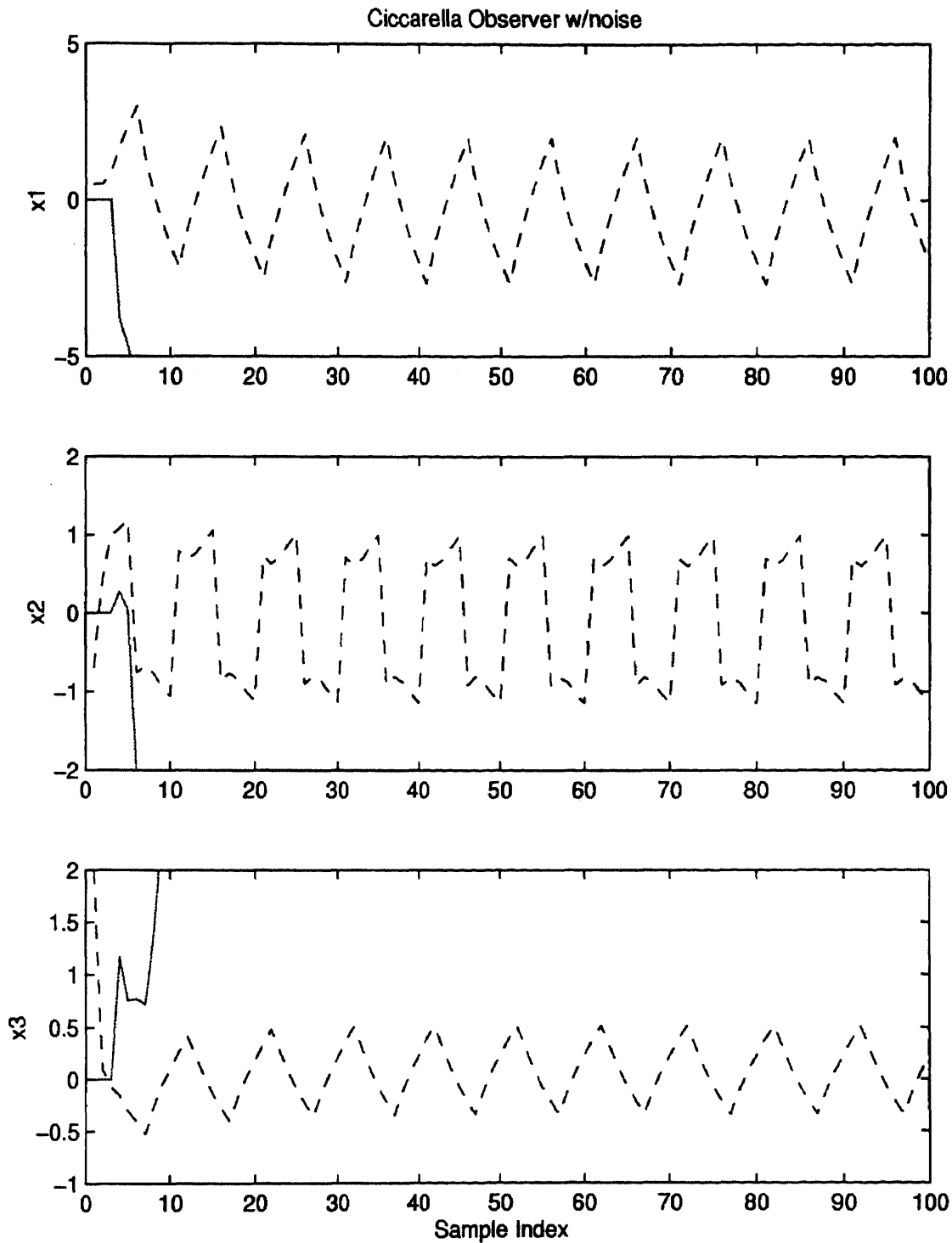


Figure 6.40 Ciccarella observer state estimate (solid) and true state (dotted), for three-state model of dog blood pressure response to medication. Arbitrary gain set ($\lambda(A - K) \in \{0.3, 0.4, 0.5\}$), no measurement noise present, no feedforward ($B = 0$). Note divergence.

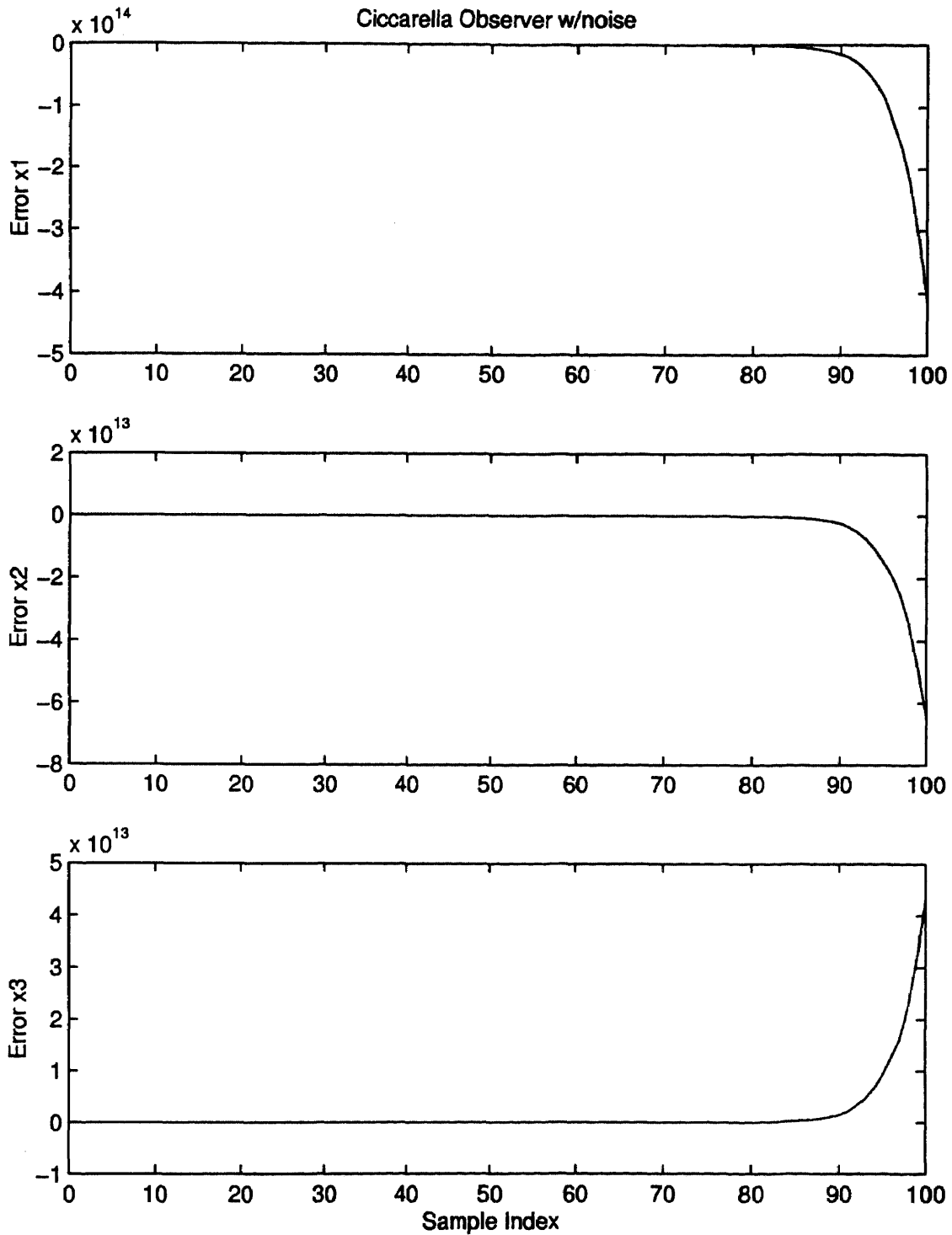


Figure 6.41 Ciccarella observer estimation error for three-state model of dog blood pressure response to medication. Arbitrary gain set ($\lambda(A - K) \in \{0.3, 0.4, 0.5\}$), no measurement noise present, no feedforward ($B = 0$). Note divergence.

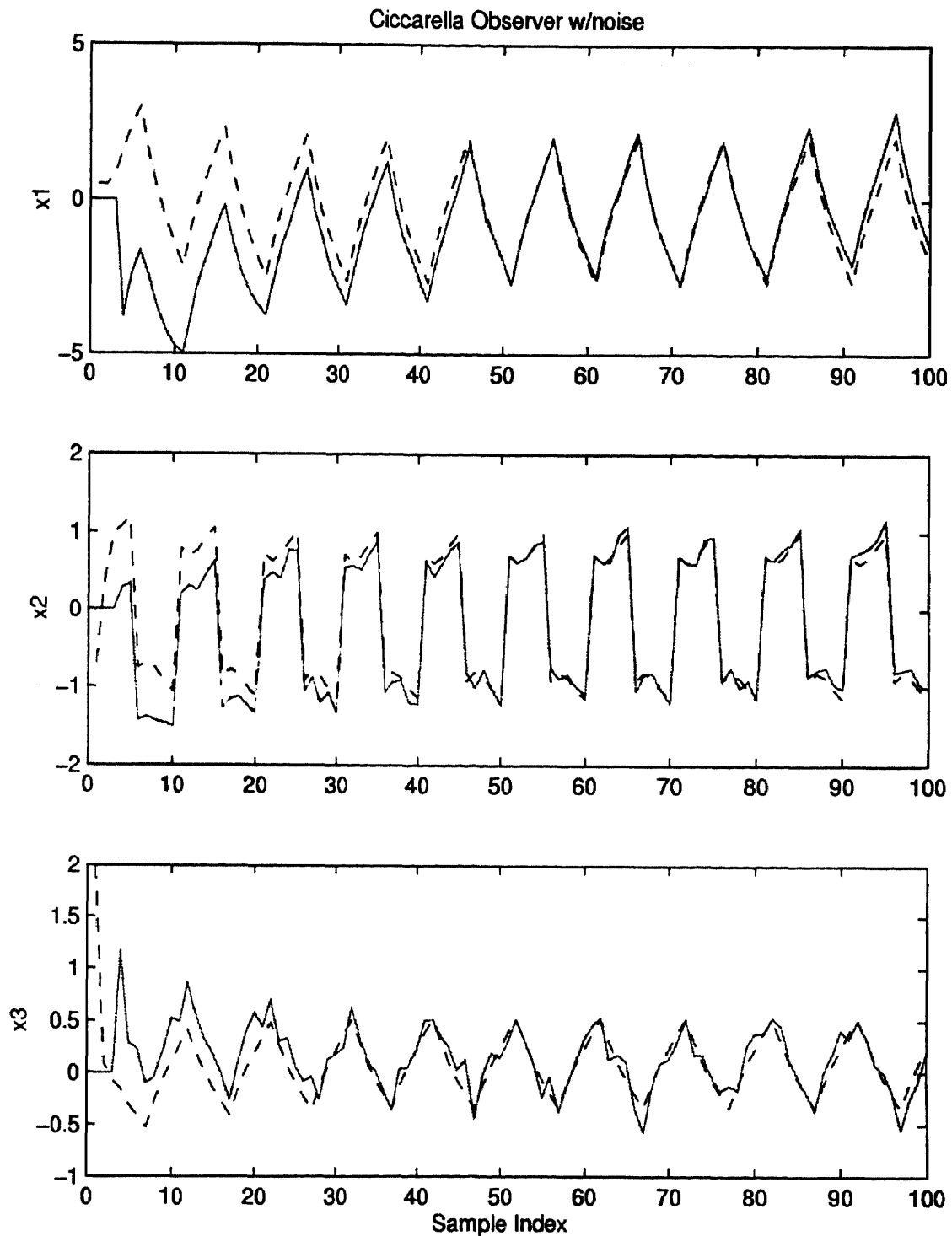


Figure 6.42 Ciccarella observer state estimate (solid) and true state (dotted), for three-state model of dog blood pressure response to medication. Reduced magnitude gain set ($\lambda(A - K) \in \{0.03, 0.04, 0.05\}$), measurement noise present, no feedforward. Observer is stabilized.

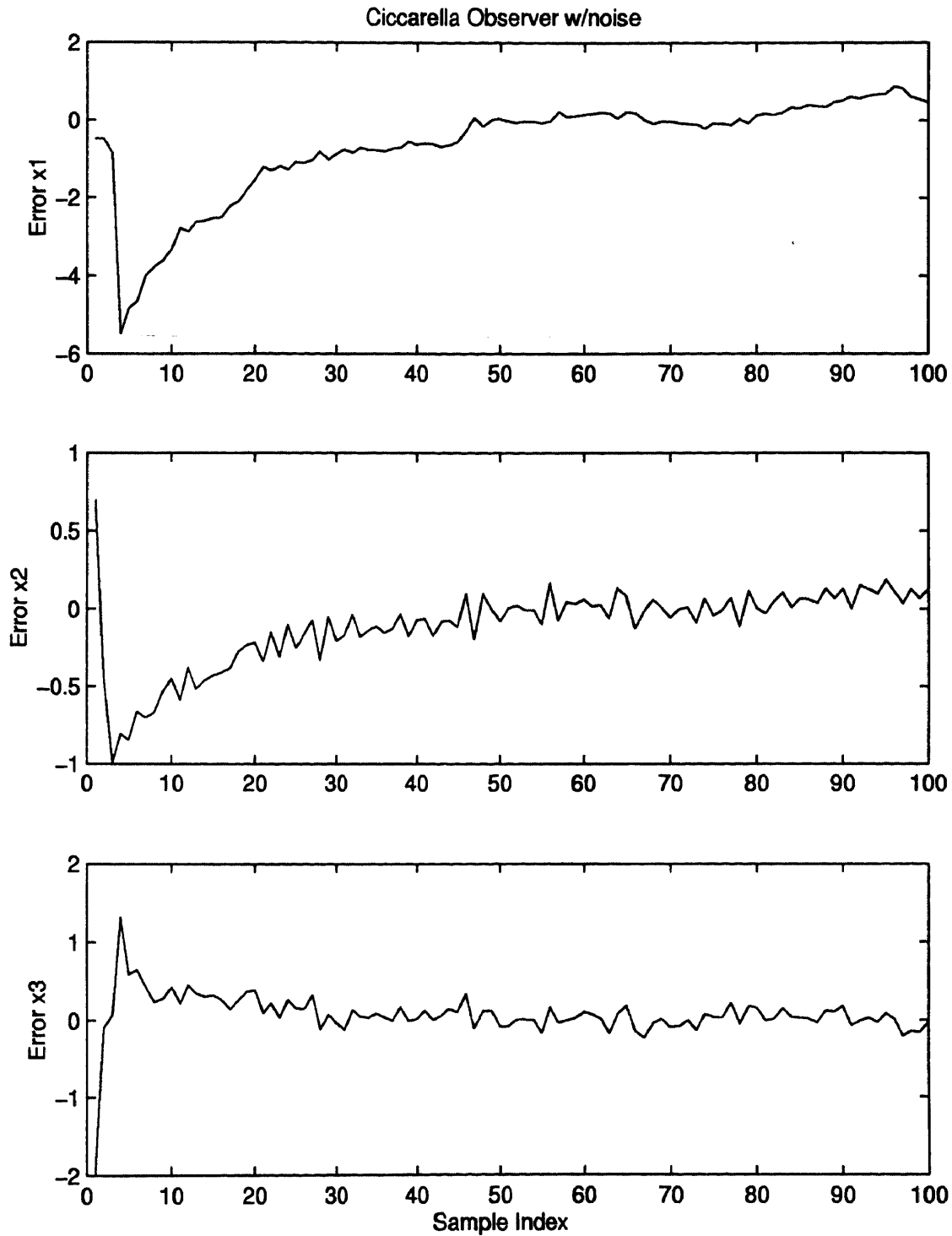


Figure 6.43 Ciccarella observer estimation error for three-state model of dog blood pressure response to medication. Reduced magnitude gain set ($\lambda(A - K) \in \{0.03, 0.04, 0.05\}$) measurement noise present, no feedforward. Observer is stabilized.

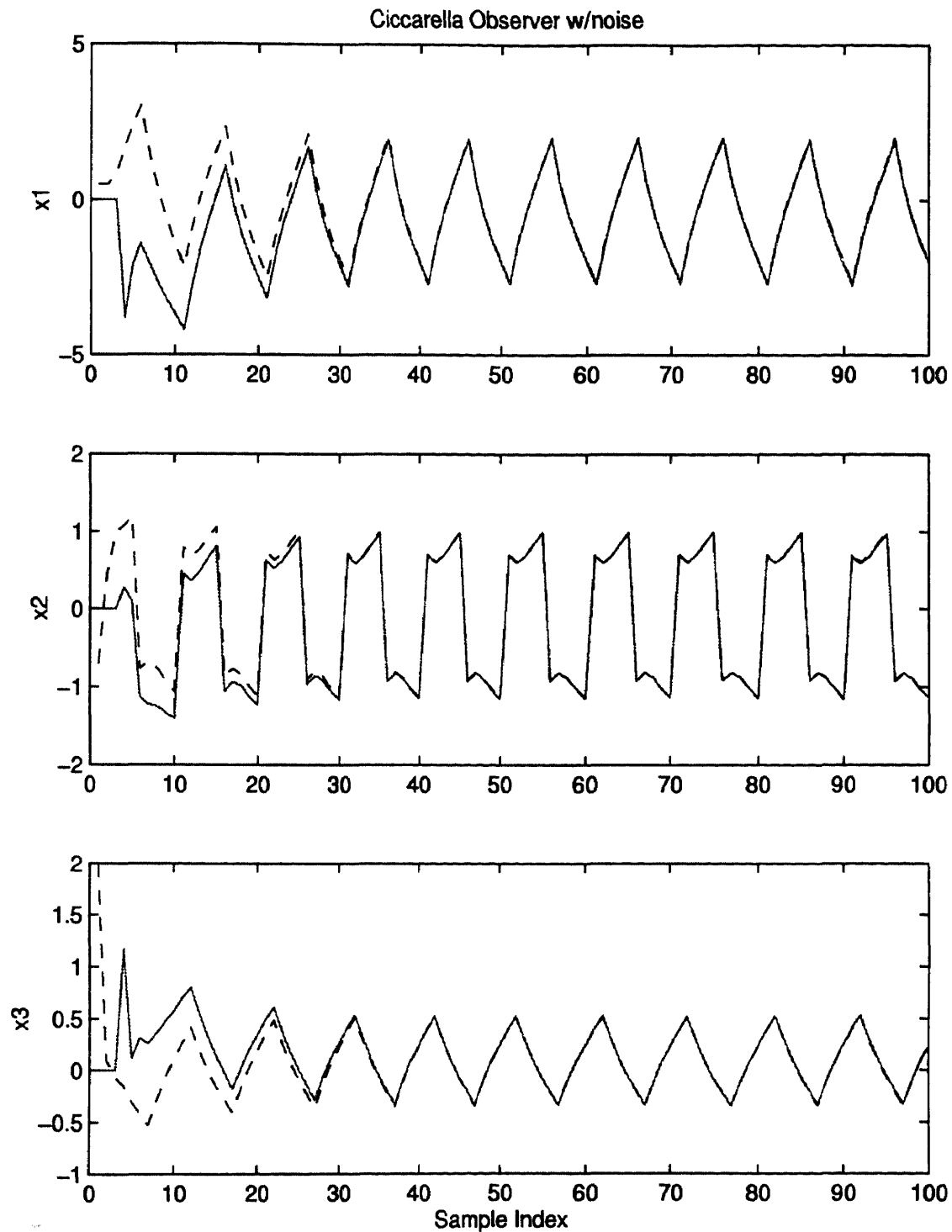


Figure 6.44 Modified Ciccarella observer estimate (solid) and true state (dotted), for three-state model of dog blood pressure response to medication. Kalman gain set, measurement noise present, no feedforward ($B = 0$). $W = 0.0183I, Q = 0.00018 \text{ diag}([0 \ 0 \ 1])$.

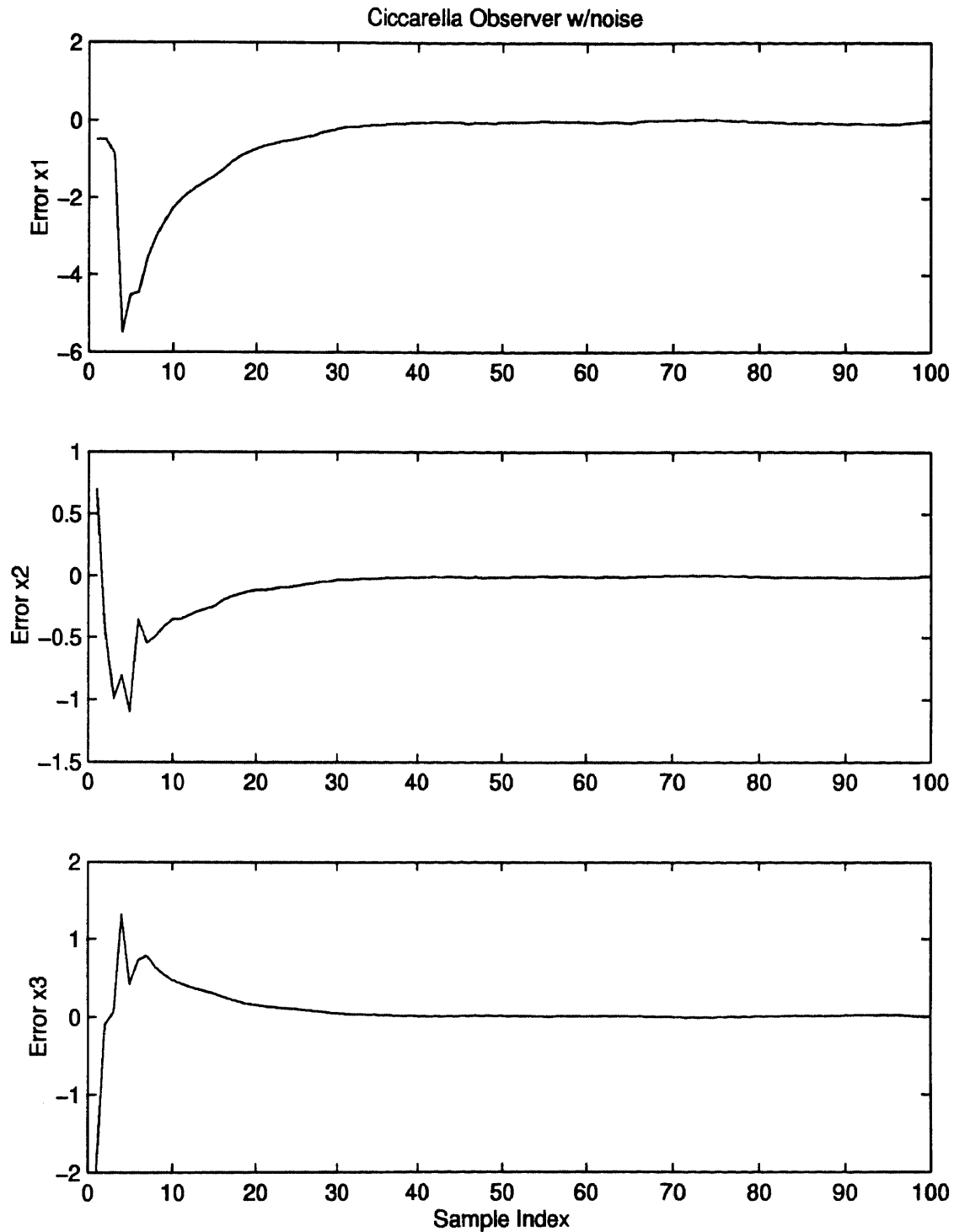


Figure 6.45 Modified Ciccarella observer estimation error for three-state model of dog blood pressure response to medication. Kalman gain set, measurement noise present, no feedforward ($B = 0$). $W = 0.0183I$, $Q = 0.00018 \text{diag}([0 \ 0 \ 1])$.

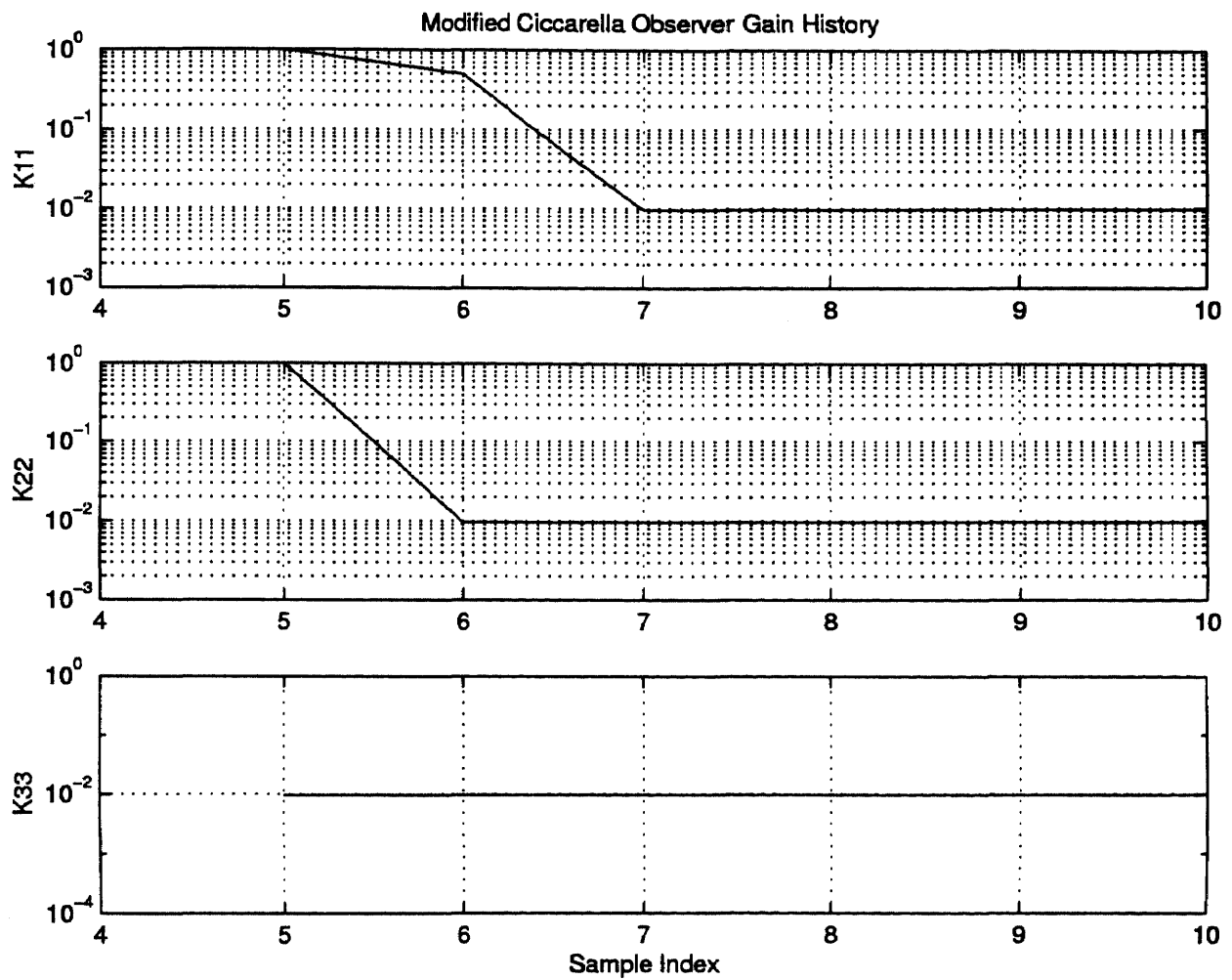


Figure 6.46 Modified Ciccarella observer gain history. $W = 0.0183I$, $Q = 0.018 \text{diag}([0 \ 0 \ 1])$.

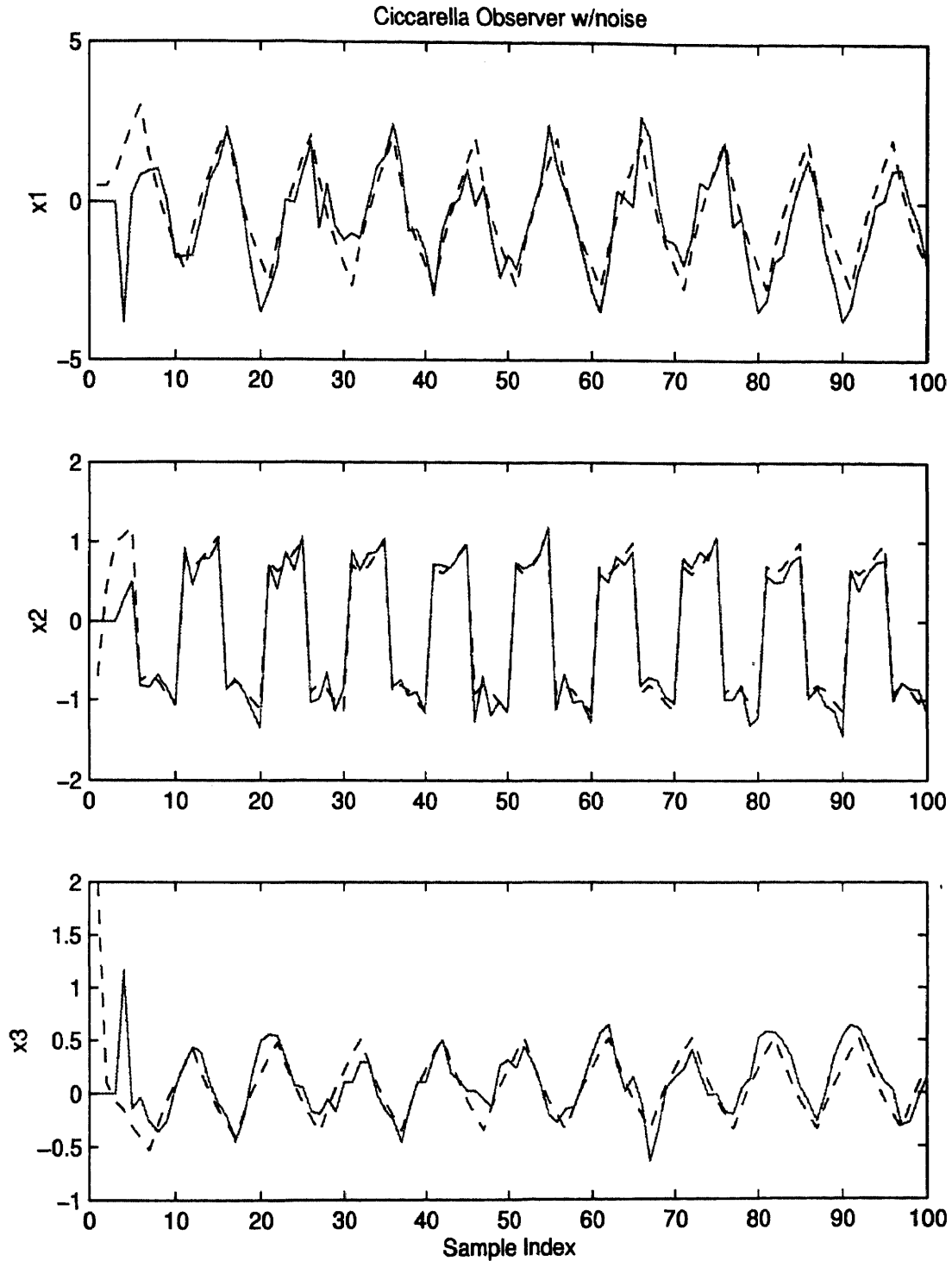


Figure 6.47 Modified Ciccarella observer estimate (solid) and true state (dotted), for three-state model of dog blood pressure response to medication. Kalman gain set, measurement noise present, no feedforward ($B = 0$). $W = 0.0183I$, $Q = 0.018 \text{diag}([0 \ 0 \ 1])$.

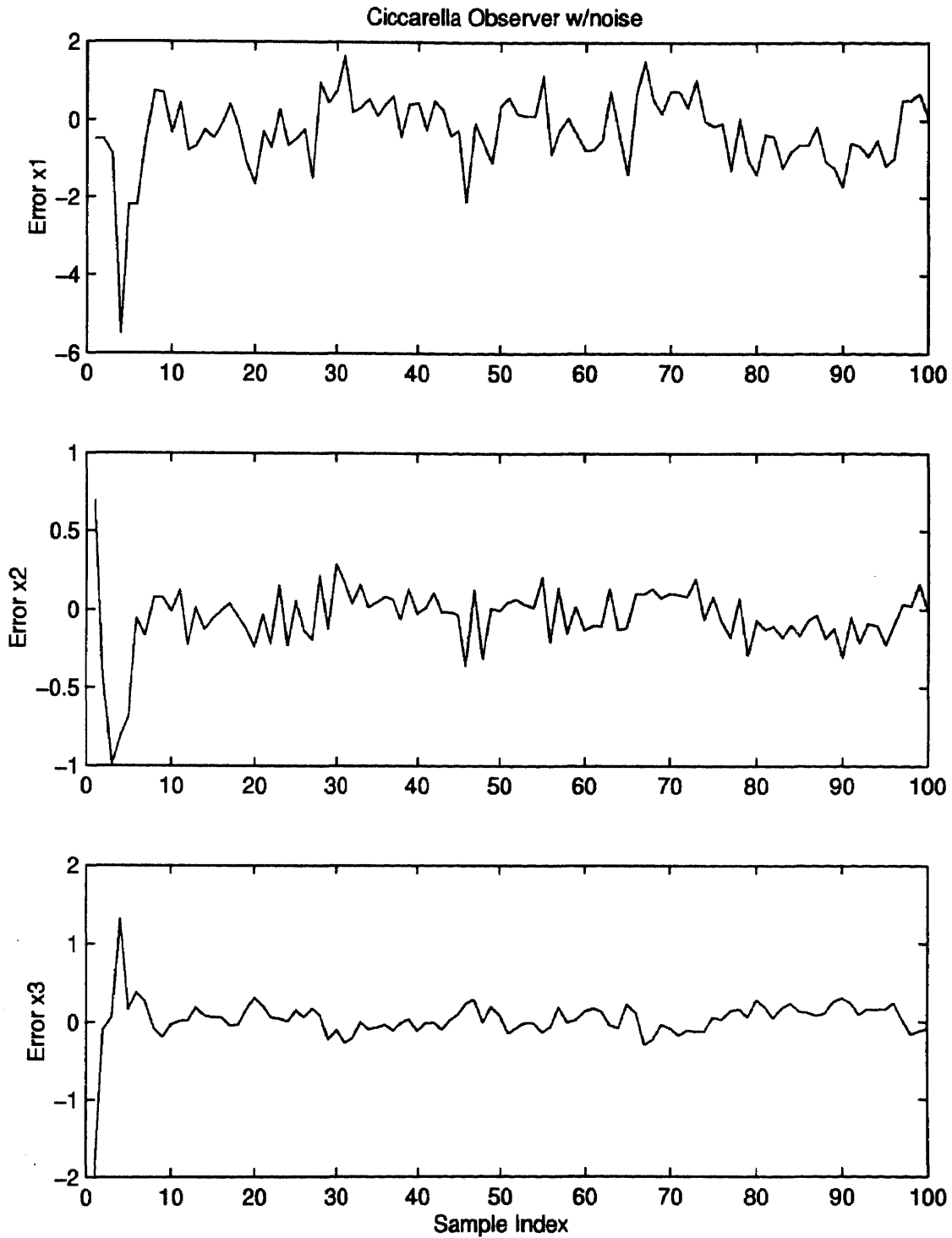


Figure 6.48 Modified Ciccarella observer estimation error for three-state model of dog blood pressure response to medication. Kalman gain set, measurement noise present, no feedforward ($B = 0$). $W = 0.0183I$, $Q = 0.018 \text{diag}([0 \ 0 \ 1])$.

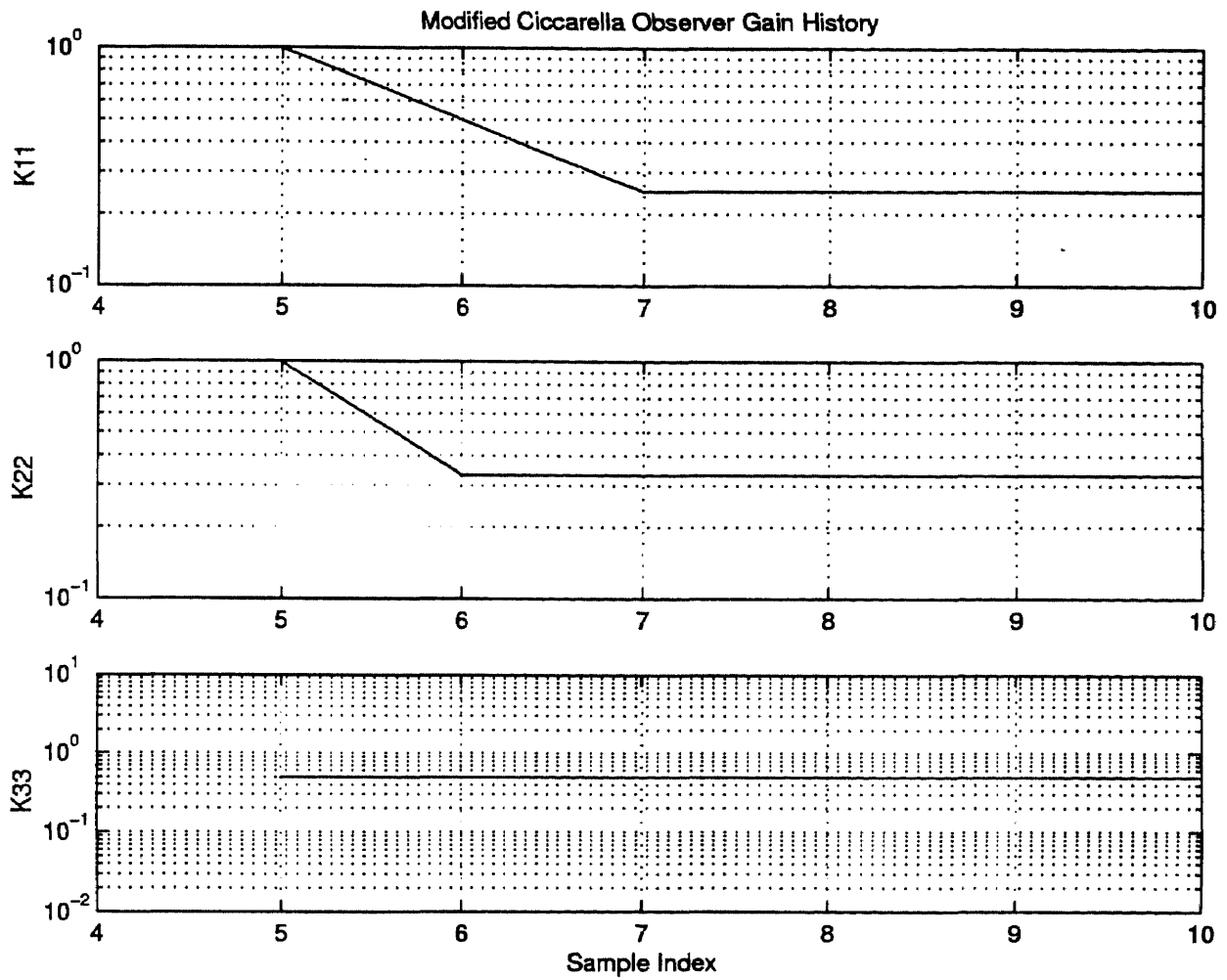


Figure 6.49 Modified Ciccarella observer gain history. $W = 0.0183I$, $Q = 0.018 \text{diag}([0 \ 0 \ 1])$.

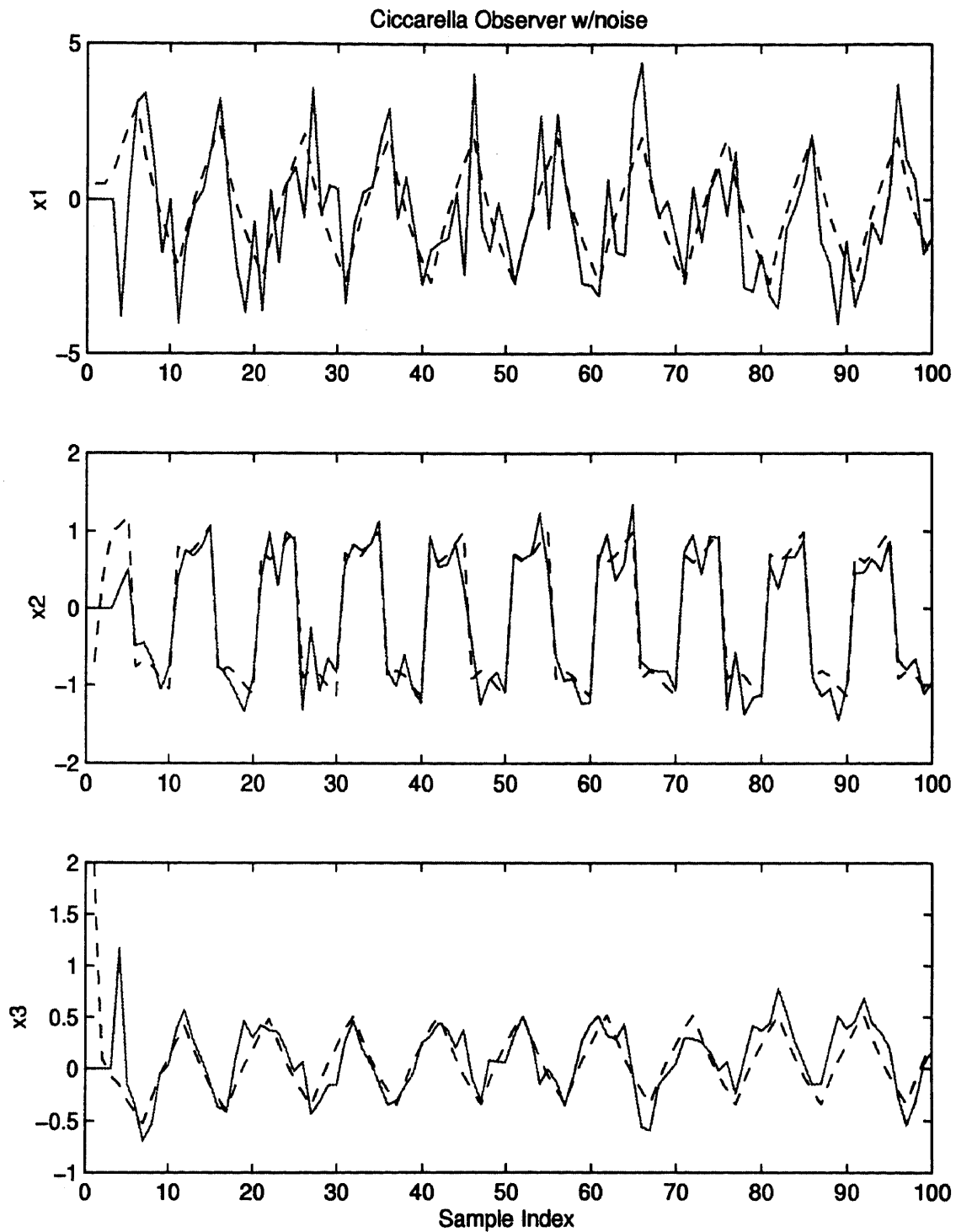


Figure 6.50 Modified Ciccarella observer estimate (solid) and true state (dotted), for three-state model of dog blood pressure response to medication. Kalman gain set, measurement noise present, *with feedforward*. $W = 0.0183I$, $Q = 0.00018 \text{diag}([0 \ 0 \ 1])$.

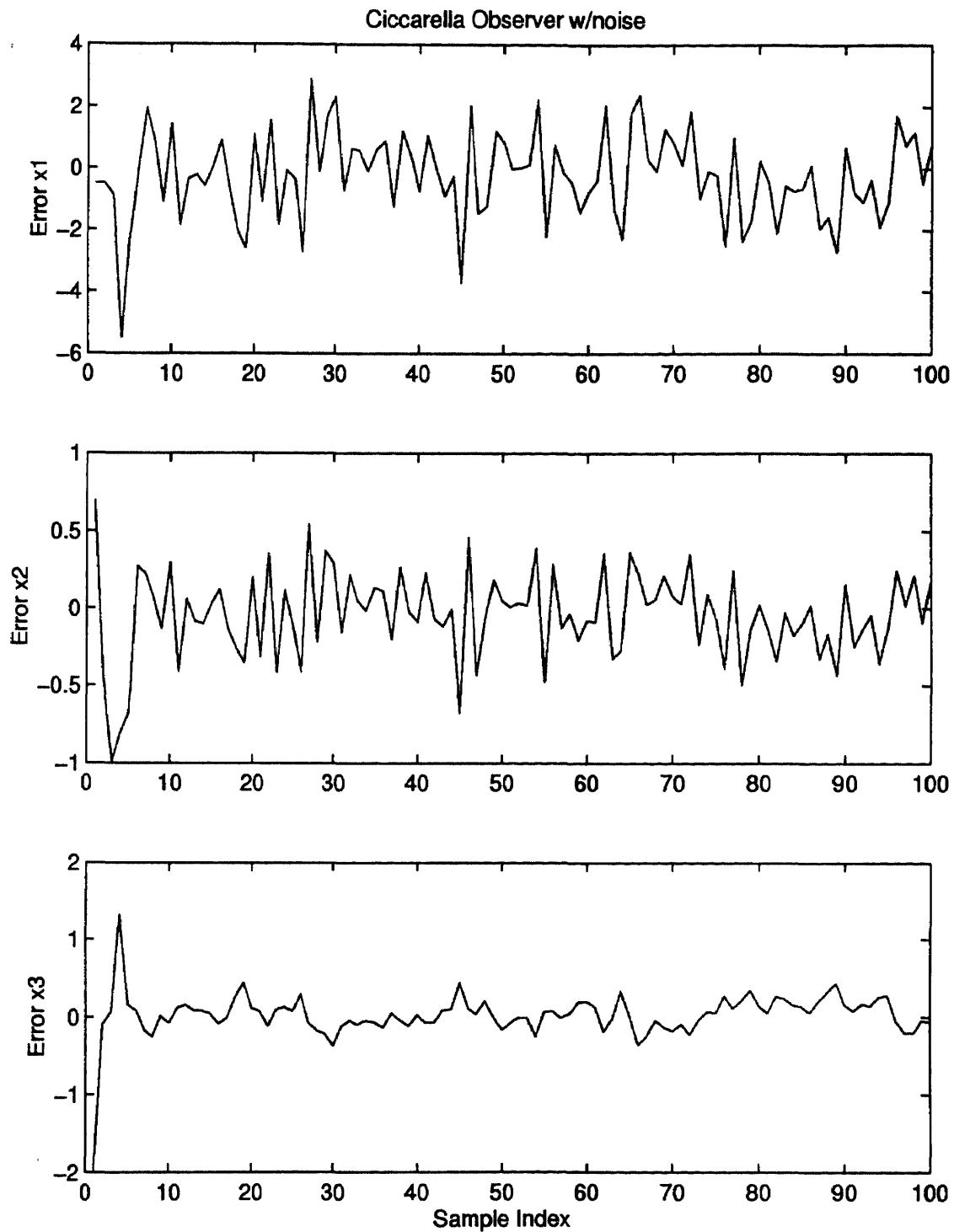


Figure 6.51 Modified Ciccarella observer state estimation error for three-state model of dog blood pressure response to medication. Kalman gain set, measurement noise present, *with feedforward*. $W = 0.0183I$, $Q = 0.00018 \text{diag}([0 \ 0 \ 1])$.

CHAPTER 7

NUMERICAL AND IMPLEMENTATION CONSIDERATIONS

At the heart of this new general observer for discrete-time nonlinear systems is the inversion of the function $z = \phi(x, u)$. A large body of knowledge exists in the related fields of numerical analysis [3] and nonlinear optimization[46] regarding this inversion. For “square” systems of equations i.e., $y = Ax$, $y \in \mathbb{R}^n$, $A \in \mathbb{R}^{n \times n}$, $x \in \mathbb{R}^n$, Newton’s Method and general Fixed-point methods are most common.

7.1 Newton’s Methods of Solving Nonlinear Systems of Equations

To solve for x in the nonlinear scalar equation $y = f(x)$ the problem is first converted to the root-finding problem for $g(x)$ where $g(x) = f(x) - y$. Newton’s method then yields improving estimates

$$\hat{x}_{k+1} = \hat{x}_k - \frac{g(\hat{x}_k)}{g'(\hat{x}_k)} \quad (7.1)$$

$$= \hat{x}_k - \frac{f(x) - y}{f'(x)}. \quad (7.2)$$

Newton’s method is extended to systems of equations by replacing the derivative with the Jacobian

$$\hat{\mathbf{x}}_{k+1} = \hat{\mathbf{x}}_k - J^{-1} \mathbf{g}(\hat{\mathbf{x}}_k) \quad (7.3)$$

$$= \hat{\mathbf{x}}_k - J^{-1} [\mathbf{f}(\hat{\mathbf{x}}_k) - \mathbf{y}_k] \quad (7.4)$$

where

$$J = \left. \frac{\partial \mathbf{g}(\mathbf{x})}{\partial \mathbf{x}} \right|_{\mathbf{x}=\hat{\mathbf{x}}_k} \quad (7.5)$$

$$= \left. \frac{\partial \mathbf{f}(\mathbf{x})}{\partial \mathbf{x}} \right|_{\mathbf{x}=\hat{\mathbf{x}}_k}. \quad (7.6)$$

(Boldface is used here to indicate vector quantities.)

In the observer presented here a full rank condition on Jacobian J is the definition of strong observability and is a prerequisite condition.

7.2 Propagation of Solver Seed

Unlike “square” systems of linear equations, which have none, one, or an infinite number of solutions, square systems of nonlinear equations $y = \phi(x)$ may have a finite number (other than one) of solutions. The proposed observer may “stumbled” onto one of the wrong solutions and yield very poor state estimates.

Formally this possibility does not exist in light of the observability requirement as defined section 3.4. For nonlinear systems it is practically difficult to demonstrate global strong observability and unless it is proved that multiple roots¹ don't exist one should presume they may.

Newton's method, like all root solvers, requires a “seed” \hat{x}_0 estimate to start. To be sure to converge to the proper root the seed need be within some unknown “observability radius” of the true root. For proper convergence of this observer, the seed must be within this radius at every time step.

It is not possible to guarantee convergence to the proper root. The best chance of doing so is to use the best seed at every time step. In this observer the best seed is achieved by *seed propagation*. For a system with state dynamics

$$x_{k+1} = f(x_k, u_k) \tag{7.7}$$

then if \hat{x}_k represents the best estimate of x at time k then $\tilde{x}_{k+1} = f(\hat{x}_k, u_k)$ represents certainly a reasonable estimate of x for the purpose of seeding the root solver for $z = \phi(x, u)$.

¹Terms “roots” and “solutions” are used synonymously in this chapter. Solutions to the system $y = f(x)$ are roots to the system $g(x)$ where $g(x) = f(x) - y$.

CHAPTER 8

MISCELLANEOUS RESULTS

8.1 The Ciccarella Observer and the Hybrid Coordinate System Kalman Filter—A heuristic Demonstration

This author introduced the Hybrid Coordinate System Kalman Filter [23] to estimate the range to a target given the location of the observer and measured line-of-sight to the target. For this problem, it was found empirically that it was better to perform the time updates in a Cartesian reference frame and the measurement updates in the so-called “modified polar” [1] reference frame. The states as described in the two coordinate systems were related exactly to each other by nonlinear algebraic equations. To the first order the covariance matrices associated with the states were related by the Jacobian of the state transformation functions. The algorithm demonstrated excellent performance.

This early work in the development of extended Kalman filter by state coordinate transformation is closely related to the later work by Ciccarella [7]. To develop his proof Ciccarella transforms the system to the Brunowski form of chain delays. The transformation presented in [23] was one which empirically demonstrated specific beneficial robustness properties. Otherwise the observers were essentially the same.¹

As is rule for most extended Kalman filter work, no rigorous proof of convergence was provided in [23]. The rigor required for a proper mathematical proof of a theorem often obfuscates an intuitive understanding of the theorem. Ciccarella provides the rigorous proof of the convergence of his observer. Presented

¹The interesting point remains that while the transformation to Brunowski form has definite desirable mathematical properties, the effect of the transformation upon the noise is ignored and remains a topic for future research. This future research may determine that transformation to non-Brunowski forms, though a more difficult form from which to develop mathematical proofs, may offer more desirable transformations of the noise and better observer performance.

here is a heuristic demonstration based upon the hybrid coordinate version of the familiar Kalman filter. Alternatively, the situation can be viewed as Ciccarella providing a rigorous proof of the hybrid coordinate system Kalman filter.

A discrete-time nonlinear dynamic system is given:

$$x_{k+1} = F(x_k) + g(x_k)u_k + v_k \quad (8.1)$$

$$y_k = h(x_k) + w_k \quad (8.2)$$

The classic extended Kalman filter equations are given:

$$\tilde{x}_{k+1} = f(\hat{x}_k) + g(\hat{x}_k)u_k \quad (8.3)$$

$$\tilde{P}_{k+1} = \Phi \hat{P}_k \Phi' + V \quad (8.4)$$

$$K = \tilde{P}_{k+1} C' (C \tilde{P}_{k+1} C' + W)^{-1} \quad (8.5)$$

$$\hat{x}_{k+1} = \tilde{x}_{k+1} + K [y_k - h(\tilde{x}_{k+1})] \quad (8.6)$$

$$\hat{P}_{k+1} = (I - KC) \tilde{P}_{k+1} \quad (8.7)$$

where

$$\Phi = \frac{\partial f(x)}{\partial x} \quad (8.8)$$

$$C = \frac{\partial h(x)}{\partial x} \quad (8.9)$$

$$V = E[vv'] \quad (8.10)$$

$$W = E[ww'] \quad (8.11)$$

Assume a one-to-one transformation exists

$$z = \phi(x) \quad (8.12)$$

$$x = \phi^{-1}(z) \quad (8.13)$$

the incremental mapping of small changes of x to small changes in z is given by

$$\delta z = J \delta x \quad (8.14)$$

$$J = \frac{\partial \phi(x)}{\partial x} \quad (8.15)$$

Define \underline{P} as the state covariance matrix for variable z , i.e.,

$$\underline{P} = E[(z - \hat{z})(z - \hat{z})']. \quad (8.16)$$

For small errors, \underline{P} is related to P and \underline{C} is related to C

$$\underline{P} = JPJ' \quad (8.17)$$

$$\underline{C} = \frac{\partial h}{\partial z} \quad (8.18)$$

$$= \frac{\partial h}{\partial x} \frac{\partial x}{\partial z} \quad (8.19)$$

$$= CJ^{-1} \quad (8.20)$$

The measurement update equations in the z coordinates are:

$$\underline{K} = \underline{\tilde{P}}_{k+1} \underline{C}' \left(\underline{C} \underline{\tilde{P}}_{k+1} \underline{C}' + \underline{W} \right)^{-1} \quad (8.21)$$

$$\underline{z}_{k+1} = \underline{\tilde{z}}_{k+1} + \underline{K} \{ y - h[\phi^{-1}(\underline{\tilde{z}}_{k+1})] \} \quad (8.22)$$

$$\underline{P}_{k+1} = (I - \underline{K} \underline{C}) \underline{\tilde{P}}_{k+1} \quad (8.23)$$

Solving for \underline{K} in terms of \underline{K} by

$$\underline{K} = \underline{\tilde{P}}_{k+1} \underline{C}' \left(\underline{C} \underline{\tilde{P}}_{k+1} \underline{C}' + \underline{W} \right)^{-1} \quad (8.24)$$

$$= J \underline{\tilde{P}}_{k+1} J' J^{-T} \underline{C}' \left(C J^{-1} J \underline{\tilde{P}}_{k+1} J' J^{-T} + W \right)^{-1} \quad (8.25)$$

$$= J \underline{\tilde{P}}_{k+1} \underline{C}' \left(\underline{C} \underline{\tilde{P}}_{k+1} \underline{C}' + \underline{W} \right)^{-1} \quad (8.26)$$

$$= JK \quad (8.27)$$

Equation (8.27) relates the Kalman gain in the z coordinates to the Kalman Gains in the x coordinates. It has a simple intuitive interpretation, viz. if the residual ρ is given by $\rho = y - h(\hat{x})$, then Kalman Gain K represents (in linear theory) optimal change in state x for a given change for the residual ρ , i.e.,

$$K = \frac{\partial x}{\partial \rho} \quad (8.28)$$

and \underline{K} is then related to K (for small ρ)

$$\underline{K} = \frac{\partial z}{\partial \rho} \quad (8.29)$$

$$= \frac{\partial z}{\partial x} \frac{\partial x}{\partial \rho} \quad (8.30)$$

$$= JK \quad (8.31)$$

For transformation ϕ , Ciccarella uses the special linearizing transformation which transforms system (8.1), (8.2) into the Brunowski normal form delay chain. He then derives limits for the gain \underline{K} which guarantees convergence of the transformed observer. The final step is to map \underline{K} back to the original system using the inverse of (8.27), i.e., $K = J^{-1}\underline{K}$.

8.2 Generalization of the Continuous-time Friedland Parameter Estimator to Continuous-time State Estimation

The continuous-time parameter estimator developed in [14] can be extended to a general state parameter observer when the unmeasured state appears affine in the dynamics.

Define a dynamic system:

$$\dot{x}_1 = f_{11}(x_1, u) + F_{12}(x_1, u)x_2 \quad (8.32)$$

$$\dot{x}_2 = f_{21}(x_1, u) + F_{22}(x_1, u)x_2 \quad (8.33)$$

$$y = x_1 \quad (8.34)$$

where x_1 is the directly measured state and x_2 is not measured.

The following reduced-order observer is proposed

$$\hat{x}_1 = y \quad (8.35)$$

$$\hat{x}_2 = K(y) + z \quad (8.36)$$

$$\dot{z} = \phi_1(y, u) + \Phi_2(y, u)\hat{x}_2. \quad (8.37)$$

The error dynamics are derived

$$e = \hat{x}_2 - x_2 \quad (8.38)$$

$$\dot{e} = \dot{\hat{x}}_2 - \dot{x}_2 \quad (8.39)$$

$$= K_y \dot{y} + \dot{z} - f_{21}(y, u) - F_{22}(y, u)x_2 \quad (8.40)$$

$$= K_y f_{11}(y, u) + K_y F_{12}(y, u)x_2 + \phi_1(y, u) + \Phi_2(y, u)\hat{x}_2 \\ - f_{21}(y, u) - F_{22}(y, u)x_2 \quad (8.41)$$

where

$$K_y = \frac{\partial K(y)}{\partial y}. \quad (8.42)$$

Substituting $\hat{x}_2 - e$ for x_2 into (8.41) yields

$$\dot{e} = K_y f_{11}(y, u) + K_y F_{12}(y, u)(\hat{x}_2 - e) + \phi_1(y, u) + \Phi_2(y, u)\hat{x}_2 \\ - f_{21}(y, u) - F_{22}(y, u)(\hat{x}_2 - e) \quad (8.43)$$

$$= [K_y f_{11}(y, u) - f_{21}(y, u) + \phi_1(y, u)] \\ + [K_y F_{12}(y, u) - F_{22}(y, u) + \Phi_2(y, u)]\hat{x}_2 \\ + [F_{22}(y, u) - K_y F_{12}(y, u)]e. \quad (8.44)$$

For the error dynamics to be independent of y , and \hat{x}_2

$$\phi_1(y, u) = f_{21}(y, u) - K_y f_{11}(y, u) \quad (8.45)$$

$$\Phi_2(y, u) = F_{22}(y, u) - K_y F_{12}(y, u). \quad (8.46)$$

The resulting error dynamics are given by

$$\dot{e} = [F_{22}(y, u) - K_y F_{12}(y, u)]e \quad (8.47)$$

which is stable when $F_{22}(y, u) - K_y F_{12}(y, u)$ is symmetric negative semi-definite.

Substituting (8.45), (8.46) into (8.37), the dynamics for z can be written

$$\dot{z} = [f_{21}(y, u) - K_y f_{11}(y, u)] + [F_{22}(y, u) - K_y F_{12}(y, u)]\hat{x}_2. \quad (8.48)$$

The observer is synthesized by choosing a function $K(y)$ such that matrix $F_{22}(y, u) - K_y F_{12}(y, u)$ is symmetric negative semi-definite. Then functions ϕ_1, Φ_2 are constructed from (8.45), (8.46) to propagate dynamics of intermediate state variable z , (8.37).

8.3 Unification of the Friedland Parameter Estimator and the Friedland Nonlinear Reduced-Order State Estimator

8.3.1 The Generalized Friedland Nonlinear Reduced-order Observer

In [14], section 6.2, Friedland describes a nonlinear reduced-order observer applicable to a general continuous-time nonlinear system where some of the state variables are directly measured. In [14], section 10.2.2, and in [15] Friedland describes a nonlinear parameter estimator for systems which are affine in the parameter and the state is directly measured. It is shown here that with a minor modification of the former, the latter is a subset of the former.

The Friedland reduced order observer is applicable to systems of the form:

$$\dot{x}_1 = f_1(x_1, x_2, u) \quad (8.49)$$

$$\dot{x}_2 = f_2(x_1, x_2, u) \quad (8.50)$$

$$y = x_1. \quad (8.51)$$

The form of the reduced-order observer is

$$\hat{x}_1 = y \quad (8.52)$$

$$\hat{x}_2 = Ky + z \quad (8.53)$$

$$\dot{z} = \phi(y, \hat{x}_2, u) \quad (8.54)$$

where

$$\phi(y, \hat{x}_2, u) = f_2(x_1, x_2, u) - K f_1(x_1, x_2, u). \quad (8.55)$$

As such, the error equation for $\epsilon = \hat{x}_2 - x_2$ is

$$\dot{\epsilon} = A(x_2)\epsilon \quad (8.56)$$

where

$$A(x_2) = \frac{\partial \phi}{\partial x_2} \quad (8.57)$$

$$= \frac{\partial f_2}{\partial x_2} - K \frac{\partial f_1}{\partial x_2} \quad (8.58)$$

and K is chosen so that $A(x_2)$ is a stable matrix.

By modifying (8.53) to be

$$\hat{x}_2 = K(y) + z \quad (8.59)$$

$$(8.60)$$

and defining

$$K_y = \frac{\partial K(y)}{\partial y} \quad (8.61)$$

the results of section 6.2 of [14] are generalized. Matrix $A(x_2)$ is still required to be stable but is now given by

$$A(x_2) = \frac{\partial f_2}{\partial x_2} - K_y \frac{\partial f_1}{\partial x_2}. \quad (8.62)$$

Admitting a state-dependent gain $K(y)$ provides for greater flexibility in designing a stable observer than using a static gain K . The observer presented in section 6.2 of [14] is a special case of this generalized version where $K(y) = Ky$.

8.3.2 Application of the Generalized Friedland Reduced-order Observer to Parameter Estimation In Systems With Affine Structure

By definition, $\dot{p} = 0$. Letting $p = x_2$ the system equations section 10.2 of [14] can be written in terms of the generalized observer of section 8.3.1

$$\dot{x}_1 = f_1(x_1, p, u) \quad (8.63)$$

$$= F(x_1, u)p \quad (\text{by supposition}) \quad (8.64)$$

$$\dot{p} = 0 \quad (8.65)$$

$$y = x_1. \quad (8.66)$$

The observer has the same form as that in section 8.3.1

$$\hat{p} = K(y) + z \quad (8.67)$$

$$\dot{z} = -K_y F(x_1, u)\hat{p}. \quad (8.68)$$

The requirement for asymptotic stability is that matrix $-K_y F(x_1, u)$ be stable. This result is identical to that presented in section 10.2.2 of [14] showing that this results in section 10.2.2 of [14] is a special case of the generalization of observer presented in section 6.2 of [14].

8.4 Quasi-Optimal Discrete-Time Friedland Observer

Consider the system

$$x_{k+1} = F(x_k, u_k)p \quad (8.69)$$

$$y_k = x_k. \quad (8.70)$$

Following section 4.4.1 the reduced-order observer is obtained

$$\hat{p}_k = \hat{p}_{k-1} + K(y_{k-1})y_k + z_k \quad (8.71)$$

$$z_{k+1} = -K(y_k)F(x_k, u_k)\hat{p}_k. \quad (8.72)$$

Equations (8.71), (8.72) can be combined to yield the observer form

$$\hat{p}_{k+1} = \hat{p}_k + K(y_k)[y_{k+1} - F(x_k, u_k)\hat{p}_k] \quad (8.73)$$

Defining the extrapolated measurement (which equals the state in this full-state measurement system), \tilde{y}_{k+1}

$$\tilde{y}_{k+1} = \tilde{x}_{k+1} = F(x_k, u_k)\hat{p}_k, \quad (8.74)$$

the observer in (8.73) can be placed into "residual" form

$$\tilde{y}_{k+1} = F(x_k, u_k)\hat{p}_k \quad (8.75)$$

$$\hat{p}_{k+1} = \hat{p}_k + K(y_k)[y_{k+1} - \tilde{y}_{k+1}]. \quad (8.76)$$

Assume that the statistics of the errors associated with measurements y and estimates \hat{p} are fairly well described by second order statistics with the properties:²

$$E[\epsilon_y] = 0, \quad E[\epsilon_y \epsilon_y'] = W, \quad (8.77)$$

$$E[\epsilon_p] = 0, \quad E[\epsilon_p \epsilon_p'] = P, \quad (8.78)$$

where ϵ_y is the error in measurement y and ϵ_p is the error in the estimate of p .

Assume further that the dynamics function $F(\cdot)$ is not known perfectly and that the associated uncertainty in propagation for a perfectly known p yields errors which are fairly well described by second order statistics:

$$E[\epsilon_F] = 0, \quad E[\epsilon_F \epsilon_F'] = Q, \quad (8.79)$$

where $\epsilon_F = \tilde{F}(x, u)p - F(x, u)p$, the process errors due to uncertainty in $F(\cdot)$.

For small ϵ_p , the errors in the extrapolated measurement \tilde{y}_{k+1} is given by,

$$\epsilon_{\tilde{y}} = F(x, u)\epsilon_p + \epsilon_F \quad (8.80)$$

²For the nonlinear problems under consideration such statistical approximations will have to suffice. The veracity of the assumption can be checked by Monte Carlo simulation.

Following Kalman filter theory and making the bold assumption of no cross-correlation of the errors in the residual $\rho = y - \tilde{y}$, the covariance of the residual is given by

$$E[\rho\rho'] = W + F(x, u)PF'(x, u) + Q. \quad (8.81)$$

The quasi-optimal discrete-time Friedland observer is then given by

$$\tilde{y}_{k+1} = F(x_k, u_k)\hat{p}_k \quad (8.82)$$

$$\tilde{P}_{k+1} = \hat{P}_k \quad (8.83)$$

$$K = \tilde{P}_{k+1}F'(x_k, u_k)[W + F(x_k, u_k)\tilde{P}_{k+1}F'(x_k, u_k) + Q]^{-1} \quad (8.84)$$

$$\hat{p}_{k+1} = \hat{p}_k + K(y_k)[y_{k+1} - \tilde{y}_{k+1}] \quad (8.85)$$

$$\hat{P}_{k+1} = [I - KF(x_k, u_k)]\tilde{P}_{k+1}. \quad (8.86)$$

CHAPTER 9

CONCLUSIONS AND RECOMMENDATIONS

9.1 Conclusion

This dissertation introduces four new observers for discrete-time nonlinear systems:

Observer 1 – The discrete-time extension of the Friedland observer applicable to systems with a special affine structure,

Observer 2 – A general discrete-time observer which is based upon an extension of the Ciccarella and Gauthier observers.

Observer 3 – A modified version of the Moraal/Grizzle observer.

Observer 4 – A modified version of the “robust” version of the discrete-time Ciccarella observer.

These observers vary in complexity. Each observer may offer certain advantages for a given application and generalizations are difficult. Table 9.1 summarizes their properties and applicability.

This dissertation develops the general observer, Observer 2, in a manner which closely parallels the 1980's development of the differential geometric system theory for nonlinear continuous-time systems. With this new formulation the discrete-time and continuous-time nonlinear system theory are represented in a conceptually analogous form. For discrete-time nonlinear systems the output mapping function is applied to a vector of multiple self-compositions of the forward dynamics function to transform the system into a Brunowski chain of delays. For continuous-time nonlinear systems the Lie derivatives of the system output are used to transform the system into a Brunowski chain of integrators.

In many applications the observers presented here are better than other commonly used state estimators. All the observers demonstrate convergence in the

Table 9.1 Nonlinear discrete-time observer application summary chart.

Observer	Recommended Application	Complexity ^{a,b}	Comments
1	All systems with appropriate affine structure, low measurement noise.	$N_f + n_x n_p^2$ ^c	Simplest observer to implement. Performance generally excellent where applicable. Requires measurement of all states in forward dynamics function. Can be very sensitive to noise.
2	Nonlinear systems with high measurement noise.	$(n+1)(N_f + N_h) + dN_J + n$ ^d	Performance generally comparable to observer 3. Allows for root finder other than Newton's method. Applicable to systems where Newton's method prone to failure. Requires observability, not necessarily strong observability.
3	Nonlinear systems with poor observability.	$(n+1)(N_f + N_h) + dN_J + n$	Excellent convergent properties in situations of poor observability while allowing for noise mitigation. Ideal for parameter estimation when convergence time is not critical and observability poor. Requires strong observability.
4	Nonlinear systems with good observability.	$(n+1)(N_f + N_h) + N_J + n$ ^e	Provides for best tuning for process noise vs measurement noise. May require closer initial estimate than observers 1 and 3. Requires strong observability.

^aOperations per step.

^b N_f, N_h, N_J - Operations associated with functions f, h , Jacobian calculation, respectively. n, d - State vector dimension, number of iterations, respectively.

^cBased upon generalized inverse, section 4.4.2. n_x - Number of directly measured states. n_p - Number of estimated states.

^dPresumes implementation with Newton's method.

^eFor fixed gain. Add $n^3/3 + n^2$ for first n steps to calculate steady-state gains.

presence of “hard” nonlinearities in contrast to the discrete-time extended Kalman filter which often diverges. These new observer can be applied to parameter estimation problems requiring “probing signals” whereas the continuous-time Gauthier and Ciccarella observers are limited in application by their restrictive relative degree requirement.

In the discrete-time parameter estimation problem where the system relative degree r is less than the system order n , implementation of the Observers 2,3, and 4 require insertion of $n - r$ delay stages. When applied to a discretized continuous-time systems, this delay limits applicability of the observer to systems in which the dominant time constant is much greater than the sampling period. This limitation is generally not restrictive given the great availability of fast and inexpensive analog-to-digital converters and computers.

The Lipschitz requirement in theorem 5.2.1 and inequality (5.42) restricts Observer 2 applicability. In practice it is not possible to know *a priori* whether these conditions are satisfied and in some applications where the initial error is large these conditions may not be satisfied. Fortunately, satisfaction of the Lipschitz condition and inequality (5.42) is *sufficient* but not *necessary* for convergence and represents upper bound on the on the radius of the closed-loop pole locations of $A - LC$. It is a conservative upper bound.

Lastly, the primary significance of the work presented here is that it provides a “toolbox” with which the systems practitioner can build observers. As illustrated by the ARMA filter example, section 6.2, some problems can be solved with different estimation methods and not all the methods yield results of equal quality. Furthermore, in these nonlinear estimation systems it is difficult to make generalizations about observer performance thus the practitioner needs this “toolbox” of methods from which to “cut and try” different solutions.

9.2 Further Research

These new observers open questions for further inquiry. It is difficult to develop a *general* line of inquiry into nonlinear systems and nonlinear observers since each nonlinear dynamical system has a particular characteristic behavior different from other nonlinear systems. Recent work on chaotic systems [44] offers some general characterizations of nonlinear systems and perhaps concepts of “attractors,” “Liapunov exponents” can be used in future observer design.¹ The only characterization used in the Ciccarella work and the present work is the single Lipschitz constant and its constraints.

It is difficult to perform further general research on Observer 1 since its gain matrix function is completely application dependent. Two questions do arise:

1. The nonlinear gain function/forward dynamics product, $F_{22} - K(y_k)F_{12}$, (4.85), needs to be a contractor. Does a general methodology exist to find this contractor?
2. Is the methodology for picking the gain function using the inverse or pseudoinverse, section 4.4.2, extendable to the continuous-time Friedland parameter estimator by setting the sample time arbitrarily small?
3. The gain matrix $K(y_k)$, (4.85), is dependent upon the measured state $y_k = x_{1k}$. How noisy can the measurement y_k be? Does it need to be measured or can it too be estimated by a dynamic observer?

With regards to Observer 2, three questions which remain unresolved are:

1. What are the *optimal* pole locations of A_{cl} , (5.32)?

¹Ott [44], pages 145-147, presents three interesting pages on the control of chaotic systems. He presents pole-placement as the design method and, like the design Observer 2 presented here, only specifies that the poles have to be stable.

2. Can the continuous-time Ciccarella and Gauthier results be recovered by making the sampling time T vanishingly small? What is the relationship between a numerical finite-difference solution of the partial differential equations inherent in the Gauthier observer and the numeric root finding of this new observer?
3. What is the relationship between static numeric root finding, static numeric optimization (solutions to nonlinear least-squares) and this dynamic observer?

9.2.1 Optimal Pole Locations

Empirically, the Lipschitz requirement, (5.42), is satisfied by increasing the “speed” of the observer, i.e., bringing all the poles of matrix A_{cl} (see (5.32)) closer to the origin of the unit circle. From understanding of linear systems it is well known that manipulating a system dynamic response by pole placement is a tricky, uncertain endeavor often leading to stable but non-robust behavior. The observer presented and the continuous-time Ciccarella observer define *only a minimum observer speed* over which convergence is guaranteed. In the continuous-time Ciccarella observer all the poles must lie in a half-plane to the left of some maximum negative number. In Observer 2, the poles must lie in a circle of some radius less than some maximum number (which has to be less than unity.) Neither observer design requirement is more specific about the pole locations.

Designing the optimal pole locations for Observer 2 is equivalent to adding “directionality” to the Liapunov proof presented in chapter 5. Just as a suboptimal observer “Kalman-like” observer using a spherical covariance matrix can be constructed, the optimal Kalman Filter observer is obtained when the covariance matrix is hyper-ellipsoidal, i.e., larger in *directions* of greater uncertainty.

This problem of optimal pole placement is further complicated when the issue of stochastic convergence is addressed. What, for instance, are the important

parameters characterizing the stochastic process? In all likelihood the probability distribution of the noise is defined in the original coordinate system. What are the properties of the noise under the $z = \phi(x)$ transformation?

Experience has shown that for “benign” transformations the central limit theorem tends to transform Gaussian noise into some well-behaved nearly Gaussian-like noise which is fairly well described by a mean and a standard deviation. However, it is sufficient for the transformation $z = \phi(x)$ to have an algebraic division to transform the Gaussian noise into a poorly-behaved distribution like the Cauchy distribution. In situations where transformation $z = \phi(x)$ maps the original noise probability distribution into some poorly behaved singular distribution, the observer is likely to fail.

9.2.2 Unification of Discrete-Time and Continuous-Time Observer Theory

The continuous-time Gauthier Observer should be recoverable from Observer 2 in the limit that sampling time $T \rightarrow 0$. Elucidating this relationship shall yield the connection between partial differential equations of the Gauthier observer and the nonlinear algebraic equations of Observer 2. It is likely that the algebraic equations of Observer 2 are the same equations which would fall out from a finite-difference discretization solution to the Gauthier PDEs.

9.2.3 Unification of the Quasi-optimal Discrete-time Friedland Observer and the Continuous-time State-dependent Riccati Equation Filter

There is probably a link between the quasi-optimal discrete-time Friedland observer presented in section 8.4 and the continuous-time State-dependent Riccati Equation Filter where the former is a discrete-time version of the latter. This relationship should be explored further to provide additional insight into the two observer forms. Furthermore, the entire relationship among Newton observers, least-squares

observers, discrete-time Friedland observers and state-dependent Riccati equation filters can be understood and unified.

9.2.4 The Dynamic Observer and Static Root finding

The problem of finding the roots of a system of n equations $f(x) = 0$ can be posed as a feedback observer problem with degenerate (i.e. static) dynamics. System $f(x) = 0$ can be written

$$x_{k+1} = x_k \quad (9.1)$$

$$y_k = h(x_k). \quad (9.2)$$

An observer for this system is in the form

$$\tilde{x}_{k-1} = \hat{x}_k \quad (9.3)$$

$$x_{k-1} = \tilde{x}_{k+1} + K \underbrace{[y_{k+1} - h(\tilde{x}_{k+1})]}_0 \quad (9.4)$$

$$= \tilde{x}_{k+1} - Kh(\tilde{x}_{k+1}) \quad (9.5)$$

where the closed-loop eigenvalues of $(I - KC)\Phi$ are stable. In this formulation $\Phi = I$ and the matrix of "observation partials" $C = J$, the Jacobian, i.e., $C = J = \partial h(x)/\partial x$. To guarantee stable eigenvalues it is sufficient that $K = \alpha J^{-1}$ where $0 < \alpha < 2$. The closed-loop error dynamic matrix becomes $(1 - \alpha)I$. The resulting observer assumes the form

$$\hat{x}_{k+1} = \hat{x}_k - \alpha J^{-1} h(\hat{x}_k) \quad (9.6)$$

which is Newton's method.

The fixed point problem, $h(x) = x$ is a variant of the root finding problem $h(x) = 0$. For the fixed point problem the observer is written in terms of a residual ρ

$$\hat{x}_{k+1} = \hat{x}_k - \alpha C^{-1} \rho \quad (9.7)$$

where

$$\rho = h(x_k) - h(\hat{x}_k) \quad (9.8)$$

$$= x_k - h(\hat{x}_k). \quad (9.9)$$

A state observer is more general and more powerful than a Newton's method root finder. The observer does not require the entire state to be instantaneously visible in the output map, i.e., $y \in \mathbb{R}^m, x \in \mathbb{R}^n, m < n$ and the root can have a forward dynamics (i.e., the root can move) and a forcing term

$$x_{k+1} = f(x_k, u_k) \quad (9.10)$$

$$y_k = h(x_k, u_k). \quad (9.11)$$

Now the root-finding part of Observer 2 can be written as an observer and the algorithm can be seen as an interplay of two observers—one static and one dynamic or, viewed in another way – one that works in space and one that works in time. From chapter 5, Observer 2 is written

$$\hat{z}_{k+1} = A\hat{z}_k + Bh[G_f^m(\hat{x}_k, u_k), u_k] + L(y_k - C\hat{z}_k) \quad (9.12)$$

$$\hat{x}_k = \phi^{-1}(\hat{z}_k, u_k). \quad (9.13)$$

In the dual observer form it is written

$$\hat{z}_{k+1} = A\hat{z}_k + Bh[G_f^m(\hat{x}_k, u_k), u_k] + L(y_k - C\hat{z}_k) \quad (\text{time}) \quad (9.14)$$

$$\tilde{x}_{k+1} = f(\hat{x}_k, u_k) \quad (\text{seed}) \quad (9.15)$$

$$\hat{x}_{j=1} = \tilde{x}_{k+1} \quad (\text{seed}) \quad (9.16)$$

$$\hat{x}_{j+1} = \tilde{x}_{k+1} - \alpha J^{-1}[\hat{z}_{k+1} - \phi(\tilde{x}_j, u_{k+1})] \quad (\text{space}) \quad (9.17)$$

where J , the Jacobian is evaluated at \tilde{x}_{k+1}

$$J = \left. \frac{\partial \phi(x, u)}{\partial x} \right|_{x=\tilde{x}_{k+1}} \quad (9.18)$$

In the present form of Observer 2 (9.17) is iterated until convergence.² Repeating the simulation on the dog's blood pressure reveals that the observer performs *better* with a *a single* calculation of (9.17) than it does when (9.17) is repeated to convergence.

This difference is *not* supported by theory and requires further investigation. This behavior is reminiscent of the often observed (yet unexplained) performance of iterated extended Kalman filters which shows they deteriorate as the number of iterations is increased beyond one or two.

Equations (9.14), (9.17) represent a set of coupled difference equations. Rewriting (9.14), (9.17) and suppressing forcing term u_k yields

$$\hat{z}_{k+1} = A\hat{z}_k + Bh[G_f^m(\hat{x}_k)] + L(y_k - C\hat{z}_k) \quad (\text{time}) \quad (9.19)$$

$$\hat{x}_{j+1} = f(\hat{x}_j) - \alpha J^{-1} \{ \hat{z}_{k+1} - \phi[f(\hat{x}_j)] \} \quad (\text{space}) \quad (9.20)$$

It would be interesting to determine whether this set of difference equations might be derivable from a discrete potential function $\Psi(j, k)$ and if it is possible to relate observer properties to some general characteristics of this potential function.

²Actually, in the examples it is iterated 20 times having noted that in all cases it converges in less than 20 iterations. It is easier to code a fixed number of iterations than to check for convergence.

APPENDIX A

SIMULATION PLOTS

A.1 Introduction

In the course of this study of nonlinear discrete-time observers it was necessary to perform many simulations. The study of nonlinear observers has a very large “parameter space” to explore. Furthermore, nonlinear observer performance is problem dependent.

By recommendation of Professor Ü. Kotta,¹ a researcher in the field of discrete-time nonlinear control systems, the canine blood pressure problem was simulated more extensively than other examples. Even in the limited scope of this one example, the simulation parameter space of the three observers is quite large. Table A.1 lists the parameters subject to variation for each observer. The number of possible simulations which cover all combinations of variations of these parameters is very large.

Table A.1 Observer simulation “parameter space.”

Observer	Parameter Subject to Variation
Grossman Observer	Prefilter gains Newton solver parameters α, d
Modified Moraal/Grizzle Observer	Newton solver parameters α, d
Modified Ciccarella Observer	Fixed filter gains Feedforward elimination Parameters P_0, Q, W

¹Institute of Cybernetics, Akadeemia tee 21, Tallinn, Estonia

In contrast to the parameter space, the “desired property” space is quite small. The desired properties of observers includes:

1. Stable convergence.
2. Fast transient response.
3. High noise rejection.
4. Robustness to modeling errors.
5. Robustness to variations in input amplitude and problem scaling.
6. Simple implementation.

Property 1, stable convergence, is the *sine qua non* of any observer. The importance placed on properties 2–6 is application dependent. Achievement of any one of these properties usually requires compromise of another property (e.g., faster transient response usually leads to reduced noise rejection). Achieving the best compromise for any given application is the observer design problem.

The simulations presented in sections A.2, A.3 of this appendix explore the compromise between achieving fast transient response and high noise rejection. In section A.2, noise-free simulation runs were performed to establish the transient response. In section A.3, Gaussian white noise added to the measurements to establish noise rejection performance.

Only a small portion of the observer parameter space was explored. For the Grossman and Moraal/Grizzle observers parameters α , d of the Newton solver were varied. For the Ciccarella observer, parameters Q , W , and the feedforward gain (0 or 1) were varied.

The simulations presented in section A.4 explore the sensitivity (or rather, insensitivity) of the three observers to input scaling. This insensitivity may be important in parameter estimation applications where a probing signal is required.

Except for the observer run shown in figure A.27, all the observers were stable.

A.2 Observer Simulations Without Noise

A.2.1 Grossman Observer Prefilter

The Grossman observer, when implemented with a Newton root finder is similar to the Moraal/Grizzle observer with a nonlinear prefilter operating on the input. The effect of this prefilter is seen in the comparisons of figure A.1 with A.2 and figure A.13 with A.14. In these simulation runs, $\alpha = 1$ which provides the maximum root-finding step. In figures A.1, A.2, $d = 1$. In figures A.13, A.14, $d = 5$. By setting $\alpha = 1$, $d = 5$, the fastest root finding is achieved, the filtering effects of the root-finding are minimized, and the effects of the prefilter of the Grossman observer are highlighted. The effects of this prefilter are to slow convergence down such that response time is about sixty sample steps for the Grossman observer compared with three steps for the Moraal/Grizzle observer.

A.2.2 Effects of Slowing Factor α and Iteration Count d

Due to the presence of the prefilter in the Grossman observer the effect of varying α , and d upon the filter response are less clear than in the Moraal/Grizzle observer.

The effect that varying α has upon convergence is seen by comparing figures A.2 and A.10. In figure A.2, $\alpha = 1$, $d = 1$, and the observer converges in three steps. In figure A.10, $\alpha = 0.1$, $d = 1$, and the observer converges in about eighteen steps. Increasing the iteration counter from $d = 1$ to $d = 5$ counters the effect of decreasing α and the deadbeat convergence in three steps is recovered as shown in figure A.22.

A.2.3 Noise-Free Ciccarella Observer Performance

In the noise-free situation the performance of the Ciccarella observer in its original form was similar to that of the Moraal/Grizzle observer, as seen from comparison

of figures A.2 and A.25. The Ciccarella observer converged in six steps rather than three steps for the Moraal/Grizzle observer.

Removal of the feedforward term in the Ciccarella observer, improves the measurement noise rejection but vitiates Ciccarella's local stability proof. Observer divergence is shown in figure A.27. Recovery of filter stability was achieved by reducing the filter gains, as shown in figure A.29.

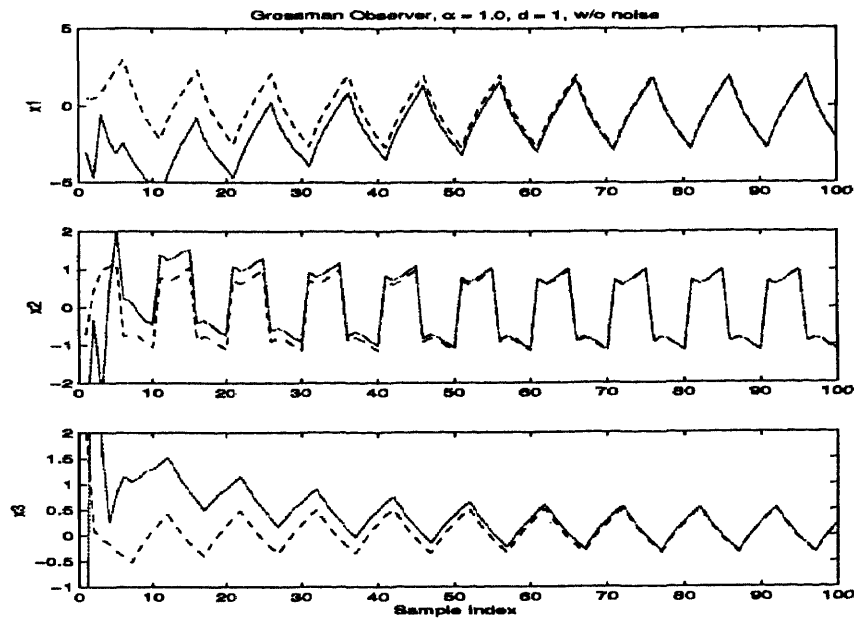


Figure A.1 Grossman observer state estimate (solid) and true state (dotted) for three-state model of dog blood pressure response to medication. $\alpha = 1.0, d = 1$, no measurement noise present.

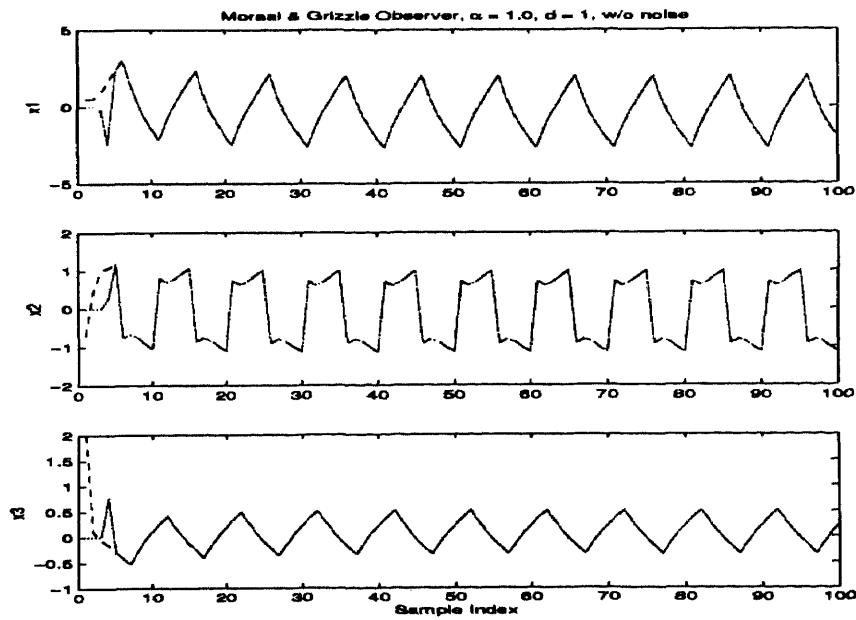


Figure A.2 Moraal/Grizzle observer state estimate (solid) and true state (dotted) for three-state model of dog blood pressure response to medication. $\alpha = 1.0, d = 1$, no measurement noise present.

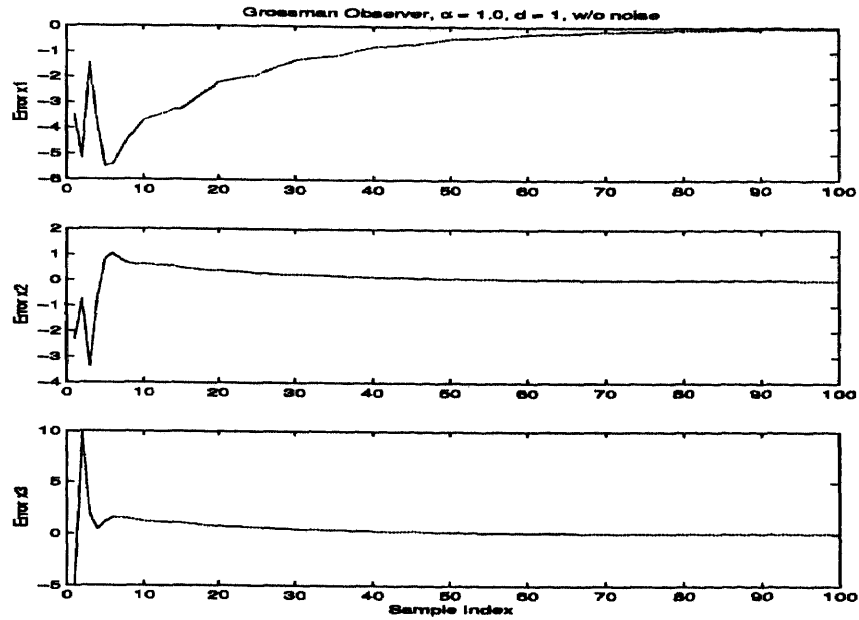


Figure A.3 Grossman observer state estimation error for three-state model of dog blood pressure response to medication. $\alpha = 1.0, d = 1$, no measurement noise present.

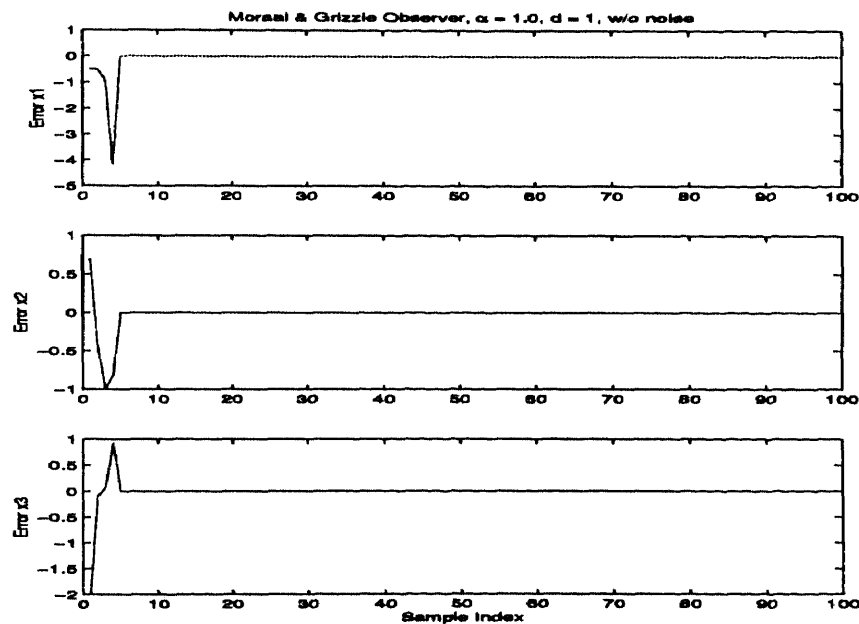


Figure A.4 Moraal/Grizzle observer state estimation error for three-state model of dog blood pressure response to medication. $\alpha = 1.0, d = 1$, no measurement noise present.

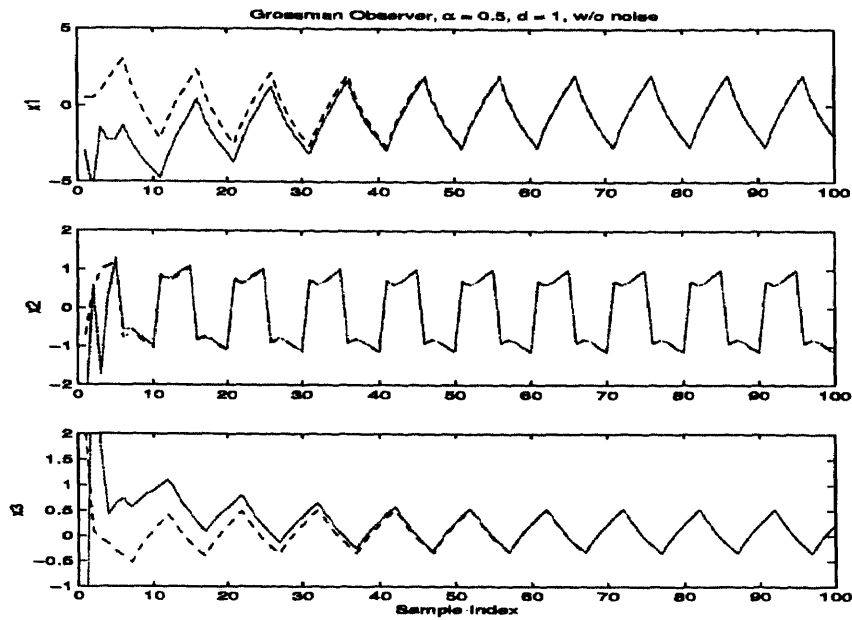


Figure A.5 Grossman observer state estimate (solid) and true state (dotted) for three-state model of dog blood pressure response to medication. $\alpha = 0.5, d = 1$, no measurement noise present.

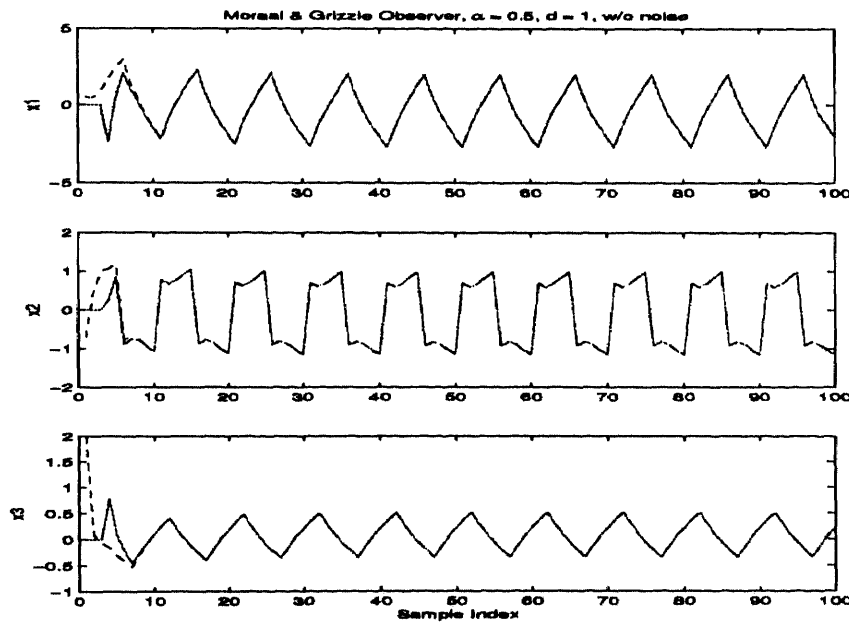


Figure A.6 Moraal/Grizzle observer state estimate (solid) and true state (dotted) for three-state model of dog blood pressure response to medication. $\alpha = 0.5, d = 1$, no measurement noise present.

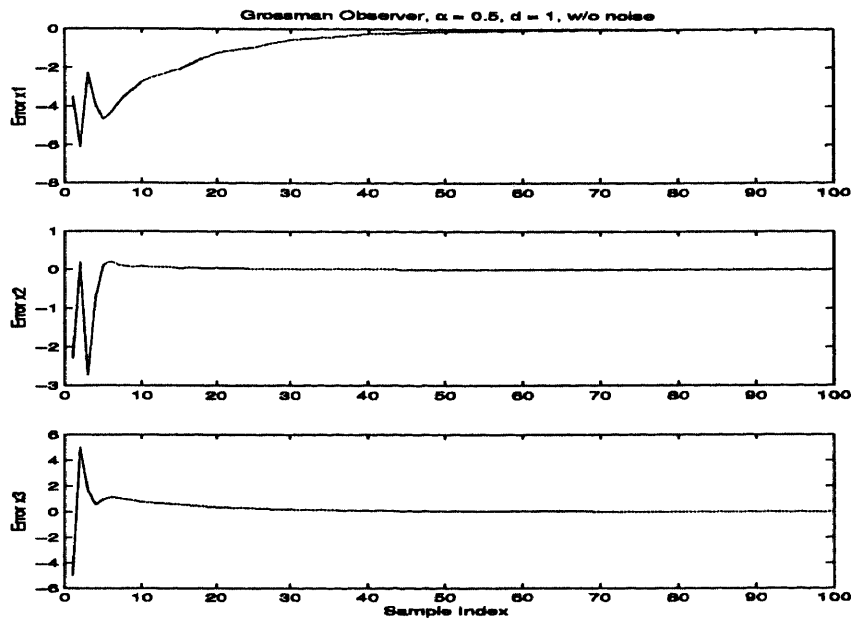


Figure A.7 Grossman observer state estimation error for three-state model of dog blood pressure response to medication. $\alpha = 0.5$, $d = 1$, no measurement noise present.

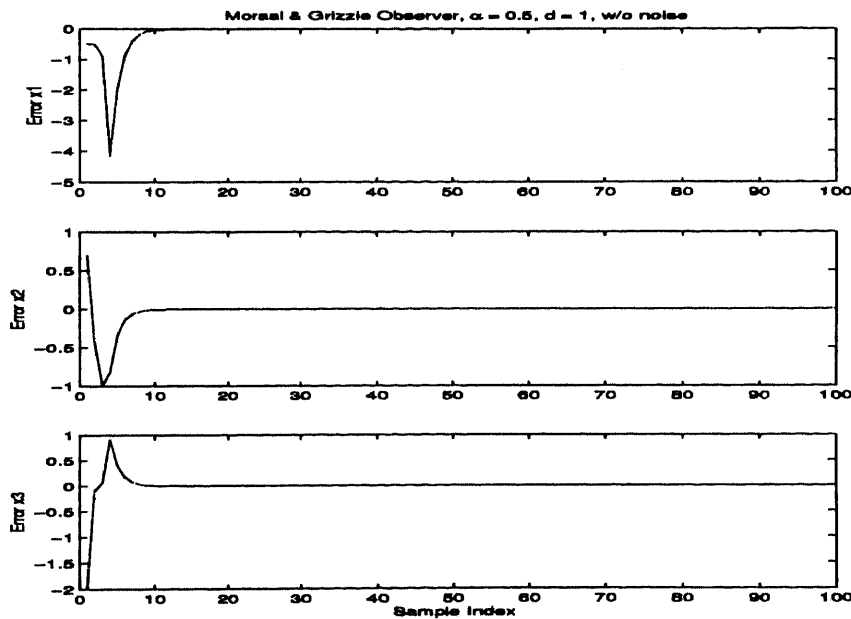


Figure A.8 Moraal/Grizzle observer state estimation error for three-state model of dog blood pressure response to medication. $\alpha = 0.5$, $d = 1$, no measurement noise present.

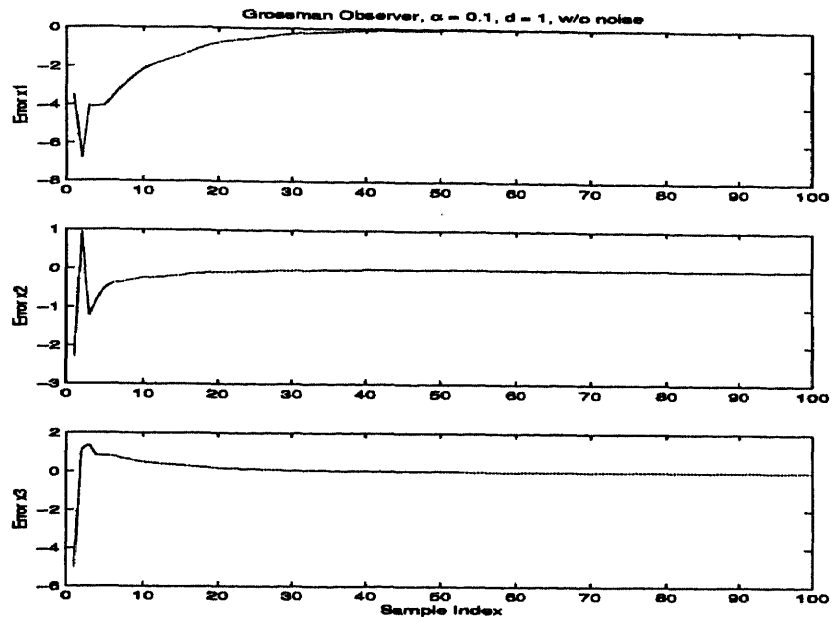


Figure A.9 Grossman observer state estimate (solid) and true state (dotted) for three-state model of dog blood pressure response to medication. $\alpha = 0.1, d = 1$, no measurement noise present.

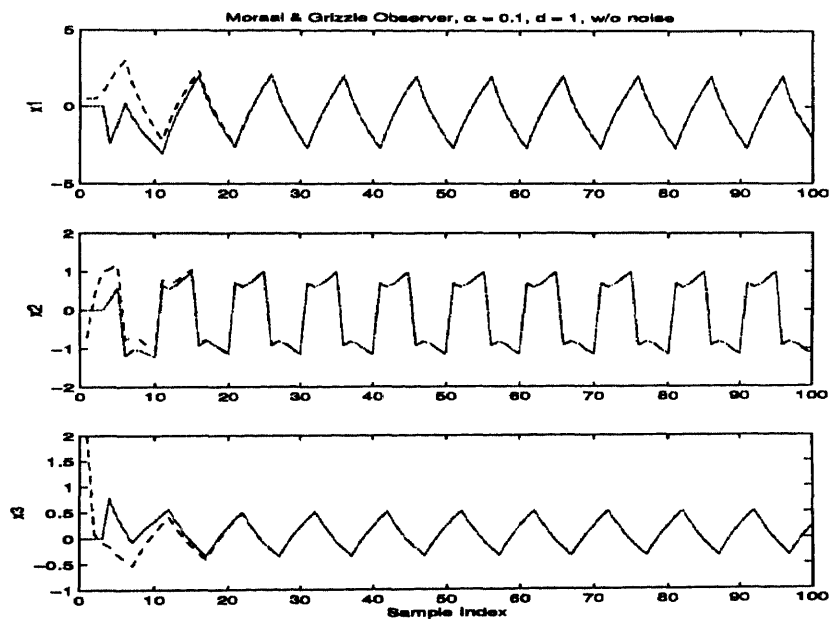


Figure A.10 Moraal/Grizzle observer state estimate (solid) and true state (dotted) for three-state model of dog blood pressure response to medication. $\alpha = 0.1, d = 1$, no measurement noise present.

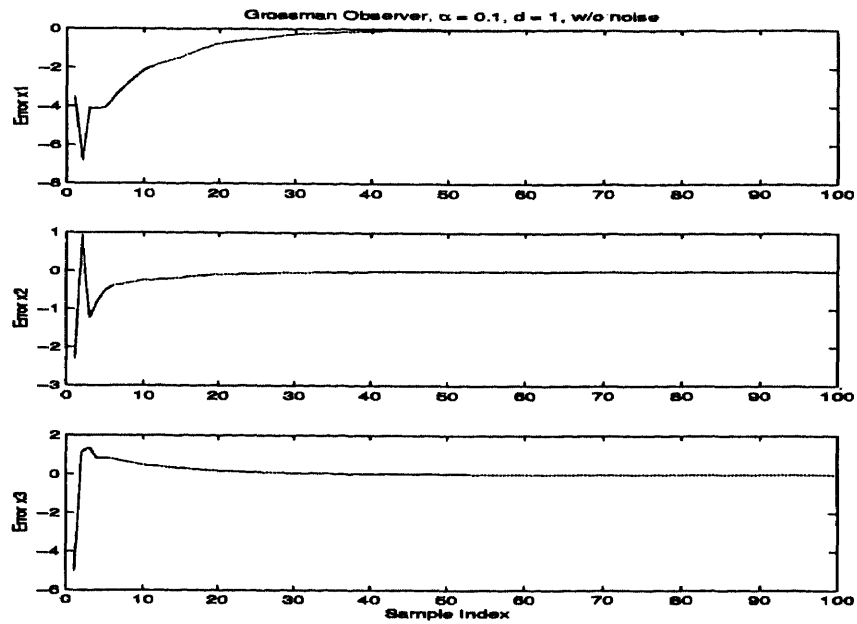


Figure A.11 Grossman observer state estimation error for three-state model of dog blood pressure response to medication. $\alpha = 0.1$, $d = 1$, no measurement noise present.

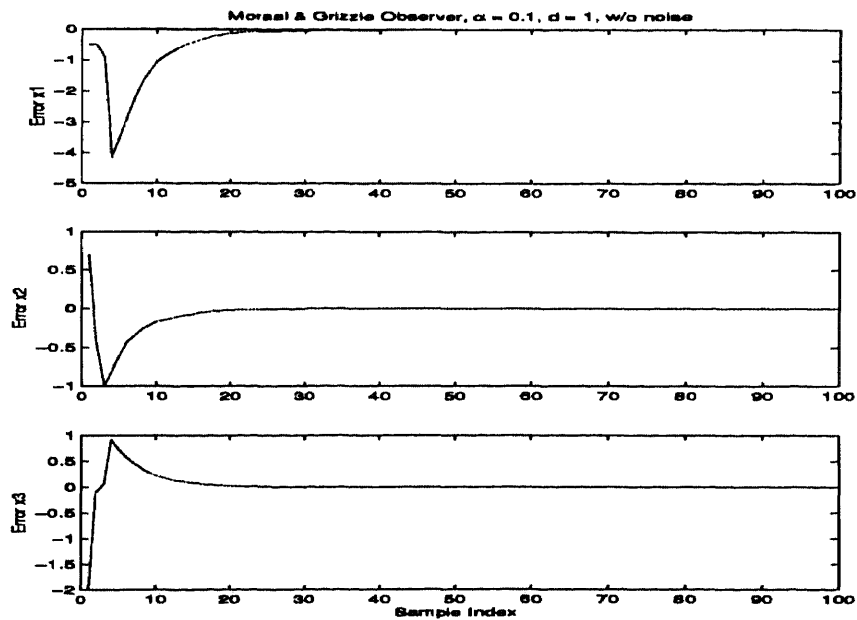


Figure A.12 Moraal/Grizzle observer state estimation error for three-state model of dog blood pressure response to medication. $\alpha = 0.1$, $d = 1$, no measurement noise present.

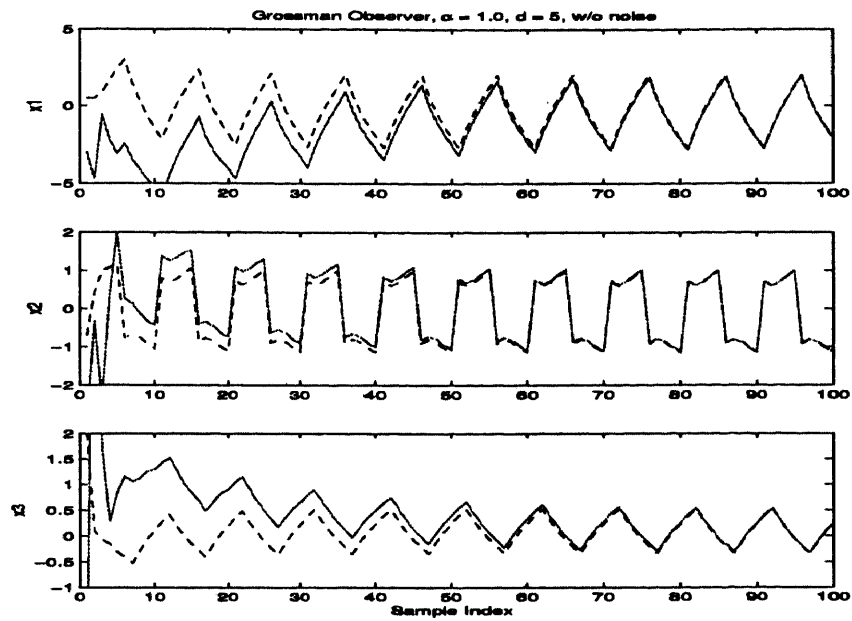


Figure A.13 Grossman observer state estimate (solid) and true state (dotted) for three-state model of dog blood pressure response to medication. $\alpha = 1.0$, $d = 5$, no measurement noise present.

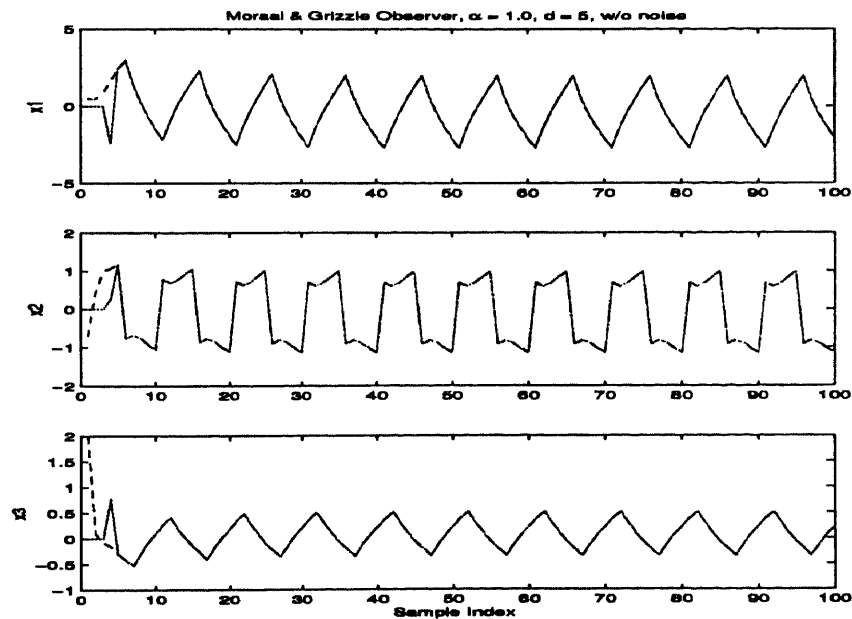


Figure A.14 Moraal/Grizzle observer state estimate (solid) and true state (dotted) for three-state model of dog blood pressure response to medication. $\alpha = 1.0$, $d = 5$, no measurement noise present.

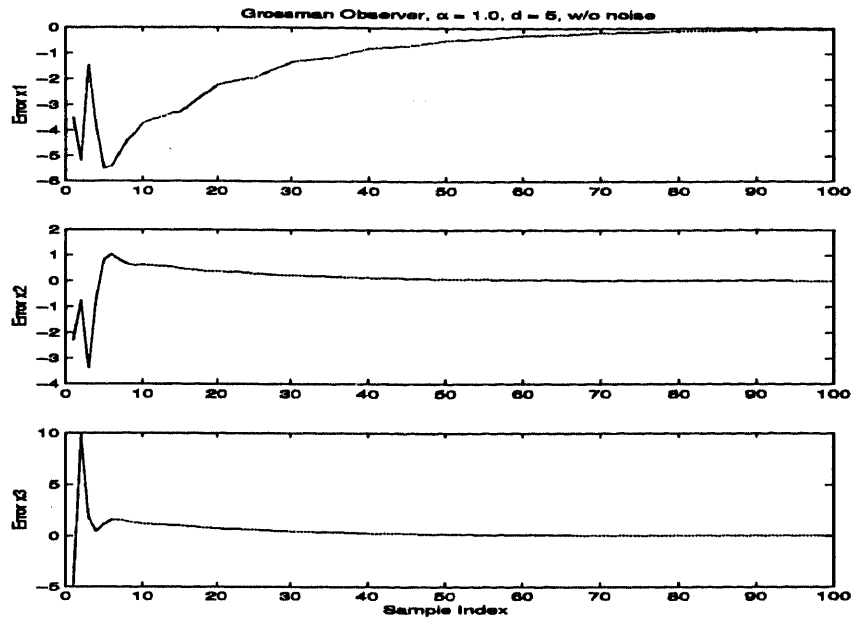


Figure A.15 Grossman observer state estimation error for three-state model of dog blood pressure response to medication. $\alpha = 1.0, d = 5$, no measurement noise present.

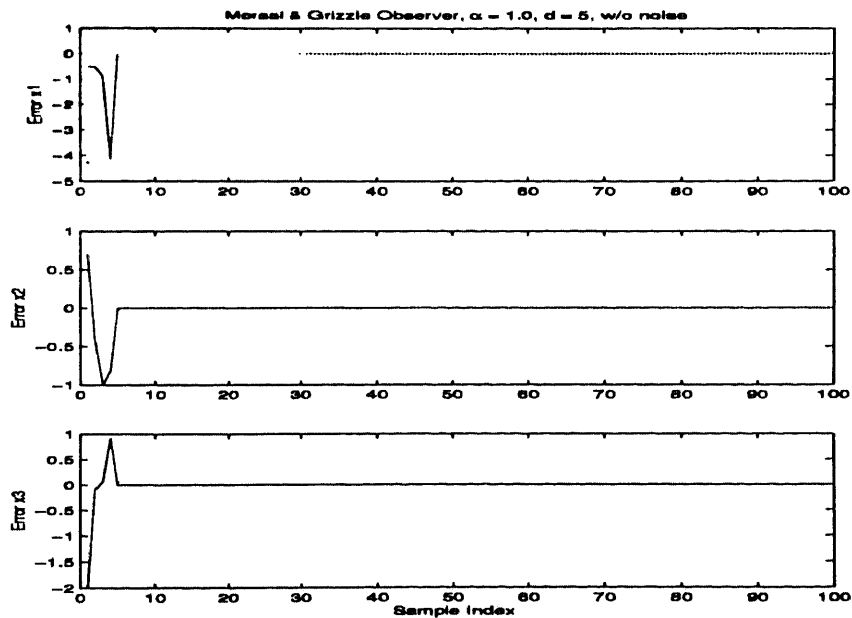


Figure A.16 Moraal/Grizzle observer state estimation error for three-state model of dog blood pressure response to medication. $\alpha = 1.0, d = 5$, no measurement noise present.

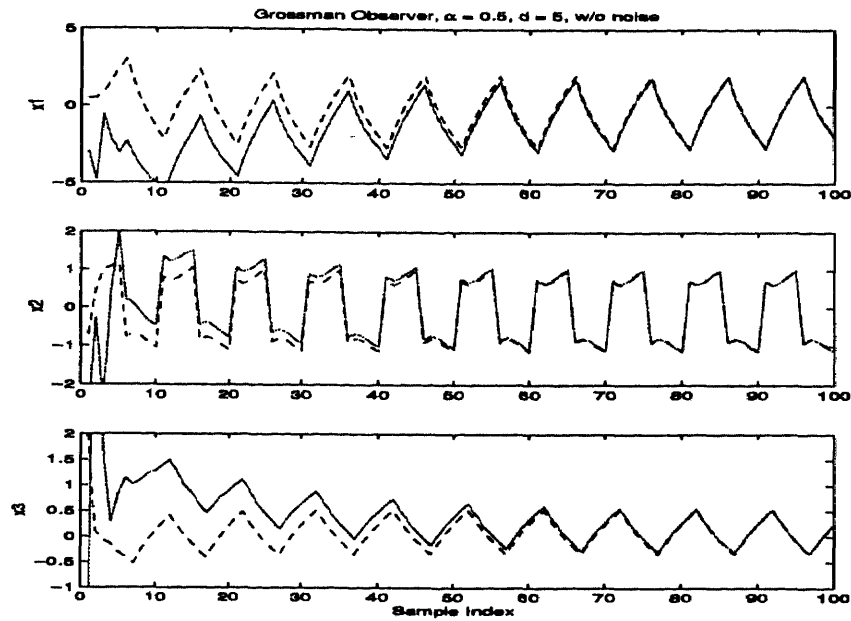


Figure A.17 Grossman observer state estimate (solid) and true state (dotted) for three-state model of dog blood pressure response to medication. $\alpha = 0.5$, $d = 5$, no measurement noise present.

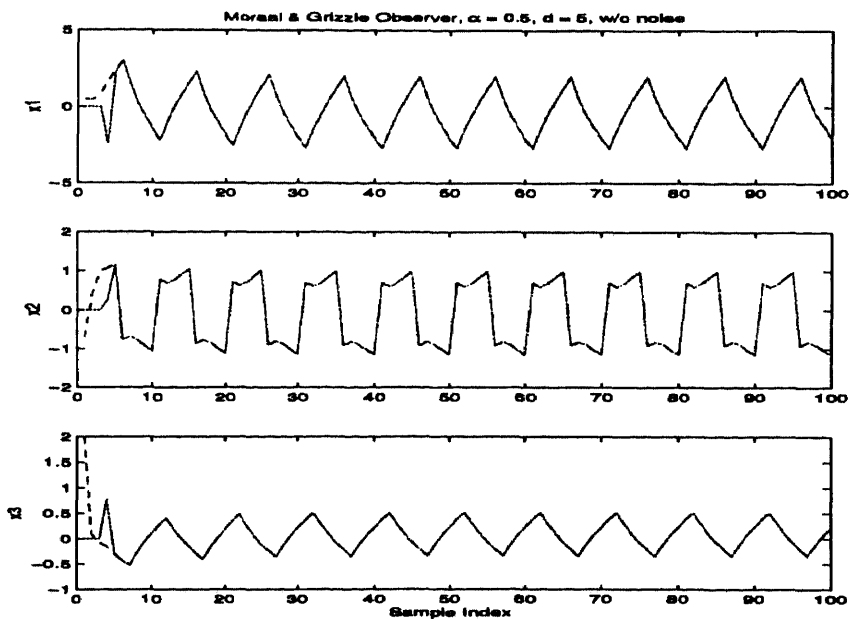


Figure A.18 Moraal/Grizzle observer state estimate (solid) and true state (dotted) for three-state model of dog blood pressure response to medication. $\alpha = 0.5$, $d = 5$, no measurement noise present.

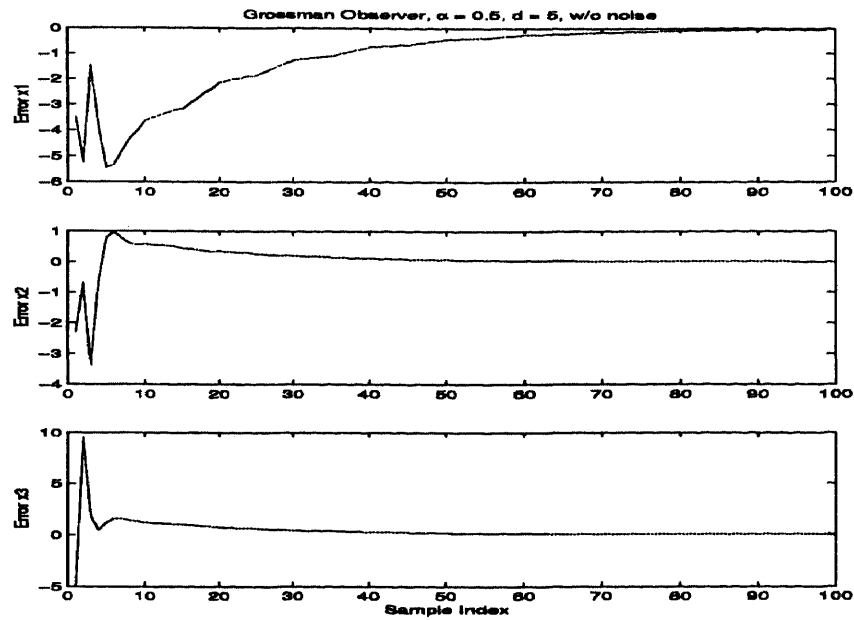


Figure A.19 Grossman observer state estimation error for three-state model of dog blood pressure response to medication. $\alpha = 0.5$, $d = 5$, no measurement noise present.

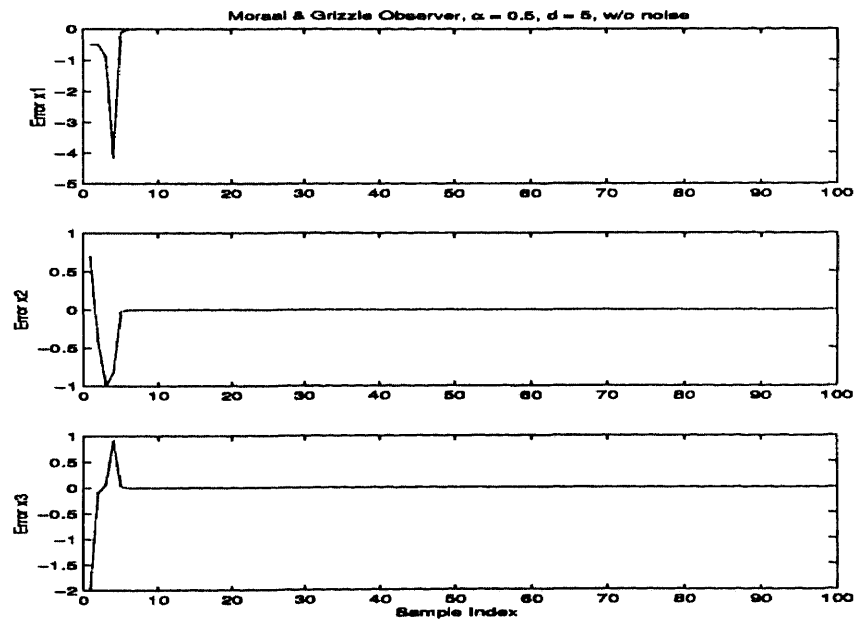


Figure A.20 Moraal/Grizzle observer state estimation error for three-state model of dog blood pressure response to medication. $\alpha = 0.5$, $d = 5$, no measurement noise present.

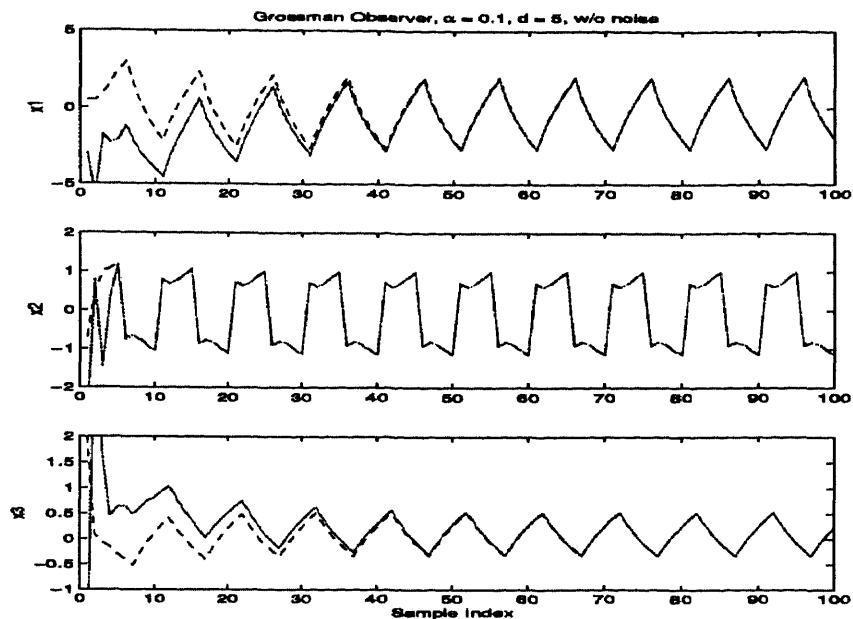


Figure A.21 Grossman observer state estimate (solid) and true state (dotted) for three-state model of dog blood pressure response to medication. $\alpha = 0.1, d = 5$, no measurement noise present.

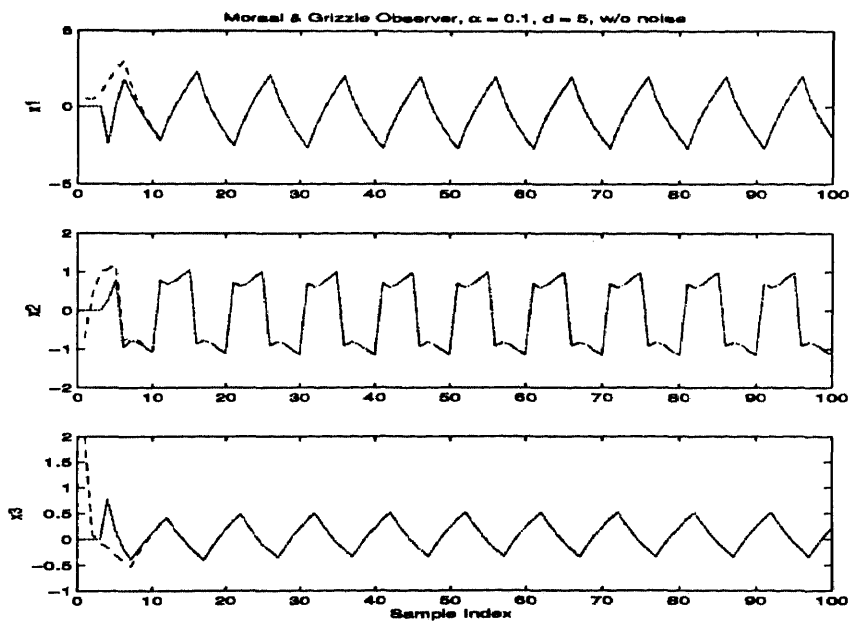


Figure A.22 Moraal/Grizzle observer state estimate (solid) and true state (dotted) for three-state model of dog blood pressure response to medication. $\alpha = 0.1, d = 5$, no measurement noise present.

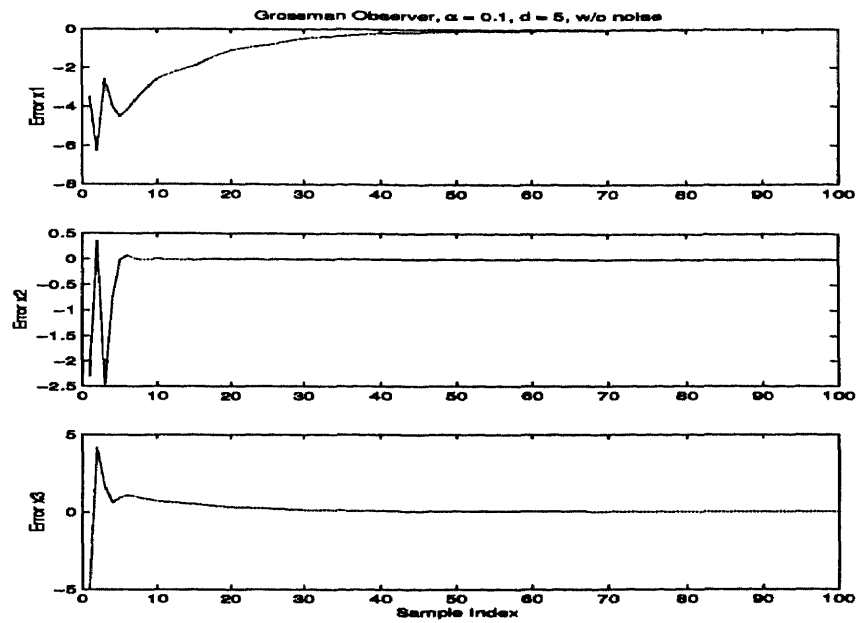


Figure A.23 Grossman observer state estimation error for three-state model of dog blood pressure response to medication. $\alpha = 0.1$, $d = 1$, no measurement noise present.

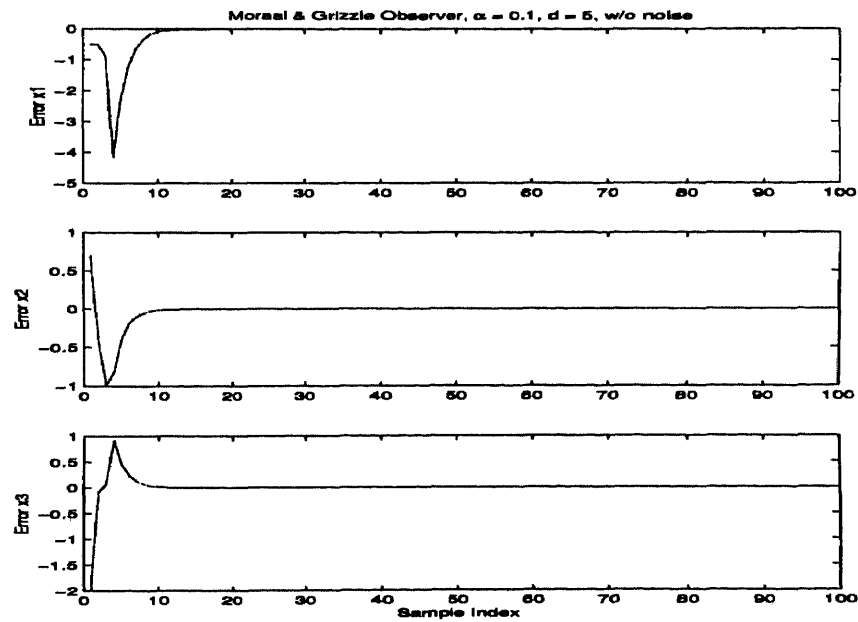


Figure A.24 Moraal/Grizzle observer state estimation error for three-state model of dog blood pressure response to medication. $\alpha = 0.1$, $d = 5$, no measurement noise present.

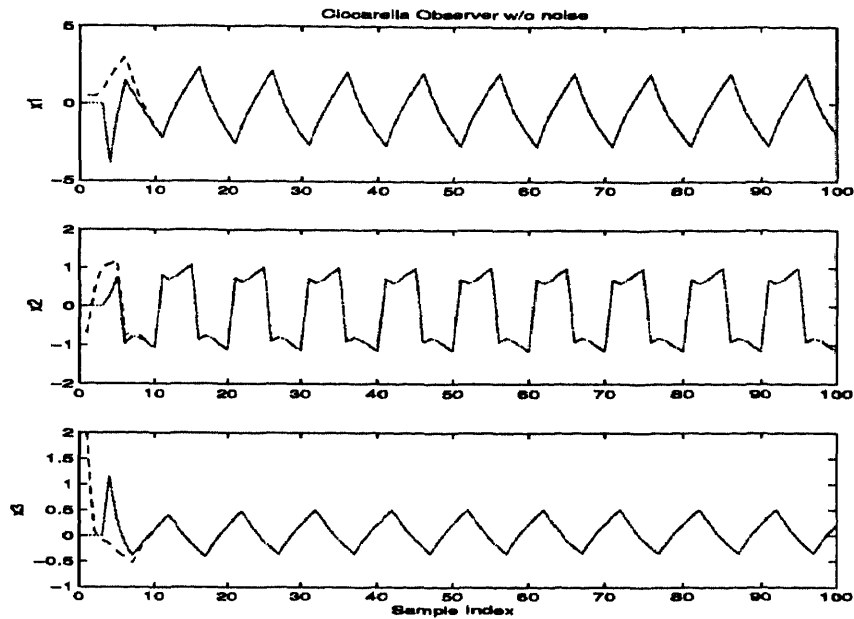


Figure A.25 Ciccarella observer estimate (solid) and true state (dotted), for three-state model of dog blood pressure response to medication. Arbitrary gain set $(\lambda(A - K) \in \{0.3, 0.4, 0.5\})$, no measurement noise present.

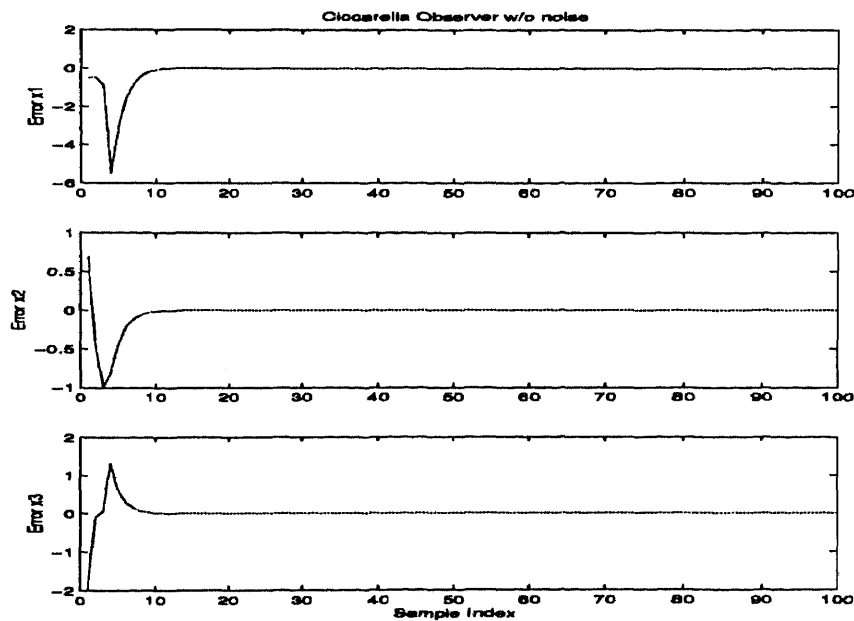


Figure A.26 Ciccarella observer state estimation error for three-state model of dog blood pressure response to medication. Arbitrary gain set $(\lambda(A - K) \in \{0.3, 0.4, 0.5\})$, no measurement noise present.

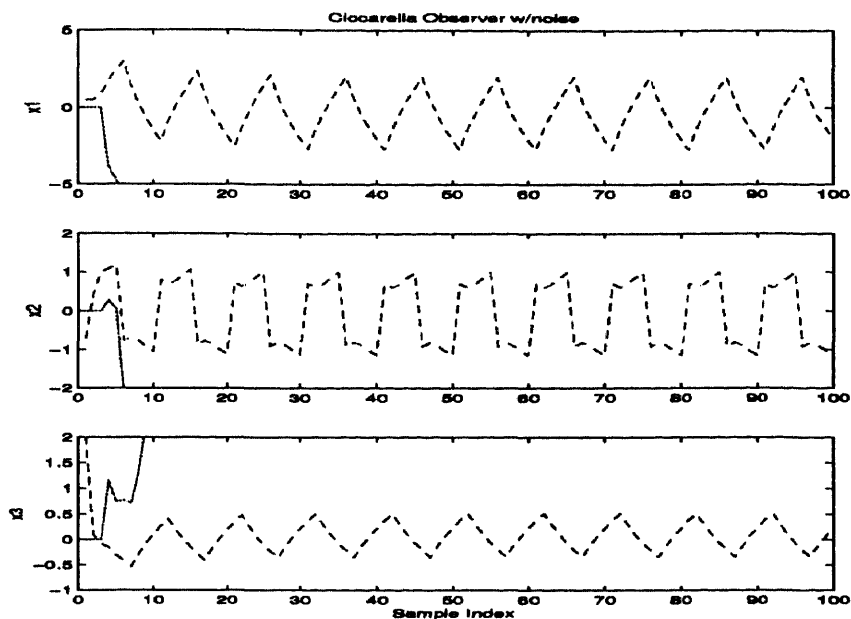


Figure A.27 Ciccarella observer estimate (solid) and true state (dotted), for three-state model of dog blood pressure response to medication. Arbitrary gain set $(\lambda(A - K) \in \{0.3, 0.4, 0.5\})$, no measurement noise present, no feedforward ($B = 0$). Note divergence.

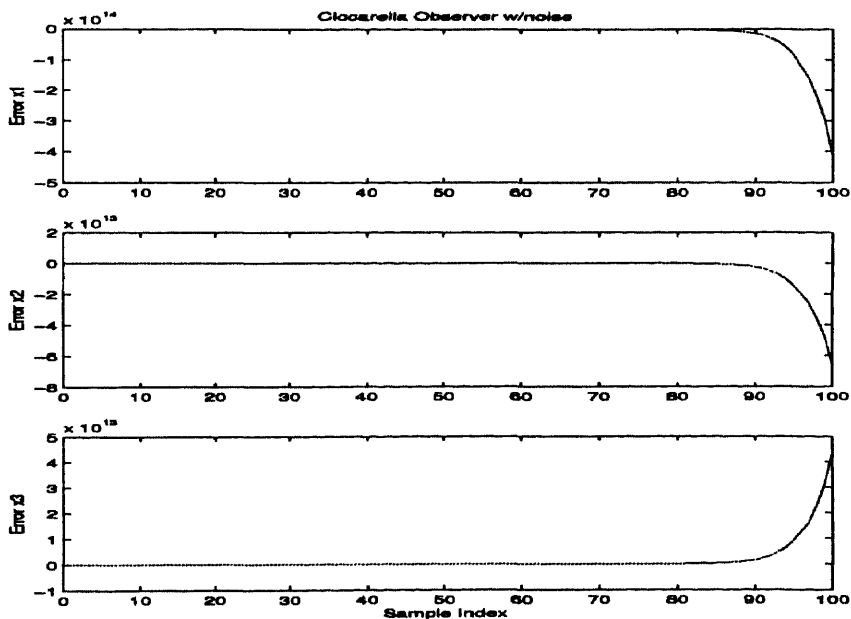


Figure A.28 Ciccarella observer state estimation error for three-state model of dog blood pressure response to medication. Arbitrary gain set $(\lambda(A - K) \in \{0.3, 0.4, 0.5\})$, no measurement noise present, no feedforward ($B = 0$). Note divergence.

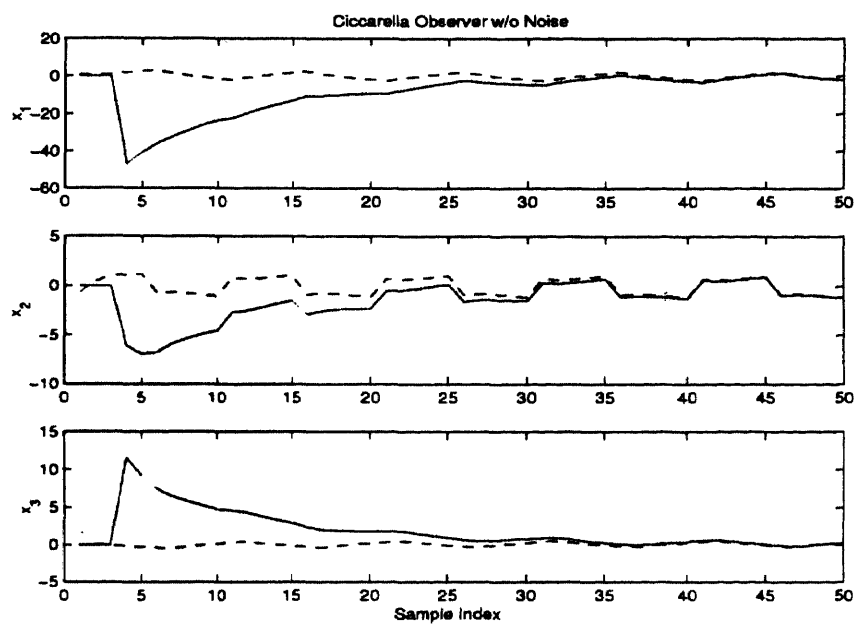


Figure A.29 Ciccarella observer estimate (solid) and true state (dotted), for three-state model of dog blood pressure response to medication. Reduced magnitude gain set ($\lambda(A - K) \in \{0.03, 0.04, 0.05\}$), measurement noise present, no feedforward. Observer is stabilized.

A.3 Observer Simulations With Noise

A.3.1 Measurement Noise Mitigation in the Grossman and Modified Moraal/Grizzle Observers

Though the Grossman observer and the Moraal/Grizzle observer are structurally related, the Grossman observer at its conception relied upon the smoothing action of its prefilter while the Moraal/Grizzle observer in its original form relied upon the smoothing action of the n -point deadbeat dynamics of the Newton solver

The measurement noise mitigation property of both observers is enhanced by exploiting the filtering action of an incomplete Newton step (by setting $\alpha < 1$) and by exploiting the incomplete solution of the nonlinear input/output equations (by setting $d = 1$).²

By setting $\alpha = 1$, $d = 5$, the filtering action of the Newton solver is minimized and the noise mitigation effect of the prefilter in the Grossman observer becomes most prominent. Comparisons of figure A.42 with A.43 and figure A.44 with A.45 show that the noise on state estimates \hat{x}_1 , \hat{x}_3 is reduced by the prefilter but that noise on state estimate \hat{x}_2 is not. Such mixed results are not uncommon in nonlinear observers.

By setting $\alpha = 0.1$, $d = 1$, the filtering action of the Newton solver is maximized.³ Comparisons of figures A.42 with A.38 and figure A.43 with A.39 demonstrate the effective filtering action of the Newton solver in both observers. This filtering comes at the expense of increased transient response time. Comparisons of figures A.38 with A.39 and figure A.40 with A.41 demonstrate comparable performance of both observers, with the Grossman observer perhaps exhibiting somewhat better tracking performance towards the end of the simulation run.

²It is interesting that both observers benefit from an effect that neither Grossman nor Moraal/Grizzle originally envisioned.

³Maximized for the values $\alpha \in \{0.1, 0.5, 1.0\}$. Clearly α can be set to $0 < \alpha < \epsilon$ with ϵ arbitrarily small.

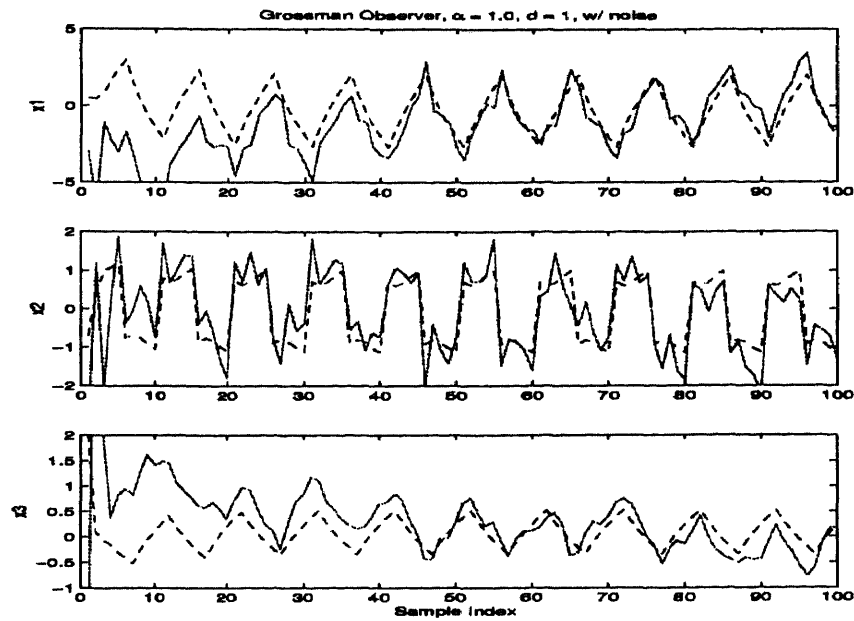


Figure A.30 Grossman observer state estimate (solid) and true state (dotted) for three-state model of dog blood pressure response to medication. $\alpha = 1.0$, $d = 1$, measurement noise present.

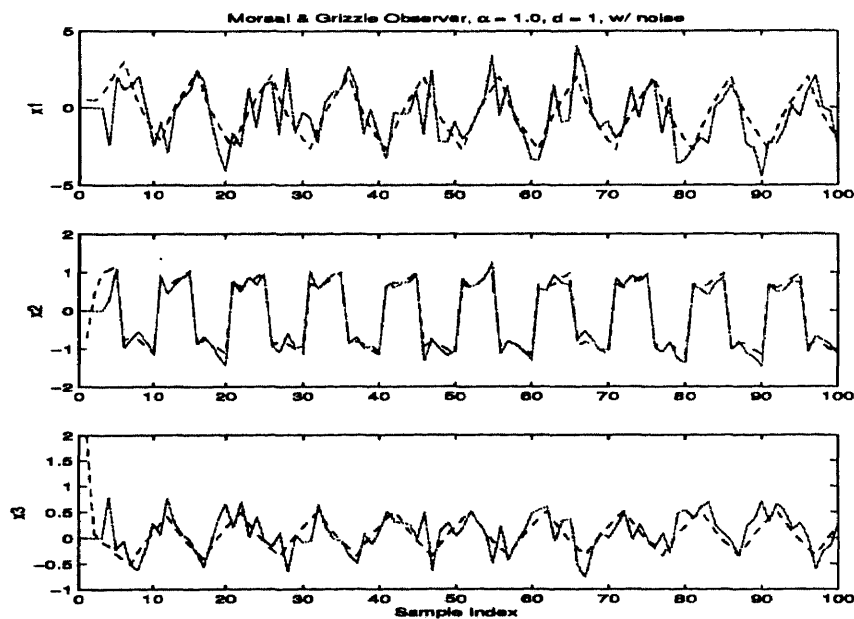


Figure A.31 Moraal/Grizzle observer state estimate (solid) and true state (dotted) for three-state model of dog blood pressure response to medication. $\alpha = 1.0$, $d = 1$, measurement noise present.

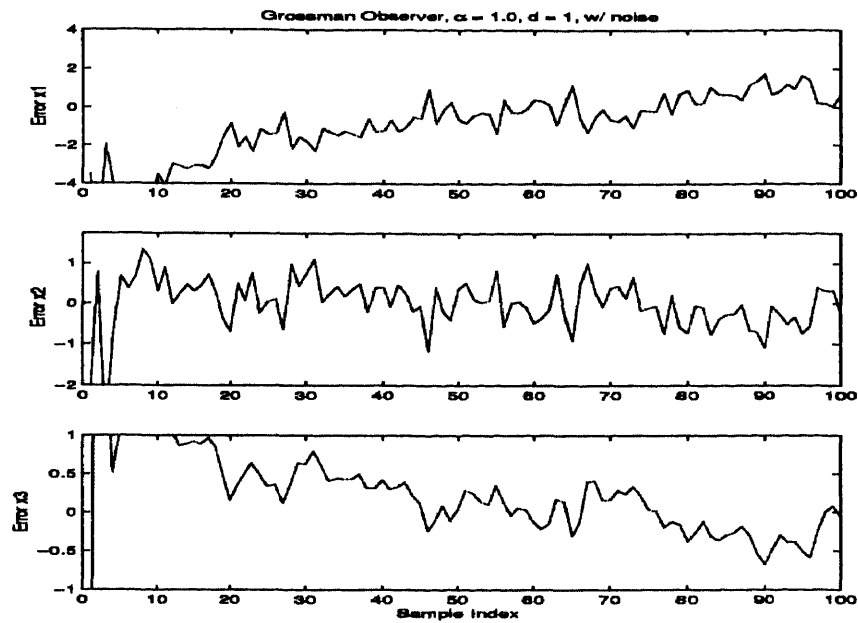


Figure A.32 Grossman observer state estimation error for three-state model of dog blood pressure response to medication. $\alpha = 1.0$, $d = 1$, measurement noise present.

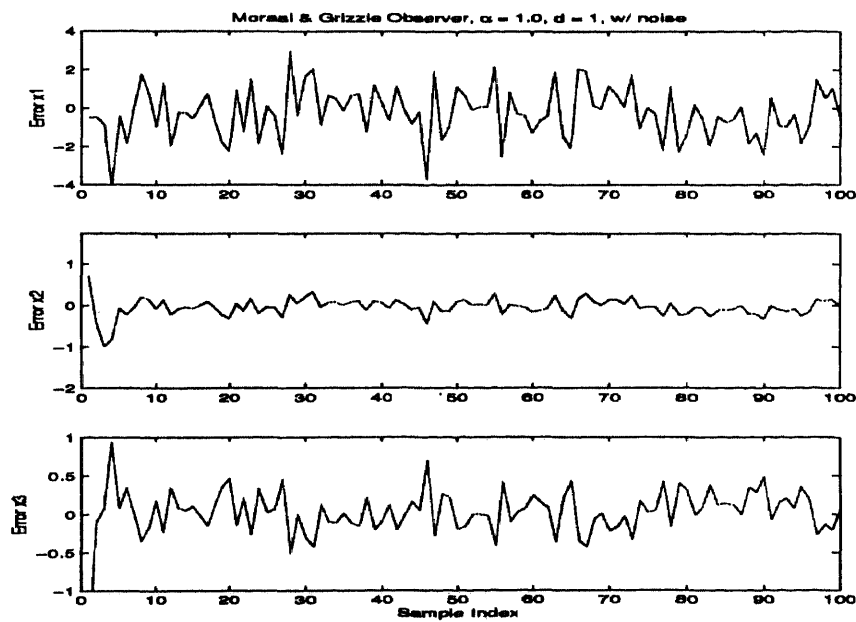


Figure A.33 Moraal/Grizzle observer state estimation error for three-state model of dog blood pressure response to medication. $\alpha = 1.0$, $d = 1$, measurement noise present.

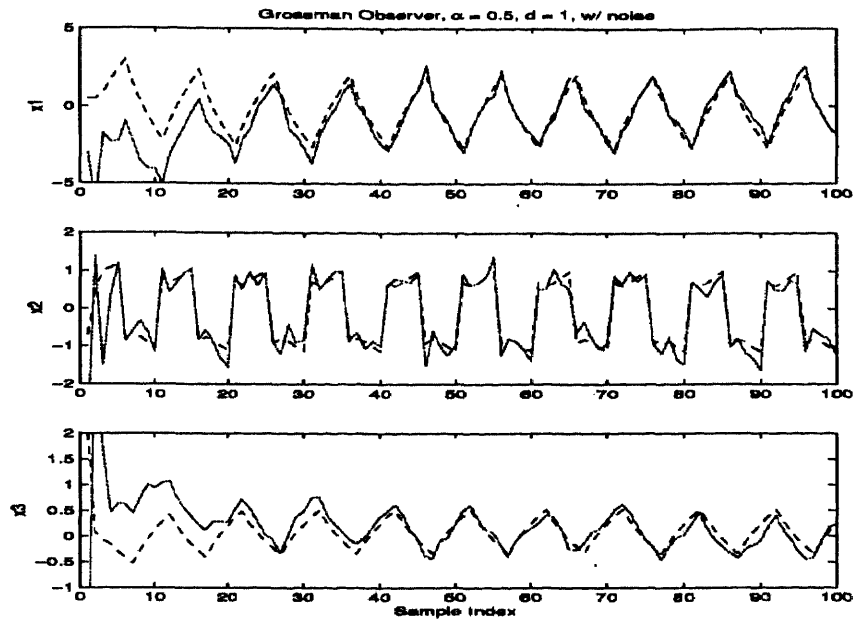


Figure A.34 Grossman observer state estimate (solid) and true state (dotted) for three-state model of dog blood pressure response to medication. $\alpha = 0.5, d = 1$, measurement noise present.

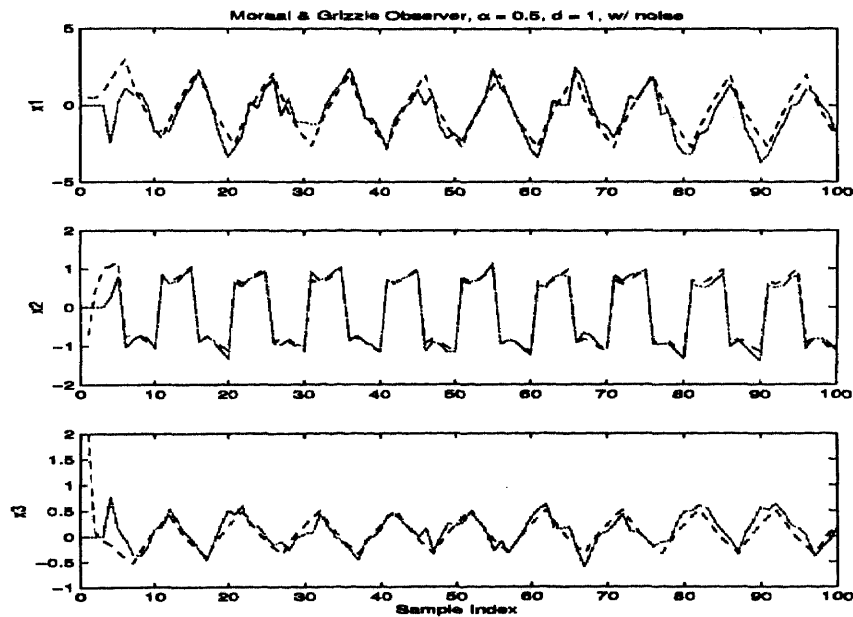


Figure A.35 Moraal/Grizzle observer state estimate (solid) and true state (dotted) for three-state model of dog blood pressure response to medication. $\alpha = 0.5, d = 1$, measurement noise present.

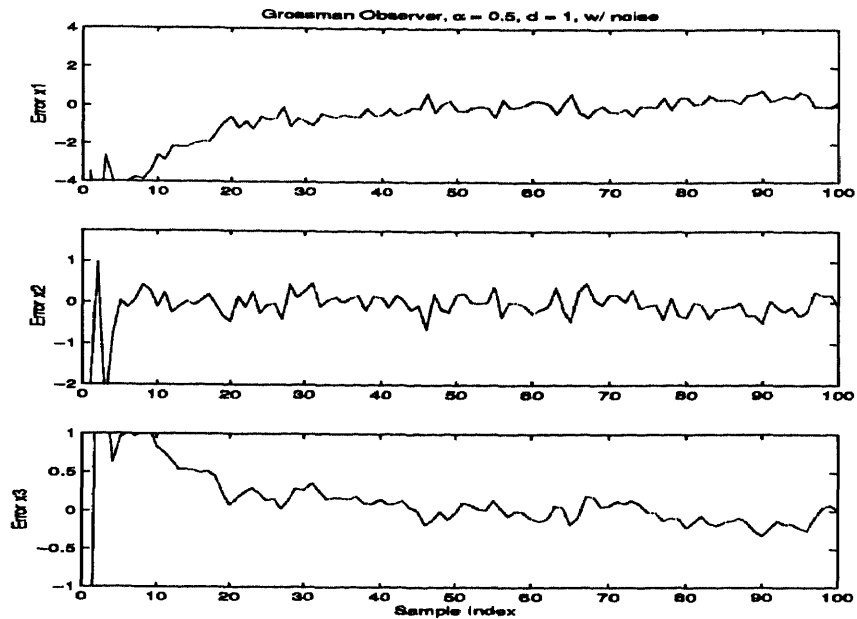


Figure A.36 Grossman observer state estimation error for three-state model of dog blood pressure response to medication. $\alpha = 0.5$, $d = 1$, measurement noise present.

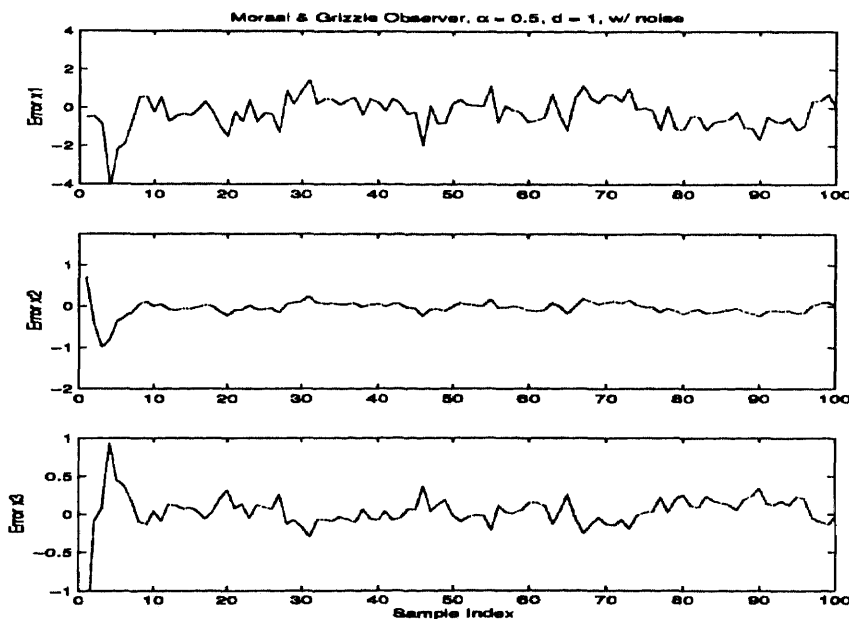


Figure A.37 Moraal/Grizzle observer state estimation error for three-state model of dog blood pressure response to medication. $\alpha = 0.5$, $d = 1$, measurement noise present.

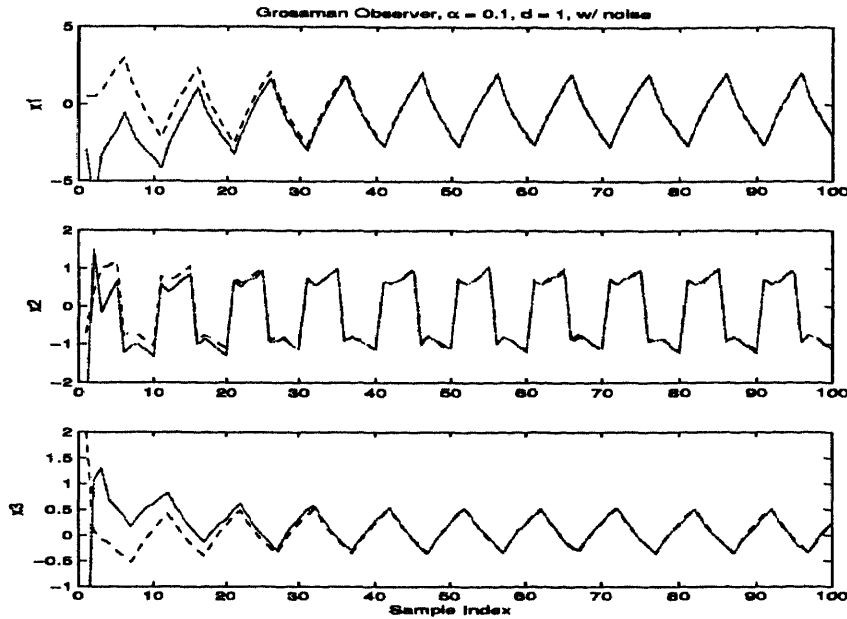


Figure A.38 Grossman observer state estimate (solid) and true state (dotted) for three-state model of dog blood pressure response to medication. $\alpha = 0.1$, $d = 1$, measurement noise present.

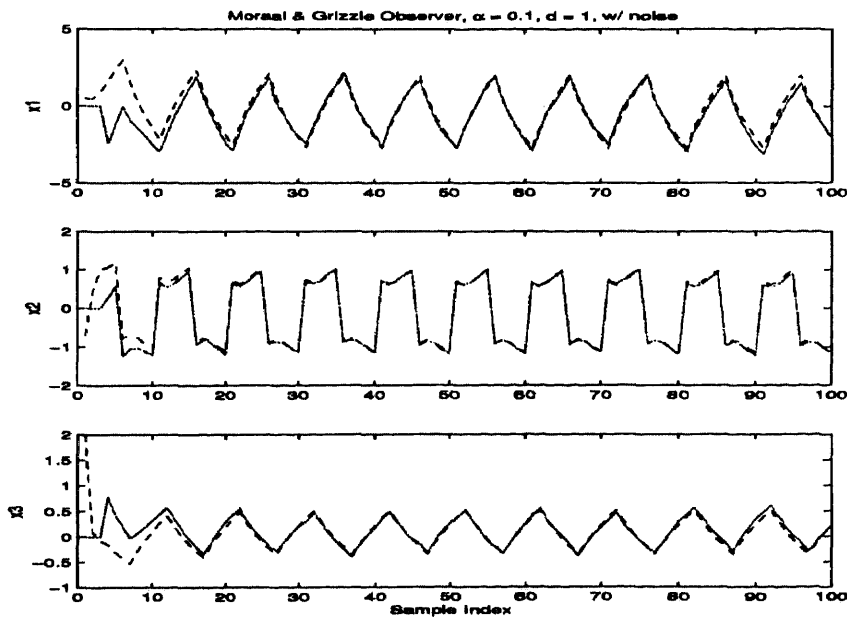


Figure A.39 Moraal/Grizzle observer state estimate (solid) and true state (dotted) for three-state model of dog blood pressure response to medication. $\alpha = 0.1$, $d = 1$, measurement noise present.

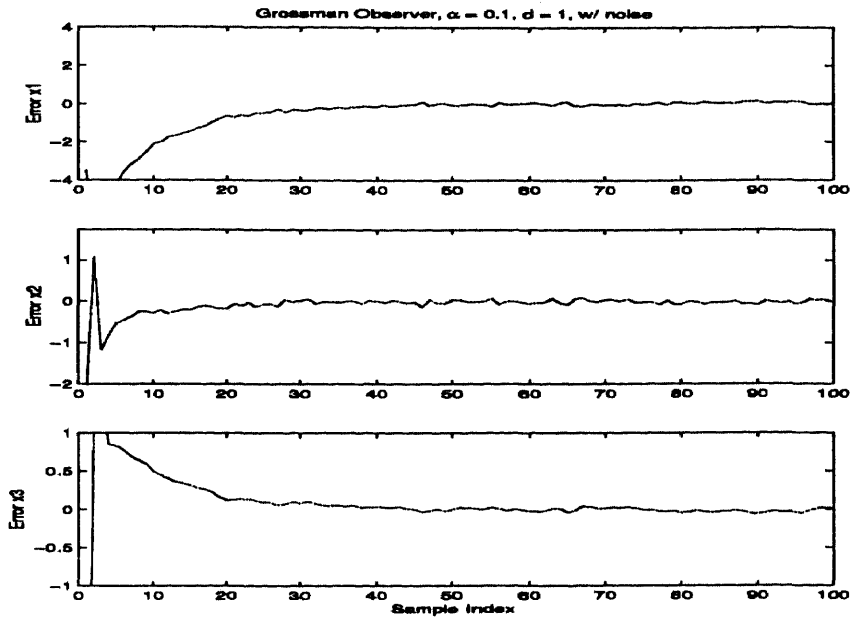


Figure A.40 Grossman observer state estimation error for three-state model of dog blood pressure response to medication. $\alpha = 0.1, d = 1$, measurement noise present.

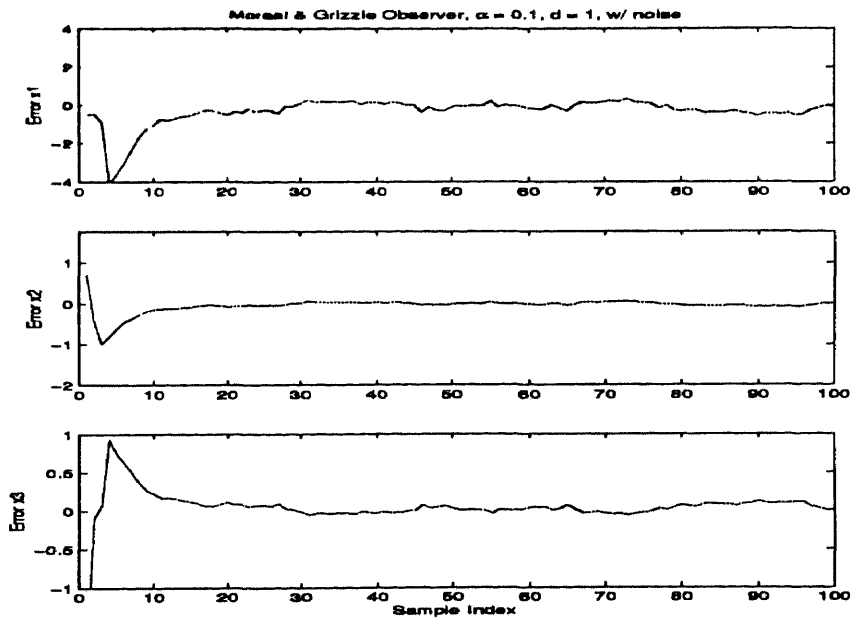


Figure A.41 Moraal/Grizzle observer state estimation error for three-state model of dog blood pressure response to medication. $\alpha = 0.1, d = 1$, measurement noise present.

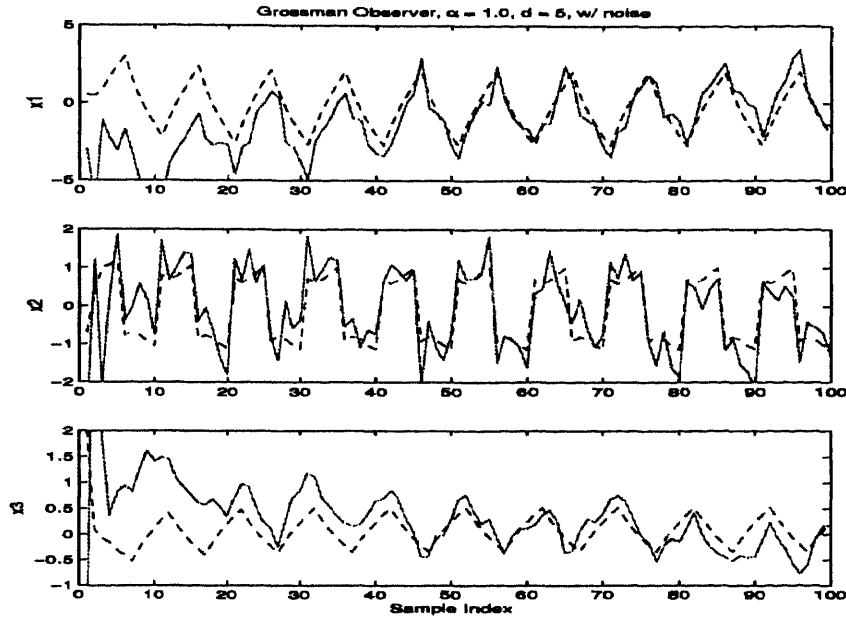


Figure A.42 Grossman observer state estimate (solid) and true state (dotted) for three-state model of dog blood pressure response to medication. $\alpha = 1.0, d = 5$, measurement noise present.

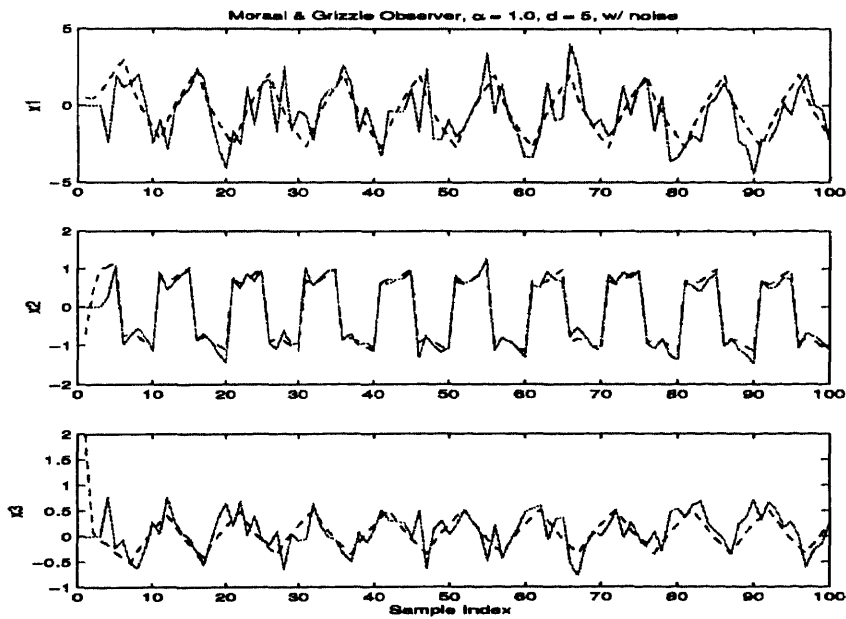


Figure A.43 Moraal/Grizzle observer state estimate (solid) and true state (dotted) for three-state model of dog blood pressure response to medication. $\alpha = 1.0, d = 5$, measurement noise present.

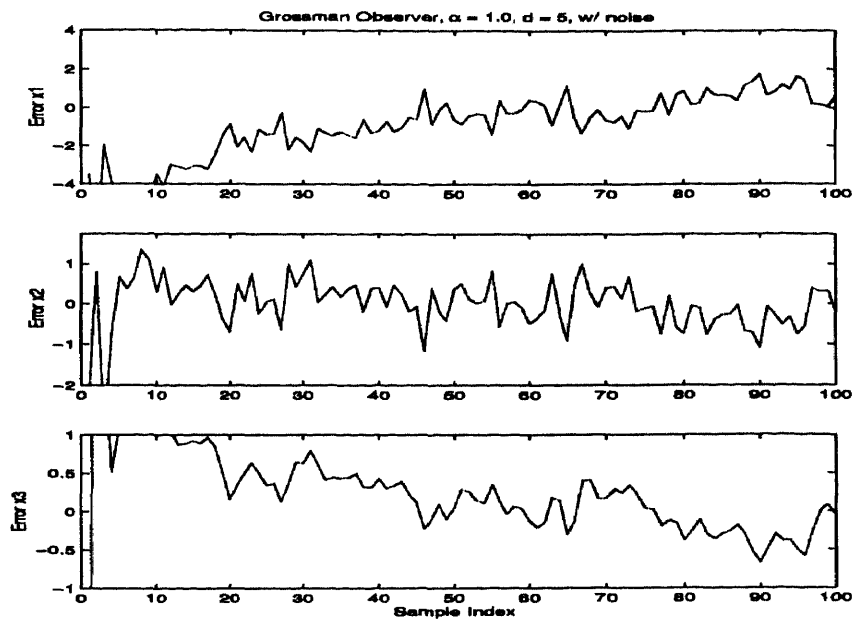


Figure A.44 Grossman observer state estimation error for three-state model of dog blood pressure response to medication. $\alpha = 1.0$, $d = 5$, measurement noise present.

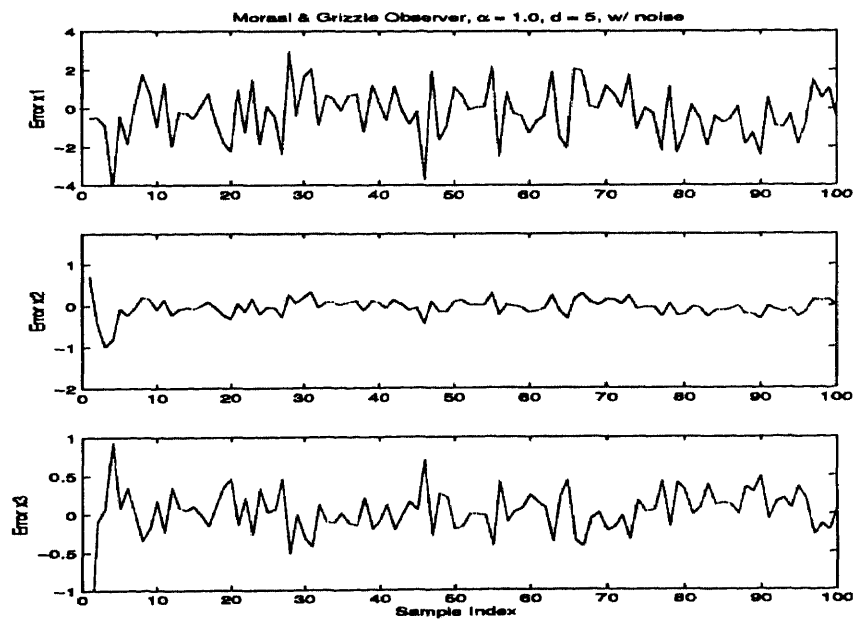


Figure A.45 Moraal/Grizzle observer state estimation error for three-state model of dog blood pressure response to medication. $\alpha = 1.0$, $d = 5$, measurement noise present.

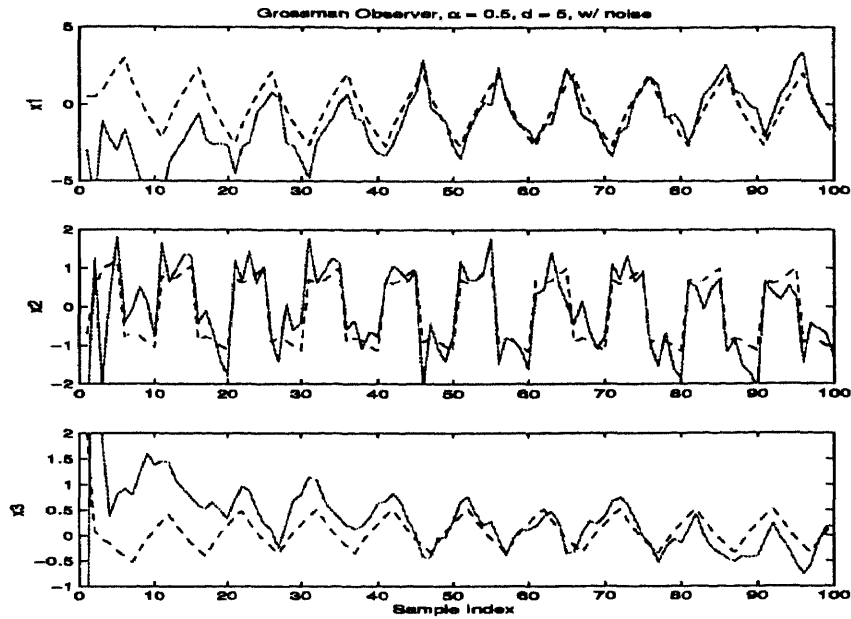


Figure A.46 Grossman observer state estimate (solid) and true state (dotted) for three-state model of dog blood pressure response to medication. $\alpha = 0.5, d = 5$, measurement noise present.

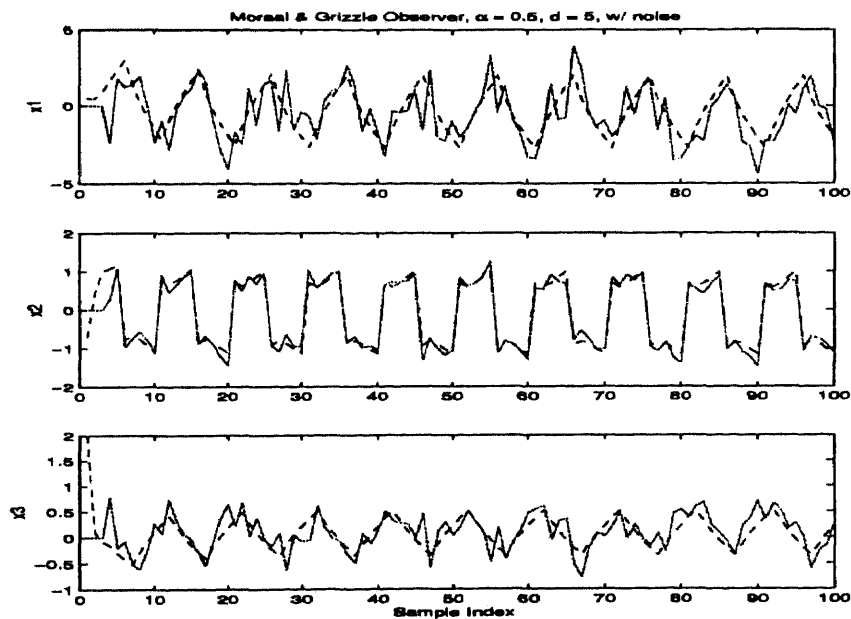


Figure A.47 Moraal/Grizzle observer state estimate (solid) and true state (dotted) for three-state model of dog blood pressure response to medication. $\alpha = 0.5, d = 5$, measurement noise present.

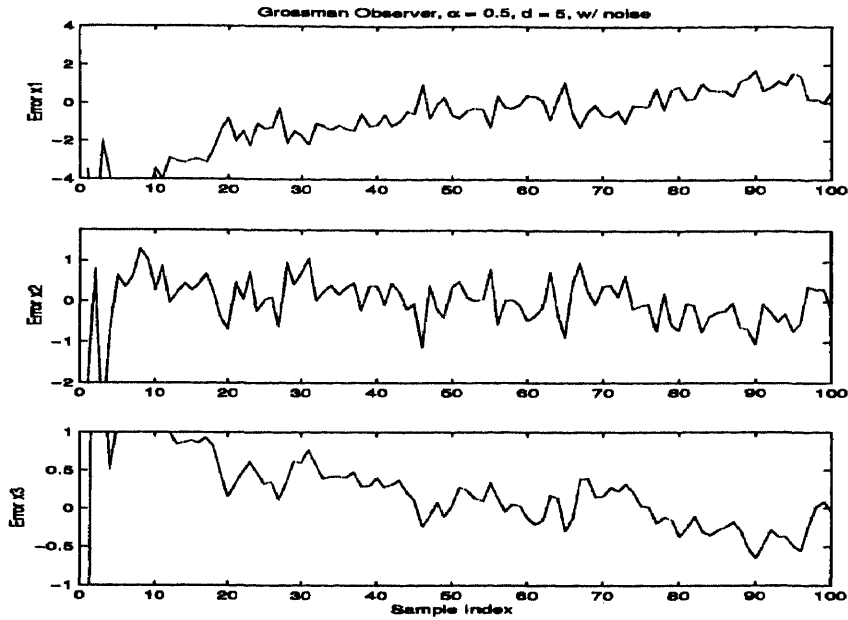


Figure A.48 Grossman observer state estimation error for three-state model of dog blood pressure response to medication. $\alpha = 0.5, d = 5$, measurement noise present.

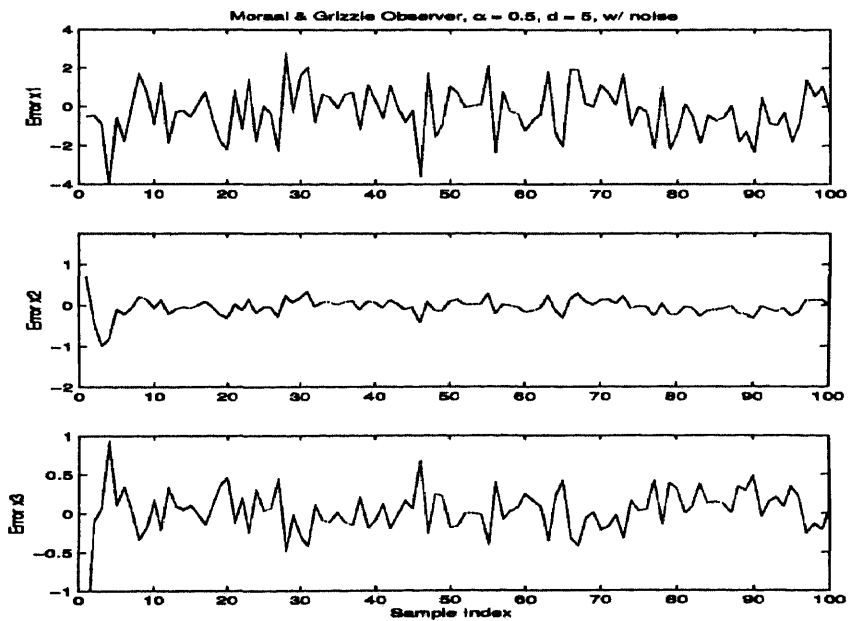


Figure A.49 Moraal/Grizzle observer state estimation error for three-state model of dog blood pressure response to medication. $\alpha = 0.5, d = 5$, measurement noise present.

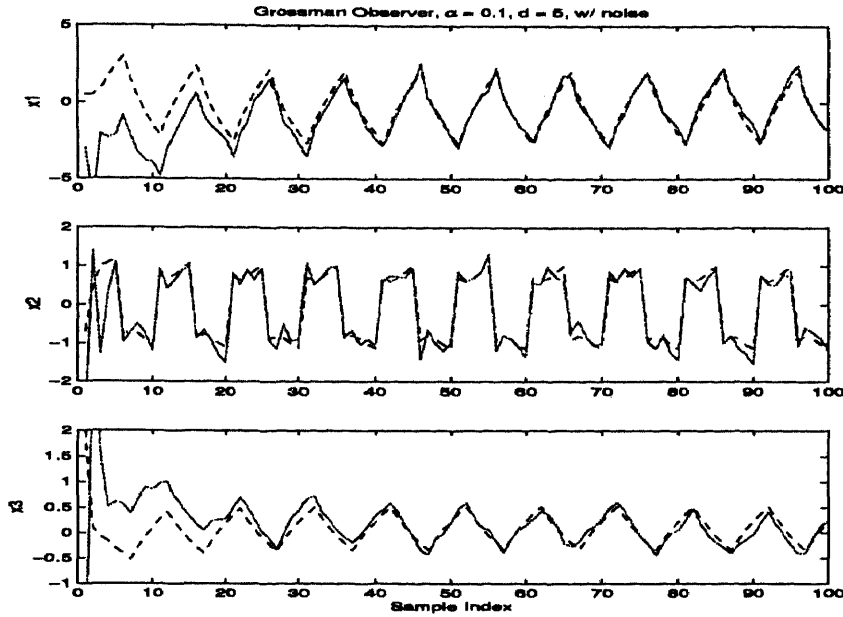


Figure A.50 Grossman observer state estimate (solid) and true state (dotted) for three-state model of dog blood pressure response to medication. $\alpha = 0.1$, $d = 5$, no measurement noise present.

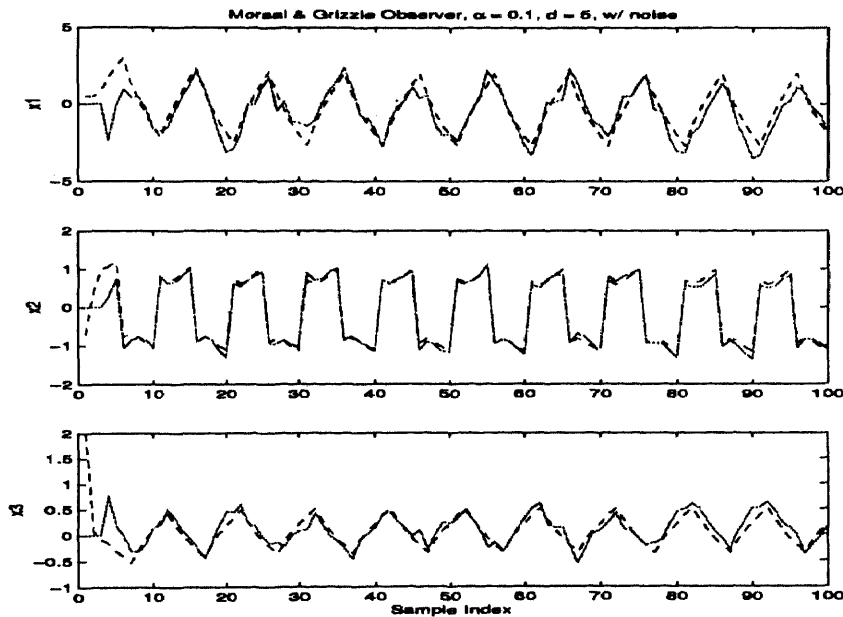


Figure A.51 Moraal/Grizzle observer state estimate (solid) and true state (dotted) for three-state model of dog blood pressure response to medication. $\alpha = 0.1$, $d = 5$, measurement noise present.

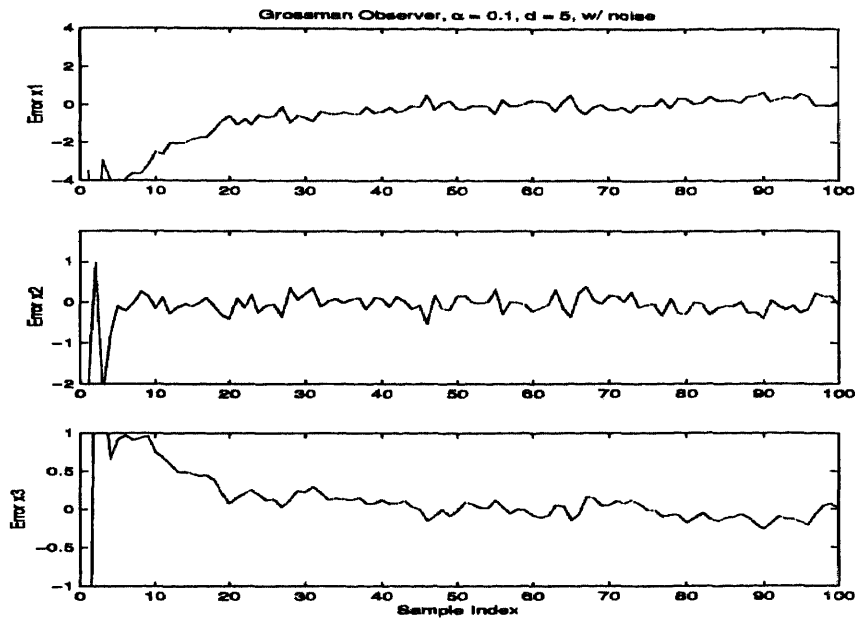


Figure A.52 Grossman observer state estimation error for three-state model of dog blood pressure response to medication. $\alpha = 0.1$, $d = 1$, measurement noise present.

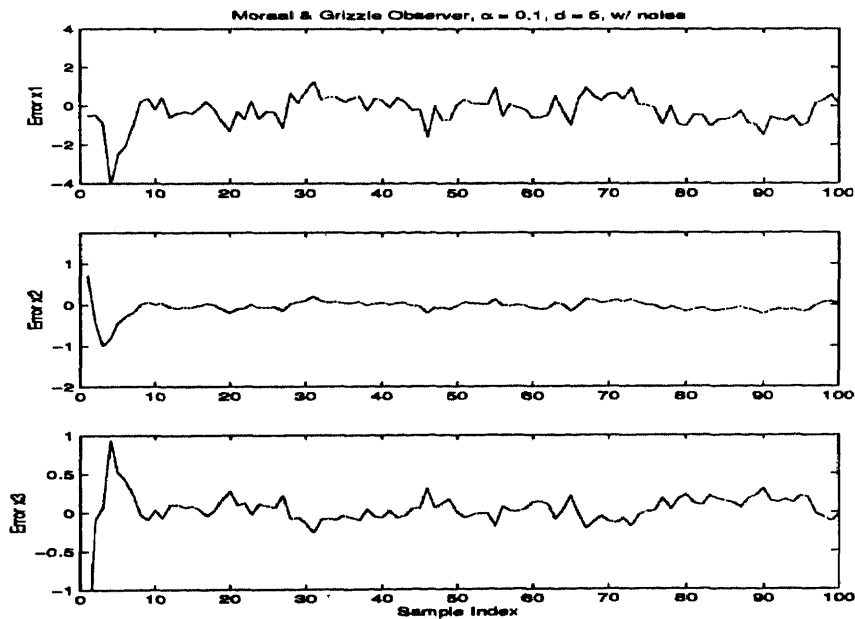


Figure A.53 Moraal/Grizzle observer state estimation error for three-state model of dog blood pressure response to medication. $\alpha = 0.1$, $d = 5$, measurement noise present.

A.3.2 Measurement Noise Mitigation in the Modified Ciccarella Observer

The modified Ciccarella observer provides process noise/measurement noise tuning capability similar to that of the Kalman filter. It can be implemented with fixed or variable gains, and it can be implemented with or without the feedforward term.⁴ Elimination of the feedforward term improves the noise mitigation properties of the observer at the risk of potentially greater observer instability.

Figure A.54 demonstrates the performance of the unmodified Ciccarella observer with a fixed gain and feedforward term. Comparison with unmodified Moraal/Grizzle observer ($\alpha = 1$, $d = 5$), figure A.43, reveals almost identical performance.

Figure A.56 demonstrates that when the feedforward term is eliminated and the fixed gains are reduced to stabilize the estimator, the noise mitigation is greatly improved. This noise mitigation is at the expense of the increased transient response time.

Figure A.57 shows the performance of the modified, variable gain Ciccarella observer without the feedforward term. The observer demonstrates near-complete elimination of the measurement noise and a short, 30 step transient response. This observer is the best performing observer of the three observers simulated.

Comparison of figure A.60 ($Q = 0.018$) with figure A.57 ($Q = 0.00018$) demonstrates the effect of increasing the value of process noise parameter Q by two orders of magnitude. As anticipated from Kalman filter theory, with the larger Q , the new state estimate depend more upon the new measurement than when Q is small. The increase in the gains caused by this increase in Q is seen by comparison of figure A.59 ($Q = 0.00018$) with A.62 ($Q = 0.018$).

⁴When the “modified” Ciccarella observer is implemented with fixed gains and feedforward, it is the original form of the filter proposed by Ciccarella and is no longer in “modified” form.

The deleterious effect of the feedforward term upon the noise mitigation of the modified Ciccarella observer is seen in the comparison of figures A.57 (no feedforward) and A.63 (with feedforward).

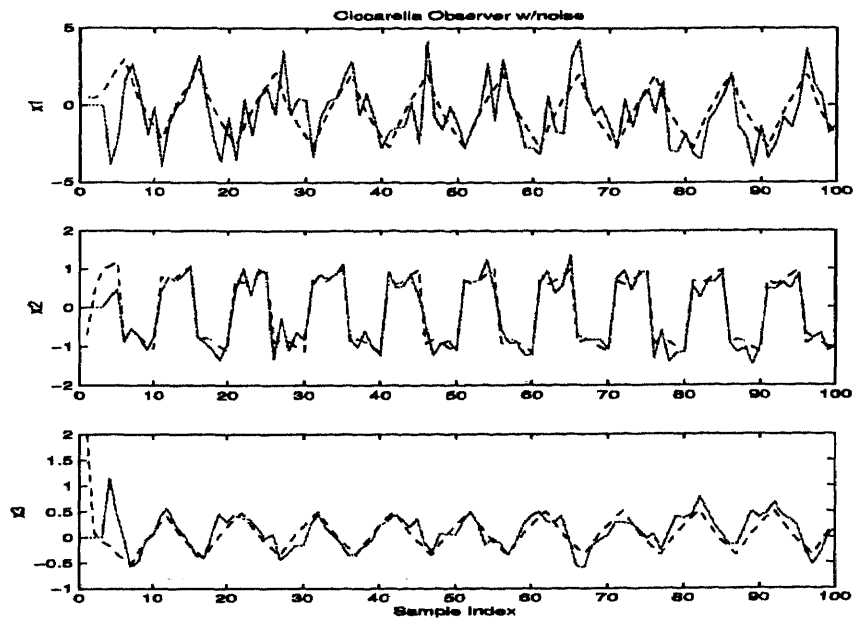


Figure A.54 Ciccarella observer estimate (solid) and true state (dotted), for three-state model of dog blood pressure response to medication. Arbitrary gain set $(\lambda(A - K) \in \{0.3, 0.4, 0.5\})$, measurement noise present.

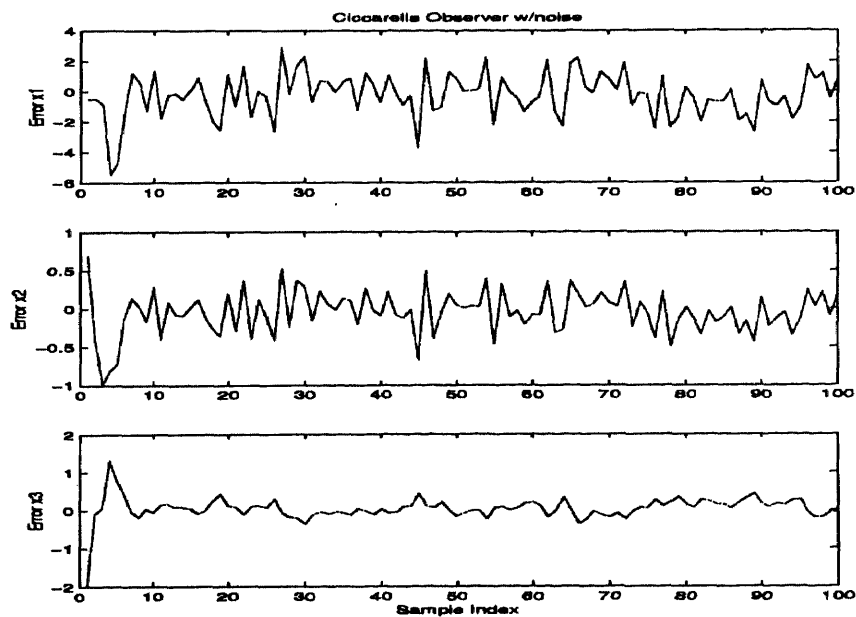


Figure A.55 Ciccarella observer state estimation error for three-state model of dog blood pressure response to medication. Arbitrary gain set $(\lambda(A - K) \in \{0.3, 0.4, 0.5\})$, measurement noise present.

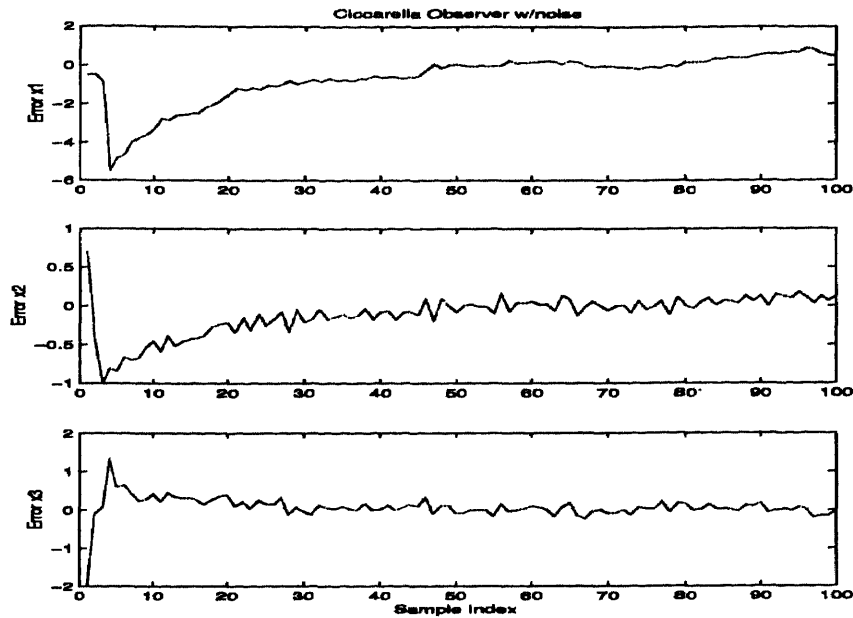


Figure A.56 Ciccarella observer state estimation error for three-state model of dog blood pressure response to medication. Reduced magnitude gain set ($\lambda(A - K) \in \{0.03, 0.04, 0.05\}$) measurement noise present, no feedforward. Observer is stabilized.

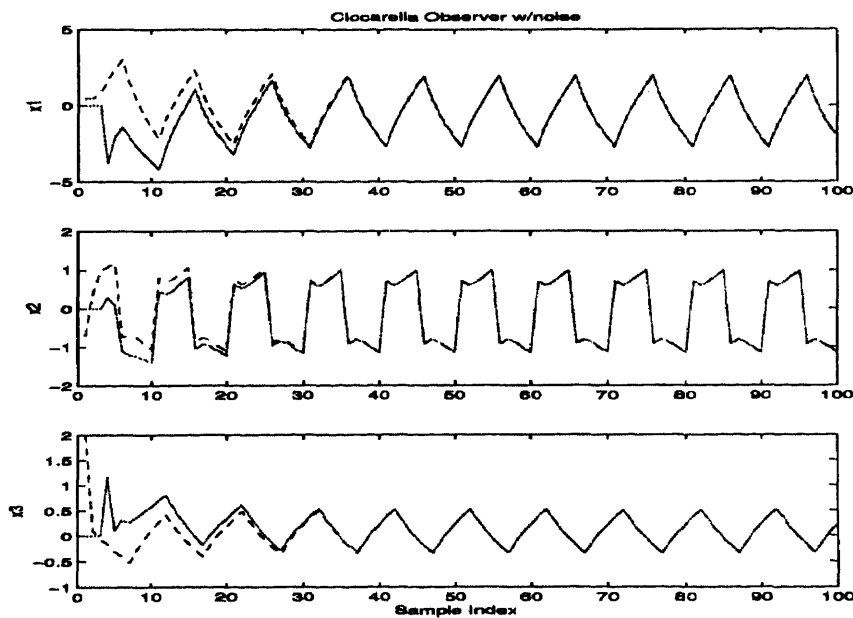


Figure A.57 Modified Ciccarella observer estimate (solid) and true state (dotted), for three-state model of dog blood pressure response to medication. Kalman gain set, measurement noise present, no feedforward ($B = 0$). $W = 0.0183I$, $Q = 0.00018 \text{ diag}([0 \ 0 \ 1])$.

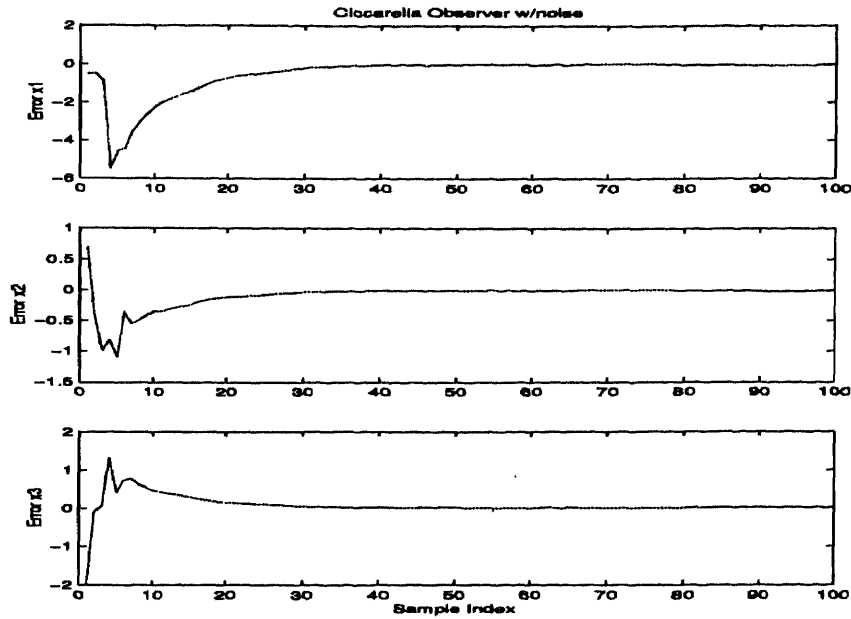


Figure A.58 Modified Ciccarella observer state estimation error for three-state model of dog blood pressure response to medication. Kalman gain set, measurement noise present, no feedforward ($B = 0$). $W = 0.0183I$, $Q = 0.00018 \text{diag}([0 \ 0 \ 1])$.

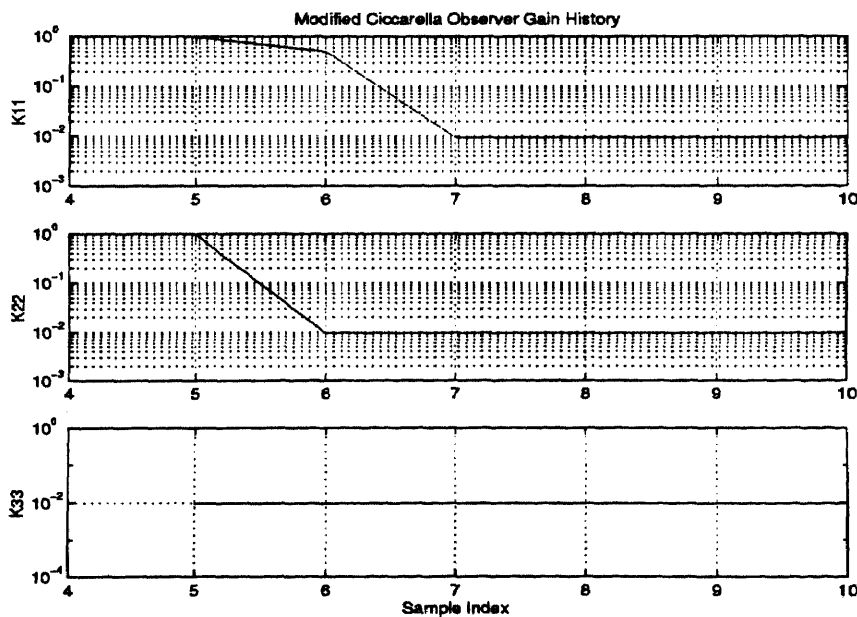


Figure A.59 Modified Ciccarella observer gain history. $W = 0.0183I$, $Q = 0.00018 \text{diag}([0 \ 0 \ 1])$.

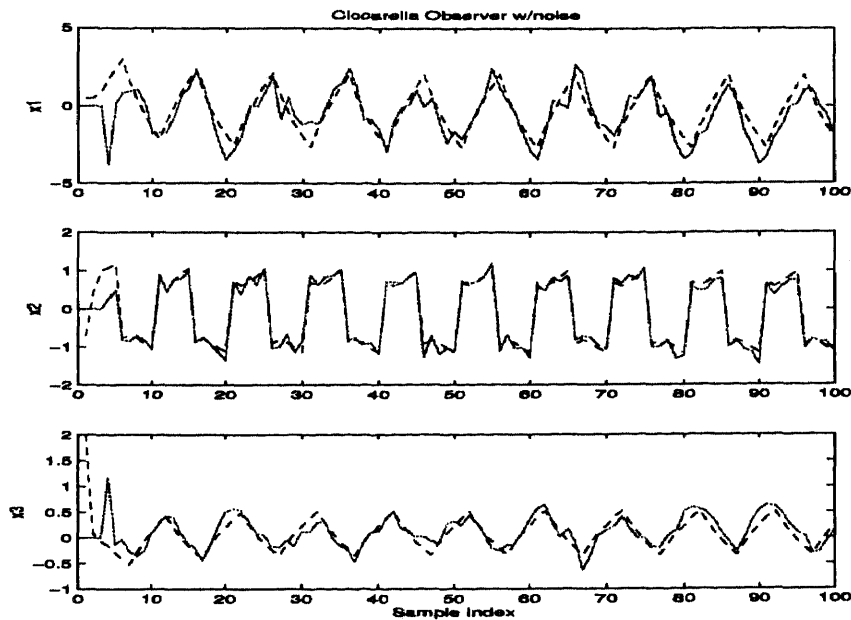


Figure A.60 Modified Ciccarella observer estimate (solid) and true state (dotted), for three-state model of dog blood pressure response to medication. Kalman gain set, measurement noise present, no feedforward ($B = 0$). $W = 0.0183I$, $Q = 0.018 \text{diag}([0 \ 0 \ 1])$.

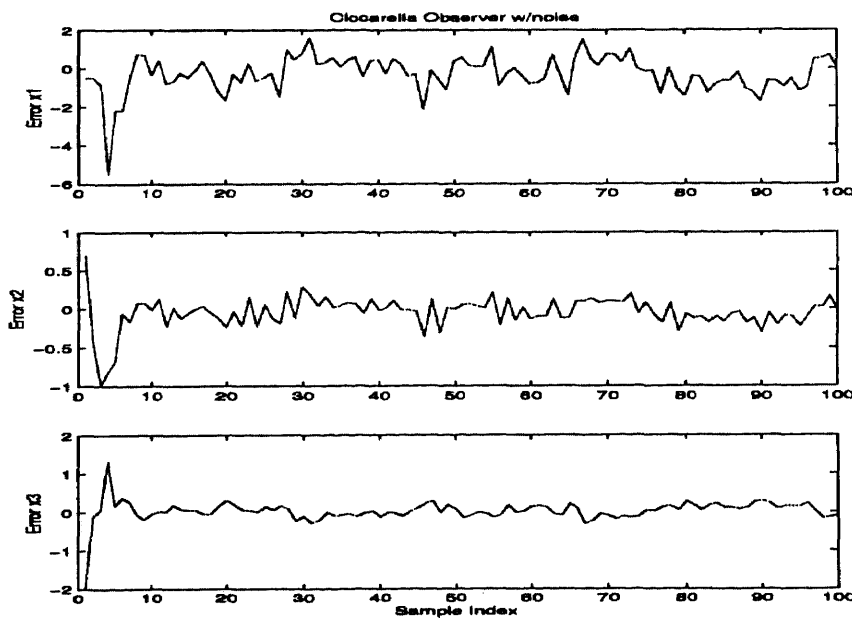


Figure A.61 Modified Ciccarella observer state estimation error for three-state model of dog blood pressure response to medication. Kalman gain set, measurement noise present, no feedforward ($B = 0$). $W = 0.0183I$, $Q = 0.018 \text{diag}([0 \ 0 \ 1])$.

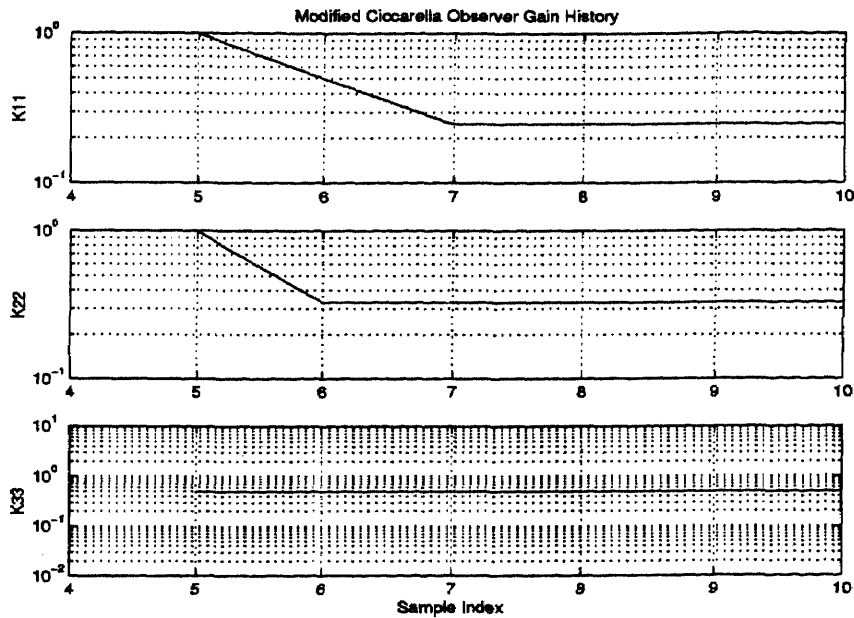


Figure A.62 Modified Ciccarella observer gain history. $W = 0.0183I$, $Q = 0.018 \text{ diag}([0 \ 0 \ 1])$.

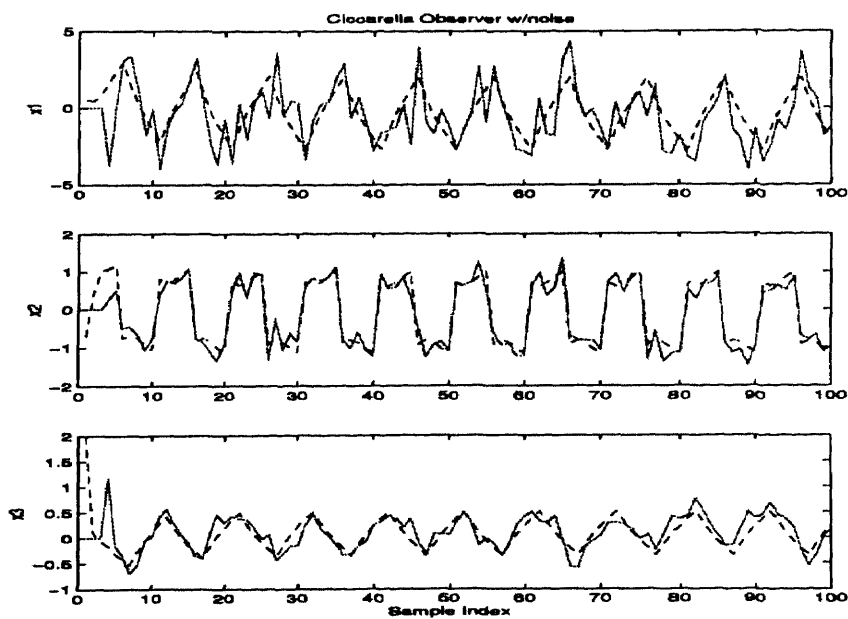


Figure A.63 Modified Ciccarella observer estimate (solid) and true state (dotted), for three-state model of dog blood pressure response to medication. Kalman gain set, measurement noise present, with feedforward. $W = 0.0183I$, $Q = 0.00018 \text{ diag}([0 \ 0 \ 1])$.

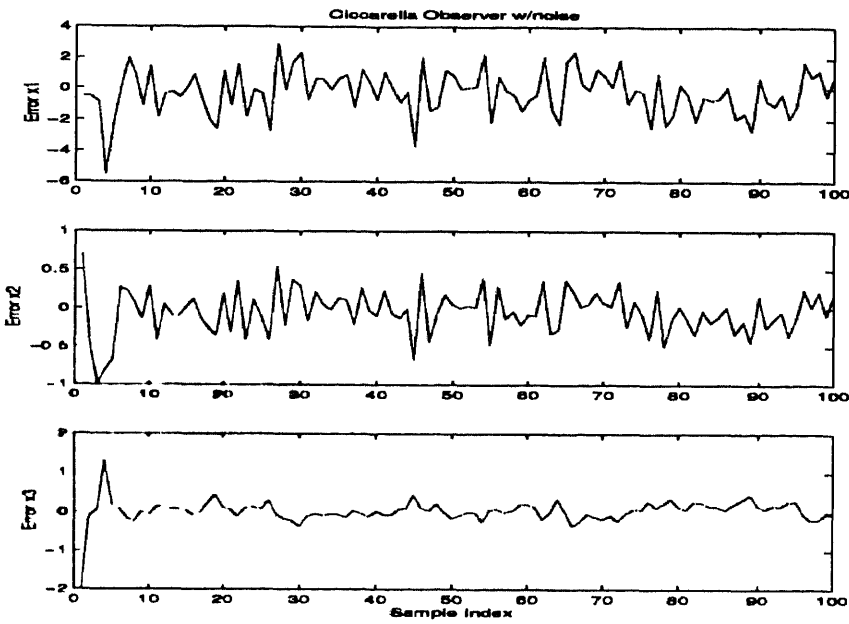


Figure A.64 Modified Ciccarella observer state estimation error for three-state model of dog blood pressure response to medication. Kalman gain set, measurement noise present, with feedforward. $W = 0.0183I$, $Q = 0.00018 \text{diag}([0 \ 0 \ 1])$.

A.4 Observer Simulations With Increased Input Amplitude

Simulations of the three observers were made with measurement noise. The input amplitude was increased by a factor of ten over the previous runs. Specifically, the control input consisted of a symmetric, 50% duty-cycle square wave of amplitude ten, with a ten-sample period, i.e.,

$$u_k = \begin{cases} 10 & \text{for } k \bmod 10 < 5, \\ -10 & \text{for } k \bmod 10 \geq 5. \end{cases} \quad (\text{A.1})$$

The measurement noise was the same *power* as the previous runs, but due to the increased amplitude of the output response, the signal-to-noise ratio was effectively increased from 3dB to 25 dB.⁵ All three observers converged with response times less than those of the previous runs with unity input.

⁵This increase in signal-to-noise ration demonstrates the technique of increasing input amplitude and system response to overcome a sensor noise floor.

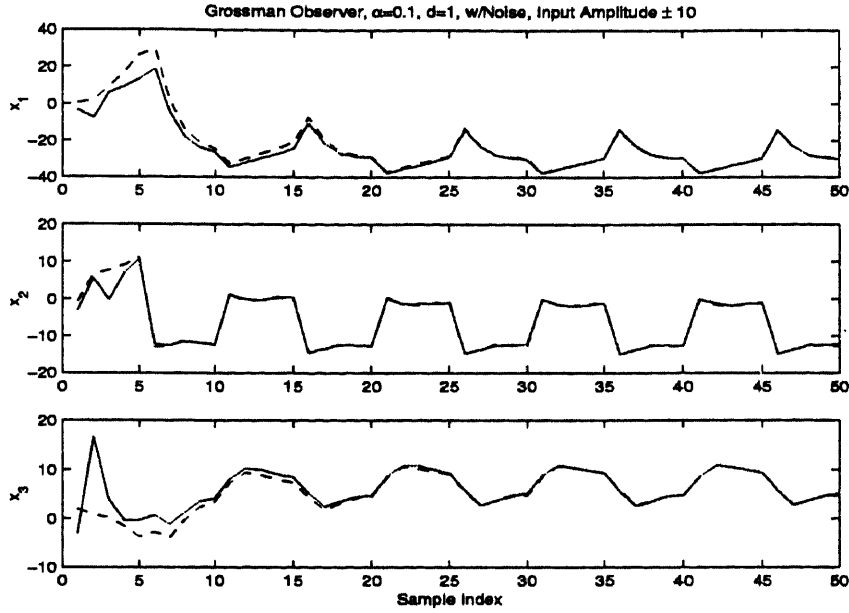


Figure A.65 Grossman observer state estimate (solid) and true state (dotted) for three-state model of dog blood pressure response to medication. $\alpha = 0.1$, $d = 1$, measurement noise present. Input amplitude $u \in \{-10, 10\}$.

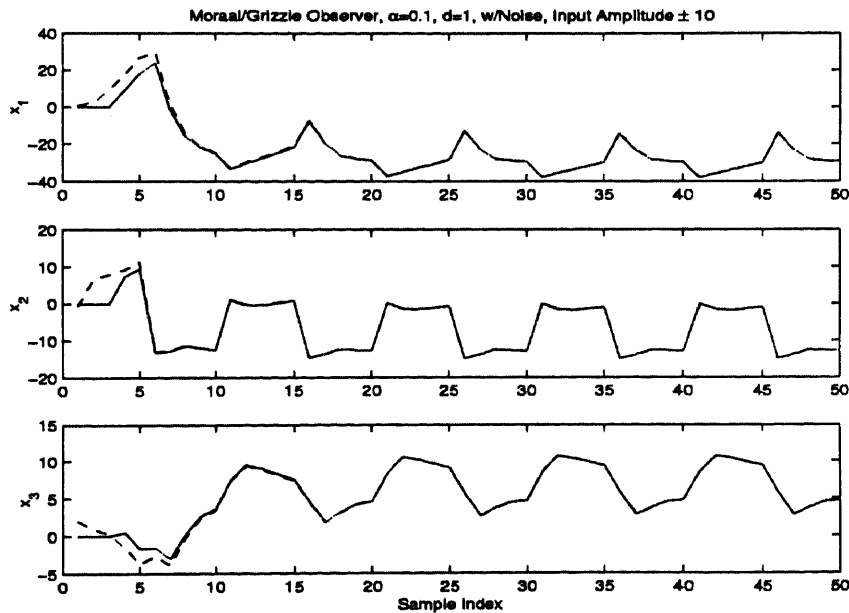


Figure A.66 Moraal/Grizzle observer state estimate (solid) and true state (dotted) for three-state model of dog blood pressure response to medication. $\alpha = 0.1$, $d = 1$, measurement noise present. Input amplitude $u \in \{-10, 10\}$.

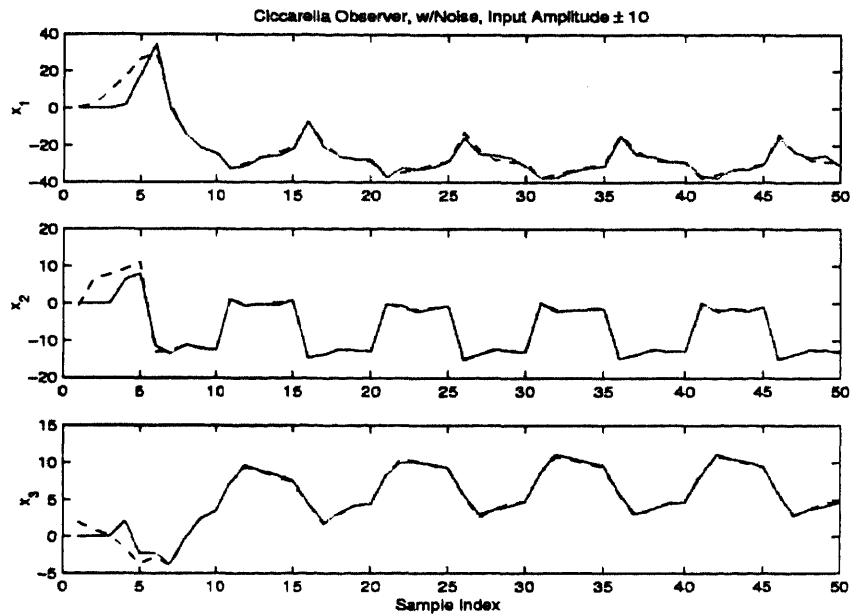


Figure A.67 Modified Ciccarella observer state estimation error for three-state model of dog blood pressure response to medication. Kalman gain set, measurement noise present, no feedforward. $W = 0.0183I$, $Q = 0.00018 \text{diag}([0 \ 0 \ 1])$. Input amplitude $u \in \{-10, 10\}$.

APPENDIX B
MATLAB CODE

B.1 Discrete-time Friedland Observer for Identification of the
Characteristic Polynomial of an Autoregressive Filter

```
function [phat,inv,u,x,z]=pest

N=5000;
x=zeros(N,2);
z=zeros(N,2);
inv=zeros(N,2);
%Generate the data
%k=1
w=[1 0]';
t=0:N-1;
f=0.1;
u=sign(sin(2*pi*f*(t+0.00001)));
%u=5*ones(N,1);
p1=0.01;
p2=0.05;
phi=[p2 p1
      1 0];
gam=[1 0]';

x(1,:)=w';
for k=1:N
    x(k,:)=w';
    w=phi*w+gam*u(k);
end

%Now estimate

%Make noise vector
sigma=1; %Adjust noise here
noise =randn(N,2)*sigma;

%Corrupt state with white Gaussian noise
x=x+noise;

%Set up filter
phat=zeros(N,2);
L=0.005;

%k=2
pkm1=0*[p2 p1]';
```



```

wkm1=x(1,:)';
ptrue=pk1;

%calculate z[2]
z(2,:)=-L*wkm1'/(wkm1'*wkm1)*(wkm1'*pk1+u(1));
%keyboard
for k=2:N
    pk=pk1+L*wkm1/(wkm1'*wkm1)*x(k,1)+z(k,:)';
    phat(k,:)=pk';

    wk=x(k,:)';
    if k<N
        z(k+1,:)=-L*wk'/(wk'*wk)*(wk'*pk+u(k));
    end
    pk1=pk;
    wkm1=wk;
end
end

```

B.2 Scalar Example of Newton Observer

```

function [xhat,noise,pole]=grizzle1(alpha)
N=2000;
h=0.1;
z=h^3;
xhat=zeros(N,1);
pole=xhat;
noise=randn(N,1)*0.1*z; % sigma=1e-4;
x1=z;
xhat(1)=x1;
for k=2:N
    L=alpha*(1/(3*x1^2));
    x1=x1+L*(z+noise(k)-x1^3);
    xhat(k)=x1;
    pole(k)=1-L;
end
end

```

B.3 Discrete-time Friedland Observer for Identification of the Characteristic Polynomial of an Autoregressive Filter

```

function phat=pest;

N=200;
x=zeros(N,2);

```

```

%Generate the data
x1=[1 0]';
t=0:N-1;
f=0.1;
u=sign(sin(2*pi*f*t));
p1=0.01;
p2=0.05;
phi=[0 1
      p1 p2];
gam=[0 1]';

x(1,:)=x1';
for k=2:N
    xx=[x1(1)^3 x1(2)]';
    x1=phi*xx+gam*u(k);
    x(k,:)=x1';
end

%Now estimate
phat=zeros(N,2);
L=.1;

z=[0 0]';
for k=3:N
    pkm1=phat(k-1,:);
    pk=pkm1+L*[x(k-1) x(k-2)]'*x(k)+z;
    phat(k,:)=pk';

    v=[x(k) x(k-1)]';
    z=-L*v*([x(k)^3 x(k-1)]*pk+u(k));

    %eig(eye(2)-L*v*v')
end

```

B.4 Simultaneous State and Parameter Estimation Applied to an Autoregressive Filter

B.4.1 Grossman Observer

```

%----- Main routine -----
function [xout,xhatout,YY,z,zhat,rho,u]=dc
%function [x,xhat,YY,z,zhat,rho,u]=dc
p1=.5;
p2=1;
xa=1;

```

```

xb=.5;

NN=100;

xhatout=zeros(NN,4);
X=[p1;p2;xa;xb];
XHAT=[0.1; 4; 1.2; 0];

k=(1:NN)';
f=15;
u=10*sign(sin(k*2*pi/f));

A=[0 1;-p1 -p2];
B=[0 1]';
C=[1 0];
D=0;
[YY,XX]=dlsim(A,B,C,D,u,X(3:4));
%YY=YY+randn(NN,1);
xout=[ p1*ones(NN,1) p2*ones(NN,1) XX];

xhatout=zeros(NN,4);
z=phi3([p1*ones(NN,1) p2*ones(NN,1) XX],u);

zhat=zeros(NN,4);

AA=[0 1 0 0
     0 0 1 0
     0 0 0 1
     0 0 0 0];

B2=[0 0 0 1]';
C=[1 0 0 0];

%Experiment with gains
%L=[ -3.0000    3.3500   -1.6500    0.3024]';
%L=[  -1.0000    0.3500   -0.0500    0.0024]';
%L=[  -2.8600    3.0671   -1.4617    0.2612]';
%L=[  -2.3490    2.0577   -0.7964    0.1147]';
%L=[  -1.8790    1.3229   -0.4134    0.0483]';
L=[ -3.9000    5.7035   -3.7069    0.9035]';

rho=zeros(NN,1);

zhat(1,:)=z(1,:)+randn(1,4)*0.3;
Z1=zhat(1,:);
xhat=XHAT;
xhatout(1,:)=xhat';

```

```

for k=1:NN-4;
    rho(k)=(YY(k)-C*Z1);
    Z1=AA*Z1+B2*(YY(k+4)+randn(1,1)*0.3);
    Z1=Z1+L*rho(k);
    xhat=invphi2(Z1,xhat,u(k+1),u(k+2));
    xhatout(k+1,:)=xhat';
    zhat(k+1,:)=Z1';
end

%----- Inversion of transformation -----
function [x,k]=invphi2(z,xhat,u0,u1)
%function [x,k]=invphi2(z,xhat,u0,u1)
%
%Solves inverse transformation for the grossman observer
alpha=0.9;
xhat1=xhat;
for k=1:10

    J=jacob01(xhat1,u0);
    xhat2=xhat1-alpha*J\(\phi2(xhat1,u0,u1)-z);
    e=norm(xhat2-xhat1);
    if (e/norm(xhat2)<0.00001)|(k==10)
        x=xhat2;
        k;
        return;
    else
        xhat1=xhat2;
    end
end
x=xhat2;

%----- Calculation of Jacobian-----
function J=jacob01(x,u0)
%function J=jacob01(x,u0)

J=zeros(4,4);
Pa=x(1);
Pb=x(2);
xa=x(3);
xb=x(4);
J(1,3)=1;
J(2,4)=1;
J(3,:)=[-xa -xb -Pa -Pb];
J(4,1)=Pb*xa-xb;
J(4,2)=2*Pb*xb+Pa*xa-u0;
J(4,3)=Pa*Pb;

```

```
J(4,4)=Pb*Pb-Pa;
```

B.4.2 Modified Moraal and Grizzle Observer

```
function [xout,xhatout,YY,u]=mgpi(alpha,d,StdNoise)
%function [x,xhat,YY,u]=mgpi(alpha,d)
if nargin<3
    StdNoise=0;
end
if nargin<2
    d=1;
end

if nargin<1
    alpha=1; %default to M&G
end

p1=.5;
p2=1;
xa=1;
xb=.5;

NN=100;

xhatout=zeros(NN,4);
X=[p1;p2;xa;xb];
XHAT=[0.1; 4; 1.2; 0];

k=(1:NN)';
f=15;
u=10*sign(sin(k*2*pi/f));

%Generate truth data
A=[0 1;-p1 -p2];
B=[0 1]';
C=[1 0];
D=0;
[YY,XX]=dlsim(A,B,C,D,u,X(3:4));
YY=YY+StdNoise*randn(NN,1);
xout=[ p1*ones(NN,1) p2*ones(NN,1) XX];

xhatout=zeros(NN,4);
zhat=[0 0 0 0]';
```

```

xhat=XHAT;
xhatout(1,:)=xhat';
N=4; %State dimension
for k=5:NN
    ztilde=f1(zhat,u(k-N));
    Y=YY(k-3:k);
    U=u(k-3:k);
    zhat=NewtonSolve(Y,U,ztilde,alpha,d);
    xhat=ForwardPropagate(zhat,U);
    xhatout(k,:)=xhat';
end

function zhat=NewtonSolve(Y,U,ztilde,alpha,d)
%function zhat=NewtonSolve(Y,U,ztilde,alpha,d)
%Solves inverse transformation for the Modified MG observer
for k=1:d
    rho=Y-H(ztilde,U);
    J=jacob01(ztilde,U);
    zhat=ztilde + alpha*(J\rho);
end

function Ytilde=H(ztilde,U)
Ytilde=[h(ztilde,U(1))
        h(f1(ztilde,U(1)),U(2))
        h(f1(f1(ztilde,U(1)),U(2)),U(3))
        h(f1(f1(f1(ztilde,U(1)),U(2)),U(3)),U(4))];

function y=h(x,u)
y=x(3);

function x2=f1(x1,u)
p1=x1(1);
p2=x1(2);

x2=[p1
    p2
    x1(4)
    -p1*x1(3)-p2*x1(4)+u];

function xhat=ForwardPropagate(zhat,U)
xhat=f1(f1(f1(zhat,U(1)),U(2)),U(3));

function J=jacob01(x,U)
%function J=jacob01(x,U)

```

```

J=zeros(4,4);
Pa=x(1);
Pb=x(2);
xa=x(3);
xb=x(4);
J(1,3)=1;
J(2,4)=1;
J(3,:)=[-xa -xb -Pa -Pb];
J(4,1)=Pb*xa-xb;
J(4,2)=2*Pb*xb+Pa*xa-U(1);
J(4,3)=Pa*Pb;
J(4,4)=Pb*Pb-Pa;

```

B.4.3 Modified Ciccarella Observer

```

function [xout,xhatout,Kout,YY,u,yres,Jcond]=ciccp1(Q,W)
%function [x,xhat,Kout,YY,u]=ciccp1(Q,W)
if nargin<2
    W=1;
end
if nargin<1
    Q=1;
end

StdNoise=sqrt(W);

p1=.5;
p2=1;
xa=1;
xb=.5;

NN=100;
Kout=zeros(NN,4);
xhatout=zeros(NN,4);
yres=zeros(NN,1);
Jcond=zeros(NN,1);
X=[p1;p2;xa;xb];
XHAT=[0.1; 4; 1.2; 0];
%XHAT=[-0.1683    0.7057   -1.5327    0.8728]';
%XHAT=[0.5; 1; 1; .50];

k=(1:NN)';

```

```

f=15;
u=10*sign(sin(k*2*pi/f));

%Generate truth data
A=[0 1;-p1 -p2];
B=[0 1]';
C=[1 0];
D=0;
[YY,XX]=dlsim(A,B,C,D,u,X(3:4));
YY=YY+StdNoise*randn(NN,1);
xout=[ p1*ones(NN,1) p2*ones(NN,1) XX];

xhatout=zeros(NN,4);
zhat=[0 0 0 0]';
zhat=XHAT;

xhat=XHAT;
xhatout(1,:)=xhat';
N=4; %State dimension

%Kalman Filter Matrices
I=eye(4);
P=0.25*I;
Q=diag([0 0 0 Q]);
W=W*I;

A=[0 1 0 0
    0 0 1 0
    0 0 0 1
    0 0 0 0];

B=1*[0 0 0 1]'; %feedforward matrix

for k=4:NN-1
    ztilde=f1(zhat,u(k-N+1));
    P=A*P*A'+Q; %Propagate Covariance
    Y=YY(k-N+1:k);
    U=u(k-N+1:k);
    Ytilde=H(zhat,U);
    rho=Y-Ytilde;
    K=P/(P+W); %Calculate gain
    J=jacob01(ztilde,U);
    Jcond(k)=cond(J);
    y=YY(k+1);
    ytilde=h(ForwardPropagate(ztilde,[U(2:4);u(k+1)]));
    zhat=ztilde+inv(J)*(B*(y-ytilde)+(K*rho)); %Update estimate

```



```

P=(I-K)*P; %update covariance
xhat=ForwardPropagate(zhat,[U(2:4);u(k+1)]);

xhatout(k+1,:)=xhat'; %Write output
Kout(k+1,:)=diag(K)'; %write gains output
yres(k)=y-ytilde;
end

```

```

function Ytilde=H(ztilde,U)
Ytilde=[h(ztilde,U(1))
        h(f1(ztilde,U(1)),U(2))
        h(f1(f1(ztilde,U(1)),U(2)),U(3))
        h(f1(f1(f1(ztilde,U(1)),U(2)),U(3)),U(4))];

```

```

function y=h(x,u)
y=x(3);

```

```

function x2=f1(x1,u)
p1=x1(1);
p2=x1(2);

```

```

x2=[p1
     p2
     x1(4)
     -p1*x1(3)-p2*x1(4)+u];

```

```

function xhat=ForwardPropagate(zhat,U)
xhat=f1(f1(f1(zhat,U(1)),U(2)),U(3));

```

```

function J=jacob01(x,U)
%function J=jacob01(x,U)

```

```

J=zeros(4,4);
Pa=x(1);
Pb=x(2);
xa=x(3);
xb=x(4);
J(1,3)=1;
J(2,4)=1;
J(3,:)=[-xa -xb -Pa -Pb];
J(4,1)=Pb*xa-xb;
J(4,2)=2*Pb*xb+Pa*xa-U(2);
J(4,3)=Pa*Pb;
J(4,4)=Pb*Pb-Pa;

```

```

function J2=jacobi5(ztilde,U);

```

```

p1=ztilde(1);
p2=ztilde(2);
x1=ztilde(3);
x2=ztilde(4);
uk=U(2);
ukp1=U(3);

J51=2*p1*x1+2*p2*x2-p2*p2*x1-uk;
J52=2*p1*x2-2*p1*p2*x1-3*p2*p2*x2+2*p2*uk-ukp1;
J53=p1*p1-p1*p2*p2;
J54=2*p1*p2-p2*p2*p2;
J2=[J51 J52 J53 J54];

```

B.5 Canine Blood Pressure Response to Nitropruside

B.5.1 Data Synthesis for Canine Blood Pressure Example

```

function [yout,xout,uout]=dog
%constants
F0=[0.8088 1 0.3614
     0.0857 0 -0.296
     -0.1692 0 0.0898];

F1=[0.0247 -0.0241 0.0049
     0.0105 0.0053 0.004
     -0.0055 -0.0025 -0.0012];

F2=[0.0002 -0.0001 0
     -0.0002 0.0002 0
     -0.0002 0.0001 0];

G1=[0 1 0]';
G2=[0.0151 -0.0289 0.0085]';
H0=[-0.1024 0.019 -0.0539];
H1=[-0.0031 -0.002 -0.0004];

N=200;
x0=[.5 -.7 2]';
x=x0;
xout=zeros(N,3);
yout=zeros(N,1);
uout=yout;

```

```

xout(1,:)=x';
for k=1:N
    u=ufun(k);
    uout(k)=u;
    yout(k)=(H0+u*H1)*x;
    xout(k,:)=x';
    x=(F0+u*(F1+u*F2))*x+u*(G1+u*G2);
end

```

```
%end %end m-file
```

```

function u=ufun(k)
if rem(k,10)<5
    u=10; %Adjust amplitude here
else
    u=-10; % and here.
end

```

B.5.2 Grossman Observer

```

function [xout,rhoOut]=dogest(y,u)
%function [xout,rhoOut]=dogest(y,u)
%Grossman estimator for Dog's blood pressure
%control example.

%First Make initial estimate
N=length(y); %length of Output matrices
xout=zeros(N,3); %Allocate State Estimate Output matrix
rhoOut=zeros(N,1); %Allocate space for residual output

% Make initial guess. Can use numerical inverse
% but, for illustration purpose, used arbitrary initial state
%u1=u(1:3); %Note 3-delay retardation required
%y1=y(1:3); %Note 3-delay retardation required
%seed=[0 0 0]';
%zhat=y(1:3); %Note 3-delay retardation required
%xhat=invphi(zhat,u(1:3),seed); %Perform nonlinear inversion

xhat=3*[-1 -1 -1]'; %Use arbitrary initial state for illustration

A=[0 1 0 %Inverted dt system matrices
    0 0 1
    0 0 0];

B=[0 0 1]';

```

```
C=[1 0 0];
```

```
K=[-0.4828      %Estimation feedback gain  
    0.0966  
   -0.0080];
```

```

zhat=y(1:3);           %Note 2-delay retardation required
rho=0;                %No initial residual
%Main loop
for k=1:N-3
    xout(k,:)=xhat';   %Store state estimate
    rhoOut(k)=rho;     %Store residual

    x2=StepX(xhat,u(k)); %Grossman bracket 1
    x3=StepX(x2,u(k+1)); %Grossman bracket 2, anti-causal by 1 delay
    x4=StepX(x3,u(k+2)); %Grossman bracket 3, anti-causal by 2 delays
    rho=y(k)-C*zhat;   %residual

    zhat=A*zhat+K*rho+B*h(x4,u(k+3)); %Estimate zhat, anti-causal 3 delays

    xhat=invphi(zhat,u(k+1:k+3),x2); %Note use of x2 as seed. Seed is
                                     %Propagated by single model step
                                     %at top of loop.
end

%=====
% z=phi(x,u) nonlinear transformation. Note implementation
%of 1st and 2d-order Grossman bracket to generate z2, z3
function z=phi(x,u)
z1=h(x,u(1));
z2=h(StepX(x,u(1)),u(2));
z3=h(StepX(StepX(x,u(1)),u(2)),u(3));
z=[z1 z2 z3]';

%=====
%Output equation
function y=h(x,u)
H0=[-0.1024 0.019 -0.0539];
H1=[-0.0031 -0.002 -0.0004];
y=(H0+u*H1)*x;

%=====
%Nonlinear function inverter using newton's method
function x=invphi(z,u,x0)
alpha=.5;
x=x0;
for k=1:20
    J=jacobi(x,u);
    z1=phi(x,u);
    x=x-alpha*(J\ (z1-z));
end

```

```
%=====
%single step of dynamics
function x1=StepX(x,u)

F0=[0.8088 1 0.3614
    0.0857 0 -0.296
    -0.1692 0 0.0898];

F1=[0.0247 -0.0241 0.0049
    0.0105 0.0053 0.004
    -0.0055 -0.0025 -0.0012];

F2=[0.0002 -0.0001 0
    -0.0002 0.0002 0
    -0.0002 0.0001 0];

G1=[0 1 0]';
G2=[0.0151 -0.0289 0.0085]';

x1=(F0+u*(F1+u*F2))*x+u*(G1+u*G2);
```

```

%=====
%Jacobian matrix calculation for root finder
function J=jacobi(x,u)

F0=[0.8088 1 0.3614
    0.0857 0 -0.296
    -0.1692 0 0.0898];

F1=[0.0247 -0.0241 0.0049
    0.0105 0.0053 0.004
    -0.0055 -0.0025 -0.0012];

F2=[0.0002 -0.0001 0
    -0.0002 0.0002 0
    -0.0002 0.0001 0];

G1=[0 1 0]';
G2=[0.0151 -0.0289 0.0085]';

H0=[-0.1024 0.019 -0.0539];
H1=[-0.0031 -0.002 -0.0004];

J1=H0+u(1)*H1;
J2=(H0+u(2)*H1)*(F0+u(1)*(F1+u(1)*F2));
J3=(H0+u(3)*H1)*(F0+u(2)*(F1+u(2)*F2))*(F0+u(1)*(F1+u(1)*F2));
J=[J1;J2;J3];

```

B.5.3 Original and Modified Moraal and Grizzle Observer

The original and modified versions of the Moraal and Grizzle Observer are the same except for the values of slowing factor α . Iteration counter d is adjustable in both forms.

```

function [xout]=grizest1(y,u,alpha,d)
%function [xout,rhoOut]=grizest1(y,u,alpha,d)
%
%Grizzle Observer for dog blood pressure

%Generate output matrices
M=length(y);
xout=zeros(M,3);
rhoOut=zeros(M,1);

%State Dimension
N=3;

```

```

%define alpha and d
if nargin < 3
    alpha=1; %Slowing factor
end
if nargin < 4
    d=1; %Number of Newton pass
end

%Make first Window
zhat=[0 0 0]';
zhat=3*[-1 -1 -1]';
for k=4:M
    %output kth point
    xhat=StepX(StepX(StepX(zhat,u(k-N)),u(k-N+1)),u(k-N+2));
    xout(k,:)=xhat';

    %Make Window
    WindowIndex=k-N+1:k;
    Yk=y(WindowIndex);
    Uk=u(WindowIndex);

    ztilde=StepX(zhat,u(k-N));
    zhat=invphi(ztilde,Yk,Uk,d,alpha);
end

function z=phi(x,Uk)
z1=h(x,Uk(1));
z2=h(StepX(x,Uk(1)),Uk(2));
z3=h(StepX(StepX(x,Uk(1)),Uk(2)),Uk(3));
z=[z1 z2 z3]';

function x1=StepX(x,u)
F0=[0.8088 1 0.3614
    0.0857 0 -0.296
    -0.1692 0 0.0898];

F1=[0.0247 -0.0241 0.0049
    0.0105 0.0053 0.004
    -0.0055 -0.0025 -0.0012];

F2=[0.0002 -0.0001 0
    -0.0002 0.0002 0
    -0.0002 0.0001 0];

G1=[0 1 0]';

```



```

G2=[0.0151 -0.0289 0.0085]';

x1=(F0+u*(F1+u*F2))*x+u*(G1+u*G2);

function y=h(x,u)
H0=[-0.1024 0.019 -0.0539];
H1=[-0.0031 -0.002 -0.0004];
y=(H0+u*H1)*x;

function J=jacobi(x,u)

F0=[0.8088 1 0.3614
     0.0857 0 -0.296
     -0.1692 0 0.0898];

F1=[0.0247 -0.0241 0.0049
     0.0105 0.0053 0.004
     -0.0055 -0.0025 -0.0012];

F2=[0.0002 -0.0001 0
     -0.0002 0.0002 0
     -0.0002 0.0001 0];

G1=[0 1 0]';
G2=[0.0151 -0.0289 0.0085]';

H0=[-0.1024 0.019 -0.0539];
H1=[-0.0031 -0.002 -0.0004];

J1=H0+u(1)*H1;
J2=(H0+u(2)*H1)*(F0+u(1)*(F1+u(1)*F2));
J3=(H0+u(3)*H1)*(F0+u(2)*(F1+u(2)*F2))*(F0+u(1)*(F1+u(1)*F2));
J=[J1;J2;J3];

function zImproved=invphi(z,Yk,Uk,d,alpha)
for k=1:d
    J=jacobi(z,Uk);
    z=z+alpha*(J\ (Yk-phi(z,Uk)));
end
zImproved=z;

```

B.5.4 Original Ciccarella Observer

```

function [xout,rhoOut,poles,Lout]=Ciccest2(y,u,L)
%function [xout,rhoOut,poles,Lout]=Ciccest2(y,u,L)

```

```

%
%Ciccarella Observer for dog blood pressure

%Ciccarella output matrices
M=length(y);
xout=zeros(M,3);
rhoOut=zeros(M,3);
Lout=zeros(M,9);
poles=zeros(M,3);

if nargin<3
    L=[ -0.95000      1      0
         0.0000  -0.95000      1
         0      0.0000  -0.95000];
end

%State Dimension
N=3;
B=0*[0 0 1]'; %feedforward control
A=[0 1 0
    0 0 1
    0 0 0];
I=eye(3);
P=3*I;
W=0.0183*I;
Q=0.00018*diag([0 0 1]);
C=I;

%Make first Window
zhat=[0 0 0]';
zhat=3*[-1 -1 -1]';
%zhat=[0.5000  -0.7000  2.0000]';
%zhat=[ 0.4815  0.4312  0.0999]';
%zhat=phi(xhat,u(1:3));
rho=[0 0 0]';
p=rho;
L=0*I;
for k=4:M-1
    %output kth point
    xhat=StepX(StepX(zhat,u(k-N+1)),u(k-N+2)); %zhat=x(k-2)
    xout(k,:)=xhat';
    rhoOut(k,:)=rho';
    Lout(k,:)=L(:)';
    poles(k,:)=p(:)';

    %Make Window
    WindowIndex=k-N+1:k;

```

```

Yk=y(WindowIndex);
Uk=u(WindowIndex);

%Covariance
P=A*P*A'+Q;
ztilde=StepX(zhat,u(k-N+1)); %x(k-1)
J=jacobi(ztilde,Uk);
ykp1hat=h(StepX(StepX(StepX(zhat,u(k-2)),u(k-1)),u(k)),u(k+1));
rho=y(k+1)-ykp1hat;

%Kalman Gain
L=P*C'/(C*P*C'+W);
zhat=ztilde+(J\ (B*rho+L*(Yk-phi(zhat,Uk))));
P=(I-L*C)*P;
p=eig(L);
end

function z=phi(x,Uk)
z1=h(x,Uk(1));
z2=h(StepX(x,Uk(1)),Uk(2));
z3=h(StepX(StepX(x,Uk(1)),Uk(2)),Uk(3));
z=[z1 z2 z3]';

function x1=StepX(x,u)
F0=[0.8088 1 0.3614
    0.0857 0 -0.296
    -0.1692 0 0.0898];

F1=[0.0247 -0.0241 0.0049
    0.0105 0.0053 0.004
    -0.0055 -0.0025 -0.0012];

F2=[0.0002 -0.0001 0
    -0.0002 0.0002 0
    -0.0002 0.0001 0];

G1=[0 1 0]';
G2=[0.0151 -0.0289 0.0085]';

x1=(F0+u*(F1+u*F2))*x+u*(G1+u*G2);

function y=h(x,u)
H0=[-0.1024 0.019 -0.0539];
H1=[-0.0031 -0.002 -0.0004];
y=(H0+u*H1)*x;

function J=jacobi(x,u)

```

```

F0=[0.8088 1 0.3614
    0.0857 0 -0.296
    -0.1692 0 0.0898];

F1=[0.0247 -0.0241 0.0049
    0.0105 0.0053 0.004
    -0.0055 -0.0025 -0.0012];

F2=[0.0002 -0.0001 0
    -0.0002 0.0002 0
    -0.0002 0.0001 0];

G1=[0 1 0]';
G2=[0.0151 -0.0289 0.0085]';

H0=[-0.1024 0.019 -0.0539];
H1=[-0.0031 -0.002 -0.0004];

J1=H0+u(1)*H1;
J2=(H0+u(2)*H1)*(F0+u(1)*(F1+u(1)*F2));
J3=(H0+u(3)*H1)*(F0+u(2)*(F1+u(2)*F2))*(F0+u(1)*(F1+u(1)*F2));
J=[J1;J2;J3];

```

B.5.5 Modified Ciccarella Observer

```

function [xout,rhoOut]=Ciccest1(y,u,L)
%function [xout,rhoOut]=Ciccest1(y,u,L)
%
%Ciccarella Observer for dog blood pressure

%Ciccarella output matrices
M=length(y);
xout=zeros(M,3);
rhoOut=zeros(M,3);

if nargin<3
    L=[ -0.03      1      0
        0.0000  -0.04000  1
        0      0.0000  -0.05000];
end

%State Dimension
N=3;
B=0*[0 0 1]';

```

```

%Make first Window
zhat=[0 0 0]';
zhat=3*[-1 -1 -1]';
%zhat=[0.5000 -0.7000 2.0000]';
%zhat=[ 0.4815 0.4312 0.0999]';
%zhat=phi(xhat,u(1:3));
rho=[0 0 0]';
for k=4:M-1
    %output kth point
    xhat=StepX(StepX(zhat,u(k-N+1)),u(k-N+2)); %zhat=x(k-2)
    xout(k,:)=xhat';
    rhoOut(k,:)=rho';

    %Make Window
    WindowIndex=k-N+1:k;
    Yk=y(WindowIndex);
    Uk=u(WindowIndex);

    ztilde=StepX(zhat,u(k-N+1)); %x(k-1)
    J=jacobi(ztilde,Uk);
    ykpihat=h(StepX(StepX(StepX(zhat,u(k-2)),u(k-1)),u(k)),u(k+1));
    rho=y(k+1)-ykpihat;
    zhat=ztilde+inv(J)*(B*rho+L*(Yk-phi(zhat,Uk)));
end

function z=phi(x,Uk)
z1=h(x,Uk(1));
z2=h(StepX(x,Uk(1)),Uk(2));
z3=h(StepX(StepX(x,Uk(1)),Uk(2)),Uk(3));
z=[z1 z2 z3]';

function x1=StepX(x,u)
F0=[0.8088 1 0.3614
    0.0857 0 -0.296
    -0.1692 0 0.0898];

F1=[0.0247 -0.0241 0.0049
    0.0105 0.0053 0.004
    -0.0055 -0.0025 -0.0012];

F2=[0.0002 -0.0001 0
    -0.0002 0.0002 0
    -0.0002 0.0001 0];

G1=[0 1 0]';
G2=[0.0151 -0.0289 0.0085]';

```

```
x1=(F0+u*(F1+u*F2))*x+u*(G1+u*G2);
```

```
function y=h(x,u)
```

```
H0=[-0.1024 0.019 -0.0539];
```

```
H1=[-0.0031 -0.002 -0.0004];
```

```
y=(H0+u*H1)*x;
```

```
function J=jacobi(x,u)
```

```
F0=[0.8088 1 0.3614
```

```
0.0857 0 -0.296
```

```
-0.1692 0 0.0898];
```

```
F1=[0.0247 -0.0241 0.0049
```

```
0.0105 0.0053 0.004
```

```
-0.0055 -0.0025 -0.0012];
```

```
F2=[0.0002 -0.0001 0
```

```
-0.0002 0.0002 0
```

```
-0.0002 0.0001 0];
```

```
G1=[0 1 0]';
```

```
G2=[0.0151 -0.0289 0.0085]';
```

```
H0=[-0.1024 0.019 -0.0539];
```

```
H1=[-0.0031 -0.002 -0.0004];
```

```
J1=H0+u(1)*H1;
```

```
J2=(H0+u(2)*H1)*(F0+u(1)*(F1+u(1)*F2));
```

```
J3=(H0+u(3)*H1)*(F0+u(2)*(F1+u(2)*F2))*(F0+u(1)*(F1+u(1)*F2));
```

```
J=[J1;J2;J3];
```

REFERENCES

1. V. J. Aidala and S. E. Hammel. Utilization of modified polar coordinates for bearings-only tracking. *IEEE Trans. Automatic Control*, AC-28(3):283–294, March 1983.
2. K. J. Åström and B. Wittenmark. *Adaptive Control*. Addison-Wesley, Reading, MA, 1989.
3. K. E. Atkinson. *An Introduction to Numerical Analysis*. John Wiley & Sons, New York, NY, 1978.
4. Y. Bar-Shalom and E. Tse. Dual effect, certainty equivalence, and separation in stochastic control. *IEEE Trans. Automatic Control*, AC-19(5):494–500, October 1974.
5. G. Ciccarella, M. Dalla Mora, and A. Germani. A luenberger-like observer for nonlinear systems. *International Journal of Control*, 57(3):537–556, 1993.
6. G. Ciccarella, M. Dalla Mora, and A. Germani. Observers for discrete-time nonlinear systems. *Systems & Control Letters*, 20:373–382, 1993.
7. G. Ciccarella, M. Dalla Mora, and A. Germani. A robust observer for discrete time nonlinear systems. *Systems & Control Letters*, 24:291–300, 1995.
8. H. Diaz and A. A. Desrochers. Modelling of nonlinear discrete-time systems from input-output data. *Automatica*, 24:629–641, 1988.
9. A. A. Fel'dbaum. Dual-control theory. I. *Avtomatika i Telemekhanika*, 21(9):1240–1249, September 1960.
10. A. A. Fel'dbaum. *Optimal Control Systems*. Academic Press, New York, NY, 1965.
11. T. Fliegner, Ü. Kotta, and H. Nijmeijer. Solvability and right-inversion of implicit nonlinear discrete-time systems. *SIAM Journal of Control and Optimization*, 34(6):2092–2115, 1996.
12. B. Friedland. *Control System Design – An Introduction to State-Space Methods*. McGraw-Hill, New York, NY, 1986.
13. B. Friedland. On the properties of reduced-order Kalman filters. *IEEE Trans. Automatic Control*, AC-34(3):321–324, March 1989.
14. B. Friedland. *Advanced Control System Design*. Prentice-Hall, Englewood Cliffs, NJ, 1995.
15. B. Friedland. A nonlinear observer for estimating parameters in dynamic systems. *Automatica*, 33(8):1525–1530, August 1997.

16. J. P. Gauthier, H. Hammouri, and S. Othman. A simple observer for nonlinear systems—applications to bioreactors. *IEEE Trans. Automatic Control*, AC-37(6):875–880, June 1992.
17. G. C. Goodwin and R. L. Payne. *Dynamic Systems Identification: Experiment Design and Data Analysis*. Academic Press, New York, NY, 1977.
18. G. C. Goodwin, M. B. Zarrop, and R. L. Payne. Coupled design of test signals, sampling intervals, and filters for system identification. *IEEE Trans. Automatic Control*, AC-19(6):748–752, December 1974.
19. M. Gopal. *Modern Control System Theory*, pages 402–405. John Wiley & Sons, New York, NY, 1984.
20. J. W. Grizzle. Feedback linearization in discrete-time systems. In *Lecture Notes in Control and Information Sciences*, 83, pages 273–281. Springer-Verlag, New York, 1986.
21. J. W. Grizzle and P. W. Kokotovic. Feedback linearization of sampled-data systems. *IEEE Trans. Automatic Control*, AC-33(9):857–859, September 1988.
22. W. Grossman. Bias and divergence in bearings-only extended Kalman filters. In *Proceedings of the 1st Regional Control Conference*, pages 137–140, Brooklyn, NY, 1992.
23. W. Grossman. Bearings-only tracking: A hybrid coordinate system approach. *AIAA J. of Guidance, Control, and Dynamics*, 17(3), May-June 1994.
24. W. Grossman. Extension of the Friedland parameter estimator to discrete-time systems. *AIAA J. of Guidance, Control, and Dynamics*, 20(5):1047–1049, 1997.
25. J. W. Hermann, R. and A. J. Krener. Nonlinear controllability and observability. *IEEE Trans. Automatic Control*, AC-22:728–740, 1977.
26. A. Isidori. Nonlinear control systems. In *Lecture Notes in Control and Information (2nd edition)*. Springer-Verlag, 1989.
27. A. H. Jazwinski. *Stochastic Processes and Filtering Theory*. Academic Press, San Diego, CA, 1970.
28. R. E. Kalman. Design of a self-optimizing control system. *Transactions of ASME*, 80:468–478, February 1958.
29. R. E. Kalman and R. S. Bucy. New results in linear filtering and prediction theory. *Transactions of ASME, J. Basic Eng.*, pages 95–108, March 1961.

30. Ü. Kotta. Inversion method in the discrete-time nonlinear control systems synthesis problems. In *Lecture Notes in Control and Information Sciences*, 205. Springer-Verlag, 1995.
31. Ü. Kotta. On right invertibility of nonlinear recursive systems. In *Proceedings of the 13th IFAC World Congress*, volume F, San Francisco, CA, 1996.
32. A. J. Krener and A. Isidori. Linearization by output injection and nonlinear observers. *Systems & Control Letters*, 3:47–52, 1983.
33. H. Kwakernaak and R. Sivan. *Linear Optimal Control Systems*, pages 390, 400–402. Wiley-Interscience, New York, NY, 1972.
34. F. L. Lewis. *Applied Optimal Control & Estimation*. Prentice Hall, Englewood Cliffs, NJ, 1992.
35. L. Ljung. Asymptotic behavior of the extended Kalman filter as a parameter estimator for linear systems. *IEEE Trans. Automatic Control*, AC-24(1):36–50, February 1979.
36. L. Ljung and T. Söderström. *Theory and Practice of Recursive Identification*, chapter 3. MIT Press, Cambridge, MA, 1986.
37. D. G. Luenberger. An introduction to observers. *IEEE Trans. Automatic Control*, AC-16(6):592–602, December 1971.
38. The Mathworks, Natick, MA. *Matlab Control System Tool Box*, 1996.
39. R. K. Mehra. On the identification of variance and adaptive Kalman filtering. *IEEE Trans. Automatic Control*, AC-15(2):175–184, April 1970.
40. R. K. Mehra. On-line identification of linear dynamic systems with applications to Kalman filtering. *IEEE Trans. Automatic Control*, AC-16(1):12–21, February 1971.
41. R. K. Mehra. Optimal input signals for parameter estimation in dynamic systems—survey and new results. *IEEE Trans. Automatic Control*, AC-19(6):753–768, December 1974.
42. P. E. Moraal and J. W. Grizzle. Observer design for nonlinear systems with discrete-time measurements. *IEEE Trans. Automatic Control*, AC-40(3):395–404, March 1995.
43. H. Nijmeijer. Observability of autonomous discrete time non-linear systems: A geometric approach. *International Journal of Control*, 36(5):867–874, 1982.
44. E. Ott. *Chaos in Dynamical Systems*. Cambridge University Press, New York, NY, 1994.

45. M. Rosenlicht. *Introduction to Analysis*, pages 173–177. Scott, Foresman and Company, Glenview, IL, 1968.
46. L. E. Scales. *Introduction to Non-Linear Optimization*. Springer-Verlag, New York, NY, 1985.
47. Eduardo D. Sontag. On the observability of polynomial systems, I: finite-time problems. *SIAM Journal Control and Optimization*, 17(1):139–151, 1979.
48. M. Spong and M. Vidyasagar. *Robot Dynamics and Control*. Wiley Interscience, New York, 1989.
49. P. Swerling. First order error propagation in a stagewise smoothing procedure for satellite observations. *Journal Astronautical Science*, 6:46–52, 1959. Autumn.
50. E. Tse and Y. Bar-Shalom. An actively adaptive control for linear systems with random parameters via the dual control approach. *IEEE Trans. Automatic Control*, AC-18(2):109–117, April 1973.
51. E. Tse and Y. Bar-Shalom. Actively adaptive control for nonlinear stochastic systems. *Proceedings IEEE*, 64:1172–1181, August 1976.
52. E. Tse, Y. Bar-Shalom, and L. Meier. Wide-sense adaptive dual control for nonlinear stochastic systems. *IEEE Trans. Automatic Control*, AC-18(2):98–108, April 1973.
53. K. Zhou, J. C. Doyle, and K. Glover. *Robust and Optimal Control*. Prentice-Hall, Upper Saddle River, NJ, 1996.